Mn(II) Oxidation by HOCl in the Presence of Iron Oxides: A Catalyzing Effect

by

William Scott Dewhirst II

Thesis submitted to the Faculty of the

Virginia Polytechnic and State University

in partial fulfillment of the requirements for the degree of

MASTER OF SCIENCE

in

ENVIRONMENTAL ENGINEERING

APPROVED:

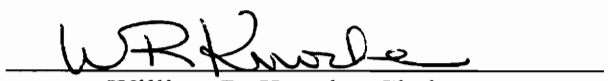

William R. Knocke, Chairman

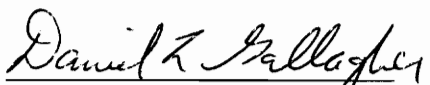

Daniel L. Gallagher

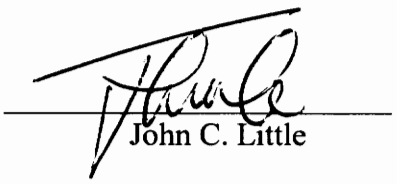

John C. Little

February, 1997

Blacksburg, Virginia

Keywords: Manganese, Iron, Oxides, Adsorption, Oxidation, Catalyzed

Mn(II) OXIDATION BY HOCL IN THE PRESENCE OF IRON OXIDES: A CATALYZING EFFECT

by

William Scott Dewhirst II

Dr. William R. Knocke, Chairman

Department of Environmental Engineering

(ABSTRACT)

The oxidation of soluble manganese (Mn(II)) to insoluble manganese dioxide ($MnO_{x\,(s)}$) is fairly well understood; however, the role of ferric hydroxide/oxides ($Fe(OH)_{3(s)}$) in catalyzing the oxidation of Mn(II) by oxidants such as free chlorine (HOCl) is one specific aspect of manganese removal via oxidation that requires further investigation. Data collected in this study indicate that the rate of Mn(II) oxidation may be beneficially catalyzed by the presence of previously formed $Fe(OH)_{3(s)}$ particles. The mechanistic means by which this enhanced oxidation is accomplished was the focal point of this research. Specifically, the research objectives were as follows:

(1) To study all possible Mn(II) removal mechanisms for a typical groundwater system to determine the necessary experimental conditions required to isolate the study of Mn(II) oxidation in the presence of ferric hydroxides/oxides ($Fe(OH)_{3\,(s)}$),

(2) To investigate the means by which ferric hydroxides/oxides ($Fe(OH)_{3\,(s)}$) may enhance the removal of Mn(II) during water treatment by interacting with HOCl; and

(3) To develop an engineered system that captures the observed catalyzing effect iron oxides have on Mn(II) oxidation by HOCl citing key system design parameters.

To complete these objectives a combination of batch and continuous flow bench-scale experiments were utilized. Batch study results indicated that the primary Mn(II) removal mechanism was a combination of adsorption and oxidation, specifically, adsorption of Mn(II) onto the iron oxide surface where Mn(II) is subsequently oxidized. A continuous flow system was developed to utilize this removal mechanism under water treatment plant conditions to improve the efficiency of iron and manganese removal. The results from experimentation with the continuous flow system indicated the following:

- Sufficient free chlorine residual in effluent insures consistent system performance,
- Initial iron oxide concentration within reactor system must have adequate adsorption capacity for initial adsorption-oxidation step to occur,
- Removal efficiency and reactor stability increase with the accumulation of manganese oxides, and
- Solution pH and reactor hydraulics affect system performance significantly.

The results suggest that this technology has the potential to change the look of conventional groundwater treatment systems that practice iron and manganese removal.

DEDICATION

This paper is dedicated to my wife, Dawn, without whose support I would not have been able to complete this work. Her patience and prayers were a source of strength during the writing of this paper. Also, this work is dedicated to my parents who have always been a source of encouragement for me and offered continuous support and motivation.

ACKNOWLEDGMENTS

The list of those to thank for their help in completing this work is immense. First, thanks go out to Dr. Knocke, my advisor, who always made time to discuss the results being observed in the laboratory and offered insight into the observations made. His motivation to complete the task as well as his thought-provoking questions were truly a stimulus. In addition, he provided a means to share the findings of this paper to the engineering profession by assisting with the preparation of abstracts for professional meetings presentations. Special thanks to Drs. Little and Gallagher for providing guidance and assistance as committee members.

Thanks also to Julie Petruska whom I depended upon a great deal in setting up the experimental apparatus, preparing chemical solutions, and with the determination of acceptable experimental methods. She was always available to help with a question and her knowledge of so many topics was a blessing.

Marilyn Grender, the laboratory technician, provided endless insight into the operation of the atomic adsorption spectrophotometer and other laboratory equipment used during data collection. Her assistance in this area improved the quality of results immensely.

To the Charles E. Via, Jr. Department of Civil Engineering and specifically to Mrs. Marion Via whose donation to the University provided scholarship and research moneys to conduct the studies presented here. Having been a Via Scholar during my undergraduate career, I owe practically my entire schooling to the Via Endowment. Thanks also to the Edna Bailey Sussman Fund for providing almost $3000 of funding for this research over a three month period. Without the financial support of these two entities, the results presented here would not have been possible.

TABLE OF CONTENTS

Abstract ii
Dedication iv
Acknowledgments v
Table of Contents vi

I. INTRODUCTION 1
A. Identification of Problem 1
B. Research Objectives 6

II. BACKGROUND 8
A. Occurrence of Iron and Manganese in Natural Waters 8
B. Chemistry of Manganese in Natural Waters 9
C. Methods for Manganese Removal from Water Supplies 11
D. Chemistry of Iron in Natural Waters 17
E. Oxidation of Soluble Iron in Natural Waters 17
F. Importance of Iron and Manganese Oxides 21
G. Summary 25

III. EXPERIMENTAL METHODS AND MATERIALS 26
A. Synthetic Water Makeup 26
B. Glassware Preparation 26
C. Preparation of Reaction Stock Solutions 28
D. pH Adjustment 30
E. Experimental Apparatus 30
F. Collection of Samples 39
G. Measurement Techniques for Data Collection 41

IV. RESULTS 44
A. Experimental Setup 44
B. Studies of Possible Mn(II) Removal Mechanisms 45
C. Mn(II) Removal via Surface Catalyzed Oxidation of Mn(II) with Fe(III) Oxides 54
D. Fe(III) Oxide Slurry Reactor System/Mn(II) Adsorption onto MnOx(s) 64
E. Model Development and Results 73

V. DISCUSSION 84
A. Studies of Possible Mn(II) Removal Mechanisms 84
B. Mn(II) Removal via Surface Catalyzed Oxidation of Mn(II) with Fe(III) Oxides 91

C. Fe(III) Oxide Slurry Reactor System/Mn(II) Adsorption onto MnOx(s) 96
D. Model Results 101

VI. SUMMARY & CONCLUSIONS 105
A. Summary of Results 105
B. Conclusions 107
B. Areas of Future Research 108

VII. REFERENCES 110

APPENDICES
Appendix A: Tabulation of Experimental Results
Appendix B: Operation and Detection Limit Determination for Atomic Adsorption-Spectrophotometry
Appendix C: Calculations
Appendix D: Model Formulation/Related Calculations

LIST OF TABLES AND FIGURES

Table 1: Summary of Field Data Collected at Groundwater Treatment Facility Treating for Iron and Manganese Removal 3
Table 2: Mn(II) Oxidation Reactions for Different Oxidants 12

Figure 1: Schematic of Conventional Groundwater Treatment Facility 4
Figure 2: Typical Iron Breakthrough Pattern for Dual-Media Filter 5
Figure 3: Manganese Potential Diagram for Mn-O_2-CO_2-H_2O), 25°C, 10^{-6} M (from Morgan[12]) 10
Figure 4: Solubility of Iron in Relation to pH and Eh at 25°C and 1 atm, Total Dissolved Sulfur 10^{-4} M; Bicarbonate Species 10^{-4} M (from Hem[41]). 18
Figure 5: Schematic of Experimental Setup for Isotherm Studies 32
Figure 6: Schematic of Experimental Setup for Catalyzed Mn(II) Oxidation in the Presence of Iron Oxides (Batch System) 34
Figure 7: Schematic of Iron Oxide Slurry Reactor System 38
Figure 8: Preliminary Studies to Determine $MnCO_{3(s)}$ Formation Potential and Mn(II) Removal via $CaCO_{3(s)}$ Adsorption 46
Figure 9: Preliminary Studies to Determine Role $CaCO_{3(s)}$ Formation has on Mn(II) Removal via Adsorption 47
Figure 10: Preliminary Studies to Determine $MnCO_{3(s)}$ Formation Potential and Mn(II) Removal via $CaCO_{3(s)}$ Adsorption 49
Figure 11: Solution Phase Oxidation via HOCl 50
Figure 12: Cartesian Plot of Adsorption of Mn(II) onto Fe(III) oxides 52
Figure 13: Langmuir Isotherm Plot of Adsorption of Mn(II) onto Fe(III) oxides 53
Figure 14: Cartesian Plot of Adsorption of Mn(II) onto Fe(III) oxides (purified iron stock) 55
Figure 15: Surface Catalyzed Oxidation of Mn(II) onto Fe(III) Oxides; Examination of Order of Addition of Metal Species 56
Figure 16: Effects of Various Fe(III) Oxide Levels on Mn(II) Oxidation Kinetics; Batch System pH 7 58
Figure 17: Effects of Various Fe(III) Oxide Levels on Mn(II) Oxidation Kinetics; Batch System pH 8 59
Figure 18: Actual versus Predicted HOCl Demand: Enhanced Mn(II) Oxidation in the Presence of Fe(III) Studies 61
Figure 19: Reaction Order and Rate Constant Determination 62
Figure 20: Mn(II) Oxidation Rate Constants as a Function of Fe(III) Concentration 63
Figure 21: Bench-Scale Continuous Flow System with Varying Fe(III) Oxide Slurry Concentration; No Additional HOCl Dose 65

Figure 22: Bench-Scale Continuous Flow System with Varying Fe(III) Oxide Slurry Concentration; Effect of HOCl Dose 66
Figure 23: Iron and Manganese Oxide Concentrations in Bench-Scale Continuous Flow System 68
Figure 24: Adsorption of Soluble Manganese (Mn(II)) onto Freshly Precipitated Manganese Oxides ($MnO_{x(s)}$) 69
Figure 25: Langmuir Isotherm for Adsorption of Mn(II) onto Freshly Precipitated Manganese Oxides ($MnO_{x(s)}$) 70
Figure 26: Bench-Scale Continuous Flow System; pH 7 71
Figure 27: Bench-Scale Continuous Flow System; pH 8 72
Figure 28: Summary of Rate Constant Values for Batch System Model at pH 8 79
Figure 29: Model Predicted and Observed Results for Batch Reactor System at pH 8 80
Figure 30: Model Predicted and Observed Results for Slurry Reactor System at pH 8 83
Figure 31: Comparison between Davies[2] Results to Observed Results 88
Figure 32: Extended Isotherm Studies to Determine Optimum Equilibrium Time for Adsorption Isotherm Determination 89
Figure 33: Experimentally Determined Rate Constants for Mn(II) Removal During Batch Studies Normalized with Respect to Fe(III) 94
Figure 34: Schematic of Proposed System 106

CHAPTER I
INTRODUCTION

A. Identification of Problem

The occurrence of iron and manganese in surface and groundwater supplies poses many challenges for the water treatment engineer and plant operator. These metals are commonly found in small to moderate concentrations in most groundwater supplies and may be prevalent in some surface water supplies, most notably reservoir impoundments during "turnover." The problems associated with these metals, although only aesthetic in nature, can be rather severe and may deter the public from consuming otherwise safe water. As consumers become more and more alarmed of the possible risks associated with their water supplies, the aesthetic properties of the water will inevitably play a significant role in their perception of an acceptable drinking water.

Various treatment techniques have been developed for removing these ions from solution. These methods range from aeration to chemical oxidation to greensand adsorption and most recently oxide-coated filter media. It is safe to say that the oxidation of each metal by conventional oxidants has been thoroughly studied and is fairly well understood. In most studies conducted to date, however, the two metals are studied independently to determine the oxidation rate or other desired parameter for each metal species. Thus, little research has been conducted that examines the interaction between the two metals during oxidation despite the fact that they are normally found together in natural waters.

The results of a field study at a groundwater treatment facility related to iron and manganese removal suggested that some interaction between the two metals may occur during conventional treatment. The field data collected indicated, as expected, that iron was effectively oxidized by aeration alone whereas manganese appeared to be unaffected. However, significant manganese removal was noted upon chlorination of the groundwater. This contradicts literature reported observations that manganese oxidation

via chlorine (HOCl) is relatively unsuccessful in the pH 7-8 range.[1] However, one significant difference between the observed conditions and those reported in the literature is the presence of oxidized iron particles in solution. A summary of the field data is provided in Table 1.

The oxidation of soluble manganese (Mn(II)) to insoluble manganese dioxide ($MnO_{x(s)}$) is fairly well understood; however, the role of ferric hydroxide/oxides ($Fe(OH)_{3(s)}$) in catalyzing the oxidation of Mn(II) by oxidants such as free chlorine (HOCl) is one specific aspect of manganese removal that requires further investigation. Previous researchers have noted catalyzed oxidation of Mn(II) via molecular oxygen in the presence of metal oxide surfaces including iron in natural water systems,[2] but the possible advantages this phenomenon may offer under water treatment conditions have yet to be fully investigated.

This treatment technology was pursued because of the problems associated with conventional groundwater treatment facilities; a schematic of such a facility is shown in Figure 1. One inherent problem associated with these groundwater treatment plants is the use of strong oxidants, most commonly potassium permanganate ($KMnO_4$). Although this chemical is very effective at oxidizing any soluble manganese, several treatment problems are associated with this method of treatment:

- the production of colloidal sized $MnO_{x\,(s)}$ particles which often pass through the filtration process[3-5]
- the sensitivity of the raw water to the dose of such a strong oxidant, resulting in over or under-treatment as the raw water quality varies
- the cost of using stronger oxidants (e.g. $KMnO_4$, ClO_2, O_3) when compared to the cost of weaker oxidants (eg. HOCl)

In addition, other problems have been noted with conventional systems employing weaker oxidants such as chlorine. Figure 2 shows a typical breakthrough curve for a dual-media filter used at such a facility to remove oxidized iron from solution. Initially, the effluent quality of the filter increases during the "ripening" period, however, the iron

Table 1: Summary of Field Data Collected at Groundwater Treatment Facility Treating for Iron and Manganese Removal

		Speciation (mg/L)**		
Oxidant	**Metal**	**Total**	**< 8 μm**	**Soluble**
Aeration	Fe	1.3	1.1	<0.1
	Mn	0.45	0.45	0.43
Aeration	Fe	1.7	1.0	< 0.1
& HOCl	Mn	0.42	0.38	0.25

**Data collected during full-scale pilot studies between pH 7.3-7.5. Treatment train: aeration, chlorine addition (if applicable), two hour detention time (no mixing), and filtration. Samples were collected, filtered, and tested following two hour detention time. Total represents influent concentration (acid digested solids), < 8 μm simulates the effluent from a dual-media filter, and soluble represents particles passing a 0.2 μm filter.

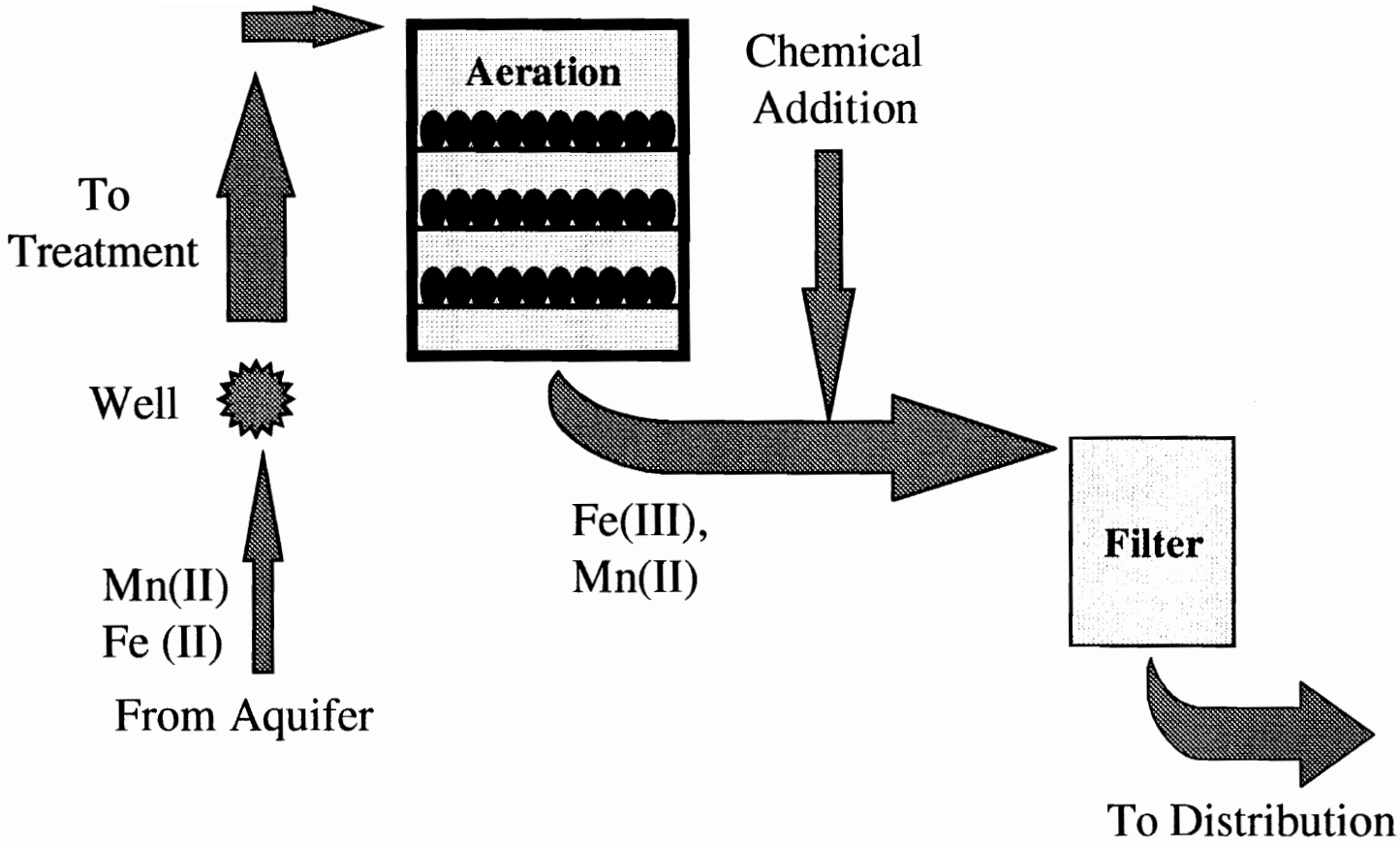

Figure 1: Schematic of Conventional Groundwater Treatment System

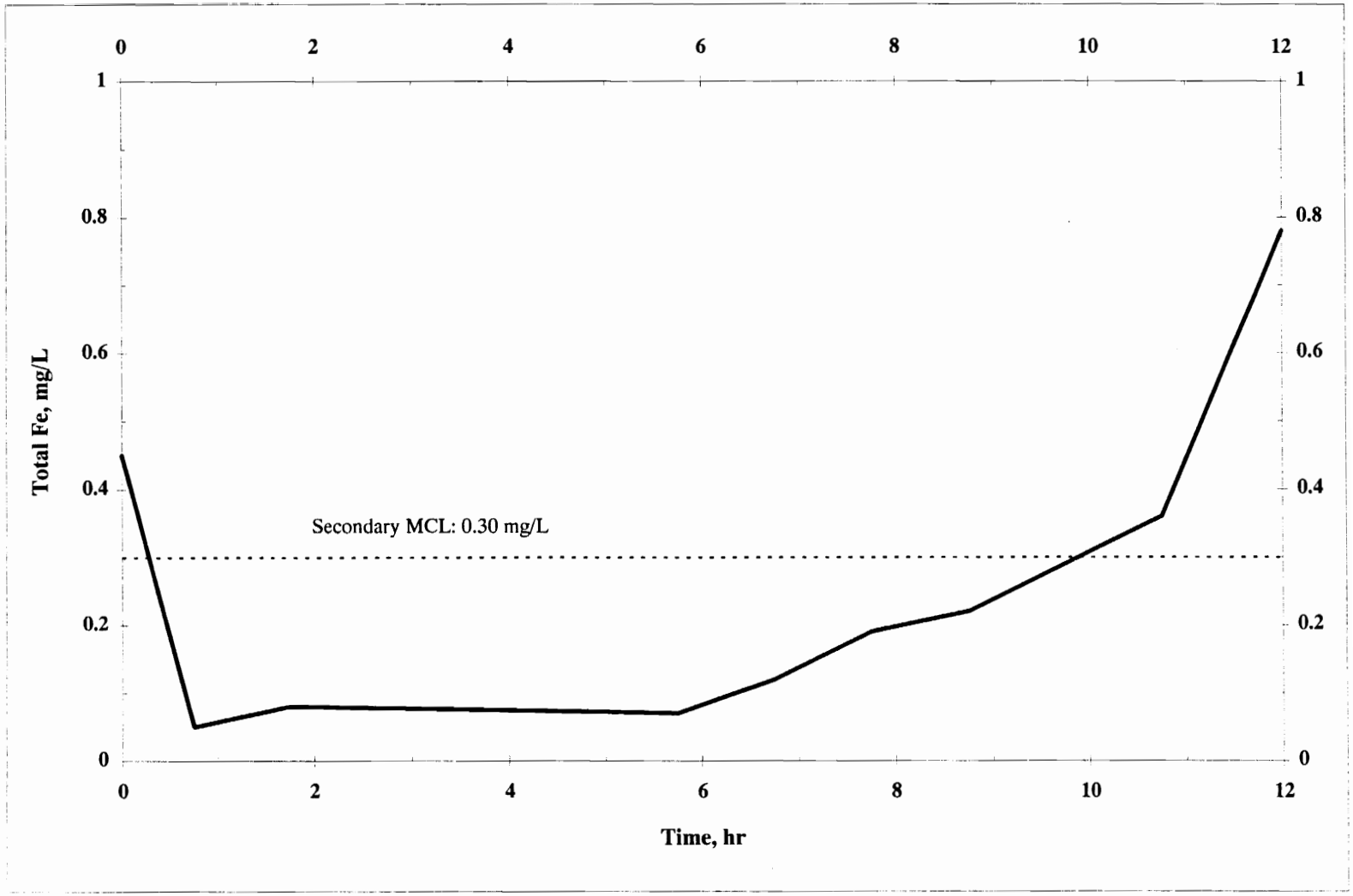

Figure 2: Typical Iron Breakthrough Pattern for Dual-Media Filter following Backwash at Conventional Groundwater Treatment Facility (Plotted Data is Acid Digested Effluent from Full-Scale Dual Media Filter)

concentration leaving the filter rapidly approaches the secondary maximum contaminant level of 0.30 mg/L within 10 hours of startup.

The goal of this study is to propose the use of a newly engineered system emphasizing chlorine for soluble Mn(II) removal. The system is geared toward improving and economizing the treatment processes at conventional groundwater treatment facilities for the removal of iron and manganese. It should be noted that the proposed process should be considered in waters with low organic content because HOCl will be used as the primary oxidant. It is well known that the interactions between chlorine and organic compounds result in the formation of trihalomethanes and other by-products regulated by the Safe Drinking Water Act.[6] In addition, previous research has indicated that iron complexed by organic material is not effectively oxidized by HOCl.[7,8]

B. Research Objectives

From the aforementioned observations several research objectives were established:

(1) To study all possible Mn(II) removal mechanisms for a typical groundwater system to determine the necessary experimental conditions required to isolate the study of Mn(II) oxidation in the presence of ferric hydroxides/oxides ($Fe(OH)_{3\,(s)}$),

(2) To investigate the means by which ferric hydroxides/oxides ($Fe(OH)_{3\,(s)}$) may enhance the removal of Mn(II) during water treatment by interacting with HOCl; and

(3) To develop an engineered system that captures the observed catalyzing effect iron oxides have on Mn(II) oxidation by HOCl citing key system design parameters.

In order to accomplish these objectives, several different types of experimental systems were arranged as described in Chapter III. First, however, a thorough review of

previous research studying the chemistry of iron and manganese as well as treatment techniques available for their removal (presented in Chapter II) was conducted. Finally, the results and discussion of the results obtained during these experiments will be discussed in Chapters IV and V, respectively, followed by the listing of formulated conclusions in Chapter VI.

CHAPTER II
BACKGROUND

A. Occurrence of Iron and Manganese in Natural Waters

The fact that iron and manganese are commonly found in most groundwaters and a portion of surface water supplies is easily explained by their abundance in the earth's crust. Iron was reported by Sung and Morgan[9] as being the fourth most abundant element by weight; Bowers and Huang[10] cite iron as being " the single most abundant micronutrient in soil systems, occurring naturally as oxides." Manganese is also widely found in nature in various oxide and mineral forms in association with silicates, carbonates, and sulfides.[11] Manganese represents approximately 0.1% of the earth's crust, making it the tenth most abundant element. Iron is more abundantly found than manganese in water supplies because of the 50:1 geochemical ratio of iron to manganese in the earth's lithosphere.[12]

The presence of iron and manganese in natural waters is a result of the dissolution of the minerals and oxides containing these metals. Often, the dissolution reactions take place under anaerobic conditions, yielding the reduced metal species manganous (Mn(II)) and ferrous (Fe(II)) oxidation states. Such manganese release has even been noted in water treatment plant sedimentation basins if insufficient oxidant is present.[13] Stone and Morgan[14-16] have shown the reduction of Mn(III) and Mn(IV) oxides by organic materials to the Mn(II) form. Significant release of iron and manganese is commonly observed in the oxygen-deficient hypolimnetic waters of reservoirs as bacteria reduce the oxide as an alternative energy source (electron acceptor). During reservoir overturn, the waters are completely mixed, explaining the seasonal occurrence of these metals in reservoir supplies. However, because of the continuous presence of iron and manganese minerals in groundwater aquifers, the presence of these metals in groundwater supplies is much more consistent.[17]

B. Chemistry of Manganese in Natural Waters

In the absence of dissolved oxygen, chlorine or other oxidants, Mn(II) is the stable form of manganese in most natural waters.[12] However, as with most metals, manganese has the capability of forming numerous compounds which can affect its solubility significantly. Among the various chemical species that may form are pyrolusite ($MnO_{2(s)}$), manganite (δ-$MnO(OH)_{(s)}$), rhodonite ($MnSiO_{3(s)}$), hausmannite, $Mn_3O_{4(s)}$, pyrochroite ($Mn(OH)_{2(s)}$), rhodochrosite ($MnCO_{3(s)}$), and alabandite ($MnS_{(s)}$). In most cases, however, manganese solubility is limited by the hydroxide (OH^-), carbonate (CO_3^{-2}), or sulfide (S^{-2}) composition of the water.[12] It is important to note that despite being the most well known oxidized form of Mn(II), $MnO_{2(s)}$ is not the only higher oxidized form of Mn(II).[18] The main chemical equilibria controlling Mn(II) solubility are summarized as follows, and a stability plot is provided in Figure 3 (all solubility products (K_{so}) and energies of formation ($\Delta F°$) are reported at 25°C by Morgan[12]):

(1)	$MnCO_{3\,(s)} \Leftrightarrow Mn(II) + CO_3^{-2}$	$K_{so} = 4.68 \times 10^{-11}$	$\Delta F° = -194.8$ kcal
(2)	$MnS_{\,(s)} \Leftrightarrow Mn(II) + S^{-2}$	$K_{so} = 7 \times 10^{-16}$	$\Delta F° = -53.0$ kcal
(3)	$Mn(OH)_{2\,(s)} \Leftrightarrow Mn(II) + 2OH^-$	$K_{so} = 9.1 \times 10^{12}$	$\Delta F° = -147.3$ kcal

Any of these reactions can control solubility in the absence of oxidants, as it is not unusual to find carbonate, hydroxide, and sulfide species in the hypolimnion of lakes or in groundwaters. Other possible, but less common, complexes include those with cyanide (CN^-), phosphate (PO_4^{-2}), and silicas.[12] The complexation observed between manganese and silica or phosphate compounds is often used to control manganese in water supplies through a process known as sequesterization.[19,20]

In waters containing organics, researchers observed that little or no complexation occurs between the organics and Mn(II) even at high dissolved organic carbon (DOC) levels.[21] Data collected by Knocke et al.[1] showed that complexation of Mn(II) by DOC increased with pH, however, the vast majority of Mn(II) remains uncomplexed by organic

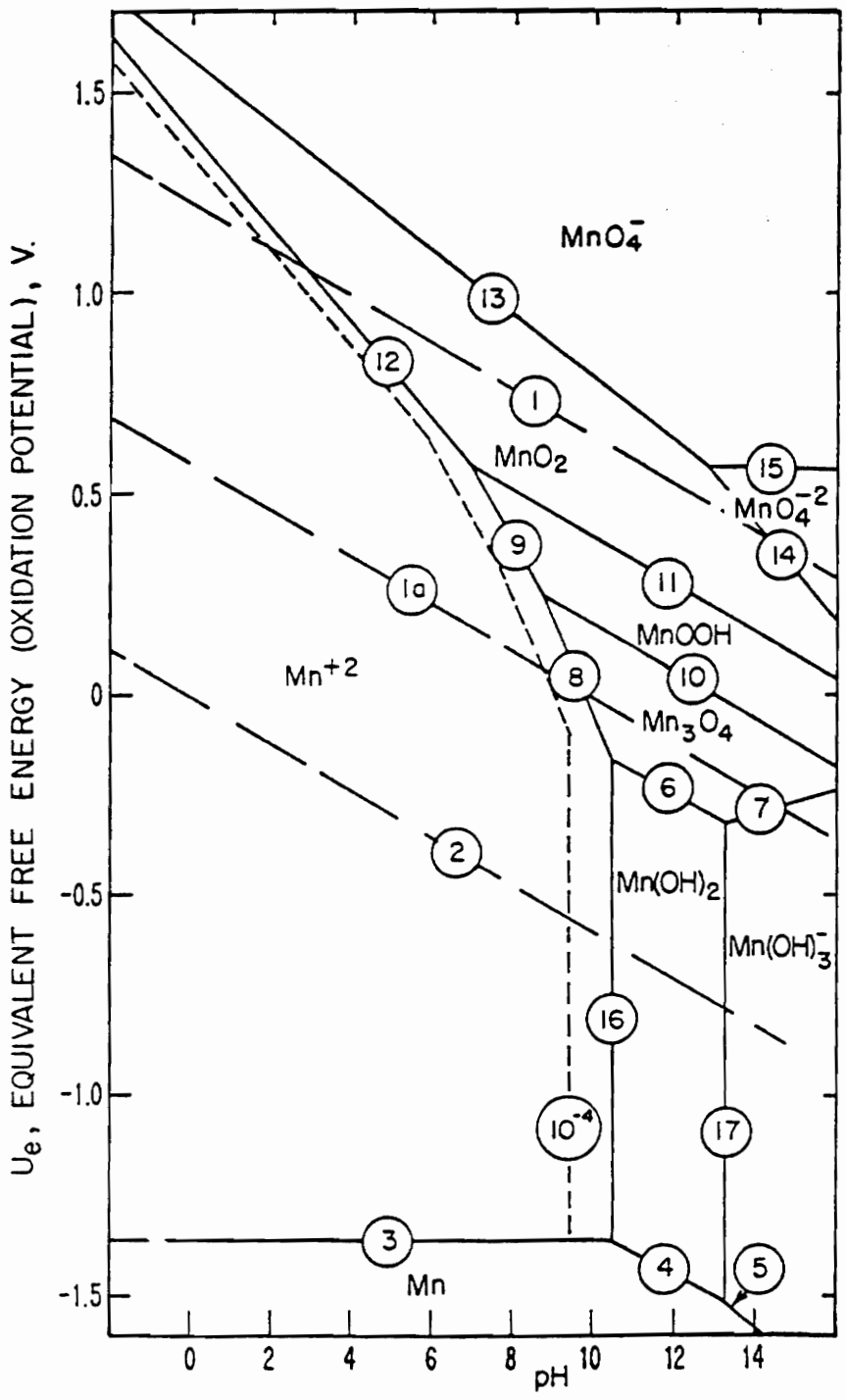

Figure 3: Manganese Potential Diagram for Mn-O_2-CO_2-H_2O, 25°C, 10^{-6}M (from Morgan[12]).

matter regardless of solution pH.

C. Methods for Manganese Removal from Water Supplies

1. Chemical Oxidation

The notorious reputation of manganese and its detrimental effect on water quality dates back to the late 19th century when Brown reported a case of black slime in an English distribution system attributed to manganese oxides.[22] Since that time a great deal of study has been devoted to alternative methods of manganese oxidation and removal before it enters the distribution system. As time has passed, the recommended means of controlling this metal have shifted from biological treatment to chemical oxidation to the use of catalysts to surface adsorption/oxidation techniques.[1,4,22-24] Each of these treatment methods have individual limitations and drawbacks making it difficult to prescribe one method to be effective on all water supplies. To better understand the various means of removal, a keen understanding of the oxidation chemistry of manganese must first be developed.

As previously discussed, the chemistry of manganese for higher oxidation states of the metal beyond the soluble Mn(II) form is very complex in that many oxidized forms can result. Table 2 summarizes chemical reduction-oxidation reactions which describe the oxidation of Mn(II) in the presence of various chemical oxidants.[1]

Although dissolved organics do not complex significantly with Mn(II), they do create an oxidant demand that must be accounted for when determining proper oxidant dosing. Generally, weaker oxidants such as oxygen and chlorine are ineffective for oxidation except at elevated pH levels or at excessive oxidant doses. However, stronger oxidants such as chlorine dioxide, potassium permanganate, and ozone, have the ability to satisfy competitive organic demands and oxidize Mn(II).[25] The oxidation of Mn(II) under low DOC levels is discussed individually by oxidant.

Table 2: Mn(II) Oxidation Reactions for Different Oxidants

Oxidant	Reaction	Stoichiometry
$O_{2(aq)}$	$Mn^{2+} + 0.5\ O_{2(aq)} + H_2O \rightarrow MnO_{2(s)} + 2H^+$	0.29 mg O_2/ mg Mn
$O_{3(aq)} \rightarrow O_{2(aq)}$	$Mn^{2+} + O_{3(aq)} + H_2O \rightarrow MnO_{2(s)} + O_{2(aq)} + 2H^+$	0.88 mg O_3/mg Mn
HOCl	$Mn^{2+} + HOCl + H_2O \rightarrow MnO_{2(s)} + Cl^- + 3H^+$	1.30 mg HOCl/ mg Mn
$KMnO_4$	$Mn^{2+} + 2KMnO_4 + H_2O \rightarrow 5MnO_{2(s)} + 4H^+$	1.92 mg $KMnO_4$/mg Mn
$ClO_2 \rightarrow ClO_2^-$	$Mn^{2+} + 2ClO_2 + H_2O \rightarrow MnO_{2(s)} + 2ClO_2^-{}_{(aq)} + 4H^+$	2.45 mg ClO_2/mg Mn

a. Mn(II) Oxidation via $O_{2\,(aq)}$. In early studies of manganese oxidation in the presence of molecular oxygen, Hem[26] found that an increase in solution pH increased the rate of Mn(II) oxidation and precipitation by aeration; further, the rate is significantly reduced when HCO_3^- and SO_4^{-2} are present. Morgan[12] used elevated initial Mn(II) concentrations of 11 mg/L to investigate these findings further. The formation of $MnCO_{3(s)}$ and the ion-pair of $MnHCO_3^+$ were cited as reasons to explain the slowing of oxidation kinetics in the presence of carbonate species; however, the presence of sulfate did not affect the oxidation kinetics significantly. The reaction rate was found to be directly proportional to temperature; as the temperature was halved the reaction rate was approximately halved. Morgan also found the oxidation of manganese by $O_{2(aq)}$ is autocatalytic in nature. However, Hem[27] reported that the catalytic effect is slowed to a pseudo-first order reaction as the amount of precipitate surface becomes large in comparison to soluble, unreacted manganese. The presence of surface catalysts or manganese bacteria have been suggested to be required for Mn(II) oxidation in some natural waters.[28]

Using x-ray diffraction, the oxidation products of manganese and oxygen were determined to be a mix of Mn(III) and Mn(IV) species.[27] The product of $O_{2(aq)}$ oxidation according to Morgan[12] resembled $Mn_3O_{4(s)}$ rather that $MnO_{2(s)}$. The overall products are generally colloidal and variable in composition from $MnO_{1.2}$ - $MnO_{1.5}$. Kessick and Morgan[29] concluded that $MnOOH_{(s)}$ is the primary product of autoxidation in aqueous solution. In other studies, temperature was found to have a significant effect on the form of precipitate; specifically as temperature was decreased the predominant precipitate was β-$MnOOH_{(s)}$ especially at temperatures less than 10°C. Eventually, however, the final form of the oxide will be $MnO_{2\,(s)}$.[27]

b. Mn(II) Oxidation via $O_{3(aq)}$. Ozone is primarily tested as an oxidant for treatment of waters with significant organic content, a condition which may limit the use of other conventional oxidants. Despite the strength of ozone as an oxidizing agent,

Weng et al.[4] found that regardless of the ozone dose, soluble manganese often remained in the finished water following filtration at levels exceeding the SMCL of 0.05 mg/L. The ozone dose utilized was sufficient to provide an ozone residual yet Mn(II) oxidation remained incomplete. Wilczak et al.[30] discovered that ozonating waters containing Mn(II) resulted in the formation of mostly colloidal $MnO_{2(s)}$. Their results also confirmed those of Weng et al.[4] in that regardless of the O_3 dose, high levels of soluble Mn(II) remained in the filtered water. For effective soluble Mn(II) removal, the authors of these articles relied on further treatment involving oxide coated filter media and permanganate addition, respectively. These methods will be discussed later.

c. Mn(II) Oxidation via HOCl. Chlorine is commonly used as an attempt to oxidize Mn(II) in water supplies. Such oxidation requires long periods of detention time depending on the pH and chlorine concentration.[31] Wong[5] suggested that the pH be maintained at pH 8.5 and that calcium be added to destabilize the net negative charge of $MnO_{2(s)}$ for improving filtration performance. Two other researchers reported the need for calcium to destabilize the colloidal MnO_2 particle to improve filtration.[32,33] Wong[5] recommended a chlorination-filtration system over aeration-filtration and potassium permanganate-manganese greensand filtration for both economic and operational reasons. Mathews[34] noted that when chlorination is used, filter media need not be coated with manganese oxides for acceptable effluent quality.

Hao et al.[23] studied the kinetics of Mn(II) oxidation by chlorine to develop a kinetic model and to study the effect various organic ligands (chelating agents) have on the Mn(II) oxidation rate. These studies utilized a very large initial Mn(II) concentration (5.5 mg/L) atypical of natural water systems. These studies concluded that the most important parameter governing the rate of oxidation was the stoichiometric ratio of chlorine to manganese. The kinetics increased as this ratio was increased as well as for increases in solution pH.

The importance of adsorption in the autocatalytic oxidation of Mn(II) has been well documented.[1,23,29]

d. Mn(II) Oxidation via Potassium Permanganate ($KMnO_4$). The use of potassium permanganate as an oxidant for Mn(II) has long been practiced.[3,22] The use of $KMnO_4$ is often favored over weaker oxidants because the rate of oxidation is much more rapid,[3] occurring almost instantaneously provided that sufficient oxidant for interaction with Mn(II) is present.[1] One problem cited with the use of $KMnO_4$ is the formation of colloidal sized $MnO_{x(s)}$ particles which pose filtration concerns.[3,4] Van Benschoten et al.[24] developed a relatively accurate kinetic model for Mn(II) oxidation via $KMnO_4$.

e. Mn(II) Oxidation via ClO_2. The use of chlorine dioxide as an oxidant for Mn(II) has not been studied extensively as this oxidant is not as popular as those previously discussed. Knocke et al.,[1] assuming only a one electron transfer product to ClO_2^-, showed similar oxidation rates to those of $KMnO_4$ with some variation occurring with the presence of organics. Also, the growing concern over residual chlorite concentration (limit of 1 mg/L) in the upcoming D-DBP Rule may further limit the use of ClO_2 as a primary oxidant for Mn(II) removal.[35]

2. Other Treatment Techniques

a. Ion Exchange. The use of ion exchange systems for Mn(II) removal is somewhat rare as treatment difficulties can easily arise if oxidation occurs in the resin bed (particularly if reduced iron becomes oxygenated). As with other ion exchange operations, the Mn(II) ions in solution are exchanged for sodium or hydrogen ions on the resin.[20] If operated correctly, such a system can be very effective, yet brine disposal is an issue.[36]

b. Manganese Greensand Adsorption-Regeneration. This "filtration" process employs filter media naturally or synthetically coated with manganese oxides. The effective size of the media is generally quite small forcing pressure filtration in many instances. Once the adsorptive capacity of the greensand has been expended, the bed is regenerated with an oxidant, normally potassium permanganate.[20] An alternative is to provide continuous regeneration with permanganate.[37] One potential drawback of these systems is the need for pump(s) to provide the pressure necessary to force the raw water through the filters; this is not a concern if well head pressures are sufficient.

c. Oxide-Coated Filter Media. Several researchers dating back to the early 20th century have noted a "natural greensand effect" occurring in filters treating manganese laden waters.[4,22, 31, 34, 38, 39] The beneficial effect the manganese oxides have on water treatment are well noted; however, significant research on the mechanistic means of the process was not conducted until recently by Knocke et al.[38,39] In removal studies using ozone, regardless of the ozone dose, effective manganese removal was not seen until the use of an oxide-coated filter media was used.[4] Knocke et al.[38] noted that the removal of Mn(II) by filtration through oxide coated media is at first an adsorption process. Generally, the uptake is very rapid, as expected based on the data presented by Morgan and Stumm[40] for Mn(II) adsorption onto previously formed $MnO_{x\,(s)}$. However, in the absence of an oxidant, the removal efficiency approached zero as the available number of adsorption sites was exhausted. Once oxidant was applied, the surface catalyzed the oxidation of the adsorbed Mn(II), resulting in the regeneration and actual growth of the manganese oxide surface around the filter media.[38]

The application of free chlorine under neutral pH conditions was found to be effective at oxidizing surface sorbed Mn(II). This mode of operation provided for continuous regeneration of the oxide coating on the filter media; thus, backwashing with a permanganate solution need not be necessary.[39]

D. Chemistry of Iron in Natural Waters

The oxidation state of iron that will be found in water is related to several different variables. Primarily, the reduction-oxidation potential of the water as well as the organic content are key factors, but alkalinity and other parameters may affect iron speciation.[8, 41, 42, 43, 44, 45] Among the most common precipitates that can be formed by interactions between iron and other species are $Fe(OH)_{3(s)}$ (hydrated ferric oxides), $FeCO_{3(s)}$ (siderite), $Fe(OH)_{2(s)}$, and $FeS_{2(s)}$ (pyrite).[41] The chemical equilibria for these reactions are summarized as follows with a stability plot provided in Figure 4:[41, 45]

(4) $Fe(OH)_{3\,(s)} \Leftrightarrow Fe(III) + 3H_20$

(5) $FeCO_{3\,(s)} \Leftrightarrow Fe(II) + CO_3^{2-}$

(6) $Fe(OH)_{2\,(s)} \Leftrightarrow Fe(II) + 2OH^-$

(7) $FeS_{2\,(s)} \Leftrightarrow Fe(II) + 2S_{\,(s)} + 2e^-$

In waters containing high levels of alkalinity, the carbonate concentration often controls iron solubility as described by equation (5).[45] Reduced Fe(II) can be removed from solution due to hydroxide or sulfide concentrations.[41] These compounds are likely to dominate under low oxygen conditions along with other possible complexes formed with cyanides, silicates, phosphates, and numerous other inorganic materials.[46] However if adequate oxygen is present in waters of neutral to alkaline pH these reactions will compete with the oxidation of iron to iron hydroxide (equation (4)) if low levels of organic material are present.[47]

E. Oxidation of Soluble Iron in Natural Waters

Similar treatment techniques for Mn(II) oxidation/removal are available for soluble iron removal (ion exchange, greensand adsorption, biological processes, chemical oxidation using O_3, $KMnO_4$, ClO_2, etc.). These methods of treatment are discussed in detail by others,[8, 19, 20, 36, 37, 48, 49] but will not be covered in this paper as the use of such

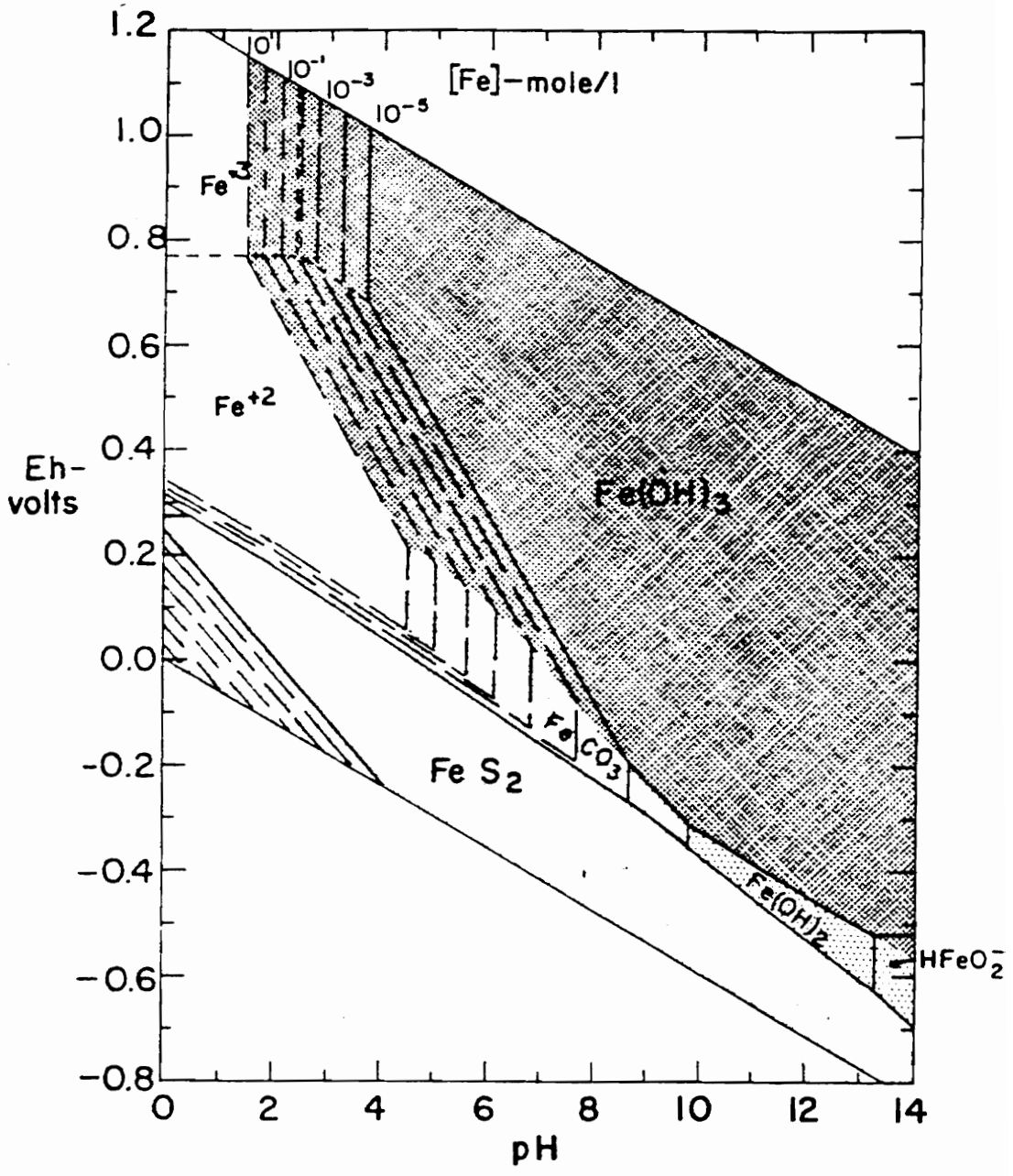

Figure 4: Solubility of Iron in Relation to pH and Eh at 25°C and 1 atm, Total Dissolved Sulfur 10^{-4} M; Bicarbonate Species 10^{-4} M (from Hem[41]).

techniques was not the focus of this work. The limits of this discussion on iron oxidation will include only oxidation via dissolved oxygen or free chlorine. These oxidants are commonly used for iron removal and have been found to be very effective in low organic waters.[1]

Numerous researchers have noted the complexation effect that organic materials have on soluble iron in water supplies.[8, 41, 42, 43, 44, 45, 47, 50] This phenomenon significantly reduces the ability of precipitates or oxidation products to form as the iron is relatively unreactive.[1] The effect organic interaction has on Fe(II) oxidation will be discussed in the upcoming section.

1. Oxidation via Dissolved Oxygen. Ghosh et al.[47] presented a study of Illinois waters to investigate the factors governing the oxidation rate of iron in natural waters via aeration. Their study indicated that in high alkalinity groundwaters, the majority of the iron precipitated following aeration was in the form of ferrous carbonate, not the oxidized form of ferric hydroxide. Several researchers refuted the results of the Ghosh et al.[47] study, citing discrepancies with the saturation levels with respect to iron and carbonate reported as well as the fact that the alkalinity concentrations used in synthetic water samples were not of the same magnitude as those found naturally.[46, 50, 51] In response to these studies, Morgan and Birkner[51] presented results from their studies indicating that Fe(II) oxidation via oxygen follows a first-order rate and that $FeCO_3$ species are less rapidly oxidized than free Fe(II) ions.

Sung and Morgan[9] demonstrated that lepidocrocite $(\gamma\text{-FeOOH})_{(s)}$ was the primary product of iron oxidation under average pH conditions. In addition, the authors noted that the reaction is autocatalytic in the presence of previously formed iron oxides at pH values greater than 7. The observed Fe(II) oxidation rate was slowed in the presence of complexing ions such as SO_4^{-2} and Cl^-, confirming the work of previous researchers.

The effects organics have on the oxygenation and oxidation of iron(II) has been well documented.[8, 41-43, 45, 47, 51] This property constitutes a major difference in

comparison to soluble Mn(II) which is only slightly complexed by organics under normal pH conditions.[1] Shapiro[44] presented a study aimed at understanding the interactions between soluble iron and organic matter in waters. His study resulted in several key conclusions:

1. the amount of iron bound by the organic matter increased with pH;
2. the metal was unaffected by exposure to air;
3. although visible by color, the metal complex could not be filtered from solution; and,
4. iron was not held solely by the mechanism known as chelation.

Researchers have hypothesized that iron may indeed be oxidized, but that it serves as the oxidant for organic material. Theis and Singer[42] and Jobin and Ghosh[43] suggested the following cyclical arrangement to explain this hypothesis:

$$Fe(II) + organics \xrightarrow{O_2} Fe(III) + complexed\ organics \xrightarrow{organics} Fe(II) + oxidized\ organics \quad (8)$$

Generally speaking, oxygenation of waters containing reduced Fe(II) complexed with organics is relatively ineffective at oxidizing the complexed iron in solution.

2. Oxidation with free chlorine. Mathews[34] performed studies to determine the effectiveness of chlorination for the oxidation of soluble iron in solution. As expected, these studies exhibited that iron oxidation with chlorination was very effective; however, if organics are present oxidation is limited. Knocke et al.[1] reported that Fe(II) oxidation by free chlorine was rapid (less than 10 seconds in most cases) in the pH range of 5.0 to 7.0 studied.

Knocke et al.[8] presented data for Fe(II) oxidation in the presence of organics which indicated that the organic material provided enough of an oxidant demand to reduce the amount of Fe(II) oxidation occurring. Only when a significant excess of chlorine was added was this oxidant effective. It should be noted that this study reported that the oxidized iron product was colloidal in size. Additional research studies indicated

that Fe(II) forms strong complexes with high molecular weight organics and weaker complexes with lower molecular weight organics.[7]

F. Importance of Iron and Manganese Oxides

The previous sections discussed the formation of oxidized forms of iron and manganese. The importance that these oxide surfaces exhibit in the natural environment and under water treatment plant conditions has been the focus of many research efforts.[10, 52-58] The research to be presented by this paper focused on the importance of the iron oxide surface in catalyzing oxidation of manganese via free chlorine. Thus, an understanding of the properties and effect the iron oxide surface has in natural water systems is of extreme importance in presenting this work. In addition, the adsorptive and catalyzing properties the manganese surface exhibits must also be considered.

1. Iron Oxides. Bowers and Huang[10] studied the adsorption of soluble metals onto various forms of iron oxides, reporting that iron is capable of forming complexes with numerous different materials. Other researchers[52] presented a study detailing the adsorption of Cu(II) onto geothite (α-FeOOH)$_{(s)}$ and reported such interactions to occur very rapidly. The same study determined that divalent cations form a monodentate innersphere surface complexes (such complexes are believed to be stronger than ionic interactions) with geothite. This property can be assumed to exist between Mn(II), a divalent cation, and geothite.[52]

Several scientists have studied the effect that the iron oxide surface has on Mn(II) oxidation, which is of great importance to the work to be presented.[55-57] Wilson[55] investigated the effect that various surfaces play on the rate of Mn(II) oxidation; one surface of particular interest was geothite. The results indicated that the geothite surface played a role in catalyzing the oxidation of Mn(II) by oxygen. Wilson hypothesized that the removal observed was most likely due to Mn(II) adsorption followed by oxidation on the iron oxide surface. He likened the catalytic effect noted to that observed in Mn(II)

oxidation when $MnO_{x(s)}$ is present. However, Wilson stated that "it is doubtful whether particulate matter would influence the oxidation process under natural loading conditions," perhaps suggesting the limited usefulness of his findings during water treatment.[55]

Wilson's study focused on geothite, an aged form of the freshly precipitated iron oxide, lepidocrocite, resulting from oxygenation of Fe(II).[55] Sung and Morgan[56] presented a similar study that focused on this "young" iron oxide form. These researchers reported that manganese has a strong affinity for the lepidocrocite (γ-FeOOH) surface, particularly at pH levels above 6.9 which is the zero point of charge (ZPC) for the oxide. Adsorption isotherms for Mn(II) onto the iron surface and data suggesting a catalyzed rate of oxidation in the presence of the iron surface were presented. Of particular interest was the kinetic model presented that found the surface rate constants for Mn(II) oxidation on the iron surface and the $MnO_{2(s)}$ surface to be the same order of magnitude.[56] It appears, however, that the authors made a faulty assumption in stating that the iron surface is not altered significantly with the surface oxidized species. One would expect that as Mn(II) is adsorbed and oxidized a $MnO_{x(s)}$ coating would develop with a high affinity for Mn(II) and catalytic effect in its oxidation. This may explain why the "iron" surface appeared to exhibit a similar surface rate constant to that of the $MnO_{2(s)}$ surface.

Davies and Morgan[57] studied the rate of Mn(II) oxidation on several different metal oxide surfaces with Mn(II) affinity ranking in the following order: lepidocrocite > geothite > silica > alumina. In this work it was assumed that a "bidentate complex" was the chemical interaction between Mn(II) and the iron oxides. In this type model, the Mn(II) ion is shared by two oxide surface sites. Again, results indicating the accelerated rate of Mn(II) oxidation in the presence of iron oxides were presented as well as two hypotheses as to why such a catalyzation effect is seen:

- A lower activation energy is required for electron transfer from Mn(II) to O_2; and

- Mn(II) oxidized by Fe(III) resulting in an oxidized Mn(III) and a reduced Fe(II); the Fe(II) is then rapidly oxidized back to Fe(III) by available oxygen

Note, however, that these authors propose a bidentate complex whereas Grossel et al.[52] had proposed a monodentate complex between Cu(II), another divalent cation, and geothite.

Another key point relating to surface chemistry was highlighted by Davies and Morgan[57] who stated that it is difficult to ascertain whether the surface (iron) or the modified surface (containing some $MnO_{x(s)}$) is responsible for the catalyzing effect unless the surface is in excess. This statement summarizes the difficulty in understanding the mechanism under study. Finally, the authors reminded future researchers that it is important to consider competition for surface sites brought about by ionic strength, [Mn(II)], [Cl^-], and specific surface areas of the oxides. A kinetic model of their findings was presented as well.

Research conducted at a full scale water treatment plant in England employing sludge blanket clarifiers indicated a similar phenomenon occurs under water treatment conditions.[59] In this system, Mn(II) adsorption onto the iron oxide surface present in the sludge blanket was observed to occur according to the Langmuir isotherm. The adsorption was noted to be enhanced and less sensitive to differences in pH as the concentration of the sorbent material (iron oxides) increased. The researchers observed that the sludge blanket assumed a darker color with time, implying $MnO_{x(s)}$ formation by oxidation with dissolved oxygen. They also noted that the sorbed Mn(II) (resulting in $MnO_{x(s)}$ formation) resulted in a surface that provided a greater sorptive capacity than the original "iron-only" surface. The study recommended that the system be analyzed using chlorine as the oxidant to provide more rapid oxidation of the Mn(II).

In other research conducted on these oxides under water treatment plant conditions, Stenkamp and Benjamin[53] observed the superiority of iron oxide coated sand media for filtration operations.

2. Manganese Oxides. Similar research has been conducted on the effect that manganese oxides may have on the scavenging of materials from natural waters.[11, 40, 60, 61] It is important to consider the adsorptive properties of these oxides as they can result as a product of Mn(II) adsorption onto iron oxides provided there is sufficient oxidant present.

As discussed previously, oftentimes the product of Mn(II) oxidation is a small, colloidal sized $MnO_{x(s)}$ particle that is difficult to remove from the water column. Posselt et al.,[33] discussed the often difficult coagulation of such particles and the need for stabilization by calcium or other divalent ions. However, of more importance for this work is the adsorptive and catalytic properties of manganese oxides studied by several researchers.[11, 40, 61] Probably the most well known work relating to properties of manganese oxides was presented by Morgan and Stumm.[40] They noted that the oxide surface served as an adsorption site for Mn(II) and served to catalyze the oxidation reaction. The zero point of charge of the colloidal manganese oxides studied during their work was 2.8 ± 0.3 pH units. It was noted that the adsorption of additional amounts of Mn(II) increased with increasing pH as the surface becomes more negatively charged. They used a Langmuir isotherm to describe the adsorption of Mn(II) onto the $MnO_{x(s)}$ surface. One key point made concerning the surface properties of the oxides was that flocculation tends to slow Mn(II) adsorption as diffusion, a slower step, occurs within the solid phase. Finally, at pH 7.5, the oxide had the capacity for 0.5 mol Mn(II) per mole of MnO_2 with very rapid adsorption rates.[40] Xyla et al.[60] reported that γ-$MnOOH_{(s)}$ (manganite) had $1/7^{th}$ the surface area of $MnO_{2(s)}$.

The adsorption of two divalent cations (cadmium and zinc) onto manganese oxides has also been studied.[61] However, researchers have reported that sorption of Mn(II) onto manganese oxides exceeds that of these metals.[11, 40] Posselt et al.[11] further studied the adsorptive properties of manganese oxides and developed the following conclusions:

- Adsorption decreased with increasing ionic strength as competitive adsorption increased;

- Mn(II) adsorption onto the oxide is greater than for any other ion studied; and
- Neutral or negatively charged particles not readily adsorbed[11]

These and other characteristics of the manganese oxide surface will be important in the understanding of the work to be presented.

G. Summary

Iron and manganese are commonly found in drinking water supplies due to natural processes. The chemistry of these metals is quite complex and can be controlled by any number of ions, the presence of organics, or reduction-oxidation conditions. This complexity can make it difficult to accurately predict the behavior of these metals amongst various oxidants.

Generally speaking Fe(II) can be easily oxidized by weaker oxidants (O_2 and HOCl) provided the Fe(II) has not formed complexes with organics, significant oxidant is present, and the pH is in the neutral to basic range. However, the same cannot be said for Mn(II) where oxidation normally requires the use of stronger oxidants ($KMnO_4$, ClO_2, O_3) to complete oxidation in a reasonable time frame. Alternative technologies such as oxide coated filter media have been developed; these technologies develop and utilize a $MnO_{x(s)}$ surface to catalyze Mn(II) oxidation. Having an oxidized surface present allows the use of weaker oxidants such as HOCl to oxidize the Mn(II) adsorbed on the $MnO_{x(s)}$ surface.

The ferric hydroxide/oxide surface has also been proven to have a catalyzing effect on Mn(II) adsorption and/or oxidation using similar oxidants. It is this interaction between the soluble Mn(II) and the oxidized Fe(III) surface that will be further investigated by this research. In addition, the ability of the oxidized Mn(IV) surface to overtake the Fe(III) surface in catalyzing Mn(II) adsorption and subsequent oxidation will be examined.

CHAPTER III

EXPERIMENTAL METHODS AND MATERIALS

The purpose of this chapter is to provide a complete description of the experimental setup and the laboratory methods used to collect the data to be presented. In cases where the laboratory method is more completely described in *Standard Methods,*[62] only a brief description is provided that highlights any alterations made to the original method.

A. Synthetic Water Makeup

For each experimental situation a synthetic water sample was prepared containing the following constituents (unless otherwise stated):

- 3 meq/L Ca^{++} (150 mg/L as $CaCO_3$)
- 3 meq/L HCO_3^- (150 mg/L as $CaCO_3$)
- 0.5 mg/L Mn(II)

The pH, HOCl dose, and ferrous iron (Fe(II)) concentrations were varied for each experiment to determine the role that each parameter may have in the adsorption/surface oxidation of Mn(II) onto the iron oxide surface. Stumm and Singer[50] cite an important difference between studies employing synthetic versus natural waters. Natural waters will contain possible catalysts or inhibitors that will affect the rate of reactions and phenomenon occurring. This fact should be considered when using the results of this research in "real-world" applications.

B. Glassware Preparation

All glassware used during these experiments was thoroughly cleaned to insure that the glassware would not be a source of metals being studied. Initially, each piece of glassware was cleaned using the following procedure:

1. Rinsed with hydroxylamine sulfate (HAS); removes oxidized metals from the surface of the glassware.
2. Rinsed with tap water, washed with soapy water, and thoroughly rinsed again with tap water.
3. Placed in a 10% nitric acid bath for at least 12 hours to ensure adequate time for ion exchange to occur.
4. Removal from the acid bath followed by three rinses with tap water and one rinse of distilled water.
5. Allowed to dry before use.

The glassware treated using this procedure included the reaction vessels (standard BOD bottles), stock solution containers, sample collection tubes, pipettes, and volumetric flasks used to prepare solutions. Following each experiment, the reaction vessels were immediately rinsed with tap water and steps 3-5 listed previously were repeated.

Several experiments were conducted at the start of the research to insure that the glassware preparation procedures were successful. Randomly selected reaction vessels were filled with Milli-Q water and allowed to stand for 24 hours after which samples were collected. The concentration of Mn(II) in the vessels tested was below the detection limit for the AA-S (results summarized in Table A-1); therefore, the acid washing procedures described were an effective means of ridding the system of unaccounted for manganese.

Next, it was desired to measure the chlorine demand of the Milli-Q water in the acid washed vessels for two reasons:

1. To ensure organic materials had been sufficiently cleaned from the glass surface; and
2. To help explain chlorine demand variability in future experimentation.

The amount of chlorine demand measured for time periods up to 1 day of detention time was found to be insignificant (see Table A-2). Thus, the chlorine demand of the Milli-Q

water and of the glass vessels should not be considered major sources of error during experimentation.

C. Preparation of the Reaction Stock Solutions

All water used to prepare each solution was deionized/distilled water which was further treated through the use of a Milli-Q water system (Millipore Corporation, Norwalk, CT) to ensure ion-free water with limited organic material present. In each case, a concentrated stock solution was prepared which was then diluted when the synthetic water was prepared. Preacidification of the Milli-Q water for the iron and manganese stock solutions was accomplished through the addition of reagent grade concentrated nitric acid (HNO_3). Such acidification minimized the potential for Mn(II) and Fe(II) oxidation in these stock solutions.

1. Manganese(II) Stock Preparation. The manganese stock solution used throughout these studies was prepared by adding reagent grade manganous sulfate monohydrate crystals ($MnSO_4 \cdot H_2O$; Fisher Scientific; Pittsburgh, PA) to preacidified (~ pH 2) Milli-Q water to obtain a concentration of 1 mg as Mn(II) per mL of solution. Because of the low pH conditions, manganese oxidation via molecular oxygen should proceed very slowly. The solution was kept in an air tight container, and the visual appearance and concentration of the solution was checked daily to insure no Mn(II) oxidation had occurred.

2. Ferrous Iron Stock Preparation. A ferrous iron stock solution was prepared in a similar fashion to the manganese solution. Ferrous iron sulfate heptahydrate crystals ($FeSO_4 \cdot 7H_2O$) were dissolved in preacidified (~ pH 2) Milli-Q water to obtain a stock solution concentration of 1 mg as Fe(II) per mL of solution. This solution was prepared weekly or bi-weekly to prevent loss of soluble iron via iron oxidation within the stock

solution. The concentration and visual appearance were checked daily so that iron oxide formation could be accurately determined.

Reagent grade American Chemical Society certified ferrous iron sulfate heptahydrate crystals with a 99%+ purity (Aldrich Chemical Company, Milwaukee, WI) was used for all experiments except for selected isotherm determinations. The impurity of the iron stock introduced background manganese (approximately 1.82×10^{-4} mg Mn per mg $FeSO_4 \cdot 7H_2O$ added) into solution which became more and more evident as the iron concentration was increased (see Table A-3). In cases where high concentrations of iron were desired (i.e. isotherm determinations at 200, 400, and 600 mg/L Fe(II)), a purified grade of iron sulfate heptahydrate (Alfa Aesar, Ward Hill, MA) was used to reduce the experimental error. In the development of isotherms, it is important to only account for the "outer" adsorptive capacity of a particular species, not that which may become entrapped within forming flocs during flocculation.

3. HOCl Stock Preparation. The chlorine stock solution was formed by diluting a stock solution of 5.25% sodium hypochlorite to a concentration of 1 mg as HOCl per mL of stock solution. This solution was stored in a sealed brown container under refrigeration to slow the degradation of the chlorine solution. The concentration of the stock solution was quantified by amperometric titration daily before use. The appropriate volume to be added to solution was then calculated based upon the measured stock concentration to insure proper chlorine dosing.

4. Hardness and Alkalinity Stock Preparation. The hardness and alkalinity stock solutions were each prepared at concentrations of 1 meq or 50 mg/L as $CaCO_3$ per mL of stock solution. The hardness solution was prepared using reagent grade calcium chloride crystals ($CaCl_2$) and sodium bicarbonate ($NaHCO_3$) was used for the alkalinity of the synthetic water. Again, Milli-Q water was used to dissolve these solids in separate containers. These stock solutions were bottled separately to prevent the possible

formation of $CaCO_{3(s)}$. The accuracy of the hardness stock ($CaCl_2$) was checked by measuring the [Ca^{++}] on a Perkin Elmer Atomic Adsorption Spectrophotometer Model 703 (AA-S).

D. pH Adjustment

The solution pH of the synthetic water samples was adjusted using nitric acid and sodium hydroxide solutions (1N), each prepared from concentrated reagent grade stock solutions. For fine adjustment of pH, dilutions of these solutions were prepared; however, care was taken to limit the amount of these solutions added to the synthetic water sample prepared to less than 0.1% by volume to minimize dilution effects. In addition, the pH was not allowed to increase more than 0.25 pH units above the target pH. This was done to minimize the potential for unnecessary chemical oxidation or precipitation. In all cases the initial pH of all test solutions was brought to within 0.10 pH units of the desired level.

E. Experimental Apparatus

1. Adsorption/Isotherm Studies. Sample solutions (500 mL each) under various pH and iron concentrations were used to determine the quantity of soluble Mn(II) that would adsorb onto iron oxide particles on a "mol Mn(II) sorbed per mol Fe(II) in solution" basis. The solution, maintained at a temperature of 10 ± 2°C using an ice water bath, was first buffered and adjusted to the desired pH, after which the calcium and iron were added to solution. The pH was again adjusted, and the solution aerated to complete the oxidation of the iron in solution. After 10-15 minutes of reaction time (measured by a stabilization in the solution pH since oxidation of Fe(II) produces acid), the aeration was halted, and an initial sample was withdrawn from the reaction vessel and acidified to provide an estimate of the Fe(III) concentration. Mn(II) was added to solution and allowed to gently mix with the iron precipitate. After 5 minutes, samples were collected to determine the amount of Mn(II) that had adsorbed to the iron particles. (The

determination of the 5 minute reaction time is discussed in the Results and Discussion Chapters of the paper.) One sample was filtered to determine the instantaneous soluble Mn(II) concentration after 5 minutes while the second was acidified to measure the initial Mn(II) in solution. All of the samples obtained by this procedure were filtered using the 0.45 μm syringe filters following the procedure outlined in Section F.1. Figure 5 shows a diagram of this experimental design.

The soluble iron in solution was oxidized prior to Mn(II) addition so that no Mn(II) ions would be incorporated within the forming iron flocs. The desire was to measure only the amount of Mn(II) adsorption onto the iron oxide surface, not the combined effects of flocculation. In addition, it was determined from several filtration experiments that the use of 0.45 μm syringe filters provided comparable results to the use of 30k ultrafiltration cells as little or no colloidal particles (less than 0.45 μm in size) were being produced. As stated earlier, it is important to account for the impurity of reagent grade iron sulfate heptahydrate and the levels of manganese its use can introduce into solution.

2. Mn(II) Removal Batch Studies. One key aspect of this research effort was to determine the kinetics of manganese adsorption/surface oxidation onto the freshly formed iron oxides in solution. For this reason it was necessary to have several reaction vessels available so that when a sample was taken at the desired time, it would not affect the results of subsequent samples collected. If a larger vessel was used and samples were withdrawn at set intervals, there is more of an opportunity to capture misrepresentative data points if the system is not thoroughly mixed. Also, the reactor(s) used must be sealed to prevent loss of CO_2 which could lead to an increase in solution pH.

For each experiment a 2L solution of synthetic water sample was prepared using Milli-Q water and the stock solutions previously discussed. In each case, the alkalinity and hardness solutions were added first followed by pH adjustment at or below the desired pH. Then, the desired soluble iron concentration was added to solution. The pH

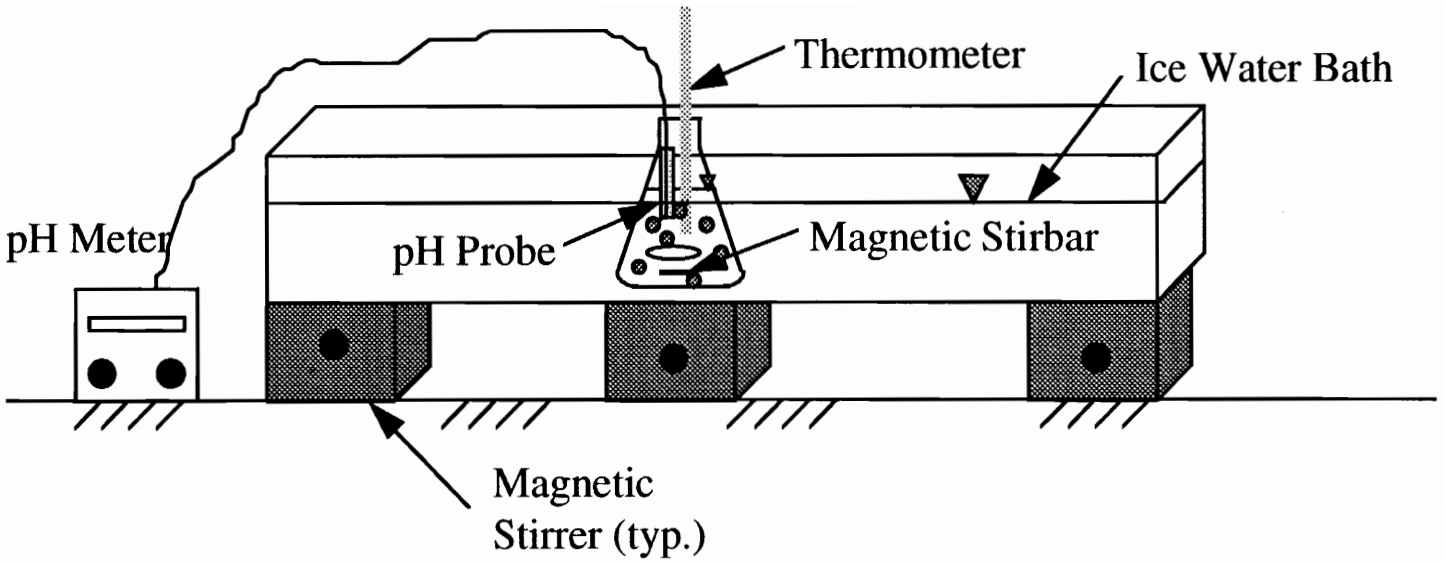

Figure 5: Schematic of Experimental Setup for Isotherm Studies

of the solution was again adjusted to the desired level and was allowed to mix for approximately five minutes to ensure complete iron oxidation via molecular oxygen dissolved in the water. Mn(II) was then added to solution at a dose of 0.5 mg/L and allowed to interact for five minutes with the iron solids present so that adsorption data could be collected. Finally, the dose of HOCl was added which represented the start of the reaction time "clock." The well mixed solution was carefully poured into six standard BOD bottles with care to limit the aeration of the sample and thus stripping of CO_2. A Teflon stirbar was placed in each bottle, and magnetic stirrers slowly mixed the samples. A schematic of this system is shown in Figure 6.

Samples were collected at the desired time by removing one of the six bottles from the water bath and measuring the pH and temperature of the solution within the vessel. Next, the sample was filtered using both a 0.45μm syringe filter and a 30k ultrafilter. The use of these size filters was an attempt to characterize the size of the particles formed, and the importance of size in the removal of Mn(II) from solution. A more detailed description of the filtration techniques is given in Section F. To simulate groundwater conditions, all of the experimental tests were conducted at 10 ± 2°C. To maintain the temperatures at this level, the reaction vessels were submerged in a cold water bath with a temperature of approximately 10°C. A refrigeration type unit was used to circulate an antifreeze-water mixture through tubing placed within the Plexiglas tank to maintain the bath at the desired temperature. In addition, the Milli-Q water used to prepare the synthetic water sample being tested was refrigerated to assist in the initial temperature adjustment of the solution.

Initially, the Mn(II) was added prior to the addition of the iron stock solution, but this resulted in a Mn(II) "sink" due to the possible entrapment of ions within the iron floc. Therefore, in later experiments, the Mn(II) was added after the iron was completely oxidized. This not only allowed for a better measurement of the change in Mn(II) in the system due to interactions with the iron oxide surface, but also permitted adsorption measurements for each of the various experimental conditions.

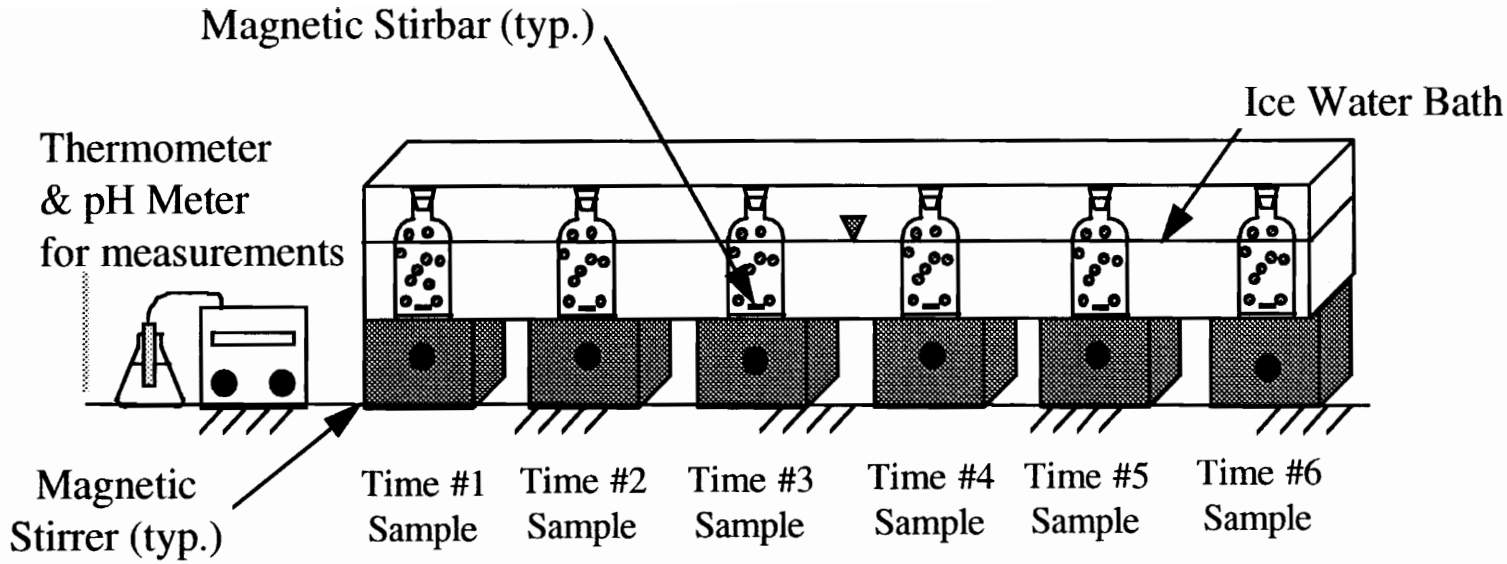

Figure 6: Schematic of Experimental Setup for Catalyzed Mn(II) Oxidation in the Presence of Iron Oxides (Batch Study).

3. $MnO_{x(s)}$ Adsorption Batch Studies. This experiment was conducted in an attempt to understand the mechanism by which the adsorptive/surface oxidation reactions continue over long periods of time. Once the initial iron oxide surface has been utilized, it was hypothesized that a manganese oxide surface may indeed serve as the main mechanism in continuing the catalyzed oxidation of soluble manganese. Therefore, this experiment was intended to serve two purposes:

1. To measure the adsorptive capacity of freshly precipitated $MnO_{x(s)}$.
2. To determine if the rate of Mn(II) removal from solution for an equivalent amount of formed manganese oxides based upon Mn(II) adsorption on the iron oxide surface from adsorption studies is similar to that noted in batch studies.

Again, a 2L sample volume was prepared similar to that outlined in the batch study procedure, but preformed manganese oxides were added instead of iron stock solution. The $MnO_{x(s)}$ solids were formed by slowly adding HOCl into a Mn(II) solution to prevent the formation of permanganate. The HOCl was added at 1.25 times the stoichiometric dose requirements based upon the approximate Mn(II) solution concentration to insure that all the Mn(II) in solution was indeed oxidized and not simply adsorbed onto the $MnO_{x(s)}$ surface. To further test the completeness of oxidation, a stock sample was filtered through a 30k ultrafilter to measure the soluble manganese concentration and the chlorine residual. The soluble manganese concentration was below detection limits, and sufficient excess chlorine was present to complete the oxidation of any sorbed Mn(II). A solid extraction using HAS was performed on the stock solution to obtain an estimate for the stock concentration of $MnO_{x(s)}$.

The adsorption data determined from the aforementioned adsorption studies (Section E.1.) was used to estimate the amount of $MnO_{x(s)}$ to be added to solution. For example, to compare the rate of removal via $MnO_{x(s)}$ versus a given iron concentration, the quantity of Mn(II) adsorbed for that iron concentration was obtained from the isotherm results. Based upon the reaction for Mn(II) oxidation to $MnO_{2(s)}$, the equivalent

amount of $MnO_{x(s)}$ surface was calculated and added to solution. In theory, this method is a conservative estimate for the amount of $MnO_{x(s)}$ surface available for adsorption as the preformed particles should have a greater surface area than those hypothesized to have formed on the outside of the iron oxide particle.

Samples were collected similarly to the procedure described in the previous section as one of the six bottles was removed from the water bath at the desired time and the pH and temperature of the solution within the vessel were measured. The sample was filtered using both a 0.45μm syringe filter and a 30k ultrafilter; the use of the 30k ultrafilters served to capture the possibly colloidal preformed $MnO_{x(s)}$ particles that may still reside in solution. The experimental setup is identical to that depicted in Figure 5.

4. Iron Oxide Slurry Reactor System. Three bench-scale slurry-type reactors were constructed to simulate a single-stage flocculation basin with a settling zone at a full-scale water treatment facility. Each was designed with a baffling system to separate the mixing and settling zones within the reactor to promote the flocculation and subsequent settling of the particles formed. The reactors each had a volume of approximately 2.3 L and were intended to have internal recycle of solids as they settled from solution. Each basin was equipped with a stirring paddle (25 rpm) which mixed the incoming constituents throughout the mixing zone of the reactor. The reactors were designed to operate in parallel as each had an effluent line that drained to a sink. The effluent line served as the sampling point for evaluating effluent quality and treatment efficiency.

It was desired to use the same synthetic water makeup for the operation of the reactors as had been used for the batch studies. Because of the limited pumping capabilities and the size of the reactors, large volumes of stock solutions were required to attain the desired detention times. In addition, because of the possible interactions that may occur between the constituents of the water makeup (i.e. Ca^{++} and alkalinity stock), the stock solutions were prepared individually to limit reactivity between ions. Therefore, a mixing unit was required to mix the solution prior to dosing each reactor. Separate

stock solutions for Mn(II), HOCl, and alkalinity were combined in the mixer with chilled tap water from a constant head tank. Three separate feed lines (one going to each reactor) were used to add this portion of the solution makeup to each reactor. A separate stock solution containing Ca^{++} (which could react with the alkalinity) and Fe(II) (which is extremely reactive with chlorine) was added separately to each reactor for the reasons cited. The iron and calcium stock solution as well as the Mn(II) stock solution were slightly acidified to pH 2.5-3 to retard the oxidation of these reduced species prior to dosing. The level of acidification was determined by titration using 0.02N sulfuric acid. A schematic of the reactor set-up is shown in Figure 7.

The temperature for these experiments was adjusted by cooling the influent tap water in the constant head tank prior to it being fed into the mixing unit. In addition, the reactors were submerged in an ice water bath throughout the experiments. Unfortunately, the temperature could not be maintained at the desired level used during other experimental studies, $10 \pm 2°C$. The actual temperatures of experimentation, 13-20°C should speed the interactions between the experimental constituents and increase the rates of reaction observed when compared to those of the batch studies conducted.

The stock solution concentrations for these constituents were adjusted as necessary to account for changes in detention time. The tap water flow was also adjusted as necessary for changes in detention time as the pumps used could only pump at a constant rate. Therefore as the detention time changed, the tap water flow was increased for shorter detention times or decreased for longer detention times to balance the volume of liquid entering and leaving the mixer. Overall, the desired water makeup follows that described in Section A with a soluble iron concentration of 2 mg/L. The chlorine dose was varied throughout the experiments to determine its importance in the reactions.

Several different sampling schemes were used to study the state and effectiveness of the continuous flow slurry systems. Effluent samples were collected periodically to study the effluent quality with frequent sampling (once every thirty minutes for at least two detention times) occurring whenever a system parameter was altered. The main focus of this sampling was to note changes in the soluble effluent manganese

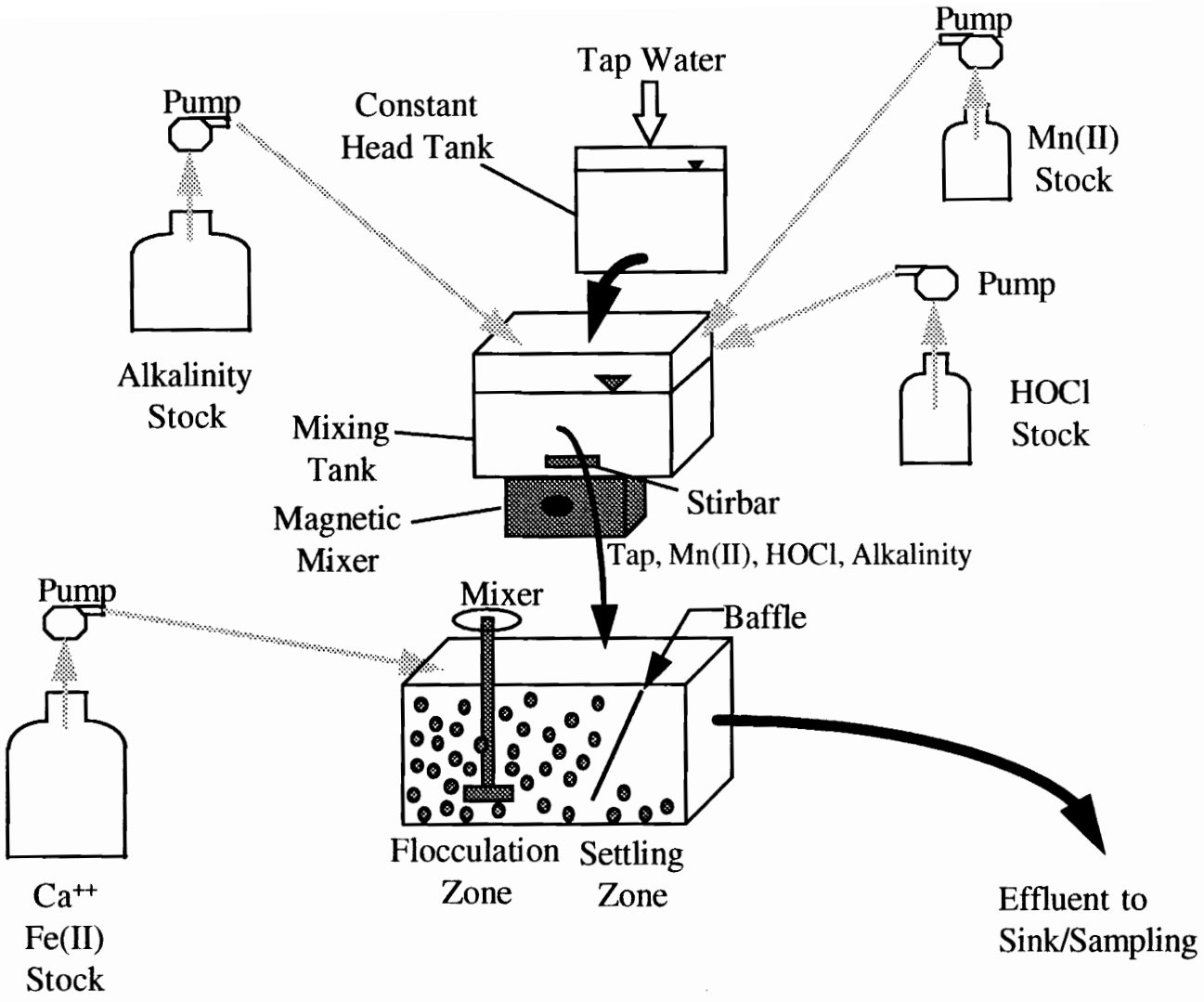

Figure 7: Schematic of Iron Oxide Slurry Reactor System

concentration; therefore, these samples were all filtered using 0.45μm filters. However, the loss of solids in the effluent was a key parameter to consider; thus, some effluent samples underwent acid digestion (no filtration) to measure the total iron and manganese in the effluent.

Samples were collected from each reactor and digested with acid as well to measure the total iron and manganese solids concentrations in the mixing zone of the reactor. An additional means of measuring the solids concentration within each reactor was the use of a standard suspended solids test. To insure that the reactors were being properly dosed, samples were taken from both the mixer (see Figure 7) and the influent lines and analyzed for Mn(II), Fe(II), and HOCl. Finally, chlorine samples were obtained from the mixer to quantify the actual chlorine dose entering the reactors. Residual chlorine from each reactor was also determined by filtering the effluent and measuring the free chlorine in solution.

F. Collection of Samples

Samples were collected from each of the experimental setups as previously described. Each sample was then filtered using one or both of the methods described below. Immediately following the filtration of each sample, two drops of concentrated nitric acid were added to the filtrate to prevent further reactions from occurring. The samples were agitated using a vortex mixer to ensure consistent solution characteristics. The procedures followed for each of these filter types are described in more detail below.

1. Syringe Filter Procedures (0.45μm). A portion of the collected sample was poured into a clean, dry 150 mL beaker. A 25mm diameter 0.45μm filter (Gelman Science, Ann Arbor, MI) was placed in the filter chamber and approximately 10 mL of Milli-Q water were passed through the filter to rinse the membrane. The syringe was filled and rinsed once with the sample to reduce likelihood of cross-contamination. A 12 mL sample was drawn into the syringe and was filtered to obtain the sample for this

reaction time. The first 2 mL of the filtrate were discarded as dilution was a concern from the residual Milli-Q water which may reside on the membrane following the rinse procedure.

2. 30k Ultrafiltration Procedures. The ultrafiltration equipment used was manufactured by Amicon (Model # 8200), and all manufacturers' specifications were followed during these experiments. The 30k filters (Amicon Diaflow Ultrafilters YM30 Membranes; Beverly, MA) were stored in the filtration chamber when not in use, soaking in a slightly acidic distilled-deionized water solution. A portion of this solution was passed through the membrane and the remainder discarded from the chamber when a sample was to be filtered. The sample to be analyzed was added to the chamber, and the solution was stirred by a magnetic stirrer and pressurized with nitrogen gas at 20 psig. The initial 10 mL of filtrate was discarded as residual amounts of the previously filtered solution occupied the filtrate effluent tube. Two 10 mL samples were then collected immediately to prevent buildup of iron particles within the membrane prior to sample collection. This could be a source of error as Mn(II) in solution that had not previously sorbed to the iron surface might do so within the filter membrane. The membrane was cleaned after each use by rinsing with pressurized distilled water to dislodge any particles trapped within the filter membrane. Again, a slightly acidic distilled-deionized water solution was added to the filtration chamber for membrane storage.

Manufacturer specifications recommend that the filters be operated at 55 psig for filter operations so that the permeability of the membrane may be constantly monitored. As previously stated the solutions were filtered at 20 psig; this lower pressure was intended to insure that the particles greater than the pore size would be retained. However, parallel tests were conducted at applied pressure of 20 and 55 psig to determine if the pressure affected the results. From the data collected, it did not appear as though the higher pressure produced results different from the 20 psig results. Also, neither

pressure condition resulted in Mn(II) concentrations different from the data collected using the syringe filters (0.45 μm.).

G. Measurement Techniques for Data Collection

1. pH and Temperature. The pH of all solutions was measured using a Fisher Accumet 710 pH meter (Fisher Scientific Co.; Pittsburgh, PA). The meter was calibrated daily using standard pH 4 and pH 7 buffer solutions refrigerated to 10°C. All temperature readings were taken using a standard alcohol thermometer (Fisher Scientific Co.; Pittsburgh, PA).

2. HOCl Residual. Monitoring of the HOCl stock solution and the residual HOCl in the test solutions was measured via amperometric titration with phenylarsine oxide (PAO) as outlined in *Standard Methods*[62] (Method # 4500-Cl D). This titration procedure requires a 200 mL sample volume; however, because of the limited amount of sample remaining following filtration procedures, a 1:1 dilution was made using Milli-Q water. To ensure the dilution would not affect the results a sample was tested using both a dilute and a full strength sample, and comparable results were obtained. The 100 mL sample volume was filtered using a 0.45μm filter to remove any oxidized particles from solution that may interfere with the titration results. To the 200 mL diluted sample, approximately 1 mL of pH 7 phosphate buffer and one gram of potassium iodide (KI) were added. The titration was then performed using a Fisher Scientific Titration Controller Model # 450 (Fisher Scientific Co.; Pittsburgh, PA) by the addition of standard 0.0054N PAO.

3. Soluble Metals Concentration. Metals analyses were performed using a Perkin Elmer Atomic Adsorption Spectrophotometer Model 703 (Perkin Elmer, Norwalk, CT). All tests were performed using the recommended settings of the manufacturer for wavelength, lamp current, etc. A detection limit test as outlined in the Perkin Elmer

Instrument Manual[63] was conducted on several occasions to determine the accuracy, reproducibility, and detection limit of the equipment used. A summary of the results from this procedure is outlined in Appendix B as well as a summary of the operating parameters used during analysis.

4. Suspended Solids Concentration. The determination of suspended solids followed the procedure outlined in *Standard Methods*[62] (Method # 2540 D.). Glass-fiber filters were prepared by passing three 20 mL aliquots of distilled water through each filter. The filters were then stored for at least one hour prior to use in a 105°C oven to evaporate any water bound to the filter. Before use, the filters were stored in a desiccator to bring them to room temperature, and subsequently weighed using a standard laboratory scale. The sample for which solids data was desired was filtered using a vacuum pump with approximately 10 pounds of applied pressure differential. Distilled water was used to rinse the sides of the filtration cone to insure all solids were captured. The volume of sample filtered was recorded, and the filter was again placed in the 105°C oven for a minimum of one hour. Again the filter was brought to room temperature in a desiccator prior to being weighed for analysis.

5. Acid Digestion of Oxidized Solids. For several experiments, the concentration of iron in solution was desired to aid in the understanding of the phenomenon under study. In most cases the iron in solution was in a solid, oxidized form which forced the development of a digestion technique to solubilize the metal ions so that AA-S could be used for concentration determination. For lower concentrations of oxidized iron, several drops of concentrated nitric acid were used for digestion, and very little dilution was noted. However, for higher concentrations of iron, concentrated hydrochloric acid was used as iron can bind with the chloride introduced as well as be solubilized by the effects of acidification. This phenomenon was unknown for earlier experiments, as its use can reduce the necessary volume of acid required significantly (reducing the dilution effects).

In cases where large amounts of acid were required, the volume added was recorded, and the dilution effects accounted for by calculation. A similar procedure was utilized to measure the quantity of manganese solids in solution as well.

CHAPTER IV
RESULTS

The experimental data collected to satisfy the research objectives will be summarized in this chapter. The order of presentation will generally follow the order the data were collected as each experiment served as a "building block" for future experiments. The intent of these studies was to explain the possible interaction that occurred between the iron oxide solids and soluble manganese at the groundwater treatment facility (field data summarized in Table 1). The experimentation was designed to study each of the possible removal mechanisms in detail to explain the observed phenomenon. Additional experimentation was conducted to develop a continuous flow system, and to cite key system parameters for the design of such a system to provide a means of more effective iron and manganese removal. All data presented in this chapter are summarized in tabular format in Appendix A. A discussion of the data presented here can be found in Chapter V.

One key note concerning the experiments conducted is the type of iron stock used. As noted in Chapter III, when larger concentrations of Fe(II) were added to solution, increasing quantities of Mn(II) were introduced into solution as well. This explains the increased amount of Mn(II) noted at time zero of the experiment(s). A summary of the impurity of the iron stock used is included in tabular format (Table A-3) in Appendix A. By using this iron stock, it is impossible to decipher whether the initial Mn(II) measured is removed by entrapment (co-precipitation) within forming flocs or by the other means to be studied during the experimentation. This should be considered when reviewing the results presented.

A. Experimental Setup

Initial experimentation was undertaken to define a set of controlled experimental conditions under which the enhanced oxidation of soluble manganese in the presence of

iron oxides and HOCl could be observed without interference from other removal mechanisms. Several experiments were first conducted to study other possible removal mechanisms for Mn(II) that could be responsible for the observed results. These mechanisms were hypothesized to include:

- Formation of $MnCO_{3\,(s)}$
- Co-precipitation with/Adsorption onto $CaCO_{3\,(s)}$
- Solution phase oxidation of Mn(II) by HOCl (no Fe(III) solids present)
- Adsorption onto iron oxides

These tests were used to determine appropriate lengths of experimentation at various pH conditions. Also, as previously mentioned, the results were used to set future experimental conditions such that any of these mechanisms would not be responsible for manganese "sinks" from the system as the investigation of enhanced oxidation of soluble manganese in the presence of iron oxides and HOCl was undertaken.

B. Studies of Possible Mn(II) Removal Mechanisms

1. Formation of $MnCO_{3\,(s)}$ and Co-precipitation with/Adsorption onto $CaCO_{3\,(s)}$. These two mechanisms were analyzed simultaneously as they occur under similar pH and solution conditions. For the experimental conditions outlined in Chapter III, the solution makeup is saturated with respect to both $MnCO_{3\,(s)}$ and $CaCO_{3\,(s)}$ at pH 9. (Solubility product calculations confirming this are included in Appendix C.) In order to account for the possible removal of Mn(II) at this solution pH, the Mn(II) concentration in solution was measured over time. The results shown in Figure 8 indicate that Mn(II) was indeed removed by one or both of these phenomena. Thus, the white chemical precipitate observed during experimentation could have been $MnCO_{3(s)}$ or $CaCO_{3(s)}$ or a combination of the two carbonate species.

Measurements of the Ca^{2+} concentration were taken which indicated that at least a portion of the precipitate was $CaCO_{3\,(s)}$; however, it was desired to determine if $MnCO_{3\,(s)}$ precipitation was occurring as well, as predicted by the solubility product of the solid. Figure 9 compares the results from the previous experiments with data obtained by

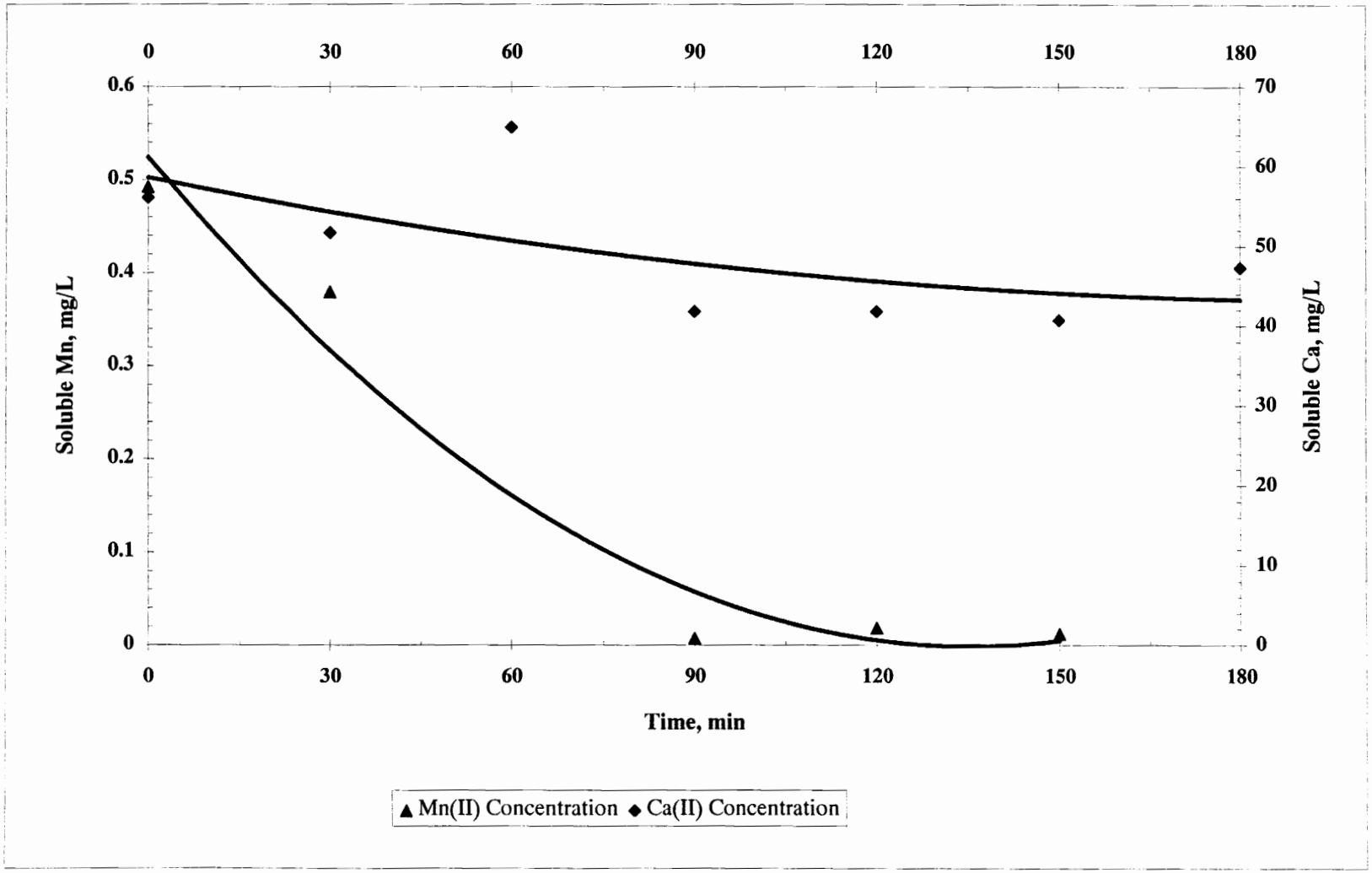

Figure 8: Preliminary Studies to Determine $MnCO_{3\,(s)}$ Formation Potential and Mn(II) Removal via Co-precipitation or Adsorption on $CaCO_{3(s)}$. Experimental Conditions: pH = 9, $[Ca^{+2}]$ = 3 meq/L, $[HCO_3^-]$ = 3 meq/L, $[Mn(II)]_O$ = 0.50 mg/L, Temperature 10°C.

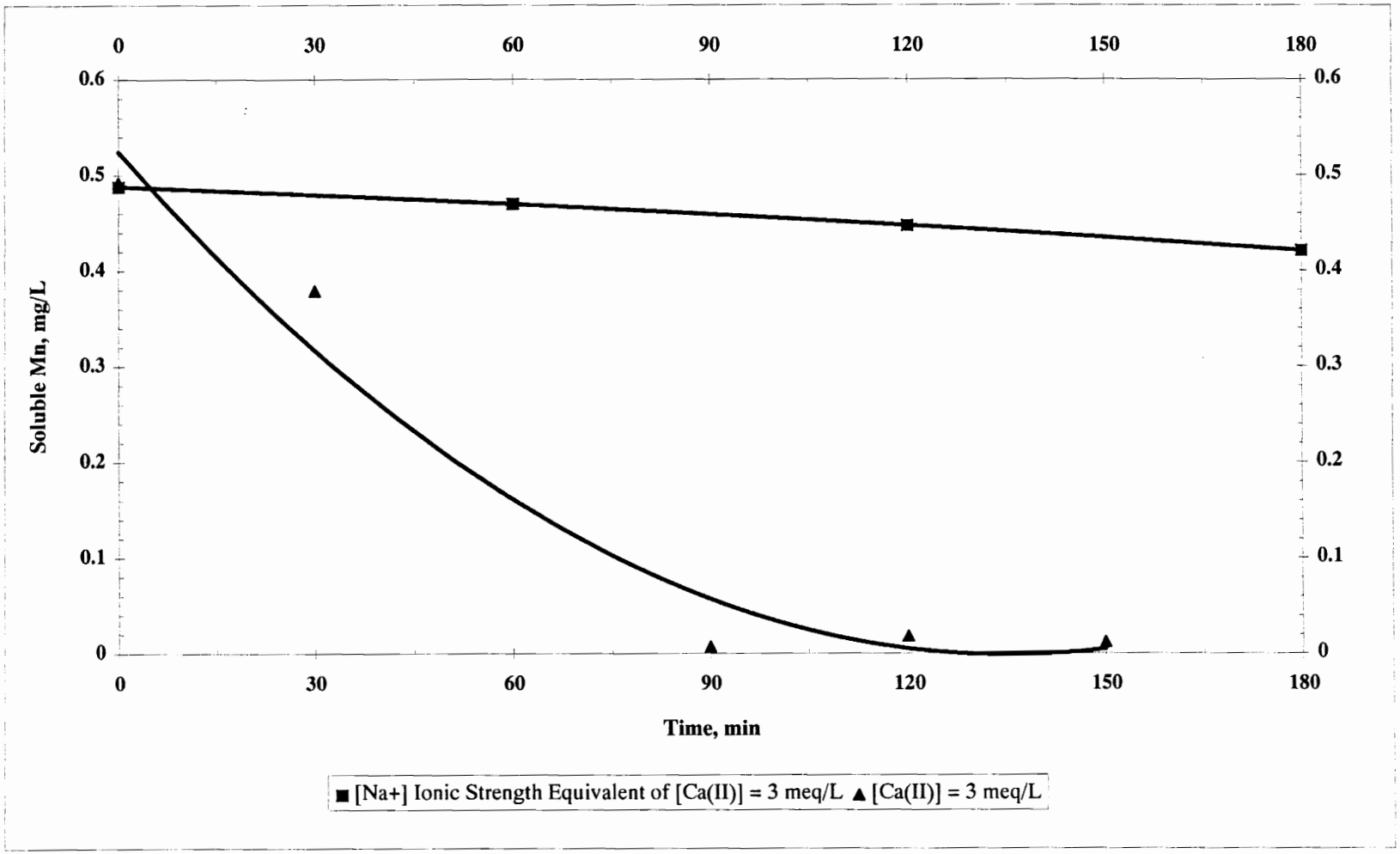

Figure 9: Preliminary Studies to Determine Role $CaCO_{3\,(s)}$ Formation has on Mn(II) Removal via Adsorption or Co-precipitation. Experimental Conditions: pH = 9, $[Ca^{+2}]$ = 3 meq/L or $[Na^{+}]$ ionic strength equivalent, $[HCO_3^{-}]$ = 3 meq/L, $[Mn(II)]_O$ = 0.50 mg/L, Temperature 10°C.

replacing $CaCl_2$ in the solution make-up with an ionic strength equivalent of NaCl, again at pH 9. The reduction in Mn(II) is minor compared to that when Ca^{2+} was in solution indicating that the majority of the Mn(II) removed in the previous experiment was a result of either adsorption onto $CaCO_{3(s)}$ or some other form of co-precipitation with Ca^{++} and CO_3^{-2}; however a small portion of the Mn(II) removed was due to the formation of $MnCO_{3\,(s)}$.

Similar experimentation was conducted at pH 8 to confirm the theoretical calculations for species' solubility which indicated that neither $MnCO_{3\,(s)}$ or $CaCO_{3\,(s)}$ is capable of forming at this solution pH. The results for this experiment, shown graphically in Figure 10, confirmed that no significant formation of either solid species occurred; thus negligible Mn(II) reductions were noted. The data for these studies is summarized in Appendix A in Tables A4-A8.

2. Solution Phase Oxidation. Solution phase oxidation was defined for this study to mean: "any oxidation that occurs in solution between a metal ion species not in contact with any surface and an available oxidant in solution." In most cases, this term will apply to Mn(II) oxidation occurring with only HOCl and the background levels of alkalinity and hardness in solution. Studies were undertaken to assess the rate and quantity of solution phase oxidation of Mn(II) via HOCl at solution pH of 7 and 8; the results of these experiments are shown in Figure 11. The amount of oxidation that occurs is negligible over the time period studied indicating that this mechanism plays a minor role in Mn(II) removal at these pH conditions. The slow oxidation kinetics for Mn(II) oxidation via HOCl at this pH as well as the reduced temperatures used in these studies help explain the depressed amount of observed oxidation.

3. Adsorption of Mn(II) onto Freshly Precipitated Iron Oxides. At most groundwater treatment facilities, any soluble iron is oxidized rapidly upon aeration resulting in the formation of iron oxides in solution with the unreacted manganese. This provides yet

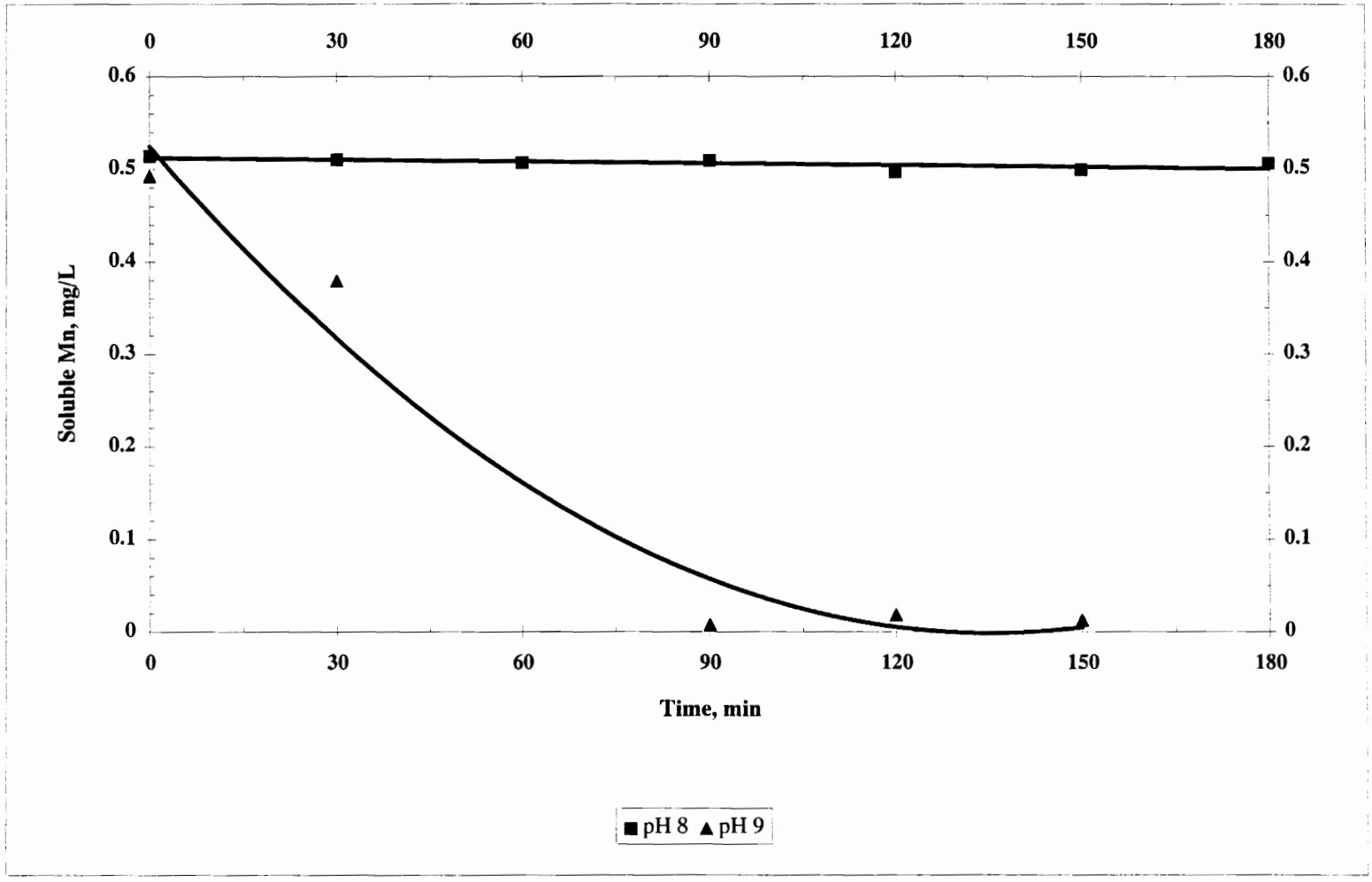

Figure 10: Preliminary Studies to Determine $MnCO_{3\,(s)}$ Formation Potential and Mn(II) Removal via $CaCO_{3\,(s)}$ Adsorption or Co-precipitation. Experimental Conditions: pH = 8 & 9, $[Ca^{+2}]$ = 3 meq/L, $[HCO_3^-]$ = 3 meq/L, $[Mn(II)]_O$ = 0.50 mg/L, Temperature 10°C.

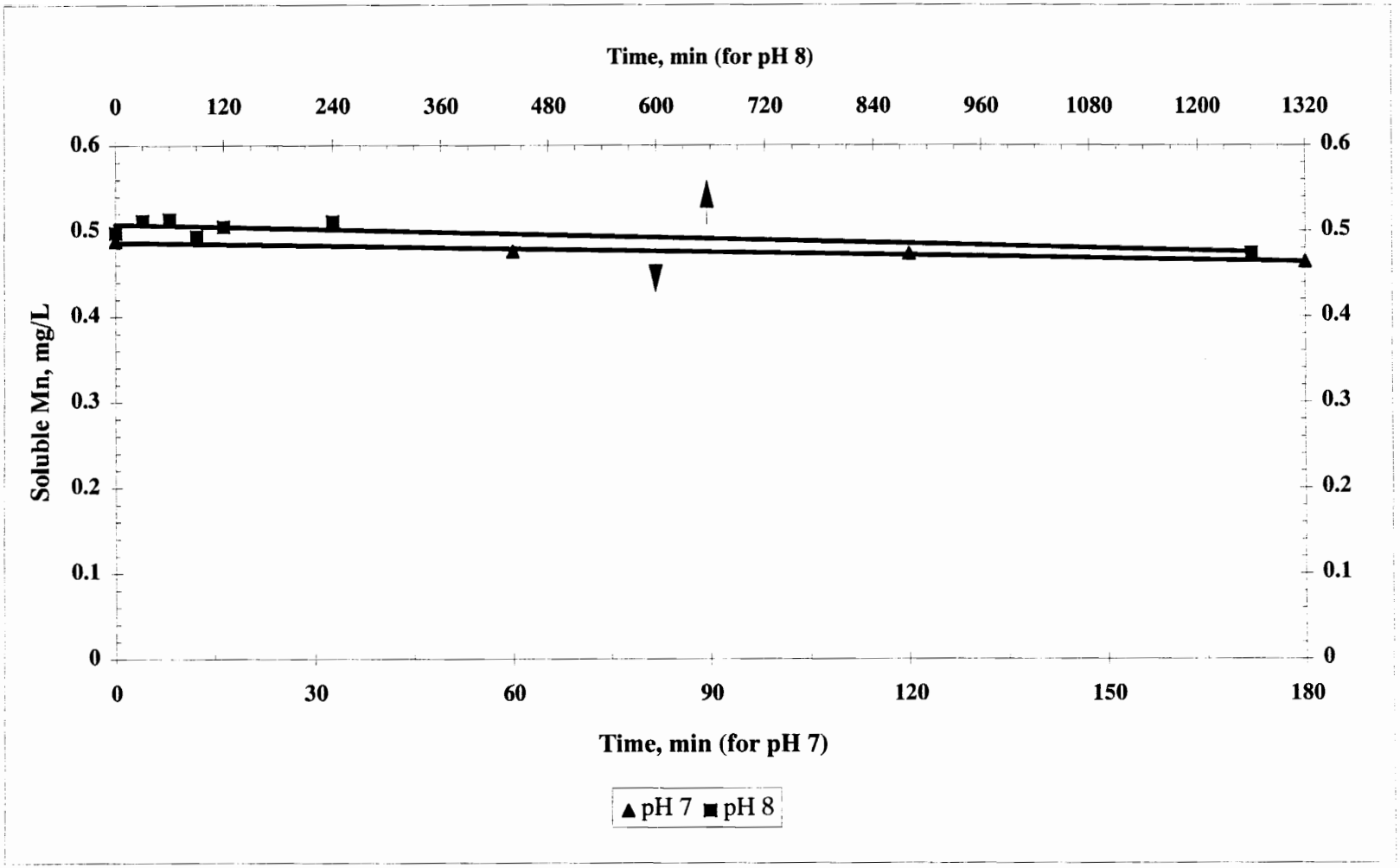

Figure 11: Solution Phase Oxidation Via HOCl. $[Ca^{+2}]$ = 3 meq/L, $[HCO_3^-]$ = 3 meq/L, $[Mn(II)]_O$ = 0.50 mg/L, [HOCl] = 2 mg/L, Temperature 10°C.

another possible means of Mn(II) removal- adsorption of Mn(II) onto freshly precipitated iron oxides. Before adsorption studies could be performed, the time required for such a phenomenon to occur was determined. Previous research[2] had indicated that a 5-minute contact time was sufficient for adsorption. For this experimentation, adsorption times of 5 minutes were used to allow for an equilibrium to develop between the iron oxides and Mn(II) in solution.

Adsorption studies were conducted at pH 7 and 8 to develop isotherms for Mn(II) sorption onto newly formed iron oxides. These data are plotted on a Cartesian coordinate system in Figure 12. The studies indicated that the adsorptive capacity of iron oxides for Mn(II) is quite small, and thus the role this mechanism, like solution phase oxidation, plays in Mn(II) removal is relatively minor and is certainly not the dominant mechanism. This observation holds true only over the range of iron oxide concentrations studied to develop the isotherm data. However, as expected, the adsorption capacity is greater at pH 8 as the iron oxide surface carries a more negative surface charge.

The data were also analyzed using Langmuirian isotherm theory as shown in Figure 13. At an equilibrium Mn(II) concentration of 0.50 mg/L, which represents the level of influent soluble manganese used throughout these studies, the maximum adsorptive capacity determined at pH 8 was 0.005 mg Mn(II)/mg Fe(III). Due to the spread of the data a best fit line could not be drawn for the data collected at pH 7 conditions for both Figures 12 and 13. Numerous attempts were made to collect more accurate isotherm data at this pH condition, but all attempts were unsuccessful as the sorbed quantities of manganese were quite small and difficult to measure.

Adsorption capacities would be expected to be even greater at higher pH conditions, however, because it has been shown that other mechanisms may dominate Mn(II) removal at higher pH values under the experimental conditions being utilized, it would be difficult to determine the role adsorption alone may have in Mn(II) removal. Therefore, the adsorption studies were only conducted to a maximum solution pH of 8 standard units.

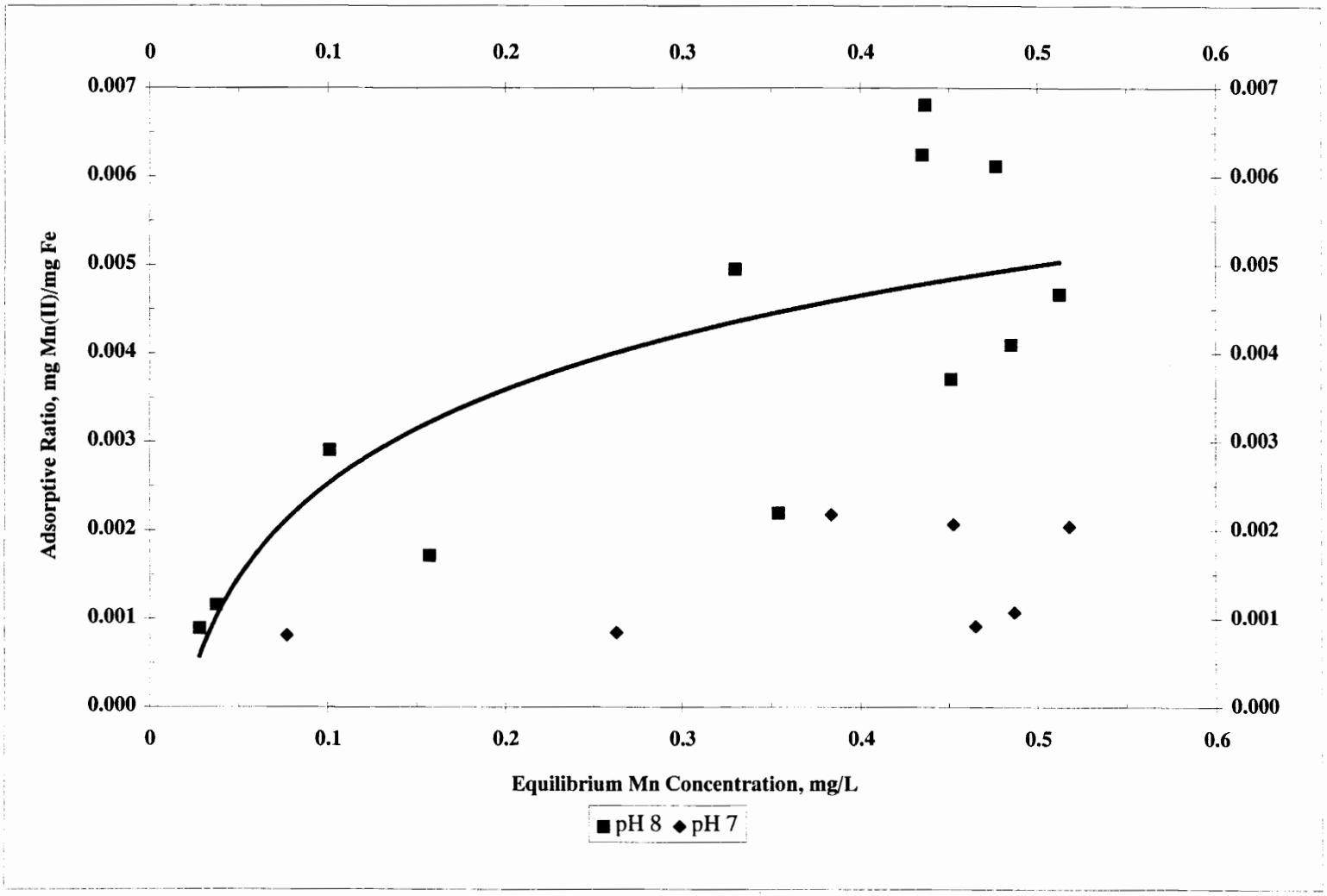

Figure 12: Cartesian Plot of Adsorption of Mn(II) onto Fe(III) oxides; Experimental Conditions: pH = 7 and 8, $[Ca^{+2}]$ = 3 meq/L, $[HCO_3^-]$ = 3 meq/L, $[Mn(II)]_o$ = 0.50 mg/L, Temperature 10°C.

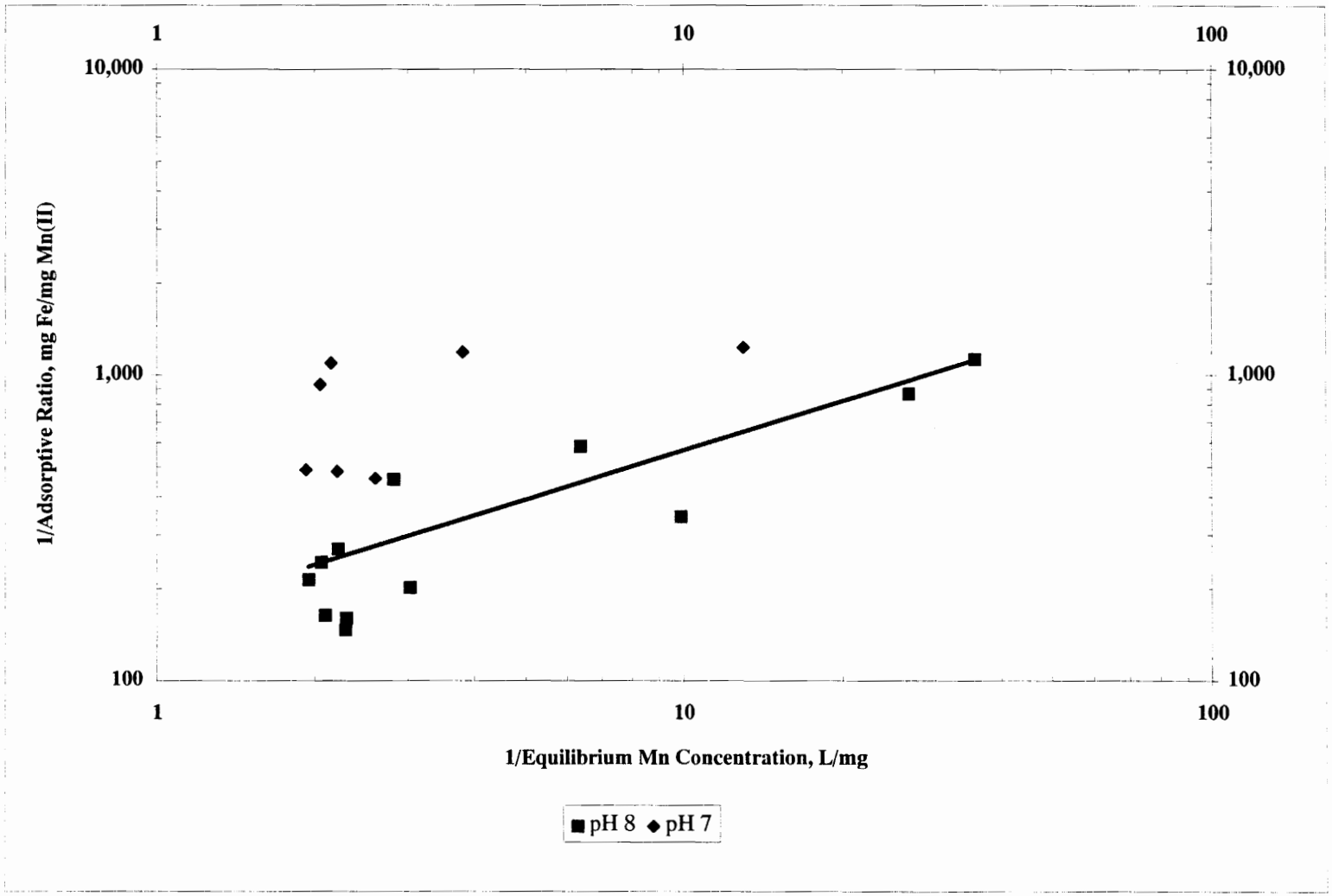

Figure 13: Langmuir Isotherm Plot of Adsorption of Mn(II) onto Fe(III) oxides; Experimental Conditions: pH = 7 and 8, $[Ca^{+2}]$ = 3 meq/L, $[HCO_3^-]$ = 3 meq/L, $[Mn(II)]_O$ = 0.50 mg/L, Temperature 10°C.

One issue noted during experimentation was the elevated levels of manganese introduced into solution as higher concentrations of iron oxides were used. This was explained by the impurity of the iron stock solution as the purity of the ferrous iron sulfate heptahydrate crystals used during experimentation was only 99%. This introduction of manganese made the adsorption studies more challenging and also allowed for the enmeshment of soluble manganese into the iron oxide flocs as they formed. For this reason, the adsorption studies presented previously may indicate greater quantities of Mn(II) were sorbed than would normally be observed.

To investigate this issue further, a purified grade (99.999%) of ferrous iron sulfate heptahydrate crystals ($FeSO_4 \cdot 7H_2O$) was obtained and adsorption studies were repeated. The results of these studies are summarized in Figure 14 and indicate that the adsorption is slightly lower than that observed using the standard iron stock solution. Adsorption capacities were determined to be 0.0001 and 0.0016 mg Mn/mg Fe(III) for pH 7 and 8, respectively for an equilibrium Mn(II) concentration of 0.35 mg/L.

C. Mn(II) Removal via Surface Catalyzed Oxidation of Manganese with Iron Oxides

In the previous adsorption experiments the reaction vessels were free of oxidants with the exception of dissolved oxygen which has little effect on soluble manganese as indicated by the field data previously presented[1]. Thus far in the experimentation, no mechanism alone has proven to be capable of the magnitude of Mn(II) removal observed in the field studies. The next set of experiments were performed to study the hypothesis that the iron surface (Fe(III)) catalyzed the reaction between Mn(II) and HOCl. This was believed to be a pseudo-combination of two mechanisms: adsorption and solution phase (chemical) oxidation.

Initially, these experiments were conducted under similar conditions to those seen at typical groundwater treatment facilities where the iron is allowed to oxidize with Mn(II) present in solution. However, as indicated in Figure 15, this resulted in greater removal of Mn(II) from solution possibly due to entrapment of the Mn(II) ions within the

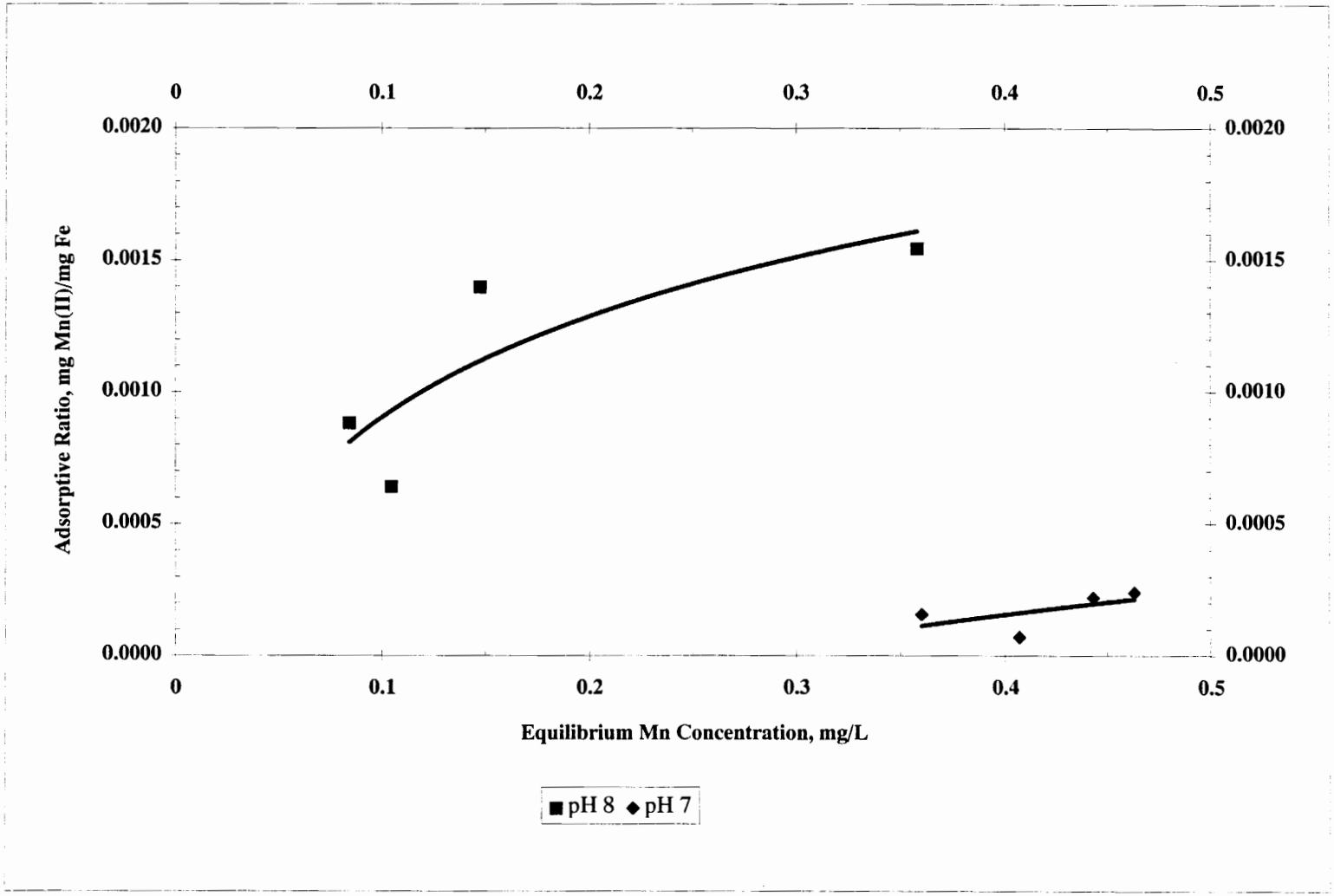

Figure 14: Cartesian Plot of Adsorption of Mn(II) onto Fe(III) oxides (purified iron stock); Experimental Conditions: pH = 7 and 8, $[Ca^{+2}]$ = 3 meq/L, $[HCO_3^-]$ = 3 meq/L, $[Mn(II)]_O$ = 0.50 mg/L, Temperature 10°C.

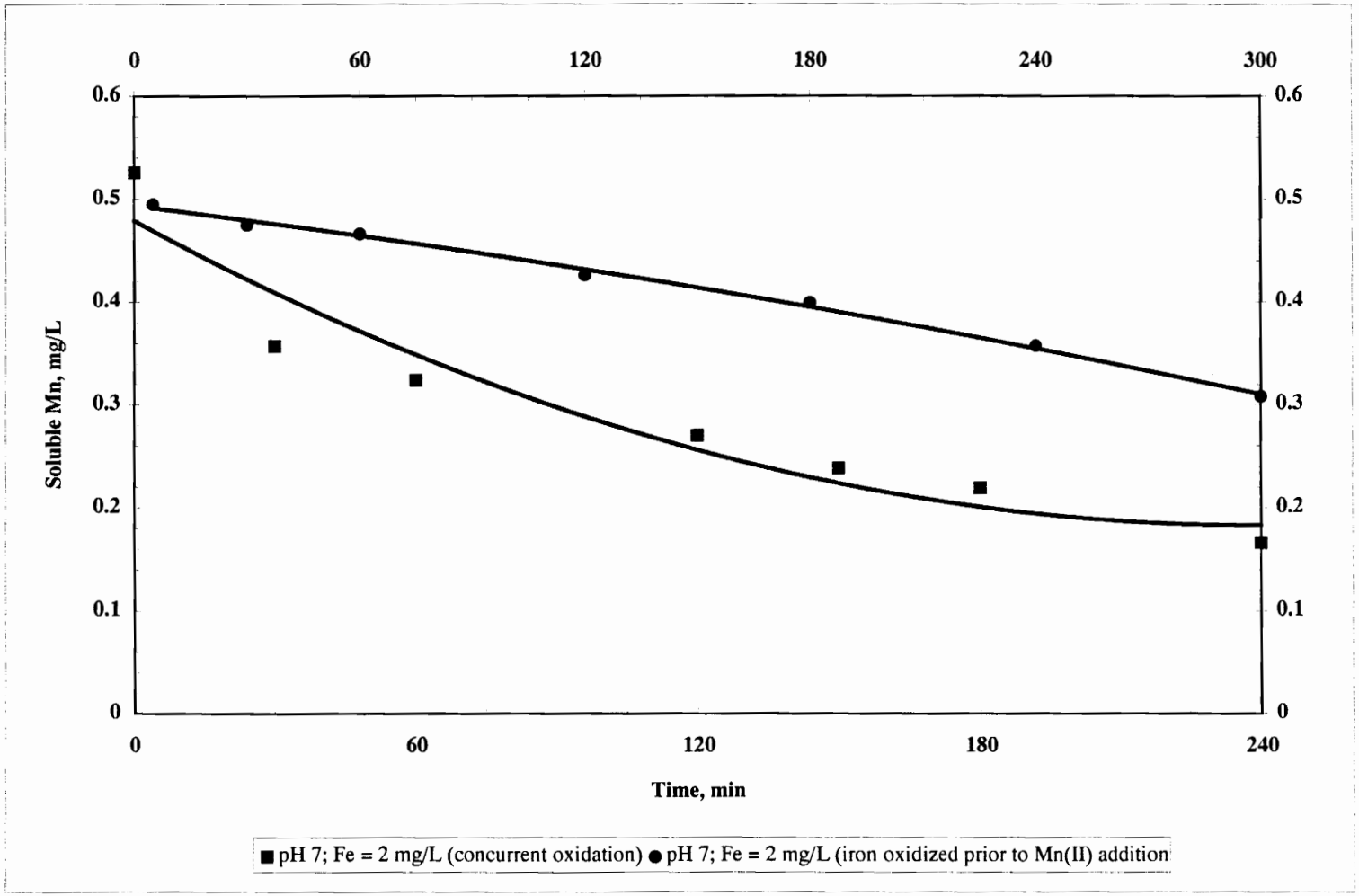

Figure 15: Surface Catalyzed Oxidation of Mn(II) onto Fe(III) Oxides: Examination of Order of Oxidation of Metal Species
Experimental Conditions: $[Ca^{+2}]$ = 3 meq/L, $[HCO_3^-]$ = 3 meq/L, $[Mn(II)]_O$ = 0.50 mg/L, Temperature 10°C, pH = 7, and Fe(III) = 2 mg/L.

iron hydroxide flocs as they were forming. It was desired to study the possible adsorption-surface oxidation step, and the entrapment phenomenon that was observed would complicate this study significantly, often making it impossible to predict the magnitude of Mn(II) removal by each mechanism. Thus, future experimentation was completed as described in Chapter III by first air oxidizing the soluble iron in solution prior to adding soluble manganese to solution. In addition, this experimental setup allows one to use the chlorine demand of the system to track the level of Mn(II) oxidation that has occurred with each time step. This is the most direct means of quantifying that portion of the Mn(II) removed from the system that has been oxidized versus that which may have only been adsorbed.

Numerous experiments were conducted at pH 7 and 8 at various iron oxide concentrations to study the surface catalyzed oxidation phenomenon. In addition to the results of these experiments, other studies were conducted concurrently that lend insight into particle sizes formed and the processes used in the collection of data. First, from the data tables provided in Appendix A, it can be seen that the concentrations of soluble manganese in the filtrate of the 0.45 μm filters and the 30k ultrafilters do not appear to be different from one another. The is confirmed by statistical calculations provided in Appendix C. For this reason, ultrafiltration was not used for these studies as it is more costly and difficult to operate. This observation also indicated that the particles being formed exceeded 0.45 μm in diameter.

The results of the surface catalyzed Mn(II) removal experiments are summarized in tabular format in Appendix A. A portion of these results have been selected and plotted in Figures 16 and 17, the results for pH 7 and 8 conditions, respectively. As indicated, the reactions are highly pH and iron concentration dependent as more rapid rates of Mn(II) removal were noted under higher pH and iron concentration conditions.

Further analysis of the data collected during these experiments, specifically HOCl demand data, suggested that the enhanced Mn(II) removal observed was the product of an adsorption step followed by surface oxidation of the sorbed Mn(II). A full summary of

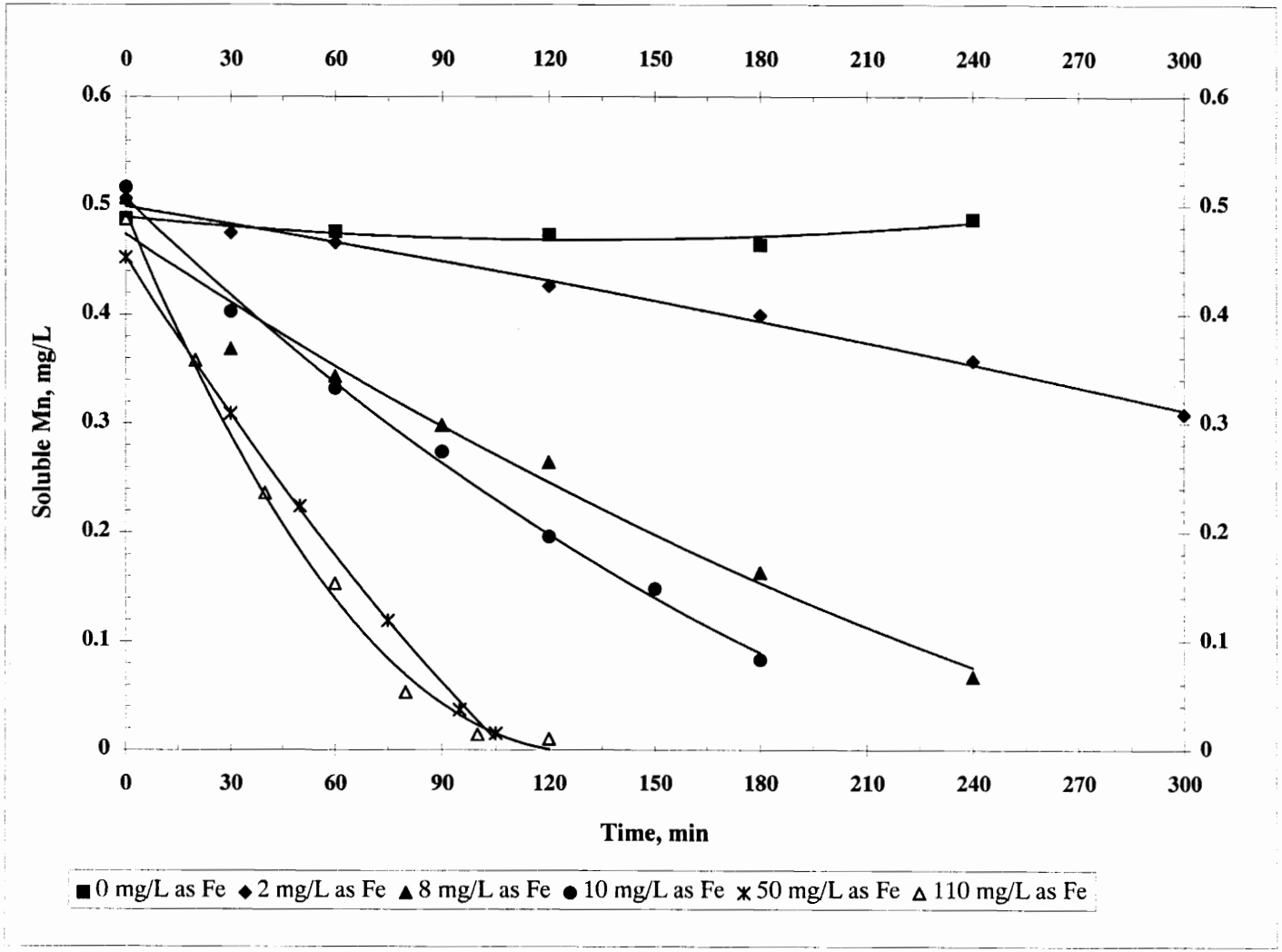

Figure 16: Effects of Various Iron Oxide Levels on Mn Removal Kinetics; Batch System. Experimental Conditions: pH = 7, $[Ca^{+2}]$ = 3 meq/L, $[HCO_3^-]$ = 3 meq/L, $[Mn(II)]_O$ = 0.50 mg/L, Temperature 10°C, Fe(III) as indicated.

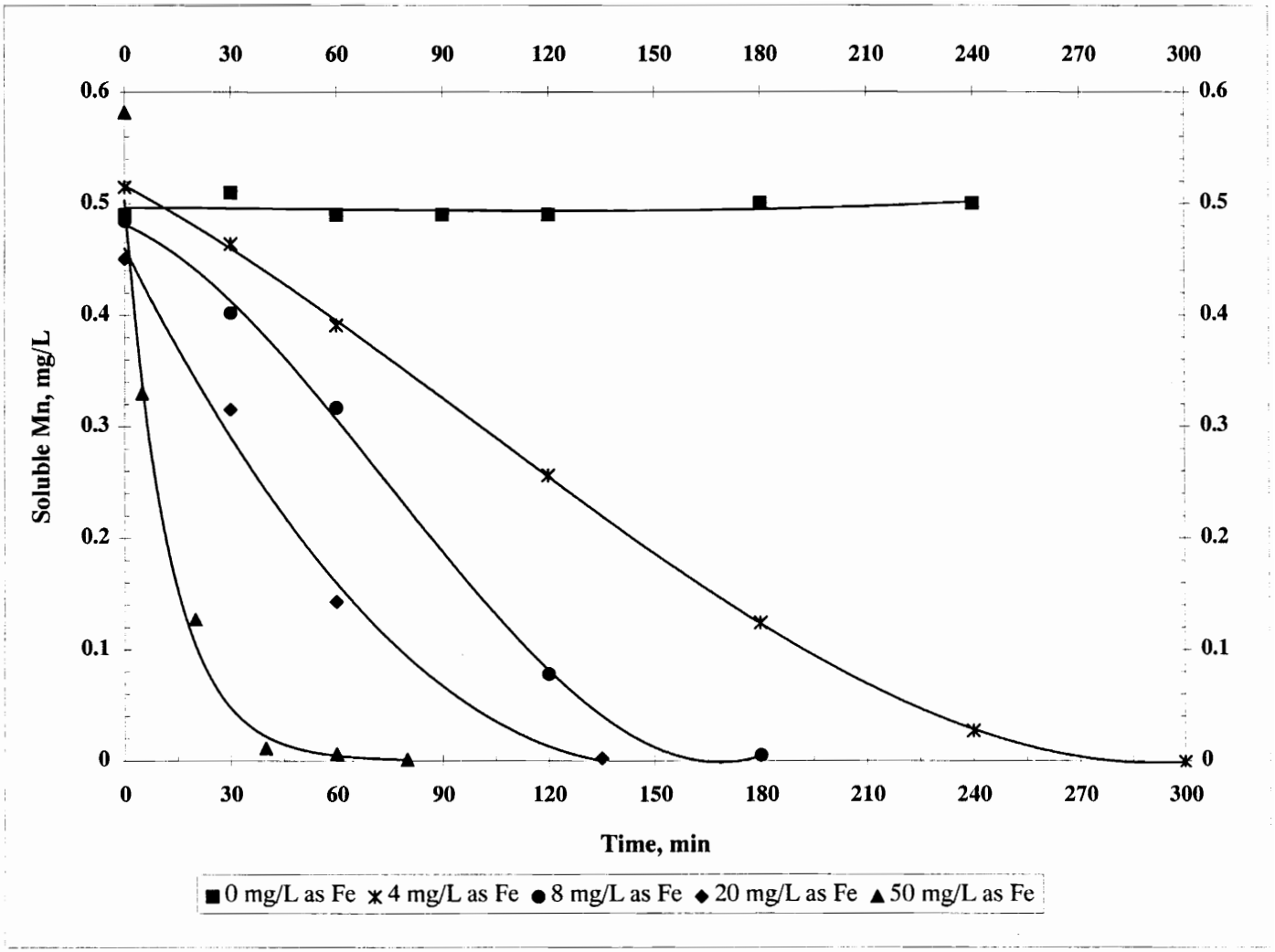

Figure 17: Effects of Various Iron Oxide Levels on Mn Removal Kinetics; Batch System. Experimental Conditions: pH = 8, $[Ca^{+2}]$ = 3 meq/L, $[HCO_3^-]$ = 3 meq/L, $[Mn(II)]_O$ = 0.50 mg/L, Temperature 10°C, Fe(III) as indicated.

the comparison between observed and predicted HOCl demand for different experimental conditions (Fe(III) and pH) is provided in Appendix A; however, the plot provided in Figure 18 provides an example of typically observed results. If Mn(II) removal was a result of oxidation via HOCl alone, one would expect the 1:1 line shown to be a "best-fit" line through the data points shown. Because the data points are located below the 1:1 line, the chlorine demand of the system lags behind what would be expected if Mn(II) removal was solely due to oxidation via HOCl. Therefore, the removal of Mn(II) from solution is the result of oxidation and a different mechanism, most likely adsorption.

Additional information gathered from these experiments was the rate of the reactions with respect to Mn(II) oxidation. Using the method outlined by Grady and Lim,[64] the rate of Mn(II) oxidation was analyzed and the order of reaction and a rate constant "k" were calculated for the results presented at pH 7 and 8. In the determination of reaction rate, the initial Mn(II) concentration was taken to be the concentration of Mn(II) following the five minute adsorption/interaction period with Fe(III) oxides, not the initial Mn(II) concentration. Otherwise, the Mn(II) removal rate would appear to be very rapid initially (most of Mn(II) removal due to adsorption) and much slower as the experiment continued (actual Mn(II) oxidation catalyzed by the Fe(III) oxides). The data for each of the experiments conducted using different Fe(III) concentrations at pH 7 and 8 were analyzed individually by plotting the log of the equilibrium Mn(II) concentration versus the log of instantaneous rate of reaction. The resulting best-fit-line provided the order of reaction (slope) as well as the rate constant for a Mn(II) concentration of 1 mg/L (y-intercept). The rate constants for a Mn(II) concentration of 0.50 mg/L were also determined using the equation of the best-fit-line on the log-log plot. An example of the determination of these parameters for a typical experiment is shown in Figure 19. The rate constants determined for each individual experiment for a given pH were then plotted versus the Fe(III) concentration to develop an equation of the rate constants with respect to Fe(III). A plot of these equations is provided in Figure 20.

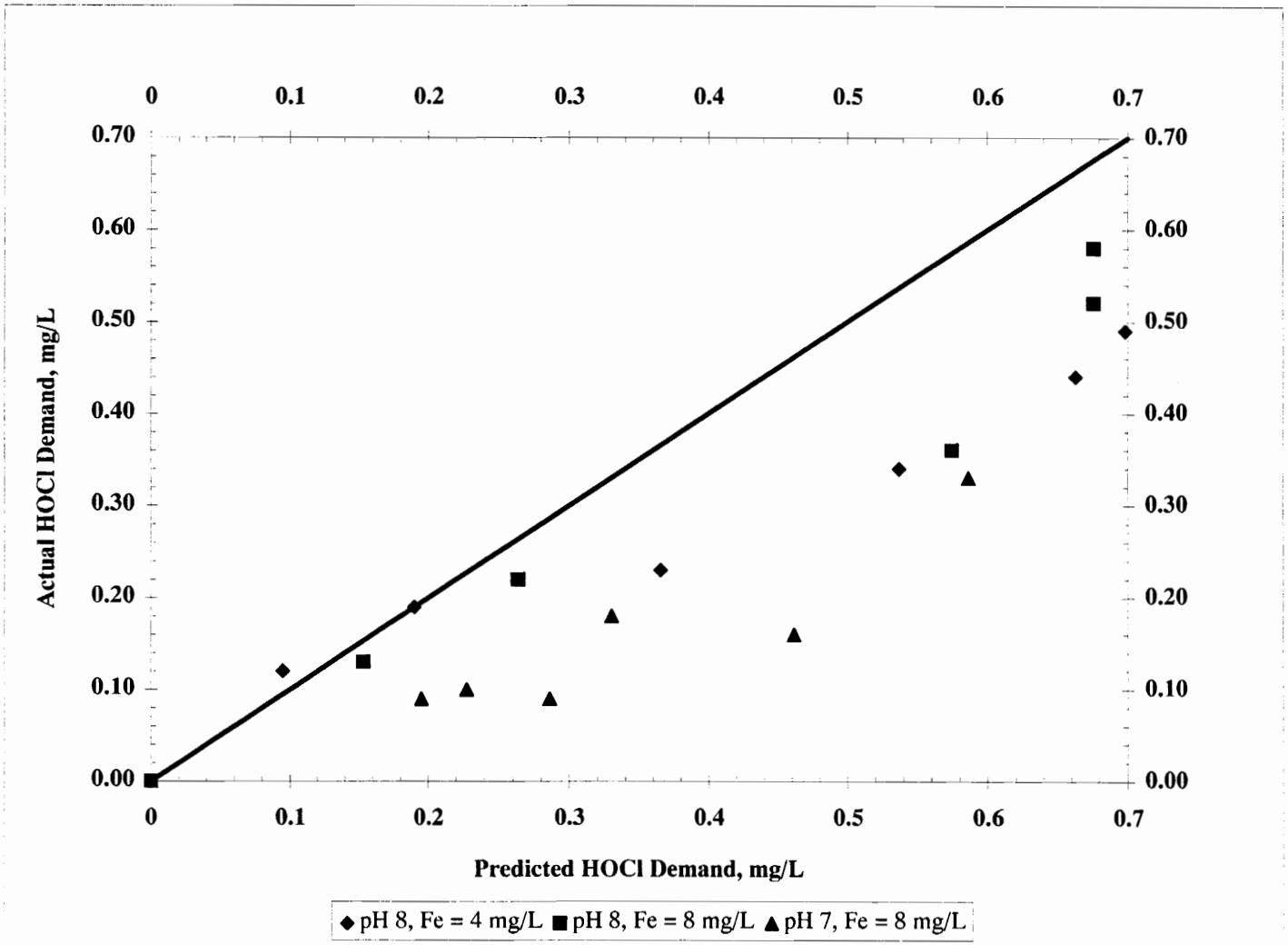

Figure 18: Comparison Between Observed and Predicted (via Stoichiometry) HOCl Demand for Various pH and Fe(III) Concentrations.

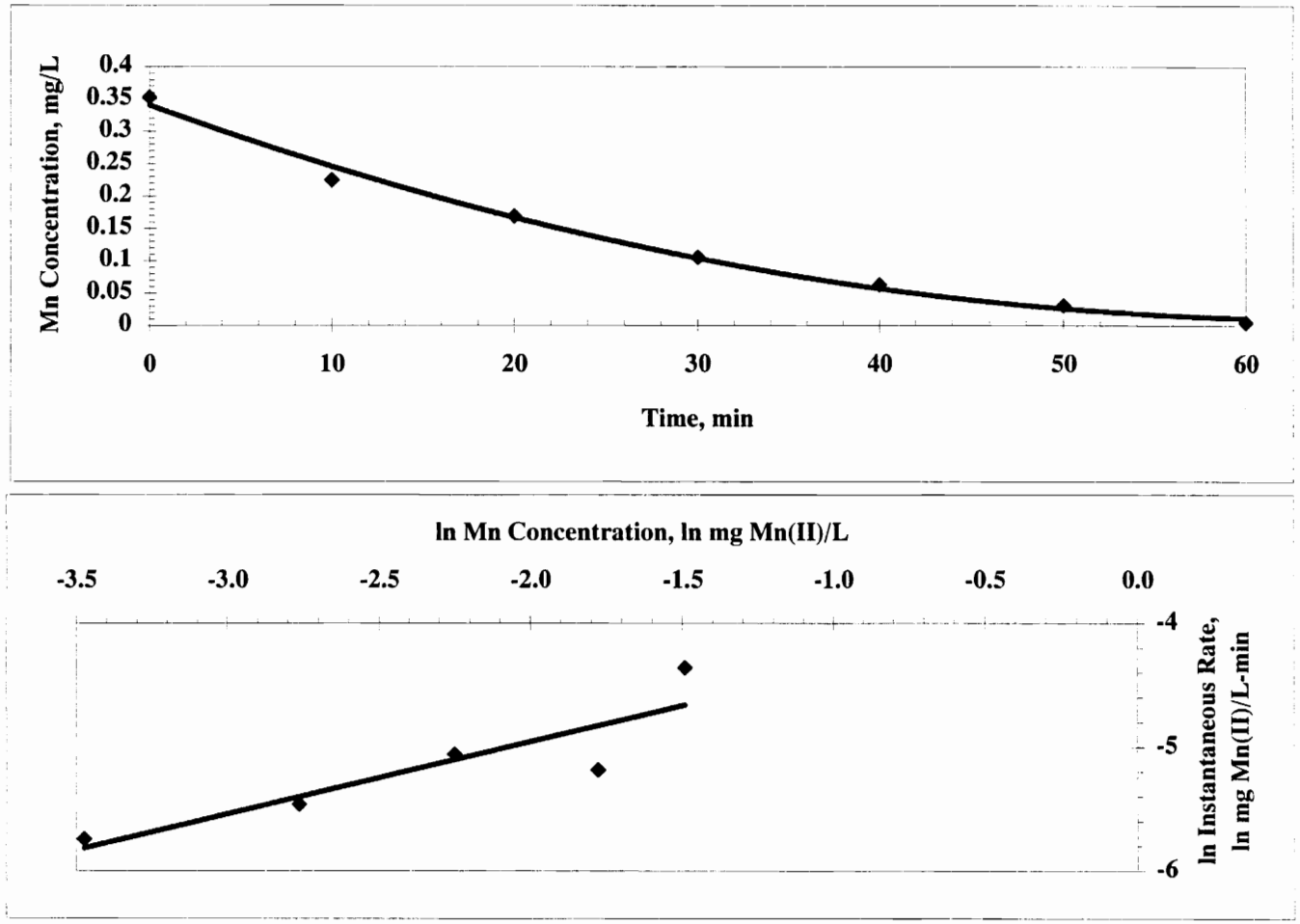

Figure 19: (a) Upper plot: Mn(II) Concenration versus Time for pH 8, Fe(III) = 100 mg/L, $[Ca^{+2}]$ = 3 meq/L, $[HCO_3^-]$ = 3 meq/L, $[Mn(II)]_O$ = 0.50 mg/L, Temperature 10°C; (b) Lower plot: Grady and Lim Method of Rate Constant k Determination for same conditions.

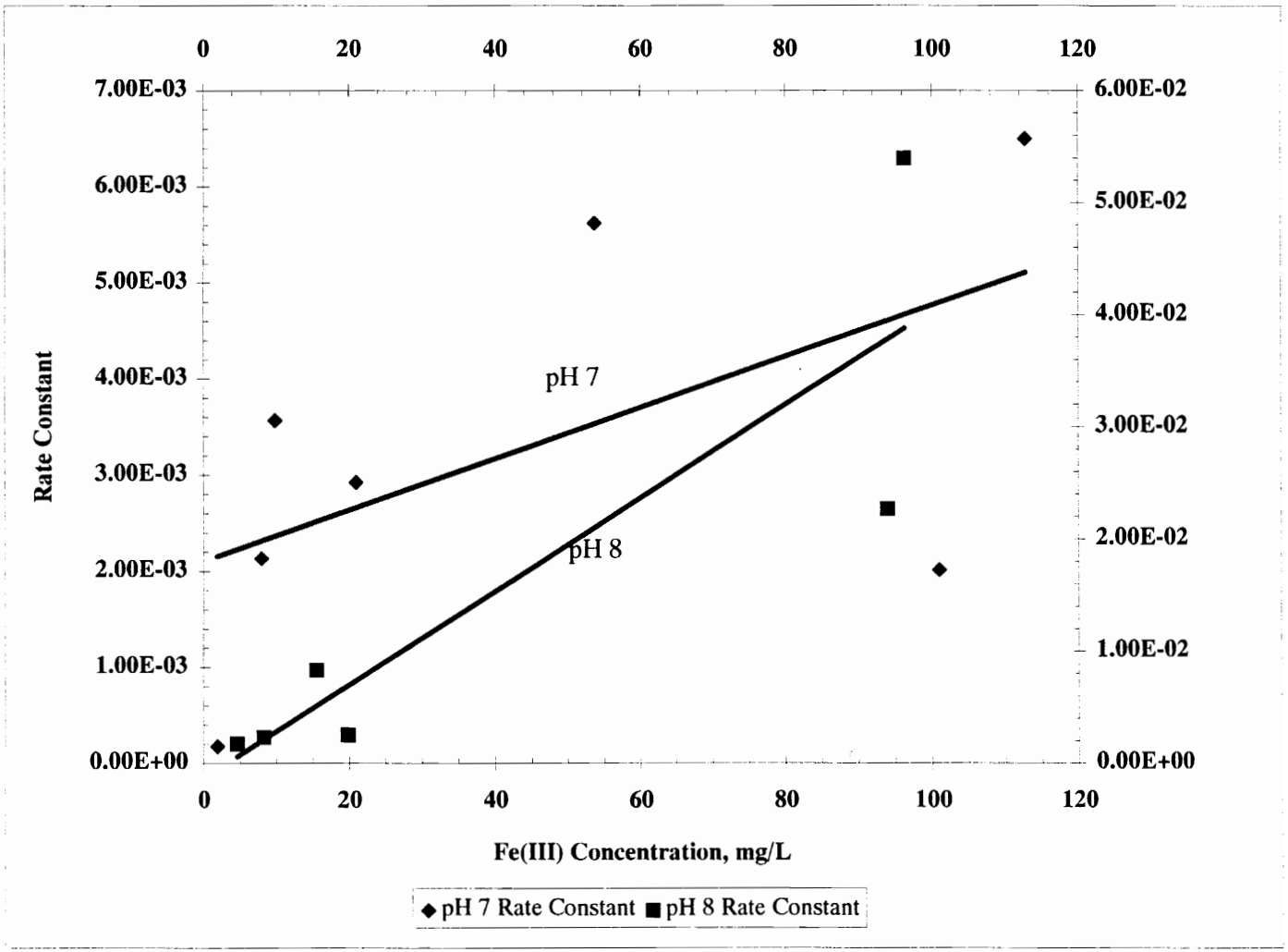

Figure 20: Experimentally Determined Rate Constants for Mn(II) Removal During Batch Studies. Experimental Conditions: $[Ca^{+2}]$ = 3 meq/L, $[HCO_3^-]$ = 3 meq/L, $[Mn(II)]_O$ = 0.50 mg/L, Temperature 10°C, Fe(III) and pH as indicated.

The next step in the research effort was to attempt to utilize this new found technology to develop a treatment system to enhance the removal of soluble iron and manganese from water supplies.

D. Iron Oxide Slurry Reactor System and Mn(II) Adsorption onto $MnO_{x(s)}$

Three bench-scale systems (described in Chapter III, Section E.4) were constructed and operated in parallel, each reactor containing a different concentration of Fe(III) oxides. Data collected from these reactors indicated that this system setup could meet the desired level of treatment for iron and manganese removal. However, caution should be taken when considering the results because of the difficulties discussed in Chapter III of maintaining the temperature during the studies at 10°C. The higher temperatures used during experimentation most likely resulted in increased rates of reaction and thus improved performance. Regardless, during the study, several key observations were made that provide further insight into the mechanistic means by which this phenomenon occurs.

Initial data collected emphasized the importance of HOCl in solution which reiterates that manganese removal is not solely an adsorptive process onto Fe(III) oxides. The reactor system failed if the stoichiometric requirements of HOCl for the influent iron and manganese levels were not satisfied. This is exhibited in Figure 21 where the system was operated with no additional HOCl dose at a detention time of 1 hour (There is a 1 mg/L residual in the tap water). For this experiment the effluent Mn(II) concentration approaches the influent concentration of 0.50 mg/L with 6½ hours. However, when the same reactor setup was tested with a HOCl concentration of 4 mg/L, an immediate reduction in Mn(II) is noted. Figure 22 shows the complete set of test results for this reactor setup indicating the point at which the chlorine dose was increased from approximately 1 mg/L (residual in tap water) to 4 mg/L. These results confirm the importance the presence of HOCl has on the effectiveness of the system.

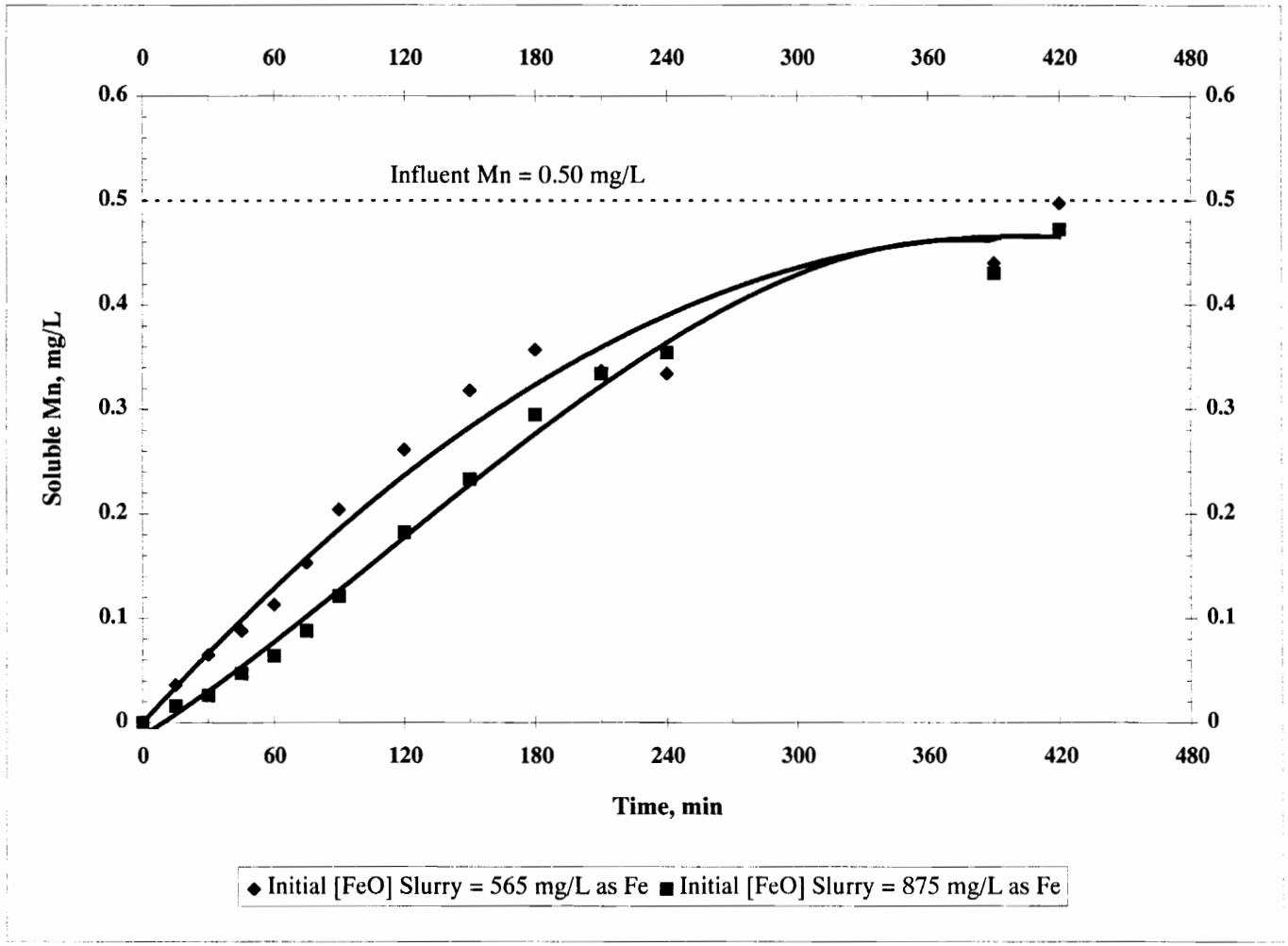

Figure 21: Bench-Scale Continuous Flow System with Varying Iron Oxide Slurry Concentrations. No Additional HOCl Dose Added (1 mg/L Residual in Source Water). pH = 6.8, $[Ca^{+2}]$ = 3 meq/L, $[HCO_3^-]$ = 3 meq/L, Influent Mn(II) = 0.50 mg/L, Temperature 10°C, Influent Fe(II) = 2 mg/L, θ_H = 1 hour.

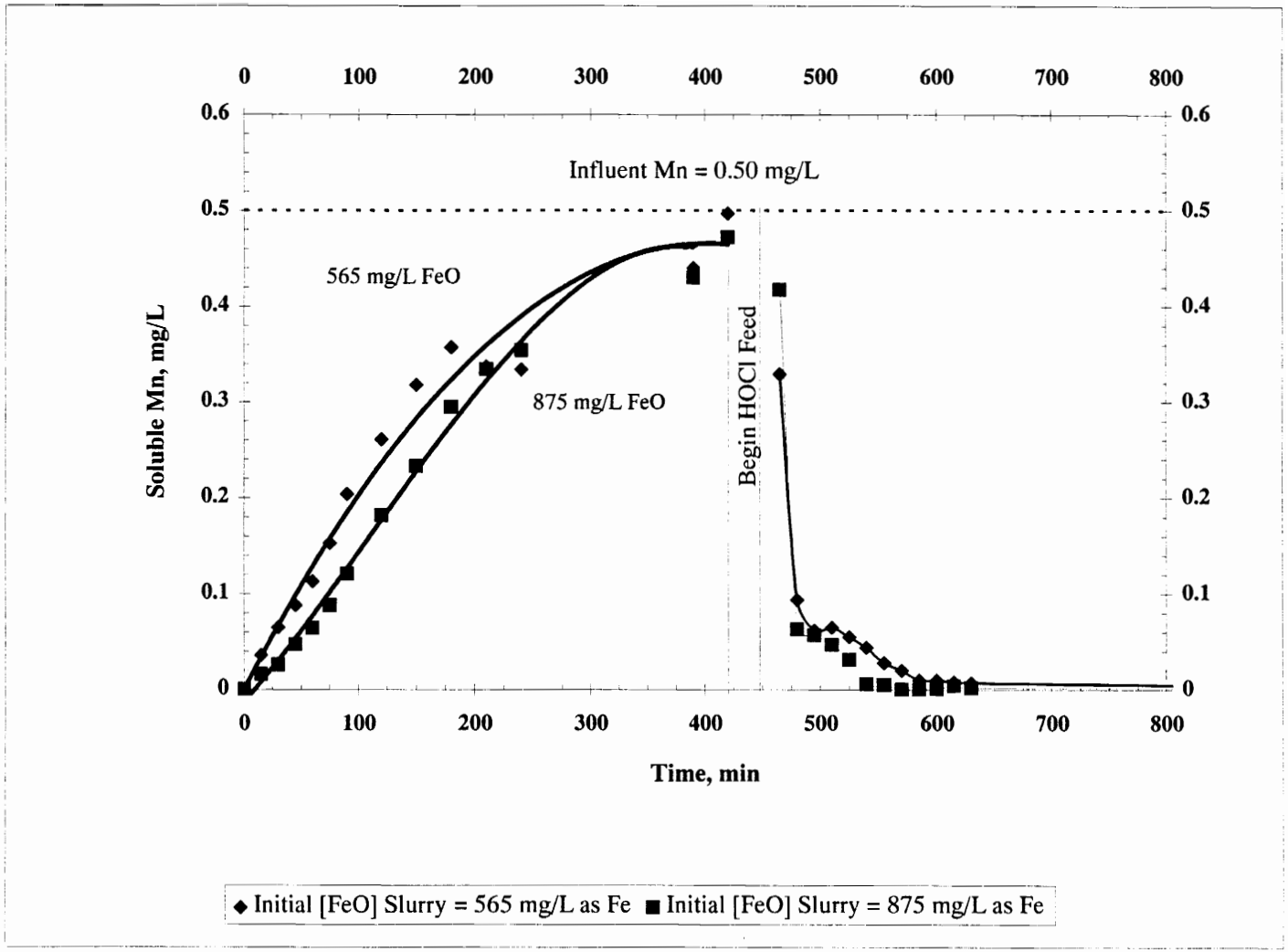

Figure 22: Bench-Scale Continuous Flow System with Varying Iron Oxide Slurry Concentrations. No Additional HOCl Dose Added (1 mg/L Residual in Source Water). pH = 6.8, $[Ca^{+2}]$ = 3 meq/L, $[HCO_3^-]$ = 3 meq/L, Influent Mn(II) = 0.50 mg/L, Temperature 10°C, Influent Fe(II) = 2 mg/L, θ_H = 1 hour.

Perhaps the most important operating phenomenon noted was the buildup of $MnO_{x\,(s)}$ in the slurry over time, provided there was sufficient chlorine to complete the Mn(II) oxidation step. Figure 23 provides a graphical representation of the data leading to this conclusion. In addition to the buildup of $MnO_{x\,(s)}$ in the slurry, another trend should be noted from Figure 23: the initial iron concentration decreases to a steady-state concentration over time. These results seem to indicate that the $MnO_{x\,(s)}$ in the slurry may take a leading role in the removal of Mn(II) from the system, in essence replacing the Fe(III) oxide as the primary Mn(II) adsorptive surface.

For these reasons, it was necessary to examine the adsorptive properties of $MnO_{x(s)}$ for Mn(II). The results of these studies are summarized in Figure 24. Again, a five minute time period was used during the adsorption studies to allow for an equilibrium relationship to develop between Mn(II) and of $MnO_{x(s)}$. Langmuir isotherm plots for the sorption of Mn(II) onto $MnO_{x\,(s)}$ are provided in Figure 25. At an equilibrium Mn(II) concentration of 0.50 mg/L, the adsorptive capacity of $MnO_{x(s)}$ for Mn(II) at pH 7 and 8 was 0.20 and 0.21 mg Mn(II)/mg $MnO_{x(s)}$, respectively. It should be noted that the adsorptive capacity of $MnO_{x\,(s)}$ for Mn(II) far exceeds that of freshly formed iron oxides (Fe(III)) as previously presented.

Several plots were prepared to exhibit slurry reactor performance under various operating conditions. Figure 26 provides an indication of typical reactor performance at pH 7 while Figure 27 represents pH 8 conditions. The system was found to be much more stable at higher pH conditions (i.e. not as sensitive to changes in system parameters such as initial Mn(II) concentration or HOCl dose). Generally, the success of the reactor systems were independent of changes in solution pH between 7 and 8. (The slight disruption noted around hour 60 for the pH 7 system was caused by an upset in the experimental setup, specifically, the constant head tank supplying tap water to the system froze overnight.) However, when the pH was reduced to 6, a level which does not promote efficient adsorption of Mn(II) onto either iron or manganese oxide surfaces, the effluent quality with respect to soluble manganese began to deteriorate rapidly despite

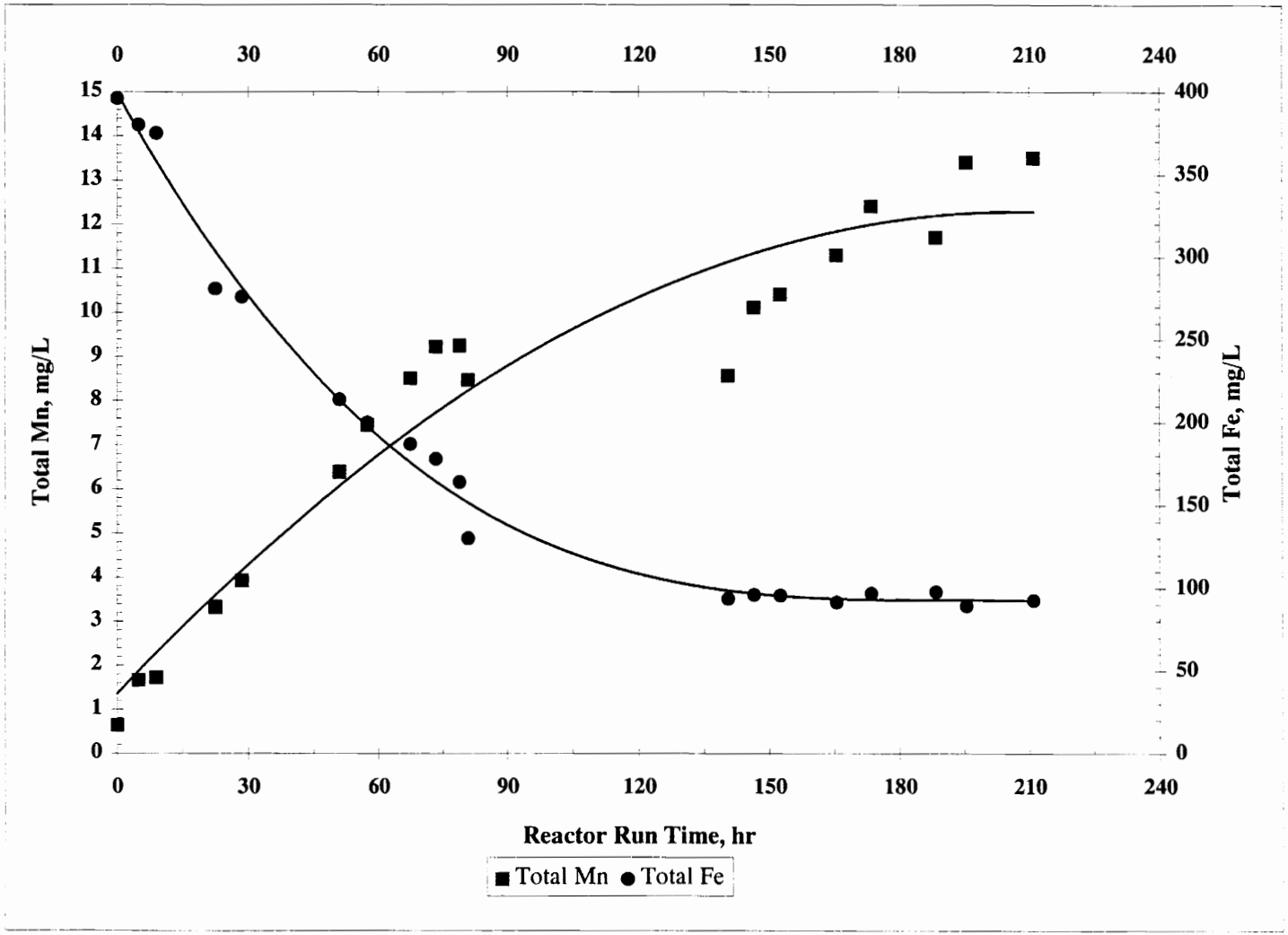

Figure 23: Iron and Manganese Oxide Concentrations in Bench-Scale Continuous Flow System; Experimental Conditions: pH = 8, $[Ca^{+2}]$ = 3 meq/L, $[HCO_3^-]$ = 3 meq/L, Influent Mn(II) = 0.50 mg/L, Influent Fe(II) = 2 mg/L, Temperature 10-15°C, HOCl Dose = 1-4 mg/L (varied), θ_H = 2 hours.

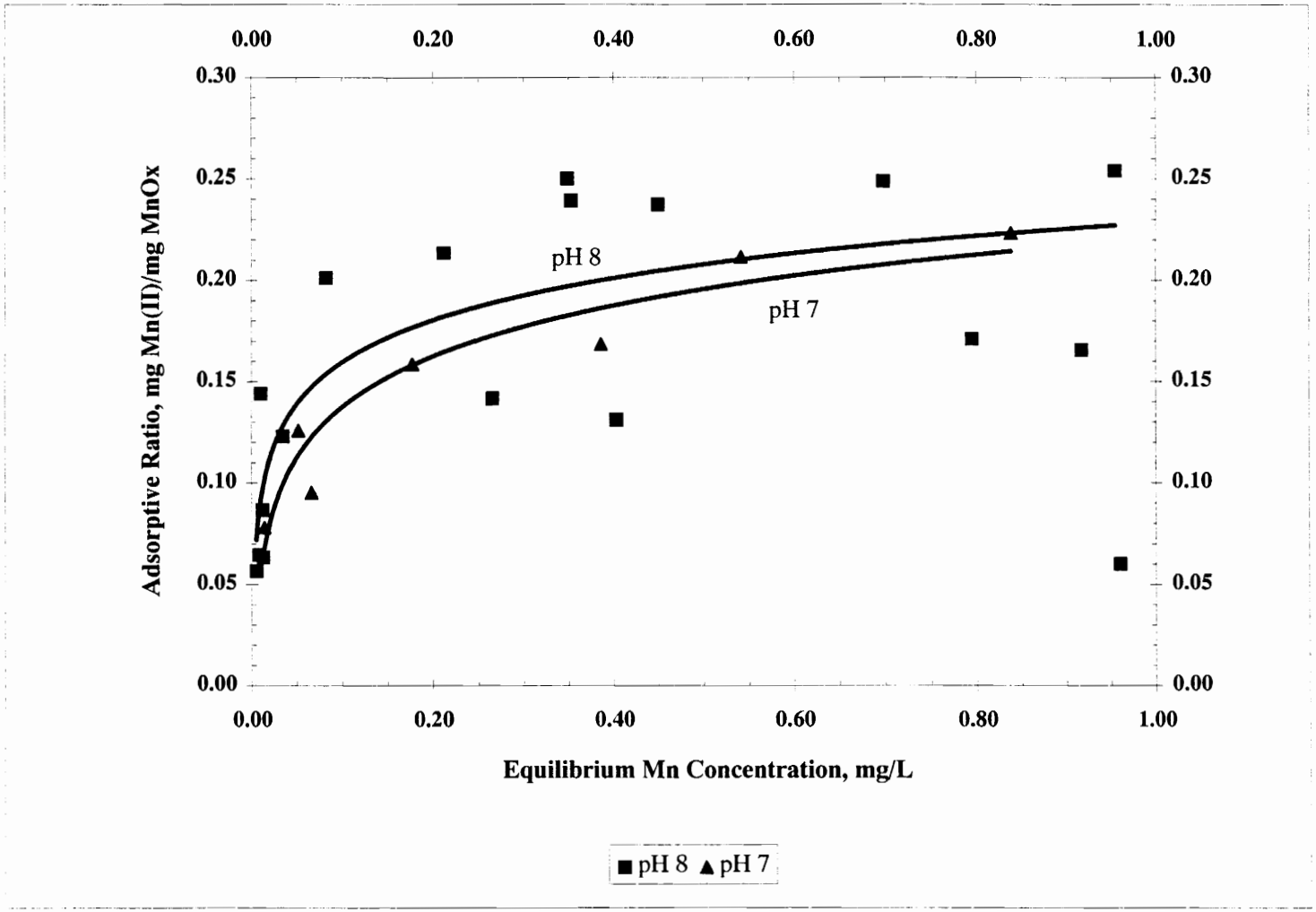

Figure 24: Adsorption of Soluble Manganese (Mn(II)) onto Freshly Precipitated Manganese Oxides (MnO_X). Experimental Conditions: $[Ca^{+2}]$ = 3 meq/L, $[HCO_3^-]$ = 3 meq/L, $[Mn(II)]_O$ = 1 mg/L, Temperature = 10°C.

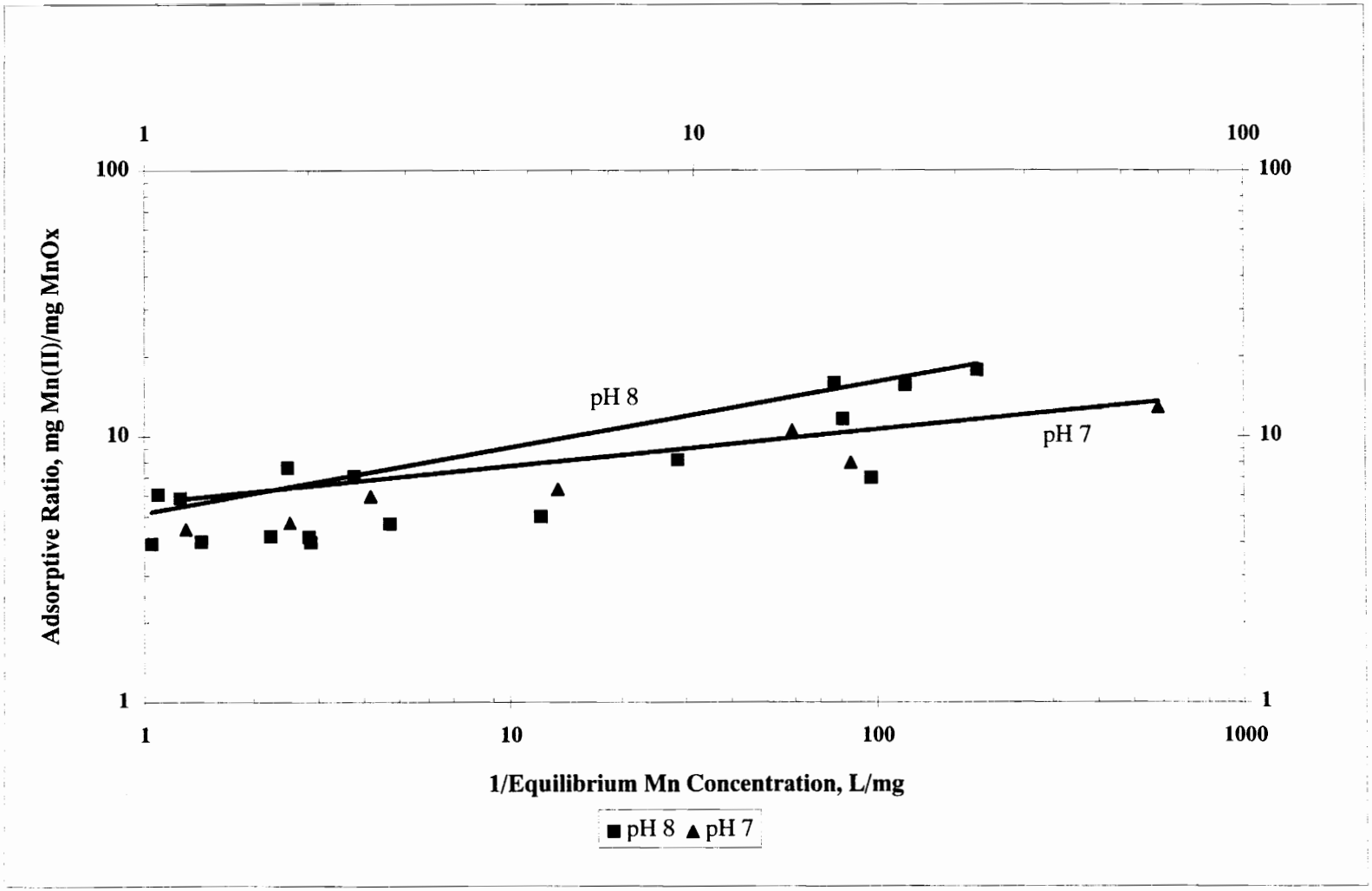

Figure 25: Langmuir Isotherm for Adsorption of (Mn(II)) onto Freshly Precipitated Manganese Oxides (MnO_X).
Experimental Conditions: $[Ca^{+2}]$ = 3 meq/L, $[HCO_3^-]$ = 3 meq/L, $[Mn(II)]_O$ = 1 mg/L, Temperature = 10°C.

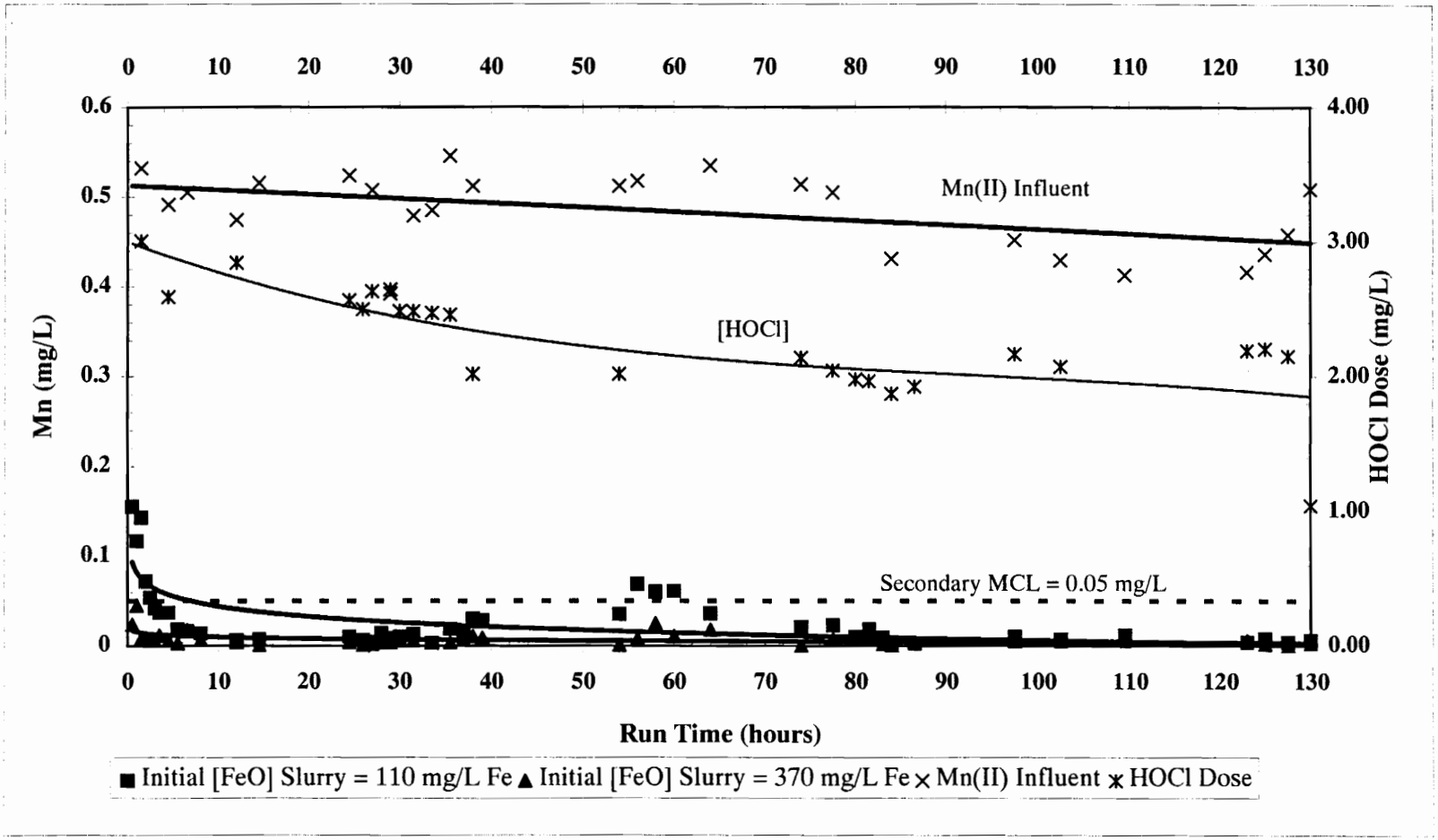

Figure 26: Bench-Sclae Continuous Flow System; Experimental Conditions: pH = 7, Influent Mn(II) = 0.50 mg/L, Influent Fe(II) = 2 mg/L, $[Ca^{+2}]$ = 3 meq/L, $[HCO_3^-]$ = 3 meq/L, Temperature = 10-15°C, HOCl Dose 2-3 mg/L (varies), θ_H = 2.5 hours.

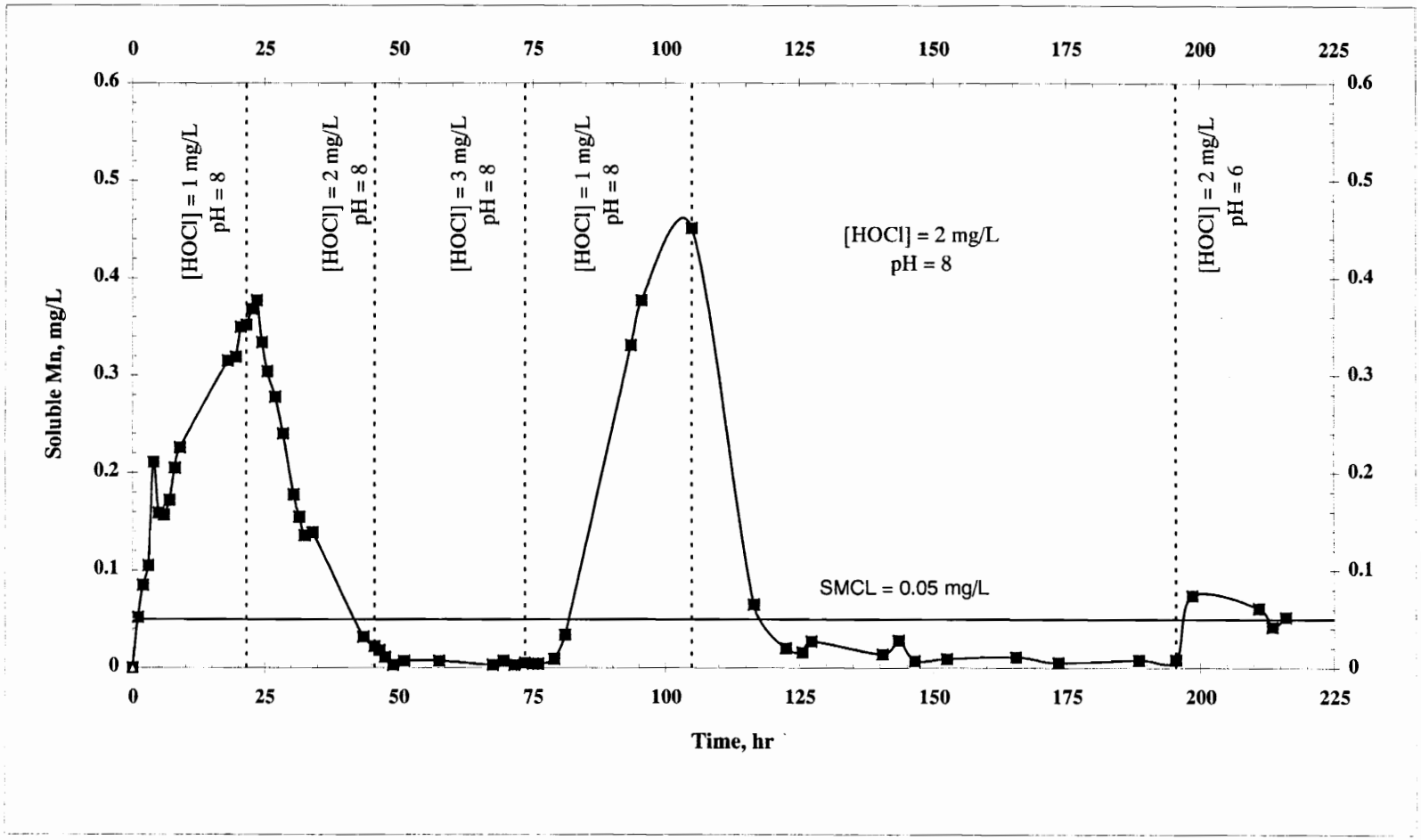

Figure 27: Bench-Scale Continuous Flow System; Experimental Conditions (unless otherwise indicated): Influent Mn(II) = 0.50 mg/L, Initial [FeO] Slurry = 280 mg/L as Fe, Influent Fe(II) = 2 mg/L, $[Ca^{+2}]$ = 3 meq/L, $[HCO_3^-]$ = 3 meq/L, Temperature 10-15°C, HOCl Dose and pH as indicated, θ_H = 2 hours.

sufficient HOCl and the large concentration of manganese oxides present in the slurry. Figure 27 also shows the performance of the system over a range of different operating conditions including the pH 6 condition.

E. Model Development and Results

These experimental observations were used to develop a mathematical model to predict the effluent water quality from a slurry reactor system, using several experimentally determined input variables. It should be noted that the laboratory experiments were not designed with this modeling effort in mind; therefore the experiments conducted do not allow for the calibration of the model or provide a means of confirming its accuracy. Note that due to concern over the accuracy of the isotherm determined for Mn(II) adsorption onto iron oxides at pH 7, the modeling exercise does not include this pH condition.

The model describes $Fe(OH)_{3(s)}$ catalyzed Mn(II) oxidation via HOCl using mass balances for manganese and chlorine. It was assumed that the reduced iron entering the slurry reactor would be immediately oxidized by the HOCl in solution as was noted in Chapter II for the pH range under study. Other assumptions made in the development of the equations are discussed in the following sections. A computer printout of the model with model simulations is provided in Appendix D. The model input parameters included:

- Influent and effluent soluble manganese concentrations
- HOCl concentration
- Initial iron and manganese oxide concentrations
- Volume of reactors and flow rate through system; sets hydraulic detention time
- Isotherm data to estimate sorbed Mn(II) on Fe(III) oxides and $MnO_{x(s)}$.
- Influent iron concentration

1. Modeling Approach. Generally, models are developed around a series of mass balance equations for several parameters within the system. This too is the case for the model to describe iron catalyzed manganese oxidation via chlorine where mass balances for manganese and chlorine were developed. The fate of Mn(II) in solution is by far the most complex of the two parameters in that its removal is made possible by several different mechanisms. Below is the equation developed for the mass balance of total manganese in the system.

$$\frac{dC_M}{dt}\cdot V+\frac{dq_F}{dt}\cdot M_{Fe}+\frac{dq_M}{dt}\cdot M_{MnO}=Q_{in}\cdot C_{M_{in}}-Q_{out}\cdot C_{M_{out}}-k_1\cdot q_F\cdot[HOCl]\cdot M_{Fe}-k_1\cdot q_M\cdot[HOCl]\cdot M_{MnO} \quad (9)$$

where: C_m = Soluble Mn (Mn(II)) in reactor (mg Mn(II)/L)

V = Volume of Reactor (L)

q_F = Amount of sorbed Mn(II) onto iron oxide surfaces as predicted by Langmuir isotherm (mg Mn(II) sorbed/mg Fe oxide)

M_{Fe} = Mass of iron oxides in system (mg Fe oxide)

q_M = Amount of sorbed Mn(II) onto iron oxide surfaces as predicted by Langmuir isotherm (mg Mn(II) sorbed/mg Mn oxide)

M_{MnO} = Mass of manganese oxides in system (mg Mn oxide)

Q_{in} = Total flow into reactor (L/min)

Q_{out} = Total flow out of reactor (L/min)

C_{Min} = Influent concentration of soluble manganese (mg Mn(II)/L)

C_{Mout} = Effluent concentration of soluble manganese (mg Mn(II)/L)

k_1 = Rate constant describing the surface catalyzed oxidation step (L/min·mg HOCl)

[HOCl] = Concentration of free chlorine in solution (mg HOCl /L)

The original idea for the model was to predict the system performance under startup conditions, however, the inclusion of the manganese oxide adsorption term and the rate of sorbed Mn(II) oxidation on the manganese oxide surface allows for the prediction of effluent quality as these oxides accumulate over time as exhibited in Figure 23. Unfortunately no experimental data were collected for the determination of the rate of Mn(II) oxidation on the manganese oxide surface. For the purposes of simulating reactor performance, the rate of oxidation on the manganese oxide surface will be assumed to be equal to that of the iron oxide surface.

Plots of the Langmuir isotherms for the determination of the "q" parameters have been presented in Figures 13 and 25. The concentrations of soluble manganese (influent and effluent), [HOCl], and oxide surface concentrations can be estimated from the data collected. [NOTE: By CSTR theory $C_M = C_{Mout}$.] The volume and flow rate through the reactors will be used to set the hydraulic detention time for each model simulation.

Next, a relationship between the amount of free chlorine in solution was developed to describe the decay or utilization of free chlorine within the system. The rate constant used in this equation is stoichiometrically related to k_1 in the mass balance relationship for manganese; both k_1, k_2, and k_3 describe the rate of surface catalyzed oxidation. Note that the decay of HOCl in the presence of Fe(II) is assumed to follow the stoichiometric requirement for oxidation of Fe(II) to Fe(III).

$$\frac{dC_{HOCl}}{dt}\cdot V = Q_{in}\cdot C_{HOCl_{in}} - Q_{out}\cdot C_{HOCl_{out}} - k_2\cdot q_F\cdot[HOCl]\cdot V - k_3\cdot q_M\cdot[HOCl]\cdot V - 0.64\cdot[Fe(II)]\cdot V \quad (10)$$

where: C_{HOCl} = HOCl in solution (mg HOCL/L)

C_{HOClin} = Influent concentration of HOCl (mg HOCl/L)

$C_{HOClout}$ = Effluent concentration of HOCl (mg HOCl/L)

k_2 = Rate constant for surface catalyzed oxidation step (mg Fe(III) oxide/mg Mn(II)·min)

k_3 =	Rate constant for surface catalyzed oxidation step (mg Mn oxide/mg Mn(II)·min)
[HOCl] =	Concentration of free chlorine in solution (mg HOCl/L)
[Fe(II)] =	Concentration of influent Soluble Iron (mg Fe(II)/L)

A mass balance for Fe(II) could not be written for the experimental system due to the lack of sufficient data for Fe(II)/Fe(III) accumulation and loss from the system. As noted previously, the iron oxide concentration decreased to a steady state value over time; however, it should be stressed again that the model intends only to predict the startup condition. In essence, an iron mass balance is not required based on this criteria, but would be required for the development of a model to predict long term reactor performance. The model could be extended to the long term performance, but it is suggested that reactor hydraulics and settling characteristics of the particles first be investigated to determine whether iron solids will accumulate over time or continue to wash out of the system as was observed during these studies. Note that the HOCl demand the influent iron exhibits was accounted for in the HOCl mass balance, as it was assumed its conversion to Fe(III) was instantaneous at these pH conditions in the presence of HOCl and that it would follow stoichiometric proportions.

A key assumption made in the writing of the mass balance equations was that the concentration of iron and manganese oxide solids in solution remains constant. As presented in Figure 23, this is unlikely. Consideration was given to including a solids accumulation or loss term, but defining the value for such a term would be difficult with the reactor setup utilized to conduct these experiments and the available data collected. As noted by the data collected and summarized in Appendix A Tables A41-A43, solids were consistently being lost from the system in the effluent. A more hydraulically stable reactor with better short circuiting prevention devices would be more successful at predicting the value of such a term.

2. Simplified Model for Batch System. Before attempting to implement the previous system of equations to the continuous flow system, a more simplified model was developed to fit the parameter k (rate constant) to existing batch study data. The equations for this model are summarized here. The first equation represents the mass balance for manganese in the system, and the second a mass balance for chlorine. It should be noted that during the batch studies, all Fe(II) in the system was completely oxidized via oxygen prior to the addition of HOCl and thus it poses little or no HOCl demand. Note that the manganese oxide concentration was assumed to be zero throughout the batch studies as these terms are not included in the following equations.

$$\frac{d[C_m]}{dt}\cdot V + \frac{dq}{dt} M_{Fe} = -k_1 \cdot [HOCl]\cdot q_F \cdot M_{Fe} \quad (11)$$

$$\frac{d[HOCl]}{dt}\cdot V = -k_2 \cdot [HOCl]\cdot q_F \cdot V \quad (12)$$

The resulting equations which must be solved simultaneously are:

$$Mn(II): \quad \frac{dC_m}{dt} = \frac{-k_1 \cdot \dfrac{a\cdot b\cdot C_m}{1+b\cdot C_m}\cdot [HOCl]\cdot M_{Fe}}{V + \dfrac{a\cdot b}{(1+b\cdot C_m)}\cdot M_{Fe}} \quad (13)$$

$$HOCl: \quad \frac{d[HOCl]}{dt} = -k_2 \cdot [HOCl]\cdot \frac{a\cdot b\cdot C_m}{1+b\cdot C_m} \quad (14)$$

where: a, b = empirical Langmuir Isotherm Constants

k_2 = k_1/A; where $A = V\cdot MW_{HOCl}/M_{Fe} \cdot MW_{Mn}$

3. Model Estimation Technique. The Runge-Kutta differential equation estimation technique for initial value problems was used to approximate the solution of the differential equations developed. The solution of the differential equations is an average of values of the equation taken at different points in the interval $x_n < x > x_{n+1}$. The formula is presented below:

$$y_{n+1} = y_n + \frac{h}{6}(k_{n1} + 2k_{n2} + 2k_{n3} + k_{n14})$$

where

$$k_{n1} = f(x_n, y_n),$$
$$k_{n2} = f(x_n + \frac{1}{2}h, y_n + \frac{1}{2}hk_{n1}),$$
$$k_{n3} = f(x_n + \frac{1}{2}h, y_n + \frac{1}{2}hk_{n2}),$$
$$k_{n4} = f(x_n + h, y_n + hk_{n3}).$$

For this model, the independent variable (x) is reaction time and the dependent variable (y) is soluble manganese concentration and HOCl concentration. The choice of the step size, h, is critical in obtaining the most accurate representation of the equation(s) being approximated. For the purposes of this model, a step size of 0.05 minutes or 3 seconds was used for approximating the mass balance equations for the batch studies and a time interval of 1-5 minutes for the CSTR estimations. For more detail on the Runge-Kutta method, please refer to the text by Boyce and DiPrima.[65]

4. Model Results for Batch Studies. The rate constant "k" used for the model calculations could not be calculated by laboratory experimentation because of the combination of mechanisms associated with this term. For this reason, a rate constant was fitted to the data for each of the batch experiments performed studying iron catalyzed manganese removal via the adsorption-oxidation process at pH 8. Figure 28 provides a summary of

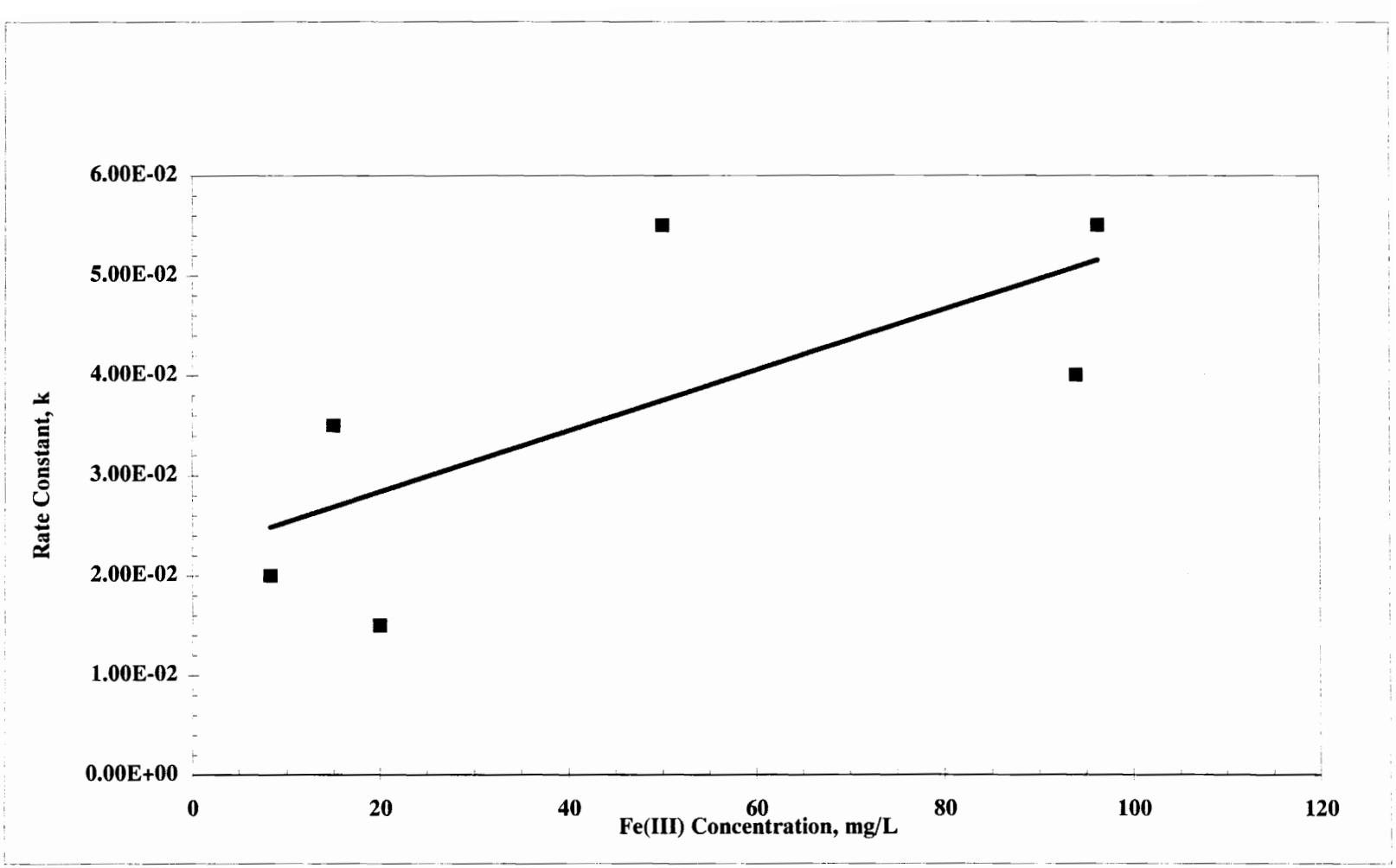

Figure 28: Summary of Rate Constant Values for Batch System Model at pH 8: Using Least Sums of Squares Fitting Techniques. Experimental Conditions as stated for batch studies.

the rate constant values determined for each of the batch experiments at pH 8. The ideal outcome of such an exercise is for the best fit "k" to be a constant value over the range of experimental conditions, signifying that the model provides a good prediction of the observed results. As noted in Figure 28, the model seemed to provide a relatively good prediction of the results as all of the rate constants predicted are within the same order of magnitude. The average 'k" value determined was 3.43×10^{-2}.

Figure 29 exhibits the fit of the rate constant value to a portion of the batch data collected at pH 8 conditions. The points represent experimental data collected and the lines a best fit of the model calculations using the optimum rate constant value (based upon the residual sums of squares) for those specific experimental conditions (i.e. Fe(III) concentration, pH, etc.).

5. Model for Continuous Flow System. The original equations (Equations 9 and 10) presented for the mass balances of Mn(II) and HOCl were modified and differentiated resulting in the following equations that must be solved simultaneously for the continuous flow system:

$$Mn(II):\frac{dC_M}{dt} =$$

$$\frac{Q_{in}\cdot C_{M_{in}} - Q_{out}\cdot C_{M_{out}} - k_1\cdot q_F\cdot[HOCl]\cdot\frac{abC_M}{1+bC_M}M_{Fe} - k_1\cdot q_M\cdot[HOCl]\cdot\frac{a'b'C_M}{1+b'C_M}M_{MnO}}{V+\frac{ab}{(1+bC_M)^2}\cdot M_{Fe}+\frac{a'b'}{(1+b'C_M)^2}\cdot M_{Mn}} \quad (15)$$

$$[HOCl]:\frac{d[HOCl]}{dt} =$$

$$\frac{Q\cdot[HOCl_{in}]-Q\cdot[HOCl]-k_2\cdot[HOCl]\cdot\frac{abC_M}{1+bC_M}\cdot V - k_3\cdot[HOCl]\cdot\frac{a'b'C_M}{1+b'C_M}\cdot V}{V} \quad (16)$$

where: a', b' = Empirical Langmuir Isotherm Constants

k_3 = k_1/B; where $B = V\cdot MW_{HOCl}/M_{MnO}\cdot MW_{Mn}$

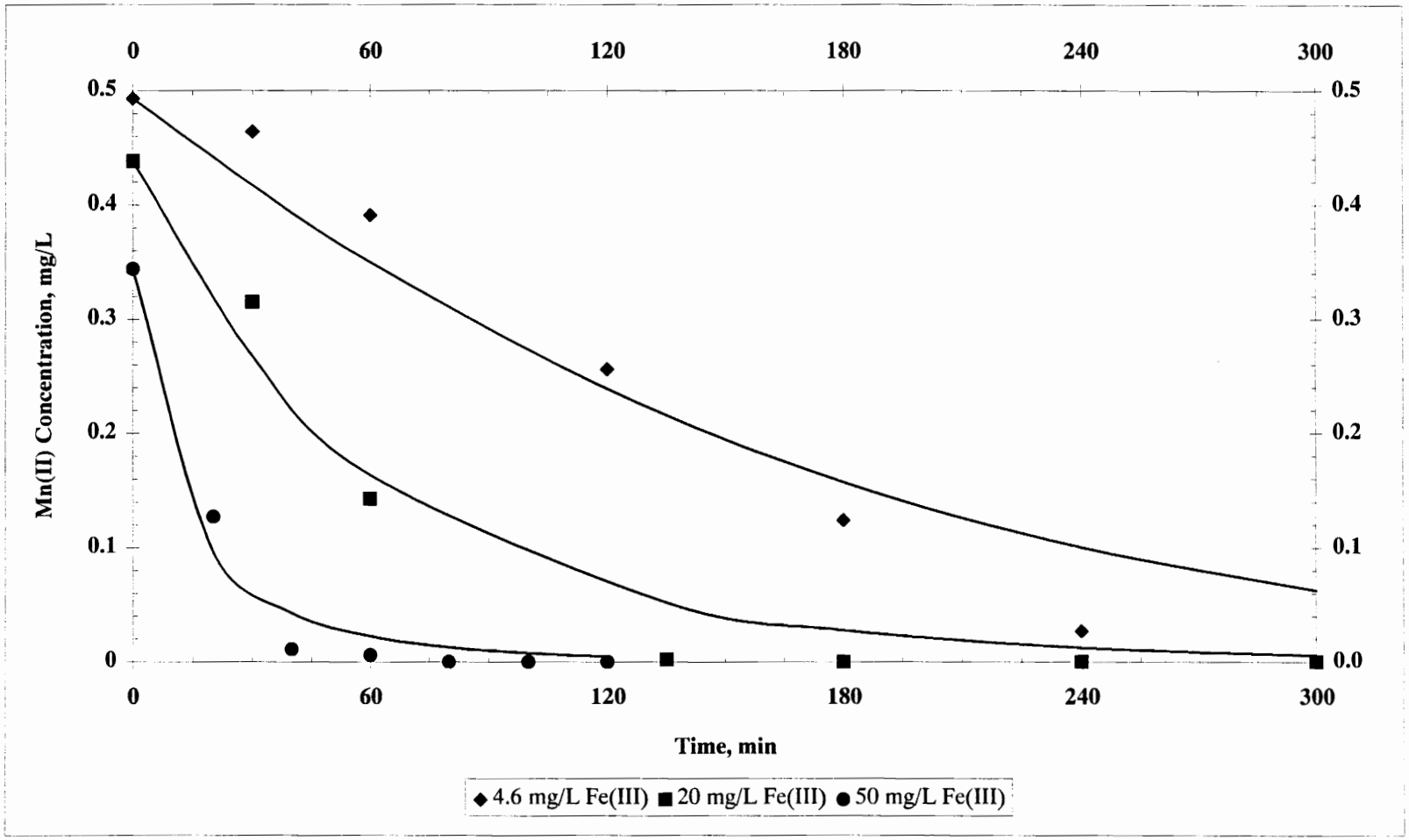

Figure 29: Model Predicted and Observed Results for Batch Reactor System at pH 8 (using best fit rate constant "k" for each Fe(III) concentration.) Experimental Conditions as stated for batch studies.

Again, the Runge-Kutta method of differential equation estimation was used to develop a solution to these equations. The resulting solution is an estimate of the effluent Mn(II) concentration for a continuous flow system for the system parameters used in the equations. The "k" value used in the model equations for the continuous flow system (slurry reactor system) is the average value determined by the batch system model under pH 8 conditions, 3.43×10^{-2}.

Figure 30 shows the model predictions for effluent Mn(II) and HOCl concentrations assuming that only iron oxides participate in the adsorption and subsequent oxidation of Mn(II). This assumption would hold only for the initial startup of the reactor system because, as shown in Figure 23, the manganese oxide concentration increases with time. One would expect that these manganese oxides would also participate in the adsorption/surface oxidation steps as previously described, resulting in lower effluent Mn(II) concentrations.

The "dip" in Mn(II) concentration predicted by the model for the conditions noted is attributed to the transition from the rapid, adsorption step to the slower, oxidation step of the reaction. Initially, the iron oxides present adsorb solution Mn(II) until the adsorptive capacity of the oxides is expended. The effluent Mn(II) concentration begins to increase until the oxidation of Mn(II) on the iron oxide surface begins resulting in a sustainable, consistent effluent quality. Additional model estimations under various operating conditions are provided in Appendix D; the bolded parameter indicates that input was changed from the previous simulation provided. Generally, the model provides a good indication of the importance of each of the key system parameters, however, because of the limited amounts of data available under this work, the quantitative accuracy of the model cannot be assessed.

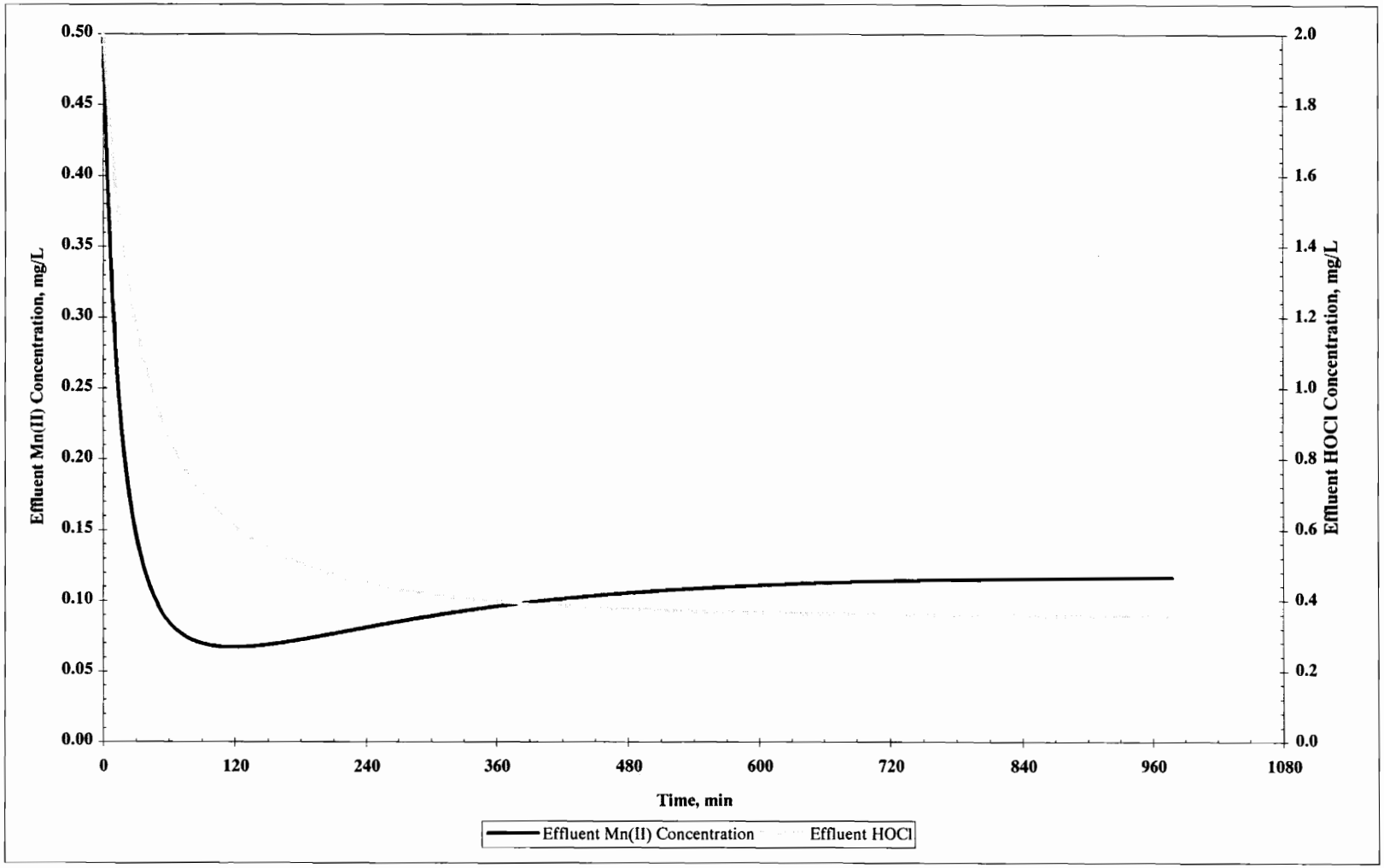

Figure 30: Predicted Results for CSTR Model: Conditions (unless otherwise indicated): Influent Mn(II) = 0.50 mg/L, Initial [FeO] Slurry = 280 mg/L as Fe, Influent Fe(II) = 2 mg/L, $[Ca^{+2}]$ = 3 meq/L, $[HCO3^{-}]$ = 3 meq/L, Temperature 10-15°C, HOCl Dose = 2 mg/L, pH = 8, θH = 2 hours.

CHAPTER V
DISCUSSION

This chapter is intended to provide a thorough discussion of the results presented in the previous chapter and to provide a basis for the development of meaningful conclusions that can be taken from these studies. From the results previously presented it appears obvious that some interaction does indeed occur between Mn(II) and oxidized iron (Fe(III)) particles in solution at pH values between 6 and 8. Some important considerations brought about during these studies are presented in the following sections.

A. Studies of Possible Mn(II) Removal Mechanisms

1. Formation of $MnCO_{3\,(s)}$ and Adsorption onto $CaCO_{3\,(s)}$. Because of the solubility relationships between Mn(II), Ca^{+2}, and CO_3^{-2} ,which are affected by solution pH, it was necessary to determine if either $MnCO_{3(s)}$ formation or $CaCO_{3(s)}$ formation could directly affect the Mn(II) concentration. Previous researchers including Davies[2] have noted the interferences on Mn(II) oxidation studies at high pH levels due to $MnCO_{3(s)}$ formation whereas others note that it is not a problem for up to 20 hours after saturation.[59]

Using the experimental parameters listed in Chapter III, a white precipitate was observed in solution after a period of approximately 60 minutes. This observed precipitate corresponded with a reduction in Mn(II) as noted in Figure 8. The Ca^{+2} in the solution makeup was replaced with an ionic strength equivalent of Na^{+} to eliminate the formation potential of $CaCO_{3(s)}$. The Mn(II) removal observed as depicted in Figure 9, was considerably less when compared to the previous experiment indicating that $MnCO_{3(s)}$ formation plays a minor role Mn(II) removal; thus, $CaCO_{3(s)}$ formation and the adsorption of Mn(II) onto its surface or co-precipitation was primarily responsible for the observed Mn(II) reduction.

At pH 8, no precipitate was observed during testing and subsequently the Mn(II) concentration was effectively unchanged as summarized in Figure 10. For this reason,

subsequent experimentation was conducted at solution pH less than 8 pH units so that these solid formations could not interfere with the iron catalyzed Mn(II) removal studies. (Recall that the field data shown in Table 1 was taken under solution pH ranging from 7.3-7.5.)

2. Solution Phase Oxidation. Several researchers have noted the ineffectiveness of HOCl to oxidize Mn(II) in solution.[1, 34] Studies were conducted to confirm these findings to ensure that the unique set of experimental conditions used during these studies would produce similar results. Studies, the results of which are shown in Figure 11, conducted at pH 7 and 8 confirmed the findings of previous researchers that Mn(II) is not effectively oxidized by HOCl at pH levels less than 8 pH units. The experiment at pH 8 was allowed to continue for a period of 21 hours at which point a reduction of only 6% of the initial Mn(II) was measured; this further indicates the slow kinetics of such oxidation. Once a $MnO_{x(s)}$ surface develops in solution, one would expect the oxidation kinetics to increase substantially as the surface serves as a site for adsorption as noted by Morgan and Stumm[40] and enhances the oxidation of the sorbed Mn(II) as observed by Hao[23]. As noted by Knocke et al.[1], however, the slower oxidation kinetics observed can be attributed to the depressed temperature of 10° C used during experimentation. The formation of $MnO_{x(s)}$ was subdued by the lower temperatures and the neutral pH conditions, both factors that affect the release of H^+ from the Mn(II) surface in turn affecting the reduction-oxidation reactions which occur via transfer of electrons (H^+).

3. Adsorption of Mn(II) onto Freshly Precipitated Iron Oxides. One hypothesis for the reduction in Mn(II) in the field studies was the adsorption of Mn(II) onto the oxidized Fe(III) surface. However, as summarized by Figures 12 and 13, the capacity for Mn(II) by the Fe(III) surface is relatively small. The observed Mn(II) adsorption was indeed solely adsorption on the Fe(III) surface rather than entrapment of Mn(II) within forming Fe(III) flocs as Mn(II) was added after Fe(II) oxidation during all adsorption studies. This

is one aspect of the experimental techniques that differs from that experienced under water treatment plant conditions. Normally, the reduced metal species are part of the raw water makeup and have the ability to interact at all phases of the treatment process. The technique used during these studies allows one to quantify that Mn(II) removal which can be solely attributed to adsorption onto the Fe(III) surface and the Mn(II) removal occurring as a result of other processes. Also, it allows for the development of isotherms for the adsorption of Mn(II) onto Fe(III).

The type of adsorption that was observed between the Mn(II) and the Fe(III) oxides and Mn(II) and $MnO_{x\,(s)}$ is hypothesized to be physical adsorption, not chemical adsorption. The bonds between the constituents in physical adsorption are typically weaker than those in chemical adsorption, and the adsorption is oftentimes reversible because of this fact. This was exhibited in the work presented by Lloyd et al.[59] for Mn(II) adsorption onto $MnO_{x(s)}$. The amount of Mn(II) that is adsorbed by the Fe(III) oxides is dependent upon the amount of Mn(II) in solution and the temperature.

Several different isotherm theories have been developed, the most well known being those by Freundlich and Langmuir. Freundlich theory most often applies to carbon adsorption where there is a linear response between the logarithm of the solute concentration and the logarithm of the amount adsorbed per unit weight of adsorbent. However, in cases where a maximum capacity is observed, Langmuirian theory applies. (The data collected during these studies were tested using both Langmuir and Freundlich theory with Langmuirian theory more closely predicted the data. These calculations are included in Appendix C.) As noted in Figure 12, a maximum capacity was observed in each of these adsorption studies. Therefore, the key assumption of Langmuirian theory is satisfied, a fixed number of sites are available for adsorption on the surface of the adsorbent.[66] Although it is difficult to conclude with the number of data points shown, the same theory could be applied to Figure 14 for the adsorption of Mn(II) onto purified Fe(III) oxides.

As previously reported the observed capacity of the Fe(III) surface for Mn(II) at pH 8 was 0.005 mg Mn(II)/mg Fe(III). When compared to the results of Davies[2] who conducted similar experiments, the values appear to be significantly lower than those Davies reported. Figure 31 shows a plot of data taken from Davies' work with the data point collected under these studies at pH 8 plotted. One would expect the point to lie closer to the line indicated for lepidicrocite rather than geothite since the Fe(III) oxides used in these studies were a "fresh" precipitate.

Naturally, when two studies are conducted using different methods by different researchers, results will differ; however, some explanation must exist for this rather large discrepancy. One key difference is in the preparation of the iron oxide particles used during experimentation. The oxides used during these studies were formed in solution immediately prior to the addition of the Mn(II). These solids were also exposed to the ionic strength of the test solution for a period of time prior to Mn(II) addition. Davies prepared his iron oxides in advance, washing them with distilled water and storing them in a plastic container. Thus, when his solids were to be used they had not been exposed to the ionic strength of the solution, instead the adsorption sites were free of sorbed particles until added to the test solution.

A key experimental parameter when conducting these studies is the length of time allowed for an equilibrium to occur between the Fe(III) surface and the Mn(II) in solution. Several initial tests using relatively small Fe(III) concentrations were conducted measuring the Mn(II) concentration over prolonged time periods. These results, plotted in Figure 32, indicated that the equilibrium between Mn(II) and Fe(III) occurred within 5 minutes of interaction as the Mn(II) concentration did not change significantly over the remainder of the reaction time. For this reason, the adsorption data collected as part of this work were collected after 5 minutes of interaction between the Mn(II) and Fe(III). An oversight in this decision was the lack of investigating the required equilibrium time when higher concentrations of Fe(III) were studied. Perhaps, because of the increased amount of surface present when higher Fe(III) concentrations are used, the time required for adsorption equilibrium to be reached may be somewhat longer. In addition, the

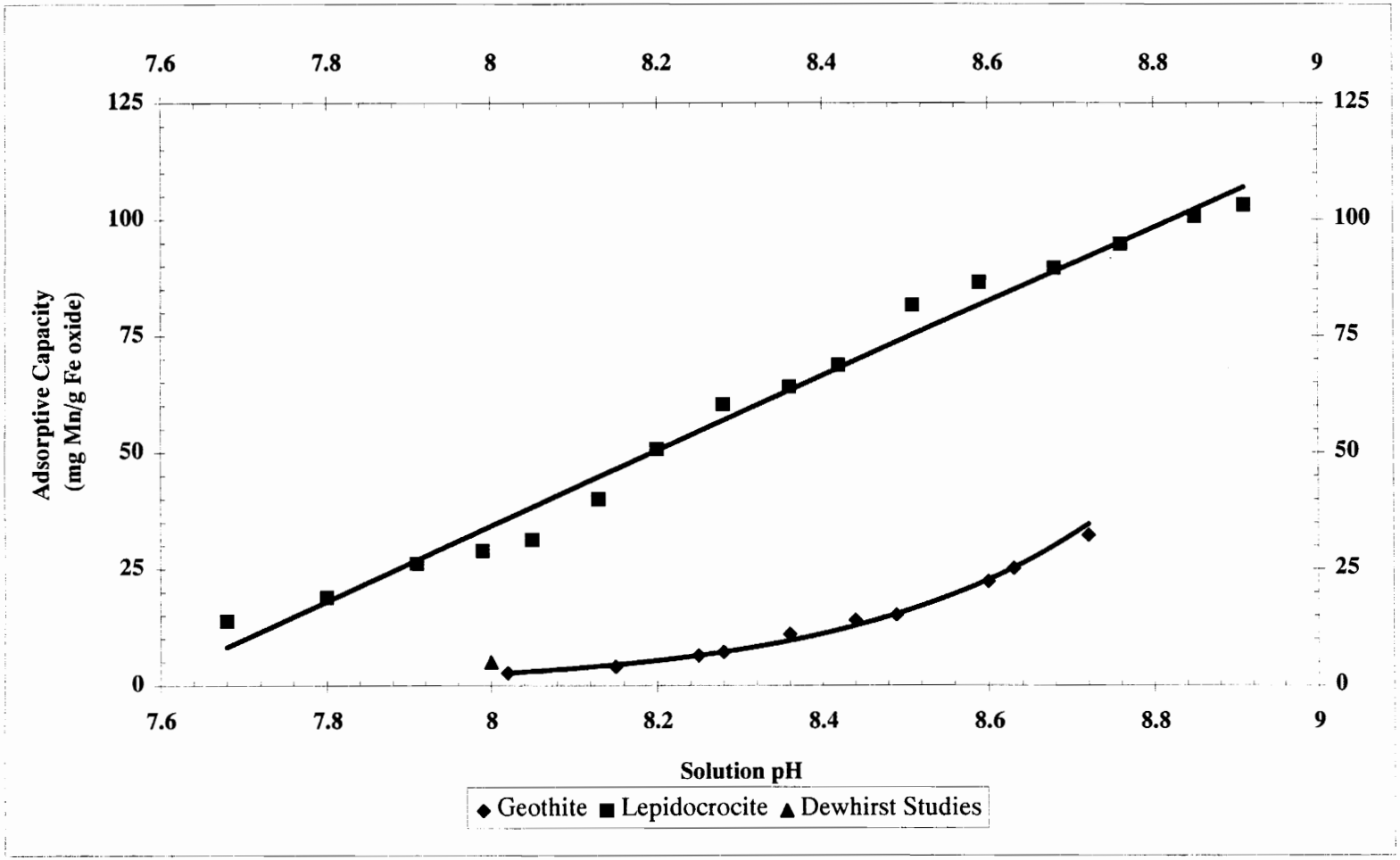

Figure 31: Comparison of Results Obtained by Davies[2] Compared with Results Obtained During These Studies (Adapted from Davies[2]; Davies experiments at 25°C; Dewhirst Studies at 10°C).

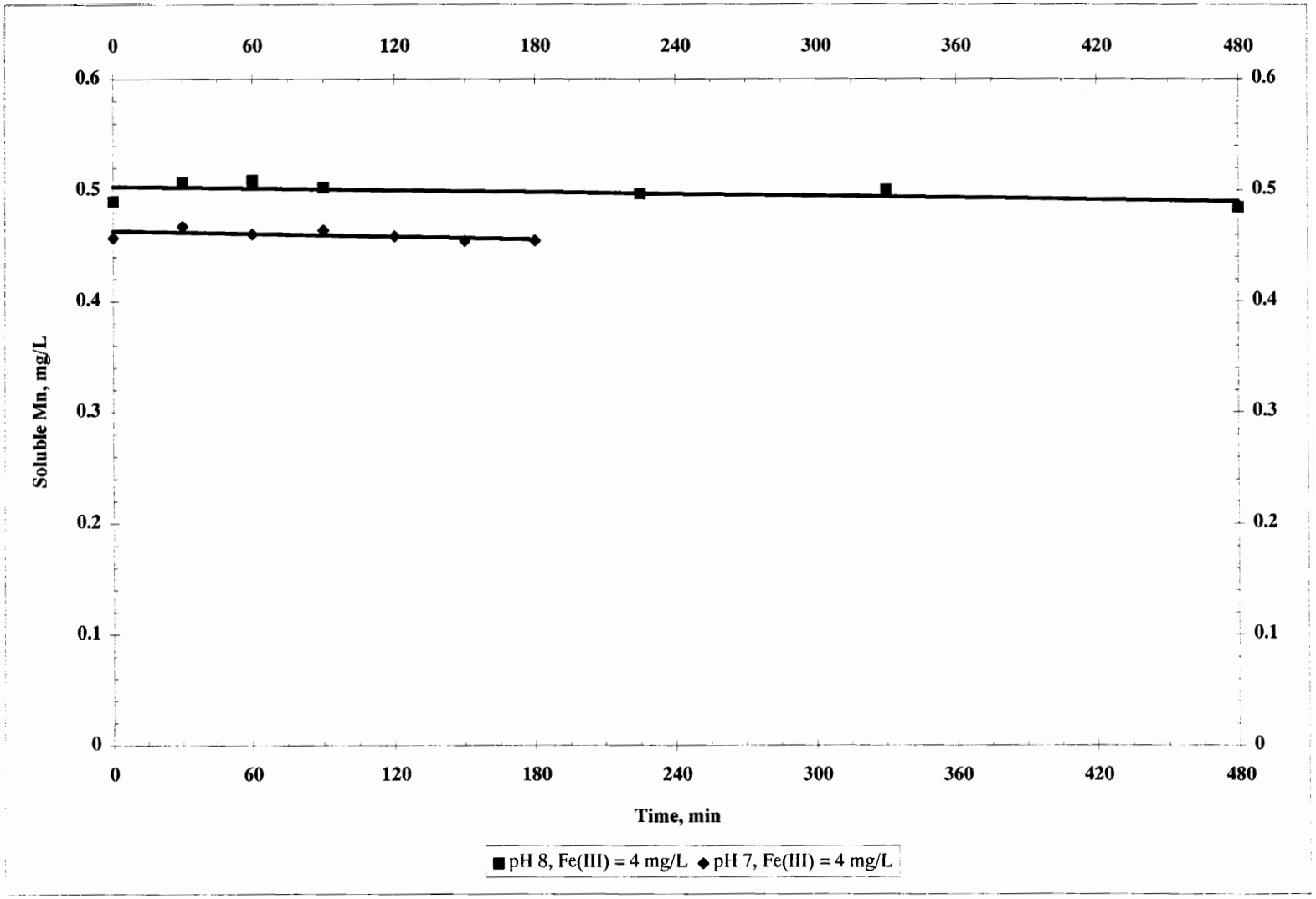

Figure 32: Extended Mn(II) Exposure to Fe(III) for Determination of Optimum Reaction Time for Isotherm Studies. Experimental Conditions: $[Ca^{+2}]$ = 3 meq/L, $[HCO_3^-]$ = 3 meq/L, $[Mn(II)]_O$ = 0.50 mg/L, Temperature 10°C, pH and Fe(III) as indicated.

depressed temperatures used during these studies (10°C) compared to the 25°C used by Davies[2] could affect the **rate** of adsorption significantly. Metcalf and Eddy, Inc.[67] suggests that lower amounts of adsorption occur at lower temperatures; this was seemingly confirmed by the results of this study. This may explain a portion of the difference noted between the results of these studies and those of Davies[2].

The results of this study could also be compared to those of Lloyd et. al.[59] who presented Langmuir isotherms for Mn(II) adsorption onto hydrated iron oxides (Fe(III)) and $MnO_{x(s)}$ at 10°C. Sung and Morgan[56] also present adsorption data for Mn(II) onto the Fe(III) which is noted only for reference. Lloyd et al.[59] noted that adsorption equilibrium was observed to occur after a period of only five minutes, the same time period used for the studies presented by this paper. The authors reported that at a solution pH of 8.0, the maximum adsorption ratio is 0.05 mg sorbed Mn(II) per mg of Fe(III) compared with a ratio of 0.005 mg Mn(II)/mg Fe(III) observed during the studies conducted for this paper. One potential cause for this order of magnitude difference in adsorption ratios is the ionic strength of the solution used during this research is approximately 2.5 times that used by Lloyd et al.[59] in the collection of their data. Therefore, numerous ions are competing for the limited number of available adsorption sites on the oxide surface; this in turn may reduce the amount of observed Mn(II) adsorption.

Obviously, a discrepancy exists between the data presented by these three studies. Most likely, these differences can be attributed to the properties of the iron oxides used in each study. The manner in which these solids were formed affects their chemical characteristics significantly. To provide a true comparison of the results between these three studies, an analysis of the surface areas of the iron oxides used would be required. Unfortunately, this was beyond the scope of this research. Thus, it is recommended that future researchers thoroughly investigate, accounting for temperature, surface area variability and other factors, the required equilibrium time that should be used to study the Mn(II) adsorption or other species adsorption onto a surface.

The noted adsorption of Mn(II) onto the Fe(III) surface obviously had some effect on the removal of Mn(II) from solution; however, the next phase of the research focused on the possible catalyzing effect the oxidized iron surface has on the sorbed Mn(II). The primary question to be addressed was whether or not the iron oxide surface could assist and serve as a catalyst in the oxidation of Mn(II), similar to the phenomenon observed when $MnO_{x(s)}$ is present in solution.

B. Mn(II) Removal via Surface Catalyzed Oxidation of Mn(II) with Fe(III) Oxides

Although the iron surface does not provide as much adsorptive capacity as an $MnO_{x(s)}$ particle with respect to Mn(II) adsorption, it is much easier to oxidize Fe(II) than Mn(II) using weaker, less expensive oxidants under normal water treatment and pH conditions. While it is possible to develop an $MnO_{x(s)}$ particle in solution using stronger oxidants, the resulting particle is often not of sufficient size nor electrostatically stable to be settled or filtered from solution. Thus, the use of the iron oxide particle as an initial adsorption surface upon which particle growth can occur is a possible Mn(II) removal scheme that appeared to be worthwhile and was further investigated during these experiments.

As noted in Figure 15, when Fe(II) is concurrently oxidized with Mn(II) in solution, a true representation of the rate of Mn(II) oxidation via catalyzation of the Fe(III) cannot be studied. Although this is the condition that would occur under water treatment plant conditions, it was first necessary to determine how much of an effect the Fe(III) surface had on Mn(II) oxidation. Thus, the remainder of the experiments conducted were performed by first oxidizing the Fe(II) to Fe(III) via oxygenation and then applying the desired concentration of Mn(II) into solution. This eliminated the potential for Mn(II) being trapped in the forming Fe(III) floc particles.

Figures 16 and 17 clearly indicate the catalyzing effect higher concentrations of iron oxides have on the oxidation and removal of Mn(II) from solution. Regardless of the solution pH, an increase in Fe(III) concentration corresponds to an increase in the rate of

Mn(II) removal. Note that the results plotted in Figures 16 and 17 show the combined effects of the removal of Mn(II) as a result of adsorption onto the Fe(III) surface as well as the surface catalyzed oxidation step. Time zero for these plots is the start of the adsorption step; chlorine was added after a period of five minutes.

Another key observation in the analysis of the data presented is the comparison between the expected versus actual HOCl demand with respect to the removal of Mn(II) from solution. Assuming that the Mn(II) is immediately oxidized once it has been adsorbed by the Fe(III) surface would be an incorrect assumption according to Figure 18. This suggests that the oxidation of Mn(II) once on the surface is slow when compared to the adsorption step. This fact was utilized in the development of the model that was presented in Chapter IV. However, the Mn(II) oxidation rate by HOCl is still enhanced by the presence of the surface in that it is much more rapid than solution phase oxidation.

Taking a closer look at the actual rate of Mn(II) removal due to the Fe(III) surface catalyzed oxidation step and adsorption, it would be expected for the reaction order to be at least one as is normally the case under a catalyzed condition. However, as exhibited in Figure 19 which provides an analysis of the surface catalyzed oxidation rate, this is not true as the reaction order actually approaches zero.

This is initially puzzling until the combination of mechanisms responsible for the observed outcome are considered. Essentially, three mechanisms are acting simultaneously to remove Mn(II) from solution:

1. Mn(II) adsorption onto Fe(III),
2. Mn(II) oxidation on Fe(III), and
3. Mn(II) adsorption onto $MnO_{x(s)}$.

The data plotted in Figure 19 remove the first mechanism from consideration as the initial data point at time zero follows the adsorption step of Mn(II) onto Fe(III). Thus, the plot exhibits the reduction in Mn(II) due to its oxidation on the Fe(III) surface and its adsorption onto the formed $MnO_{x(s)}$ surface on the Fe(III) particle. The combination of

these mechanisms may indeed result in an overall zero order reaction. Unfortunately, these two mechanisms could not be separated for individual study to determine the role each plays in Mn(II) removal. However, the development of an $MnO_{x(s)}$ surface on the Fe(III) oxide, as also noted by Lloyd et al.,[59] may provide an explanation for the constant rate of Mn(II) removal observed. As the Mn(II) concentration decreases in solution (as it is adsorbed and oxidized on the Fe(III) surface), the $MnO_{x(s)}$ surface that develops has a greater affinity for Mn(II) than the Fe(III) surface. The result is what appears to be a constant Mn(II) removal rate; actually the catalyzed Mn(II) oxidation rate has slowed, but the $MnO_{x(s)}$ adsorption has counteracted this reduction in the rate of catalyzed Mn(II) oxidation.

When analyzing the reaction rates for Mn(II) oxidation in the presence of Fe(III), the rate is observed to increase with an increase in the Fe(III) concentration as exhibited in Figure 20. (Note, however, that the rate over the Fe(III) concentrations studied does not change a great deal based on the range of the y-axis values.) However, if the reaction rate is normalized with respect to the iron oxide concentration, as shown in Figure 33, the opposite is true as the reaction rate decreases with increase in Fe(III) concentration. This outcome is not surprising based upon the nature of the oxidized iron product, predominately $Fe(OH)_{3(s)}$. The product is somewhat amorphous and flocculent, therefore some agglomeration of iron oxide particles will occur. Assuming such interaction between the iron particles, not all of the iron added to solution results in additional Fe(III) surface for catalyzing Mn(II) oxidation.

The interaction noted during these experiments between the Fe(III) oxides and Mn(II) have also been noted by other researchers as well.[2,55,56,59] Lloyd et al.[59] noted that during the adsorption experiments for Mn(II) onto Fe(III), the adsorbent color changed from the orange associated with iron to a chocolate brown indicating the possible presence of $MnO_{x(s)}$ as well. Wilson[55] also noted that Mn(II) oxidation is indeed catalyzed by the iron surface similarly to that observed in the presence of $MnO_{x(s)}$. Sung and Morgan[56] reported that the oxidation rate of Mn(II) on freshly precipitated Fe(III) was

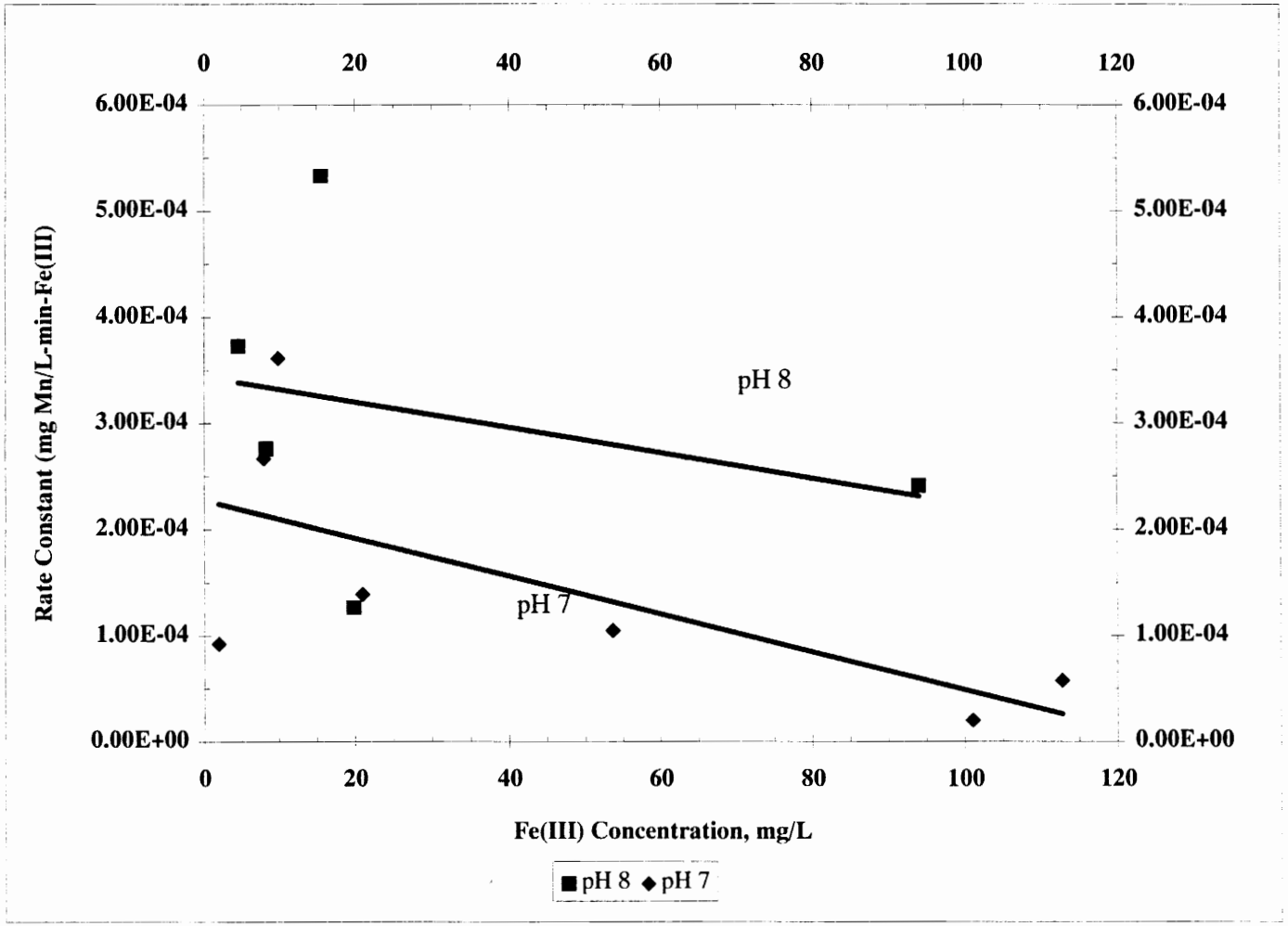

Figure 33: Experimentally Determined Rate Constants for Mn(II) Removal During Batch Studies Normalized with Respect to Fe(III). Experimental Conditions: $[Ca^{+2}]$ = 3 meq/L, $[HCO_3^-]$ = 3 meq/L, $[Mn(II)]_O$ = 0.50 mg/L, Temperature 10

approximately equal to that of Mn(II) onto $MnO_{x(s)}$. However, an assumption made when analyzing the rate data appears to be unacceptable based upon the findings of this work; it was assumed that "the surface is not altered significantly with the surface oxidized species." Several researchers[2,55,56] used excessive concentrations of Mn(II) (2.75-5.5 mg/L) to study the induced oxidation rates. The reaction rate would be expected to slow as Mn(II) is reduced; therefore, the catalyzing effect is more evident when higher Mn(II) concentrations are used. The studies presented under this work were intended to study the catalyzed oxidation under more typically observed Mn(II) concentrations for water treatment.

Each of the previous researchers'[2,55,56,59] results discussed conducted their experiments in the presence of oxygen whereas the testing conducted during this research used a more powerful oxidant, chlorine. As noted by studying the results presented by Wilson[55] and Lloyd et al.,[59] elevated pH values are required for Mn(II) oxidation to occur in a timely manner. Lloyd et al.[59] also noted that as a result of higher pH values being used, as $MnO_{x(s)}$ develops in solution, the suspension of particles becomes more difficult to settle as the zero point of charge for $MnO_{x(s)}$ lies between 2.8 and 4.5 pH units. Because of the elevated pH used by Lloyd et al.,[59] Ca^{+2}, which could normally help to stabilize the $MnO_{x(s)}$,[33] may instead be precipitated out of solution as $CaCO_{3(s)}$. As noted previously, the solution pH used during this research does not allow for the precipitation of $CaCO_{3(s)}$, leaving Ca^{+2} available for stabilizing the $MnO_{x(s)}$ that forms. Also, through the use of a stronger oxidant such as chlorine, the reactions proceed much more rapidly, allowing for treatment under typical water treatment conditions without requiring longer detention times.

The next phase of the research simulated water treatment plant conditions, to test a high solids reactor system that can be utilized to remove both iron and manganese from solution using chlorine as an oxidant. The use of such system appears to be a more viable option that the typical groundwater treatment system employed currently (Figure 1).

C. Fe(III) Oxide Slurry Reactor System and Mn(II) Adsorption onto $MnO_{x(s)}$

From the discussion presented thus far, it is apparent that Mn(II) oxidation can indeed be enhanced by the presence of Fe(III) and the use of HOCl as an oxidant. This portion of the research sought to develop an acceptable bench scale reactor system that could be employed at a water treatment facility for the removal of Mn(II) and Fe(II) from solution. The system presented here could also be used for surface water supplies containing Fe(II) and Mn(II), but the water must have a low organic content as HOCl is used as the oxidant which is known to form harmful by-products, trihalomethanes and haloacetic acids.

One note when considering the results presented for the slurry reactor system is that the experimental design was unable to maintain the temperature throughout the experiments at 10°C, instead the temperatures within the reactors were maintained between 13-20°C. This should improve performance as adsorption and oxidation rates should increase with temperature.

The initial results presented in Figure 21, prove how vital the presence of an oxidant is and that the observed phenomenon is not merely an adsorptive process. In a matter of hours the effluent Mn(II) concentration approaches that of the influent concentration. This result occurs once the adsorptive capacity of the large concentration of Fe(III) oxides has been expended. (Note that breakthrough occurred first in the reactor that contained a smaller concentration of Fe(III) oxides.) The pH of the solution is slightly less than 7 which is not conducive to adsorption processes which prefer higher pH conditions (resulting in a more negatively charged particle as H^+ is expended from the surface site). Also note that no additional HOCl was added to solution to assist with Mn(II) removal, but there was a 1 mg/L residual in the tap water fed through the system. However, this amount of HOCl is inadequate to oxidize the Fe(II) being fed to the system which would require a minimum of 1.28 mg/L HOCl as dictated by stoichiometry[1]. Thus, little or no HOCl was available for Mn(II) oxidation.

Following the addition of supplemental HOCl to the system (Figure 22), the effluent Mn(II) concentration rapidly decreased to levels well below the SMCL of 0.05 mg/L despite the pH being held less than 7 standard units. The use of chlorine in the system provides several advantages over the conventional oxidants used for Mn(II) removal:

- Stronger oxidant than oxygen allowing for more rapid reaction times at lower pH values,
- Provides a disinfectant residual which will be required following the implementation of the Groundwater Treatment Rule,
- Allows the Mn(II) to be adsorbed onto larger Fe(III) particles rather than oxidizing the individual Mn(II) particles (as potassium permanganate would do) providing for the settling or filtration of the combined particles from solution,
- HOCl is more flexible to changes in raw water quality; permanganate will turn water pink if overdosed due to sudden decrease in Mn(II).

As alluded to previously, however, HOCl would not be an acceptable choice for waters laden with organic materials. In general, the successful performance of the system required that a residual of HOCl exist in the effluent. This indicated that the oxidant demand of the system had been satisfied. Normally, a HOCl residual of 0.50 mg/L was associated with superior reactor performance.

Part of the discussion in the previous section suggested that $MnO_{x(s)}$ developed on the iron surface or was intermixed with the iron particles as the process continued over a period of time. A portion of the work conducted on this new system was devoted to understanding the effect that each of these oxide forms had on the removal of Mn(II) from solution. Data were collected in all experiments on the influent, effluent, and in-reactor concentrations of Mn(II) and Fe(II)/Fe(III) to study the possible "growth" of

$MnO_{x(s)}$ within the system. A portion of the data collected is plotted in Figure 23 which provides some enlightening information to the processes occurring within the slurry reactor system. Note the extended time period over which these results were taken as well as the trends that are evident. While the concentration of Fe(III) in the reactor decreased to a relatively constant value, the concentration of $MnO_{x(s)}$ within the system increased.

This observation is important for several reasons; first, it is believed that during the initial stages of operation only this steady-state concentration of iron particles participates in catalyzing Mn(II) oxidation. These particles, encapsulated by a $MnO_{x(s)}$ coating, grow in size helping them to settle rather than "washing out" of the reactor. Once a sufficient coating of $MnO_{x(s)}$ develops, this surface is believed to dominate the adsorption and oxidation of Mn(II) in solution. The freshly precipitated iron particles formed via oxidation and those remaining from the initial slurry do not participate and are washed out of the system because of their smaller size. Thus the steady-state iron slurry concentration most likely represents those particles initially encapsulated by $MnO_{x(s)}$ coatings.

Another point that should be noted from these observations and the data summarized in Appendix A is the importance of reactor hydraulics and design. The reactor system used in these experiments was not optimum as was evidenced by the loss of solids from the system. Ideally, these solids should settle from solution, and the slurry concentration would increase with time. Thus, a wasting of solids similar to the practices of a wastewater treatment plant would be used to maintain system control. The use of a settling aid polymer was not investigated, but is recommended during future studies if similar problems persist.

Based upon the data collected, the lack of settling cannot be solely attributed to the formation of particles (i.e. $MnO_{x(s)}$) that are far from their zero point of charge. The loss of solids was a problem continuously experienced by the system and periodically small upsets due to reactor hydraulics would result in additional loss of solids. The

reactors used in these experiments were indeed "bench-scale"; because of this fact they were unable to absorb minor system changes as well as a full scale reactor would. However, improvement was noted in retention of solids when the hydraulic detention time within the reactor was increased from 1 hour to 2 hours. The results presented were all observed using a 2 hour hydraulic detention time with the exception of the data presented in Figures 21 and 22.

The lack of defined mixing conditions is another deficiency of the conventional groundwater treatment facility for iron and manganese removal. The use of gentle mixing proved to be very beneficial to the success of the system. Without providing for interaction between the particles, adsorption would be curbed as well as the exposure of the adsorbed metal species to an oxidant source. However, mixing intensities should be maintained at levels consistent with flocculation, not rapid mix. The floc particles that were observed during these studies were very fragile in nature. As previously mentioned, the inability to stabilize and rectify the negative surface charge of $MnO_{x(s)}$ particles can lead to failure of the system.

The previous point provides insight into another benefit of the proposed system, the increased opportunity for particle interaction and flocculation. Flocculation theory for orthokinetic flocculation (equation shown) indicates the rate of flocculation is proportional to the square of number of particles and to the cube of the particle diameter.

$$Rate\ of\ Orthokinetic\ Flocculation = \frac{-2\xi G D^3 N^2}{3} \qquad (17)$$

where: ξ = *collision efficiency factor*
G = *velocity gradient*
D = *particle diameter*
N = *particle concentration*

Thus, the slurry reactor system (which resembles that of a solids contact unit) provides a significant number of particles for interaction. Also, because the particles grow via adsorption and subsequent oxidation, the diameter of the particles is

continuously growing. In this manner the flocculation of the particles is significantly enhanced allowing for the formation of larger, more settleable particles. Based upon the experimental methods used the particle sizes exceeded 0.45μm as minimal difference was noted between the filtrate of the 30k ultrafilters and the 0.45μm filters.

Because of the seemingly dominant role $MnO_{x(s)}$ has in catalyzing Mn(II) oxidation over time, its adsorptive properties for Mn(II) for use in this study were investigated. The adsorptive capacity observed for Mn(II) by $MnO_{x(s)}$ was reported earlier as 0.20 and 0.21 mg Mn(II)/mg $MnO_{x(s)}$ at solution pH of 7 and 8, respectively. Lloyd et al.[59] conducted similar experimentation at 10°C and reported a maximum adsorption ratio at pH 8 of 0.7 mg Mn(II)/mg $MnO_{x(s)}$. In the well known work of Morgan and Stumm[40], the adsorptive capacities of $MnO_{x(s)}$ for Mn(II) were observed to be 0.31 and 0.76 mol Mn(II)/mol $MnO_{2(s)}$ at pH 7 and 8, respectively (these values translate to 0.20 and 0.48 mg Mn(II)/mg $MnO_{x(s)}$, respectively). Again, a wide range of results is noted between the different results reported. Most likely this can be attributed to the formation and the chemical properties of the $MnO_{x(s)}$ particles formed by each researcher. Again, without taking a measurement of the surface areas it is difficult to say that the $MnO_{x(s)}$ particles formed by each are "equal."

Regardless of which values are compared versus the results previously presented for Mn(II) adsorption onto Fe(III), the capacity of the $MnO_{x(s)}$ surface far exceeds that of the Fe(III) surface. This explains the outstanding performance of the slurry reactor system once sufficient $MnO_{x(s)}$ surface had been developed within the reactor. As noted in Figures 26 and 27, only when the system is starved of HOCl does it approach a failure condition. Figure 27 provides a glimpse of the system performance under various chlorine conditions. After approximately 20 hours of operation at a 1 mg/L dose of HOCl, the HOCl dose is increased to 2 mg/L, a minimal amount for the influent levels of Fe(II) and Mn(II) entering the system (stoichiometry dictates that just under a 2 mg/L dose of HOCl will satisfy the requirements for the influent Mn(II) and Fe(II)). Reactor performance is outstanding for this minimal dose of oxidant. The presence of the $MnO_{x(s)}$

particles in solution provide stability to the system as well as absorbing slight fluctuations in influent Mn(II) and HOCl concentrations. The Fe(III)-oxide only system does not offer the same abilities primarily due to its lack of Mn(II) adsorptive capacity.

However, as previously mentioned the Fe(III) particles do serve a vital purpose in the system performance in that they are believed to be the initial site of Mn(II) adsorption and subsequent $MnO_{x(s)}$ formation. This provides for the formation of larger, more settleable particles that can be removed via conventional solids-liquid separation technologies. As has been stated previously, the oxidation of Fe(II) and Mn(II) can be accomplished rather simply using stronger oxidants, however, the removal of the oxidized particles from solution can be difficult. Treatment for the removal of iron and manganese is a two step process:

(1) oxidize the metal species to an insoluble form and

(2) remove the oxidized particle(s) form the finished water.

The second item is often overlooked when devising an effective iron and manganese removal strategy!

From the previous discussion and results presented it is apparent that the proposed reactor system will provide acceptable levels of effluent Mn(II) provided sufficient HOCl is provided. However, the same cannot be said of reactor performance at pH 6 as depicted in Figure 27 toward the end of the experimentation. What was observed under this scenario appeared to be **desorption** of Mn(II) and an upset in system performance. At the lower pH conditions, adsorptive capacities decrease as the H^+ ions more effectively compete for adsorptive sites on the surface of the oxide particles. This in turn reduces the ability of the oxides to enhance Mn(II) oxidation.

D. Model Results

1. Batch System Model. The batch system model was primarily used as a means of determining an appropriate rate constant value (k) to be used in the continuous flow model to be discussed in the next section. The results of the batch system model

provided some insight into the mechanisms of Mn(II) removal that were observed during experimentation.

The model does not appear to fully account for all of the Mn(II) removal mechanisms that occur at the various Fe(III) concentrations as there was some variability in the rate constant values determined. Under a perfect modeling condition, the model would predict the observed data over the range of conditions under study with no variability in the rate constant value. However, as observed in Figure 28, this was not the case for the pH condition modeled by this work as there is minor variability in the model predicted rate constants as the slope of the line indicates.

As the model was developed it was formulated using Freundlich isotherm theory and also formulated using Langmuir isotherm theory. The two models were conducted in a "side-by-side" comparison to determine which provided a better representation of the observed data. The comparison showed that the Langmuirian model provided a better fit of the predicted results to those observed in the laboratory as the residual sums of squares was lower. (The results of this comparison are provided in Appendix D.) It should be noted that other isotherm theory exists that was not considered under this work, therefore, it should not be implied that the Langmuir isotherm used in this modeling exercise will hold true in future research efforts. It is important to again note that the oxide particles formed during experimentation are somewhat unique and can be site specific, and thus future researchers should investigate all isotherm theories for the proper representation of their data.

2. Slurry Reactor System Model. As shown in Figure 30, the model developed provided a good representation of the importance of the key system parameters noted in previous discussion of the slurry reactor system. As previously mentioned, the quantity of data collected under these experiments was insufficient to conduct a full comparison on the quantitative accuracy of the model presented. However, several model simulations have been provided in Appendix D under various operating conditions, changes in detention

time, iron concentration, HOCl concentration, influent Mn(II), etc., to exhibit the importance and effect each of these parameters have on system performance. The model seems to be able to predict trends, similar to those observed during the laboratory studies.

One parameter that was included in the model equations that was not included in the modeling exercise was the adsorption of Mn(II) onto the $MnO_{x(s)}$ that is hypothesized to form on the outside surface of the iron oxide particles. As exhibited in the results presented, this surface has a much greater adsorptive capacity and has been observed to serve as a catalyst for Mn(II) oxidation.[23] Also, it was previously noted that this oxide surface does indeed provide stability to the system under conditions where the system would normally be stressed and approach failure. The inclusion of this term in the model should be considered further in future research. This will require more data collection to include the oxidation rate of Mn(II) in the presence of $MnO_{x(s)}$ and quite possibly a term to describe the growth of $MnO_{x(s)}$ in the system over time as was observed and noted in Figure 23. Model simulations including this term and the surface oxidation term for Mn(II) adsorbed onto the MnOx(s) surface are included in Appendix D.

The same type of solids accumulation term should be included for the iron oxides within the reactor system. Although from the data collected during these studies the iron oxide concentrations within the reactor system were observed to decrease to a steady state concentration over time, this was believed due to the hydraulics of the system used. Thus, it would be expected that the iron oxide concentration would also increase as the influent Fe(II) is oxidized to a solid Fe(III) particle.

Overall, the model presented here offers insight into the mechanisms that were observed to affect the removal of Mn(II) from the system. Generally speaking, it does predict the response in the effluent quality that would be expected from the changes made in the system parameters. Thus, this model provides a good baseline for the development of future models describing this phenomenon. These future models may provide additional input parameters, the ability to input a specific pH condition, or simply use a larger data set for comparisons between the model predicted results and those observed

experimentally. It is vital that prior to using the model developed herein, that sufficient data be collected for model calibration.

CHAPTER VI
SUMMARY & CONCLUSIONS

A. Summary of Results

An important consideration concerning the oxidation of Mn(II) is its subsequent removal from solution by solid-liquid separation techniques (i.e. filtration, etc.). This often poses more of a problem than actual oxidation as the species formed following oxidation carry a significant negative particle charge which must be neutralized for effective settling and/or filtration. Although the oxidation of Mn(II) can be accomplished, it is important to understand that Mn(II) removal is a two-step process; oxidation followed by removal of the insoluble manganese product from solution.

The results of these studies suggest that surface catalyzed oxidation by the iron surface may be a valuable technology to utilize for both iron and manganese removal. These data confirmed the field observations that soluble manganese interacts with iron oxide solids. It was hypothesized that the manganese in solution initially adsorbs to the iron surface after which the catalyzed oxidation occurs.

While this indicates that $Fe(OH)_{3\,(s)}$ could enhance Mn(II) removal via HOCl oxidation (catalyzed oxidation), the low concentrations of iron present in most waters would not provide enough surface to significantly improve Mn(II) removal. Thus, an engineered system was developed involving oxidized iron particles in a slurry reactor similar to solids contact units. By increasing the number of iron particles within the treatment basin, flocculation and removal of iron can be significantly improved. This in turn will enhance manganese removal because of the adsorptive/oxidative interaction it has with the iron surface.

The proposed system which is depicted in Figure 34, offers several advantages over the conventional groundwater treatment system for iron and manganese removal. These include:

- Increased number of particles (for flocculation)

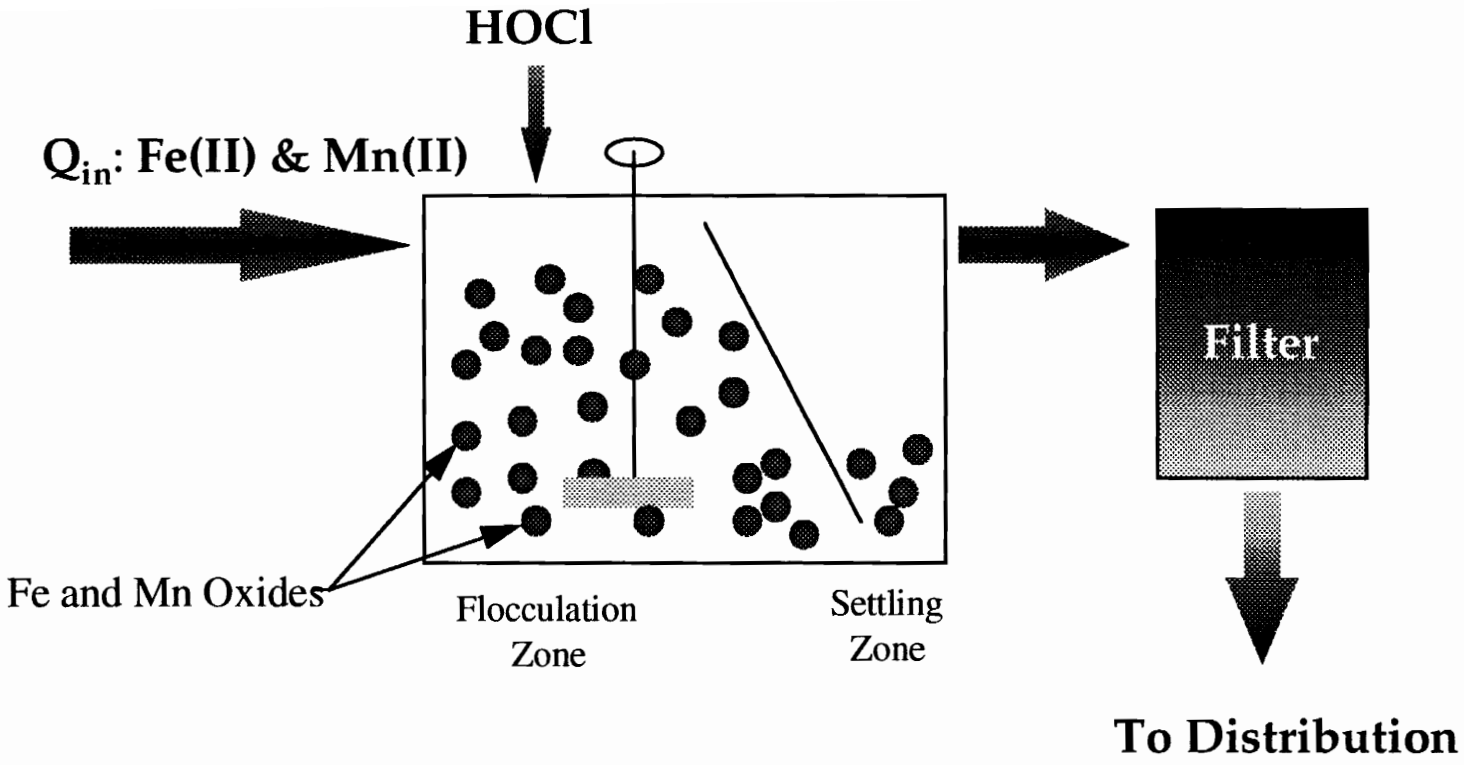

Figure 34: Schematic of Proposed Slurry Reactor System

- More economical; HOCl relatively inexpensive oxidant for Mn(II) removal
- Groundwater Disinfection Rule will require disinfection
- Larger particles; increased sedimentation decreasing filter loading
- More flexible to changes in water quality (chemical dosing not as critical with HOCl)

Additional information concerning the performance of the newly engineered reactor system was also discovered under this research effort. The most critical observation was the dominance that the $MnO_{x(s)}$ that forms over time has on system performance. Because of its high adsorptive capacity for Mn(II), $MnO_{x(s)}$ provides the system with additional stability which allows for minor changes in HOCl dose or Mn(II) concentration to be adsorbed by the system.

The success of the slurry reactor system as reported by these studies indicates that it has potential for improving the conventional means of groundwater treatment for iron and manganese removal. However, additional research is required to better define key system parameters and to develop a more detailed model for such a system. Also, the problems associated with the settling of the particles should be further assessed to determine if it is solely due to reactor hydraulics, and if polymer addition can alleviate the problem.

B. Conclusions

Several conclusions can be drawn from the results presented in this paper:

(1) The interaction noted between Mn(II) and Fe(III) at the groundwater treatment facility under study is the result of a combined adsorption-surface oxidation reaction that occurs on the surface of the iron oxide particle.

(2) The rate of Mn(II) adsorption-surface oxidation increased with increasing concentration of iron oxides.

(3) The proposed slurry reactor system offers an effective solution to the Mn(II) removal problems encountered by existing groundwater treatment systems by utilizing the interactions observed.

(4) The key system parameters for the slurry reactor system include iron oxide concentration, pH, chlorine concentration, and detention time.

(5) Over long periods of operation, the manganese oxide surface dominates the adsorption-surface oxidation of Mn(II) in the system resulting in improved performance and greater system stability.

C. Areas of Future Research

The results of these studies indicated that the conventional treatment schemes used currently can be done more efficiently and with higher levels of performance. However, to fully grasp the potential that the system presented by these studies offers, additional work should be performed. The system parameters that should be used in the design of a full-scale system should be better defined. The results presented by this study indicated that the following are key design parameters:

- hydraulic detention time
- oxidant dose
- relative concentrations of iron and manganese oxides within the system
- solution pH

However, additional research is required to better define the recommended limits of these parameters and to develop a more detailed model for such a system.

The problems associated with the settling of the particles should be further assessed to determine if it due to reactor hydraulics or other factors such as detention time, clarifier overflow rates, or mixing intensity. The use of a polymer to assist in the

flocculation and settling of the particles should also be studied to determine if this could alleviate the problem.

Finally, the model presented has several deficiencies that should be addressed in the development of a new model that allows for more variation in system parameters. For example, the model presented with this work only applied to the pH 8 conditions as accurate isotherm and oxidation rates were only measured for this condition. A model with a pH term included would add a great deal of flexibility to determining optimum ranges of operation. Secondly, the model presented also assumes that the iron and manganese oxide concentrations remain constant which as presented previously is not the case. This was an assumption made to simplify the model that should be allowed to vary in future modeling efforts on the system presented. These are two examples of model deficiencies that currently exist with the model presented herein that should be addressed in future work. Again, it is stressed that prior to using the model developed during these studies further, it should be calibrated to insure its accuracy.

The results presented in this paper will hopefully stimulate future researchers to further investigate this apparently useful phenomenon.

CHAPTER VII

REFERENCES

1. Knocke, William R. *et al.* American Water Works Association Research Foundation Report: Alternative Oxidants for the Removal of Soluble Iron and Manganese. March 1990.

2. Davies, Simon H.R. Thesis, Mn(II) Oxidation in the Presence of Metal Oxides. California Institute of Technology. 1985.

3. Adams, Reginald B. "Manganese Removal by Oxidation with Potassium Permanganate." *Journal of the American Water Works Association*, 52:2:219-228 (February 1960).

4. Weng, Cheng-nan *et al.* "Ozonation: An Economic Choice for Water Treatment." *Journal of the American Water Works Association*, 78:11:83-89 (November 1986).

5. Wong, James M. "Chlorination-Filtration for Iron and Manganese Removal." *Journal of the American Water Works Association*, 76:1:76-79 (January 1984).

6. Ponitus, Frederick W. "Complying With the New Drinking Water Regulations." *Journal of the American Water Works Association*, 82:2:32 (February 1990).

7. Knocke *et al.* "Impact of Dissolved Organic Carbon on the Removal of Iron During Surface Water Treatment." Unpublished Article.

8. Knocke, William R. ET AL."Examining the Reactions Between Soluble Iron, DOC, and Alternative Oxidants During Conventional Treatment." *Journal of the American Water Works Association*, 86:1:117-127 (January 1994).

9. Sung, Windsor and Morgan, James J. "Kinetics and Product of Ferrous Iron Oxygenation in Aqueous Systems." *Environmental Science & Technology*. 14:5:561-568 (May 1980).

10. Bowers, A.R. and Huang, C.P. "Role of Fe(III) in Metal Complex Adsorption by Hydrous Solids." *Water Research*. 21:7:757-764 (1987).

11. Posselt, Hans S. *et al.* "Cation Sorption on Colloidal Hydrous Manganese Dioxide." *Environmental Science & Technology*. 2:12:1087-1093 (December 1968).

12. Morgan, James J. Chemical Equilibria and Kinetic Properties of Manganese in Natural Waters (1967). in: *Principles and Applications of Water Chemistry*, Samuel D. Faust and Joseph V. Hunter. eds., John Wiley and Sons, New York, 561-624.

13. Hoehn, Robert C. ET AL. "Effects of Storage and Preoxidation on Sludge and Water Quality." *Journal of the American Water Works Association*. 79:6:62 (June 1987).

14. Stone, Alan T. and Morgan, James J. "Reduction and Dissolution of Manganese (III) and Manganese (IV) by Organics: 1. Reaction with Hydroquinone." *Environmental Science & Technology*. 18:6:450-456 (June 1984).

15. Stone, Alan T. and Morgan, James J. "Reduction and Dissolution of Manganese (III) and Manganese (IV) by Organics: 2. Survey of the Reactivity of Organics." *Environmental Science & Technology*. 18:8:617-624 (August 1984).

16. Stone, Alan T. "Reductive Dissolution of Manganese (III/IV) Oxides by Substituted Phenols." *Environmental Science & Technology*. 21:10:979-987 (October 1987).

17. Bourg, Alaln C.M. and Bertin, Clotilde. "Seasonal and Spatial Trends in Manganese Solubility of an Alluvial Aquifer." *Environmental Science & Technology*. 28:5:868-876 (May 1994).

18. Morgan, J.J. and Stumm, Werner. "Analytical Chemistry of Aqueous Manganese." *Journal of the American Water Works Association*, 57:1:107-119 (January 1965).

19. Robinson, R. Bruce ET AL. "Iron and Manganese: Sequestration Facilities Using Sodium Silicate." *Journal of the American Water Works Association*, 84:2: 77-82 (February 1992).

20. McFarland, Wayne E. "Groundwater Treatment Alternatives for Industry: Part I: Iron and Manganese Removal." *Plant Engineering*. 62-66. July 11, 1985.

21. LaZerte, Bruce D. and Burling, Kirsten. "Manganese Speciation in Dilute Waters of the Precambrian Shield, Canada." *Water Research*. 24:9:1097-1101 (1990).

22. Zapffe, Carl. "The History of Manganese in Water Supplies and Methods for its Removal." *Journal of the American Water Works Association*, 25:5:655-676 (May 1933).

23. Hao, Oliver J. ET AL. "Kinetics of Manganese(II) Oxidation with Chlorine." *ASCE Journal of Environmental Engineering*." 117:3:359-374 (May/June 1991).

24. Van Beschoten, John E. ET AL. "Kinetic Modeling of Manganese(II) Oxidation by Chlorine Dioxide and Potassium Permanganate." *Environmental Science & Technology*. 26:7:1327-1333 (July 1992).

25. Knocke, William R. ET AL. "Using Alternative Oxidants to Remove Dissolved Manganese from Waters Laden with Organics." *Journal of the American Water Works Association*, 79:3:75-79 (March 1987).

26. Hem, J. D. U.S. Geological Survey Water Supply Paper 1667-A pp. 52-59 (1963).

27. Hem, John D. "Rates of Manganese Oxidation in Aqueous Systems." *Geochimica et Cosmochimica*. 45:1369-1374 (1981).

28. Diem, Dieter and Stumm, Werner. "Is dissolved Mn^{2+} being oxidized in absence of Mn-bacteria or surface catalysts?" *Geochimica et Cosmochimica*. 48:1571-1573 (1984).

29. Kessick, Michael A. and Morgan, James J. "Mechanism of Autoxidation of Manganese in Aqueous Solution." *Environmental Science & Technology*. 9:2:157-159 (February 1975).

30. Wilczak, Andrzej *et al.* "Manganese Control During Ozonation of Water Containing Organic Compounds." *Journal of the American Water Works Association*, 85:10:98-104 (October 1993).

31. Griffin, Attmore E. "Manganese in Water Supplies." *Journal of the American Water Works Association*, 52:10:1326-1334 (October 1960).

32. Jenkins, Stephen R. and Engeset. "The Cost of Effective Manganese Removal from Wyoming Waters." *Journal of the American Water Works Association*, 83:11:631-633 (November 1975).

33. Posselt, Hans S. *et al.* "Coagulation of Colloidal Hydrous Manganese Dioxide." *Journal of the American Water Works Association*, 60:1:48-68 (January 1968).

34. Mathews, Everett R. "Iron and Manganese Removal by Free Residual Chlorination." *Journal of the American Water Works Association*, 37:7:680-686 (July 1947).

35. Ponitus, Frederick W. "An Update of the Federal Regs." *Journal of the American Water Works Association*, 88:3:36-46 (March 1996).

36. Alsentzer, Harry A. "Ion Exchange in Water Treatment." *Journal of the American Water Works Association*, 55:6:742-752 (June 1963).

37. Willey, Benjamin F. and Jennings, Harry. "Iron and Manganese Removal with Potassium Permanganate." *Journal of the American Water Works Association*, 55:6:729-734 (June 1963).

38. Knocke, William R. ET AL. "Soluble Manganese Removal on Oxide-Coated Filter Media." *Journal of the American Water Works Association*, 80:12:65-70 (December 1988).

39. Knocke, William R. ET AL. "Removal of Soluble Manganese by Oxide-Coated Filter Media: Sorption Rate and Removal Issues." *Journal of the American Water Works Association*, 83:8:64-96 (August 1991).

40. Morgan, James J. and Stumm, Werner. "Colloid-Chemical Properties of Manganese Dioxide." *Journal of Colloid Science*. 19:347-359 (1964).

41. Hem, John D. Equilibrium Chemistry of Iron in Ground Water (1967). in: *Principles and Applications of Water Chemistry*, Samuel D. Faust and Joseph V. Hunter. eds., John Wiley and Sons, New York, 625-643.

42 Theis, Thomas L. and Singer, Philip C. "Complexation of Iron (II) by Organic Matter and Its Effect on Iron (II) Oxygenation." *Environmental Science & Technology*. 8:6:569-573 (June 1974).

43. Jobin, Robert and Ghosh, Mriganka. "Effect of Buffer Intensity and Organic Matter on the Oxygenation of Ferrous Iron." *Journal of the American Water Works Association*, 64:9:590-595 (September 1972).

44. Shapiro, Joseph. "Effect of Yellow Organic Acids on Iron and Other Metals in Water. *Journal of the American Water Works Association*, 56:8:1062-1081 (August 1964).

45. Olson, Larry L. and Twardowski Jr., Charles J. "$FeCO_3$ vs. $Fe(OH)_3$ Precipitation in Water Treatment." *Journal of the American Water Works Association*, 67:3:150-153 (March 1975).

46. Winklehaus, Charles ET AL. Discussion on "Precipitation of Iron in Aerated Ground Waters." *ASCE Journal of the Sanitary Engineering Division*. 92:SA6:129-137 (December 1966).

47. Ghosh, Mriganka M. ET AL. "Precipitation of Iron in Aerated Ground Waters." *ASCE Journal of the Sanitary Engineering Division*. 92:SA1:199-213 (February 1966).

48. Cromley, J. Timothy and O'Connor, John T. "Effect of Ozonation on the Removal of Iron from a Ground Water." *Journal of the American Water Works Association*, 68:6:315-319 (June 1976).

49. Mouchet, Pierre. "From Conventional to Biological Removal of Iron and Manganese in France." *Journal of the American Water Works Association*, 84:4:158-167 (April 1992).

50. Stumm, Werner and Singer, Philip C. Discussion on "Precipitation of Iron in Aerated Ground Waters." *ASCE Journal of the Sanitary Engineering Division.* 92:SA5:120-124 (October 1966).

51. Morgan, James J. and Birkner, Francis B. Discussion on "Precipitation of Iron in Aerated Ground Waters." *ASCE Journal of the Sanitary Engineering Division.* 92:SA6:137-143 (December 1966).

52. Grossl, Paul R. "Rapid Kinetics of Cu(II) Adsorption/Desorption on Geothite." *Environmental Science & Technology*. 28:8:1422-1429 (August 1994).

53. Stenkamp, V. Susie Benjamin, Mark M. "Effect of Iron Oxide Coating on Sand Filtration." *Journal of the American Water Works Association*, 86:8:37-50 (August 1994).

54. Edwards, Marc. "Chemistry of Arsenic: Removal During Coagulation and Fe-Mn Oxidation." *Journal of the American Water Works Association*, 86:9:64-78 (September 1994).

55. Wilson, Donald E. "Surface and Complexation Effects on the Rate of Mn(II) in Natural Waters." *Geochimica et Cosmochimica*. 44:1311-1317 (1980).

56. Sung, Windsor and Morgan, James J. "Oxidative Removal of Mn(II) from Solution Catalyzed by the γ-FeOOH (lepidocrocite) Surface." *Geochimica et Cosmochimica*. 45:2377-2383 (1981).

57. Davies, Simon H.R. and Morgan, James J. "Manganese(II) Oxidation Kinetics on Metal Oxide Surfaces." *Journal of Colloid and Interface Science*. 129:1:63-77 (April 1989).

58. Jenne, E.A. "Controls on Mn, Fe, Co, Ni, Cu, and Zn Concentrations in Soils and Water: the Significant Role of Hydrous Mn and Fe Oxides." in *Trace Inorganics in Water*. Robert A. Baker ed. American Chemical Society. Washington. 337-387. 1968.

59. Lloyd, A. *et al.* "The Removal of Manganese in Water Treatment Clarification Processes." *Water Research.* 17:11:1517-1523 (1983).

60. Xyla, Aglaia G. *et al.* "Reductive Dissolution of Manganese(III, IV) (Hydr)oxides by Oxalate: The Effect of pH and Light." *Langmuir.* 8:1:95-103 (1992).

61. Zasoski, R.J. and Burau, R.G. "Sorption and Sorptive Interaction of Cadmium and Zinc on Hydrous Manganese Oxide." *Soil Sci. Soc. Am. J.* 52:81-86 (1988).

62. American Water Works Association and Water Pollution Control Federation. Greenberg, Arnold E., Clesceri, Lenore S., and Eaton, Andrew D. Editors for *Standard Methods for the Examination of Water and Wastewater.* 18th edition. 1992.

63. Instructions for Perkin Elmer Atomic-Adsorption Spectrophotometer Model 703 Norwalk, CT. May 1978.

64. Grady, C.P.L. and Lim, H.C. *Biological Wastewater Treatment.* Marcel Dekker, Inc. New York. 1980.

65. Boyce, William E. and DiPrima, Richard C. *Elementary Differential Equations and Boundary Value Problems.* John Wiley & Sons. New York. 1986.

66. Reynolds, Tom D. *Unit Operations and Processes in Environmental Engineering.* PWS-Kent Publishing Company. Boston. 1982.

67. Metcalf and Eddy, Inc. *Wastewater Engineering: Treatment, Disposal, and Reuse: 2nd Edition.* McGraw-Hill, Inc. New York. 1979.

OTHER SOURCES

Anderson, Dewy R. ET AL. "Iron and Manganese Studies of Nebraska Water Supplies." *Journal of the American Water Works Association*, 65:10:635-641 (October 1973).

Baadsgaard, Marinus and Pai, Punda. "Iron and Manganese Removal in Groundwater Wells." *Public Works.* 122:2:59 (February 1991).

Bourg, Alaln C.M. and Richard-Raymond, Francoise. "Spatial and temporal variability in the water redox chemistry of the Drac River calcareous alluvial aquifer (Grenoble, France). *Journal of Contaminant Hydrology.* 15:93-105 (1994).

Chadik, Paul A. and Amy, Gary L. "Removing Trihalomethane Precursors from Various Natural Waters by Metal Coagulants." *Journal of the American Water Works Association.* 75:10:532-536 (October 1983).

Cleasby, John L. "Iron and Manganese Removal- A Case Study." *Journal of the American Water Works Association*, 67:3:147-149 (March 1975).

"Committee Report: Research Needs for the Treatment of Iron and Manganese." *Journal of the American Water Works Association*, 79:9:119-121. (September 1987).

Knocke, William R. and Van Benschoten, John E. Discussion of "Kinetics of Manganese(II) Oxidation with Chlorine." (*ASCE Journal of Environmental Engineering.*" 117:3:359-374). *ASCE Journal of Environmental Engineering.*" 119:2:390-399 (March/April 1993).

"Removing Iron and Manganese" *Public Works.* 122:5:C-19-C-20.

Welch, W. Arthur. "Potassium Permanganate in Water Treatment." *Journal of the American Water Works Association*, 55:6:735-741 (June 1963).

APPENDIX A:

TABULATION OF

EXPERIMENTAL RESULTS

Table A-1: 2 Blanks to Insure Proper Glassware Preparation (Mn(II) Removal)
3 meq/L Ca^{++}, 3 meq/L HCO_3^-, No Fe(II), Mn(II), or HOCl

BOD	0.45 um Filtered		30k Ultrafiltered # 1		30k Ultrafiltered # 2	
Bottle #	Tube #	Mn (mg/L)	Tube #	Mn (mg/L)	Tube #	Mn (mg/L)
61	1	0.012	2	0.016	5	0.02
231	3	0.017	4	0.019	6	0.021

Table A-2: Check HOCl Demand of Milli-Q Water
3 meq/L Ca^{++}, 3 meq/L HCO_3^-, 2 mg/L HOCl, No Fe(II) or Mn(II)

Time	pH 7	pH 8
(min)	HOCl (mg/L)	HOCl (mg/L)
0	2.04	2.03
135	1.94	1.9
1440	1.86	1.92

Table A-3: Introduction of Mn(II) by Addition of Reagent Grade A.C.S. Certified Ferrous Sulfate Heptahydrate (>99%); Aldrich Chemical Co.

Date	mg $FeSO_4*7H_2O$ Added	Volume (L)	Mn (mg/L)	mg Mn/mg $FeSO_4*7H_2O$
11/18/94	200	0.2	0.194	1.94E-04
11/18/94	400	0.2	0.368	1.84E-04
11/18/94	600	0.2	0.559	1.86E-04
Rerun	400	0.2	0.3595	1.80E-04
Rerun	600	0.2	0.541	1.80E-04
9/11/94	497.8	2	0.094	3.78E-04
9/11/94	4978.2	2	0.1725	6.93E-05
9/12/94	4978.2	2	0.22	8.84E-05
11/23/94	248.9	0.25	0.195	1.96E-04
11/23/94	497.8	0.25	0.375	1.88E-04
11/23/94	659.6	0.25	0.475	1.80E-04
		AVERAGE VALUE:		**1.84E-04**

* Although the results are somewhat variable, the average value seems to be a good estimate based upon specific tests conducted to determine this value.
Also there are inherent laboratory errors which render exact repetition impossible.

Preliminary Research Studies
Mn(II) Removal via $CaCO_3$ and $MnCO_3$ Ppt.

Table A-4: $CaCO_3/MnCO_3$ Interference Tests 6/12/94

pH = 8; 3 meq/L Ca^{++}, 3 meq/L HCO_3^-, 0.5 mg/L Mn(II), No Fe(II) or HOCl, 10°C

Time (min)	BOD Bottle #	Final pH	Temp. (C)	0.45 um Filtered Samples		30k Ultrafiltered # 1		30k Ultrafiltered # 2		Avg. Ultra
				Tube #	Mn (mg/L	Tube #	Mn (mg/L)	Tube #	Mn (mg/L)	
0	Blank	7.98	10.2	7	0.271	8	0.267	9	0.268	0.2675
30	6	7.85	10.8	10	0.269	11	0.284	12	0.273	0.2785
60	15	7.85	10.2	13	0.275	14	0.273	15	0.272	0.2725
90	50	7.86	11	16	0.273	17	0.273	18	0.273	0.273
180	123	ND	ND	19	0.27					
				20	0.278					

* There was an error in preparing the water makeup as Mn is approximately half of the intended concentration.

Table A-5: $CaCO_3/MnCO_3$ Interference Tests 6/13/94

pH = 9; 3 meq/L Ca^{++}, 3 meq/L HCO_3^-, 0.5 mg/L Mn(II), No Fe(II) or HOCl, 10°C

Time (min)	BOD Bottle #	Final pH	Temp. (C)	0.45 um Filtered Samples			30k Ultrafiltered Sample # 1			30k Ultrafiltered Sample # 2		Avg. Ultra
				Tube #	Ca (mg/L)	Mn (mg/L	Tube #	Ca (mg/L)	Mn (mg/L)	Tube #	Mn (mg/L)	
0	Blank	9.06	10.3	1	56.1	0.492	2	60.5	0.478	3	0.463	0.4705
30	6	8.91	12	4	51.7	0.379	5	48.4	0.281	6	0.217	0.249
60	15	8.95	11.5	7	64.9	0.479	8	60.5	0.451	9	0.461	0.456
90	37	8.28	11.5	10	41.8	0.007	11	40.7	0.022	12	0.021	0.0215
120	50	8.28	11.6	15	41.8	0.018	13	44	0.017	14	0.014	0.0155
150	61	8.17	11.2	16	40.7	0.012	17	40.7	0.015	21	0.014	0.0145
180	231	8.58	10.3	22	47.3	0.187	23	46.2	0.197	24	0.191	0.194
Stock Solution Check				25		0.496	26		0.289	27	0.334	0.3115

Preliminary Research Studies
Mn(II) Removal via CaCO3 and MnCO3 Ppt.

Table A-6: $CaCO_3/MnCO_3$ Interference Tests 6/13/94; Check of Previous Test
pH = 9; 3 meq/L Ca^{++}, 3 meq/L HCO_3^-, 0.5 mg/L Mn(II), No Fe(II) or HOCl, 10°C

Time (min)	BOD Bottle #	Final pH	Temp. (C)	0.45 um Filtered	
				Tube #	Mn (mg/L)
0	Blank	9	~ 10	A	0.49
120	ND	ND	ND	B	0.047
120	ND	ND	ND	C	0.067
120	ND	ND	ND	D	0.05

Table A-7: $CaCO_3/MnCO_3$ Interference Tests 6/15/94
pH = 8; 3 meq/L Ca^{++}, 3 meq/L HCO_3^-, 0.5 mg/L Mn(II), No Fe(II) or HOCl, 10°C

Time (min)	BOD Bottle #	Final pH	Temp. (C)	0.45 um Filtered	
				Tube #	Mn (mg/L)
0	Blank	8.01	10.2	50	0.514
30	41	8	10.4	51	0.51
60	57	7.98	10.4	52	0.507
90	73	8	10.3	53	0.509
120	97	8.01	10.1	54	0.497
150	309	8.01	10.1	55	0.499
180	356	8.12	10.3	56	0.506

Table A-8: $CaCO_3/MnCO_3$ Interference Tests 6/15/94
pH = 9; 3 meq/L Na^+, 3 meq/L HCO_3^-, 0.5 mg/L Mn(II), No Fe(II) or HOCl, 10°C
Replaced $CaCl_2$ in solution with NaCl (same ionic strength)

Time (min)	BOD Bottle #	Final pH	Temp. (C)	0.45 um Filtered	
				Tube #	Mn (mg/L)
0	Blank	9.01	10.2	57	0.488
60	ND	8.91	9.2	58	0.47
120	ND	8.92	10	59*	0.447
180	ND	8.8	10.5	61	0.421

* Filter was torn; not noted until sample had been discarded

Table A-9: 6/22/94: pH = 8; 2 mg/L as HOCl; 0.5 mg/L as Mn(II); Ca^{++} & HCO_3^- = 3 meq/L; NO Fe(II), 10°C

Time	Final	Temp.	0.45 um Filtered Samples			30k Ultrafiltered Sample # 1			30k Ultrafiltered Sample # 2			Avg.
(min)	pH	(C)	Tube #	Fe (mg/L)	Mn (mg/L)	Tube #	Fe (mg/L)	Mn (mg/L)	Tube #	Fe (mg/L)	Mn (mg/L)	Ultra
0	7.99	10	109		0.498	110		0.494	111		0.492	0.493
30	7.8	10.5	112		0.512	113		0.509	114		0.52	0.5145
60	7.89	10.5	115		0.514	116		0.494	117		0.49	0.492
90	7.91	10.1	118		0.494	119		0.491	120		0.495	0.493
120	7.92	10.6	121		0.505	122		0.499	123		0.493	0.496
240	7.9	10	124		0.511	125		0.497	126		0.494	0.4955
1260	7.8	9.5?	127		0.474	128		0.461	129		0.465	0.463

Table A-10: 7/7/94: pH = 7; 2 mg/L as HOCl; 0.5 mg/L as Mn(II); Ca^{++} & HCO_3^- = 3 meq/L; NO Fe(II), 10°C

Time	Final	Temp.	0.45 um Filtered Samples			30k Ultrafiltered Sample # 1			30k Ultrafiltered Sample # 2			Avg.	HOCl
(min)	pH	(C)	Tube #	Fe (mg/L)	Mn (mg/L)	Tube #	Fe (mg/L)	Mn (mg/L)	Tube #	Fe (mg/L)	Mn (mg/L)	Ultra	(mg/L)
0	7.01	9.8	105		0.481								2.01
0	7.01	9.6	106		0.481								
0	Acidified		107		0.488								
60	6.85	9.8	108		0.476	109		0.47	110		0.475	0.4725	1.95
120	6.81	9.7	111		0.473	112		0.462	113		0.469	0.4655	1.98
180	6.75	9.8	114		0.464	115		0.459	116		0.455	0.457	1.82
240	6.85	10	117			118			119			ND	1.94

Long Mn(II) Adsorption onto Fe(III)

Table A-11: 6/21/94: pH = 8; 4 mg/L as Fe(II); 0.5 mg/L as Mn(II); Ca^{++} & HCO_3^- = 3 meq/L; NO HOCl, 10°C

Time	Final	Temp.	0.45 um Filtered Samples			30k Ultrafiltered Sample # 1			30k Ultrafiltered Sample # 2			Avg.
(min)	pH	(C)	Tube #	Fe (mg/L)	Mn (mg/L	Tube #	Fe (mg/L)	Mn (mg/L	Tube #	Fe (mg/L)	Mn (mg/L	Ultra
0	8.03	10.2	66	0	0.455	67	-0.008	0.458	68	-0.004	0.456	0.457
30	7.96	11.2	69	-0.005	0.467	70	-0.005	0.467	71	0.004	0.468	0.4675
60	7.97	9.8	72	ND	ND	73	-0.005	0.46	74	0.003	0.461	0.4605
90	8	9	75	-0.014	0.459	76	-0.012	0.461	77	-0.01	0.467	0.464
120	8	9.8	78	-0.011	0.464	79	-0.015	0.459	80	-0.011	0.458	0.4585
150	8	10	81	-0.011	0.458	82	-0.007	0.454	83	0	0.454	0.454
180	8	10.1	84	ND	ND	85	-0.009	0.451	86	-0.019	0.458	0.4545

Table A-12: 6/22/94: pH = 7; 4 mg/L as Fe(II); 0.5 mg/L as Mn(II); Ca^{++} & HCO_3^- = 3 meq/L; NO HOCl, 10°C

Time	Final	Temp.	0.45 um Filtered Samples			30k Ultrafiltered Sample # 1			30k Ultrafiltered Sample # 2			Avg.
(min)	pH	(C)	Tube #	Fe (mg/L)	Mn (mg/L	Tube #	Fe (mg/L)	Mn (mg/L	Tube #	Fe (mg/L)	Mn (mg/L	Ultra
0	7.03	10.1	87	0.235	0.489	88	0.177	0.49	89	0.138	0.49	0.49
	Acidified		90	3.691	0.517							
30	6.81	10	91	0.402	0.508	92	0.409	0.509	93	0.365	0.505	0.507
60	6.79	10	94	0.207	0.499	95	0.184	0.51	96	0.174	0.508	0.509
90	6.82	10.1	97	0.073	0.514	98	0.061	0.505	99	0.066	0.5	0.5025
225	6.78	9.1	100	0.008	0.503	101	0.049	0.495	102	0.03	0.498	0.4965
330	6.79	9.8	103	0.005	0.498	104	0.18	0.499	105	-0.012	0.501	0.5
480	6.89	10.2	106	0.003	0.491	107	0.035	0.484	108	0.001	0.485	0.4845

Mn(II) Adsorption onto Fe(III)

Table A-13: Isotherm Data Summary

pH, Fe as indicated, $[Mn(II)]_0$ = 0.50 mg/L $[Ca^{++}]$ = 3 meq/L, $[HCO_3^-]$ = 3 meq/L

pH 8

Type Fe	Date	Lab Bk. Page	Avg. Fe	Initial Mn	Final Mn	Δ Mn	Ratio Mn/Fe	Ce/(X/M)	ln q	ln Ce	1/Ce	1/Ratio	Comments
Regular	7/28/95	9	8.302	0.519	0.485	0.034	0.0041	118.4256	-5.4979	-0.7236	2.0619	244.1765	
Regular	7/28/95	10	19.425	0.523	0.451	0.072	0.0037	121.6760	-5.5977	-0.7963	2.2173	269.7917	
Regular	8/3/94	11	8.672	0.553	0.5125	0.0405	0.0047	109.7383	-5.3666	-0.6685	1.9512	214.1235	
Regular	8/3/94	11	8.337	0.5275	0.4765	0.051	0.0061	77.8937	-5.0966	-0.7413	2.0986	163.4706	
Regular	8/3/94	11	20.03	0.56	0.435	0.125	0.0062	69.7044	-5.0767	-0.8324	2.2989	160.2400	
Regular	8/3/94	11	20.72	0.5775	0.4365	0.141	0.0068	64.1438	-4.9901	-0.8290	2.2910	146.9504	
Regular	8/9/94	12	50.715	0.581	0.33	0.251	0.0049	66.6771	-5.3085	-1.1087	3.0303	202.0518	
Regular	9/11/94	16	205	0.696	0.101	0.595	0.0029	34.7983	-5.8422	-2.2926	9.9010	344.5378	1000 Fe was goal; dilution???
Regular	???	30	200	0.5	0.157	0.343	0.0017	91.5452	-6.3683	-1.8515	6.3694	583.0904	
Regular	???	30	400	0.5	0.0375	0.4625	0.0012	32.4324	-6.7626	-3.2834	26.6667	864.8649	
Regular	???	30	530	0.5	0.028	0.472	0.0009	31.4407	-7.0237	-3.5756	35.7143	1122.8814	
Regular	12/29/94	35	96.3	0.5655	0.354	0.2115	0.0022	161.1830	-6.1210	-1.0385	2.8249	455.3191	

pH 7

Type Fe	Date	Lab Bk. Page	Avg. Fe	Initial Mn	Final Mn	Δ Mn	Ratio Mn/Fe	Ce/(X/M)	ln q	ln Ce	1/Ce	1/Ratio	Comments
Regular	7/21/94	8	1.882	0.528	0.492	0.036	0.0191	25.7207	-3.9566	-0.7093	2.0325	52.2778	Not Plotted
Regular	8/15/94	14	21.05	0.561	0.518	0.043	0.0020	253.5791	-6.1935	-0.6578	1.9305	489.5349	
Regular	8/25/94	15	101.69	0.605	0.3835	0.2215	0.0022	176.0637	-6.1293	-0.9584	2.6076	459.0971	
Regular	8/25/94	15	53.67	0.5635	0.4525	0.111	0.0021	218.7899	-6.1811	-0.7930	2.2099	483.5135	
Regular	9/11/95	16	112.77	0.608	0.487	0.121	0.0011	453.8760	-6.8373	-0.7195	2.0534	931.9835	
Regular	9/11/95	17	215.5	0.662	0.465	0.197	0.0009	508.6675	-6.9975	-0.7657	2.1505	1093.9086	
Regular	11/23/94	31	378.7	0.582	0.263	0.319	0.0008	312.2197	-7.0793	-1.3356	3.8023	1187.1473	
Regular	11/23/94	31	490	0.475	0.077	0.398	0.0008	94.7990	-7.1157	-2.5639	12.9870	1231.1558	
Pure	12/6/94	33	200	0.511	0.463	0.048	0.0002	1929.1667	-8.3349	-0.7700	2.1598	4166.6667	1 hr samples
Pure	12/6/94	33	402	0.435	0.407	0.028	0.0001	5843.3571	-9.5720	-0.8989	2.4570	14357.1429	1 hr samples
Pure	12/6/94	33	577	0.45	0.36	0.09	0.0002	2308.0000	-8.7658	-1.0217	2.7778	6411.1111	1 hr samples
Pure	12/20/94	33	712.3	0.6	0.443	0.157	0.0002	2009.8656	-8.4200	-0.8142	2.2573	4536.9427	

Investigation of Order of Oxidation of Metal Species; Fe(II) and Mn(II) added simultaneously

Table A-14: 6/27/94: pH = 8; 4 mg/L as Fe(II); 0.5 mg/L as Mn(II); Ca^{++} & HCO_3^- = 3 meq/L; HOCl = 2 mg/L, 10°C

Time	Final	Temp.	0.45 um Filtered Samples			30k Ultrafiltered Sample # 1			30k Ultrafiltered Sample # 2			Avg.	HOCl
(min)	pH	(C)	Tube #	Fe (mg/L)	Mn (mg/L)	Tube #	Fe (mg/L)	Mn (mg/L)	Tube #	Fe (mg/L)	Mn (mg/L)	Ultra	(mg/L)
0	8.03	9.3	1	-0.005	0.435	2	0.01	0.425	3	0.02	0.431	0.428	1.61
30	7.83	10	4	-0.028	0.375	5*	2.959	0.45	6*	3.15	0.452	0.451	1.85
60	7.81	10	7	0.027	0.34								1.67
90	7.81	10.2	8	0.014	0.211								1.65
150	7.85	10	9	0.02	0.064								
240	7.73	10	10	0.001	0								
360			11	-0.012									

* Suspect that membrane tore or punctured; rapid flow rate & high concentrations.

Table A-15: 6/28/94: pH = 8; 4 mg/L as Fe(II); 0.5 mg/L as Mn(II); Ca^{++} & HCO_3^- = 3 meq/L; HOCl = 2 mg/L,m 10°C

Time	Final	Temp.	0.45 um Filtered Samples			30k Ultrafiltered Sample # 1			30k Ultrafiltered Sample # 2			Avg.	HOCl
(min)	pH	(C)	Tube #	Fe (mg/L)	Mn (mg/L)	Tube #	Fe (mg/L)	Mn (mg/L)	Tube #	Fe (mg/L)	Mn (mg/L)	Ultra	(mg/L)
0	8	9.3	12	0.02	0.448	13	-0.015	0.445	14	0.533	0.44	0.4425	1.63
30	7.94	8.8	15	0.141	0.412	16	-0.022	0.402	17	-0.026	0.407	0.4045	1.69
60	7.92	9.2	18	0.017	0.344	19	0.003	0.334	20	-0.006	0.337	0.3355	1.72
90	7.91	10	21	-0.013	0.281	22	-0.01	0.286	23	-0.003	0.288	0.287	1.66
120	7.9	10.3	24	0.019	0.224	25	0.015	0.222	26	-0.029	0.211	0.2165	1.47
180	7.87	10.5	27	-0.004	0.056	28	-0.004	0.054	29	-0.014	0.051	0.0525	1.47
180	7.88	10.2	30	-0.006	0.068	31	0.008	0.067	32	0.008	0.068	0.0675	1.45

Investigation of Order of Oxidation of Metal Species; Fe(II) and Mn(II) added simultaneously

Table A-16: 6/29/94: pH = 7; 4 mg/L as Fe(II); 0.5 mg/L as Mn(II); Ca^{++} & HCO_3^- = 3 meq/L; HOCl = 2 mg/L, 10°C

Time (min)	Final pH	Temp. (C)	0.45 um Filtered Samples			30k Ultrafiltered Sample # 1			30k Ultrafiltered Sample # 2			Avg. Ultra	HOCl (mg/L)
			Tube #	Fe (mg/L)	Mn (mg/L)	Tube #	Fe (mg/L)	Mn (mg/L)	Tube #	Fe (mg/L)	Mn (mg/L)		
0	6.98	9.3	33	-0.003	0.452								1.76
	Acidified*		34	2.794	0.494								
	Acidified*		35	3.81	0.504								
30	6.83	8.8	36	0.041	0.438	37	0	0.432	38	-0.003	0.433	0.4325	1.84
60	6.89	9.2	39	0.001	0.413	40	0.006	0.408	41	-0.014	0.412	0.41	1.84
90	6.85	10	42	-0.005	0.376	43	0.001	0.374	44	-0.002	0.374	0.374	1.79
120	6.84	10.3	45	-0.006	0.331	46	-0.01	0.327	47	-0.006	0.322	0.3245	1.57
260	6.81	10.5	48	-0.012	0.062	***Ultrafiltration equipment not available for use***							1.51
360	6.8	10.2	50	-0.041	0.011	51	-0.013	0.013	52	-0.03	0.012	0.0125	1.50

* Acidified Samples not allowed enough reaction time to resuspend all colloidal iron; some visible on filter.

HOCl Blank = 2.77 mL Titrant; 2.05 mg/L as HOCl

Table A-17: 6/30/94: pH = 7; 2 mg/L as Fe(II); 0.5 mg/L as Mn(II); Ca^{++} & HCO_3^- = 3 meq/L; HOCl = 2 mg/L, 10°C

Time (min)	Final pH	Temp. (C)	0.45 um Filtered Samples			30k Ultrafiltered Sample # 1			30k Ultrafiltered Sample # 2			Avg. Ultra	HOCl (mg/L)
			Tube #	Fe (mg/L)	Mn (mg/L)	Tube #	Fe (mg/L)	Mn (mg/L)	Tube #	Fe (mg/L)	Mn (mg/L)		
0	7.02	9.8	78	2.051	0.524								
0			79	2.053	0.526								
30	6.92	9.7	60	-0.005	0.357	61	-0.012	0.345	62	-0.01	0.351	0.348	1.35
60	6.96	10	63	-0.014	0.324	64	-0.002	0.325	65	0.004	0.321	0.323	1.30
120	7.06	10	66	0.007	0.27	67	0.06	0.267	68	0.003	0.267	0.267	1.26
150	7.06	10	69	0.001	0.238	70	-0.001	0.236	71	-0.008	0.234	0.235	1.27
180	7.02	10	72	-0.015	0.219	73	-0.018	0.216	74	-0.021	0.215	ND	1.26
240	7.01	9.8	75	-0.01	0.166	76	0	0.164	77	-0.012	0.159	0.1615	1.18

* HOCl Target = 2 mg/L; Check = 2.79 mL Titrant = 2.06 mg/L

Fe(II) Oxidized Prior to Mn(II) Addition

Table A-18: 7/20/94: pH = 8; Fe(II) Target = 4 mg/L; 0.5 mg/L as Mn(II); Ca^{++} & HCO_3^- = 3 meq/L; HOCl = 2 mg/L; 10°C

Time	Final	Temp.	0.45 um Filtered Samples			30k Ultrafiltered Sample # 1			30k Ultrafiltered Sample # 2			Avg.	HOCl
(min)	pH	(C)	Tube #	Fe (mg/L)	Mn (mg/L)	Tube #	Fe (mg/L)	Mn (mg/L)	Tube #	Fe (mg/L)	Mn (mg/L)	Ultra	(mg/L)
0	8.04	11.5											
0	Acidified		127	4.552	0.537	128	4.621	0.545	129	4.634	0.542	0.54	ND
5	Adsorb		124	-0.026	0.493	125	-0.024	0.501	126	-0.022	0.505	0.50	ND
30	7.88	10.8	1	-0.01	0.464	2	-0.017	0.452	3	-0.013	0.447	0.45	1.98
60	7.87	11	4	-0.007	0.391	5	-0.011	0.404	6	0.003	0.398	0.40	1.91
120	7.87	11	7	-0.008	0.256	8	-0.008	0.261	9	-0.011	0.252	0.26	1.87
180	7.83	10.2	10	-0.001	0.124	11	-0.011	0.12	12	-0.01	0.118	0.12	1.76
240	7.79	11	13	-0.013	0.027	14	-0.013	0.027	15	-0.021	0.025	0.03	1.66
300	7.79	11.2	16	-0.014	-0.001	17	-0.016	0.001	18	-0.019	0	0.00	1.61

* It is believed that the initial HOCl dose exceeded 2 mg/L; probably ~ 2.1 mg/L

Table A-19: 7/21/94: pH = 7; Fe(II) Target = 2 mg/L; 0.5 mg/L as Mn(II); Ca^{++} & HCO_3^- = 3 meq/L; HOCl = 2 mg/L; 10°C

Time	Final	Temp.	0.45 um Filtered Samples			30k Ultrafiltered Sample # 1			30k Ultrafiltered Sample # 2			Avg.	HOCl
(min)	pH	(C)	Tube #	Fe (mg/L)	Mn (mg/L)	Tube #	Fe (mg/L)	Mn (mg/L)	Tube #	Fe (mg/L)	Mn (mg/L)	Ultra	(mg/L)
0	6.99	10.8											
0	Acidified		21	1.827	0.518	40	1.936	0.536	41	1.84	0.531	0.53	ND
5	Adsorb		19	-0.003	0.495	20	-0.024	0.489					2.00
30	6.91	9.2	22	-0.011	0.475	23	-0.018	0.478	24	-0.015	0.47	0.47	1.85
60	6.9	9.8	25	-0.011	0.466	26	-0.011	0.462	27	-0.013	0.457	0.46	1.85
120	6.9	10	28	-0.011	0.426	29	-0.008	0.425	30	-0.018	0.416	0.42	1.82
180	6.91	8.2	31	-0.019	0.399	32	-0.011	0.393	33	-0.026	0.392	0.39	1.76
240	6.87	11	34	-0.023	0.357	35	-0.013	0.353	36	-0.023	0.353	0.35	1.67
300	6.89	10.2	37		0.308	38		0.319	39		0.305	0.31	1.63

* "Zero" sample represents the amount of Mn that is initially adsorbed onto the oxide surface.

Fe(II) Oxidized Prior to Mn(II) Addition

Table A-20: 7/28/94: pH = 8; Fe(II) Target = 8 mg/L; 0.5 mg/L as Mn(II); Ca^{++} & HCO_3^- = 3 meq/L; HOCl = 2 mg/L; 10°C

Time	Final	Temp.	0.45 um Filtered Samples			30k Ultrafiltered Sample # 1			30k Ultrafiltered Sample # 2			Avg.	HOCl
(min)	pH	(C)	Tube #	Fe (mg/L)	Mn (mg/L)	Tube #	Fe (mg/L)	Mn (mg/L)	Tube #	Fe (mg/L)	Mn (mg/L)	Ultra	(mg/L)
0	Acidified		47	8.518	0.528								ND
0	Acidified		48	8.086	0.51								1.97
5	7.99	10.8	42	0.032	0.481								
5	Adsorb		43	-0.004	0.488								
30	7.87	9.8	44	ND	0.402	45	ND	0.395	46	ND	0.393	0.39	1.84
60	7.88	10	49	ND	0.317	50	ND	0.311	51	0.021	0.307	0.31	1.75
120	7.87	10.2	52	ND	0.078	53	ND	0.078	54	ND	0.077	0.08	1.61
180	7.83	9.7	55	0.027	0.001	56	ND	0.004	57	ND	0	0.00	1.45
240	7.95	9.5	58	ND	0	59	ND	0.001	60	ND	0	0.00	1.39
300	7.91	9.6	61	ND	0.005	62	ND	0.003	63	ND	0.003	0.00	1.39

Table A-21: 7/28/94: pH = 8; Fe(II) Target = 20 mg/L; 0.5 mg/L as Mn(II); Ca^{++} & HCO_3^- = 3 meq/L; HOCl = 2 mg/L; 10°C

Time	Final	Temp.	0.45 um Filtered Samples			30k Ultrafiltered Sample # 1			30k Ultrafiltered Sample # 2			Avg.	HOCl
(min)	pH	(C)	Tube #	Fe (mg/L)	Mn (mg/L)	Tube #	Fe (mg/L)	Mn (mg/L)	Tube #	Fe (mg/L)	Mn (mg/L)	Ultra	(mg/L)
0	Acidified		65	19.4	0.517								ND
0	Acidified		66	19.45	0.529								2.03
5	7.99	10	68	0.008	0.463								ND
5	Adsorb		69	ND	0.438								ND
30	7.99	10	70	ND	0.315	71	ND	0.305	72	ND	0.314	0.31	1.75
60	7.7	9.2	73	ND	0.143	74	ND	0.135	75	ND	0.126	0.13	1.56
135	7.74	9.8	76	ND	0.002	77	ND	0.002	78	0.013	0.001	0.00	1.38
180	7.67	10	79	ND	0	80	ND	0.003	81	ND	-0.001	0.00	1.42
240	7.65	10	82	0.025	-0.003	83	ND	0	84	ND	-0.005	0.00	1.35
300	7.67	10	85	ND	-0.001	86	ND	-0.004	87	ND	-0.002	0.00	1.35

* Another acidified sample: # 89: Fe = 20.695 & Mn = 0.536

Fe(II) Oxidized Prior to Mn(II) Addition

Table A-22: 8/9/94: pH = 8; Fe(II) Target = 50 mg/L; 0.5 mg/L as Mn(II); Ca^{++} & HCO_3^- = 3 meq/L; HOCl = 2 mg/L; 10°C

Time	Final	Temp.	0.45 um Filtered Samples			30k Ultrafiltered Sample # 1			30k Ultrafiltered Sample # 2			Avg.	Bottle Conc. (mg/L)		HOCl
(min)	pH	(C)	Tube #	Fe (mg/L)	Mn (mg/L)	Tube #	Fe (mg/L)	Mn (mg/L)	Tube #	Fe (mg/L)	Mn (mg/L)	Ultra	Mn	Fe	(mg/L)
0	Acidified		1	53.03	0.592										ND
0	Acidified		2	48.4	0.571										1.48
5	8.05	10.3	3	ND	0.315										ND
5	Adsorb		4	0.011	0.344										ND
20	7.87	10.5	5	ND	0.127	6	ND	0.119	7	ND	0.106	0.11			ND
40	7.94	11	8	ND	0.011	9	ND	0.014	10	ND	0.004	0.01	0.57	49.95	ND
60	7.93	11	11	ND	0.006	12	ND	0.004	13	ND	0.004	0.00	0.60	50.14	1.33
80	7.74	8	14	ND	0.001	15	ND	0.001	16	ND	-0.002	0.00	0.59	51.33	ND
100	7.93	8	17	-0.025	0.002	18	ND	0.003	19	ND	0.003	0.00	0.58	50.09	ND
120	7.86	9.3	20	ND	0.001	21	ND	0	22	ND	0.002	0.00	0.58	50.40	1.27

* Possibly some of the HOCl was used to complete the oxidation of Fe(II). Average Fe (8) = 50.48 +/- 1.42 & (2) 50.72 mg/L

Table A-23: 8/11/94: pH = 7; Fe(II) Target = 8 mg/L; 0.5 mg/L as Mn(II); Ca^{++} & HCO_3^- = 3 meq/L; HOCl = 2 mg/L; 10°C

Time	Final	Temp.	0.45 um Filtered Samples			30k Ultrafiltered Sample # 1			30k Ultrafiltered Sample # 2			Avg.	Bottle Conc. (mg/L)		HOCl
(min)	pH	(C)	Tube #	Fe (mg/L)	Mn (mg/L)	Tube #	Fe (mg/L)	Mn (mg/L)	Tube #	Fe (mg/L)	Mn (mg/L)	Ultra	Mn	Fe	(mg/L)
0	Acidified		38	8.01	0.513										ND
0	Acidified		39	ND	0.522										1.66
5	7.01	10	40	ND	0.505										ND
5	Adsorb		41	0.032	0.509										ND
30	6.97	10	42	ND	0.368	43	ND	0.373	44	ND	0.383	0.38	0.53	7.50	1.57
60	7.03	9	46	ND	0.343	47	ND	0.337	48	ND	0.348	0.34	0.53	7.72	1.56
90	6.96	9.3	50	ND	0.298	51	0.018	0.307	52	ND	0.307	0.31	0.54	7.56	1.57
120	6.99	9.3	54	ND	0.264	55	ND	0.253	57	ND	0.244	0.25	0.52	7.79	1.48
180	6.99	9.8	58	ND	0.163	59	ND	0.156	60	ND	0.161	0.16	0.51	7.02	1.50
240	7	9.2	62	ND	0.067	63	ND	0.067	64	ND	0.062	0.06	0.52	7.95	1.33

* Possibly some of the HOCl was used to complete the oxidation of Fe(II). Average Fe (7) = 7.65 +/- 0.33 & (1) 8.01 mg/L

Fe(II) Oxidized Prior to Mn(II) Addition

Table A-24: 8/15/94: pH = 7; Fe(II) Target = 10 mg/L; 0.5 mg/L as Mn(II); Ca^{++} & HCO_3^- = 3 meq/L; HOCl = 2 mg/L; 10°C

Time	Final	Temp.	0.45 um Filtered Samples			30k Ultrafiltered Sample # 1			30k Ultrafiltered Sample # 2			Avg.	Bottle Conc. (mg/L)		HOCl
(min)	pH	(C)	Tube #	Fe (mg/L)	Mn (mg/L)	Tube #	Fe (mg/L)	Mn (mg/L)	Tube #	Fe (mg/L)	Mn (mg/L)	Ultra	Mn	Fe	(mg/L)
0	Acidified		103	9.87	0.533										ND
0	Acidified		104	9.88	0.535										1.84
5	7.01	10	105	ND	0.515										ND
5	Adsorb		106	ND	0.519										ND
30	6.98	10.2	107	ND	0.403	108	ND	0.4	109	ND	0.412	0.41	0.53	9.94	1.54
60	7.04	10.2	111	ND	0.332	112	ND	0.335	113	ND	0.336	0.34	0.53	9.72	1.58
90	6.98	10	115	-0.011	0.274	116	ND	0.271	117	ND	0.268	0.27	0.52	9.86	1.56
120	7.03	10	119	ND	0.196	120	ND	0.194	121	ND	0.189	0.19	0.52	9.76	1.48
150	7.05	9.8	123	ND	0.148	124	ND	0.139	125	ND	0.14	0.14	0.48	9.97	1.47
180	6.98	10	127	ND	0.083	128	-0.011	0.08	129	ND	0.076	0.08	0.52	9.69	1.33

* Possibly some of the HOCl was used to complete the oxidation of Fe(II). Average Fe (8) = 9.835 +/- 0.13 & (2) 9.875 mg/L

Table A-25: 8/15/94: pH = 7; Fe(II) Target = 20 mg/L; 0.5 mg/L as Mn(II); Ca^{++} & HCO_3^- = 3 meq/L; HOCl = 2 mg/L; 10°C

Time	Final	Temp.	0.45 um Filtered Samples			30k Ultrafiltered Sample # 1			30k Ultrafiltered Sample # 2			Avg.	Bottle Conc. (mg/L)		HOCl
(min)	pH	(C)	Tube #	Fe (mg/L)	Mn (mg/L)	Tube #	Fe (mg/L)	Mn (mg/L)	Tube #	Fe (mg/L)	Mn (mg/L)	Ultra	Mn	Fe	(mg/L)
0	Acidified		75	20.98	0.566										ND
0	Acidified		76	21.08	0.556										1.81
5	7.03	9	77	ND	0.513										ND
5	Adsorb		78	ND	0.523										ND
15	6.92	10.8	79	ND	0.451	80	ND	0.457	81	ND	0.444	0.45	0.59	20.49	ND
30	7.02	9.3	83	ND	0.424	84	ND	0.419	85	ND	0.409	0.41	0.55	21.84	ND
45	7.03	10	87	-0.039	0.387	88	ND	0.384	89	ND	0.379	0.38	0.55	21.22	ND
60	7.04	10	91	ND	0.328	92	ND	0.336	93	ND	0.318	0.33	0.55	20.60	1.50
75	7.05	10	95	ND	0.281	96	ND	0.292	97	-0.008	0.282	0.29	0.56	20.74	ND
90	7.03	10.2	99	ND	0.241	100	ND	0.241	101	ND	0.236	0.24	0.57	20.79	1.48

* Possibly some of the HOCl was used to complete the oxidation of Fe(II). Average Fe (8) = 20.97 +/- 0.43 & (2) 21.03 mg/L

Fe(II) Oxidized Prior to Mn(II) Addition

Table A-26: 8/25/94: pH = 7; Fe(II) Target = 50 mg/L; 0.5 mg/L as Mn(II); Ca^{++} & HCO_3^- = 3 meq/L; HOCl = 2 mg/L; 10°C

Time	Final	Temp.	0.45 um Filtered Samples			30k Ultrafiltered Sample # 1			30k Ultrafiltered Sample # 2			Avg.	Bottle Conc. (mg/L)		HOCl
(min)	pH	(C)	Tube #	Fe (mg/L)	Mn (mg/L)	Tube #	Fe (mg/L)	Mn (mg/L)	Tube #	Fe (mg/L)	Mn (mg/L)	Ultra	Mn	Fe	(mg/L)
0	Acidified		29	54.89	0.567										ND
0	Acidified		30	52.45	0.56										ND
5	6.99	10.2	31	ND	0.447										ND
5	Adsorb		32	ND	0.458										ND
30	6.81	10	33	ND	0.309	34	ND	0.294	35	ND	0.293	0.29	0.56	51.85	ND
50	6.88	10	37	ND	0.224	38	ND	0.225	39	ND	0.218	0.22	0.56	52.29	ND
75	6.86	9.5	41	ND	0.119	42	ND	0.116	43	ND	0.103	0.11	0.55	53.83	ND
95	6.84	9.3	45	ND	0.037	46	ND	0.035	47	ND	0.036	0.04	0.60	52.58	ND
105	6.84	10	49	ND	0.015	50	ND	0.013	51	ND	0.009	0.01	0.55	50.95	ND
135	6.81	9.4	53	ND	0.003	54	ND	0.001	55	ND	0.006	0.00	0.57	50.28	ND

* Possibly the drop in pH was due to Fe oxide formation (H+ released). Average Fe (8) = 52.39 +/- 1.47 & (2) 53.67 mg/L

Table A-27: 8/25/94: pH = 7; Fe(II) Target = 100 mg/L; 0.5 mg/L as Mn(II); Ca^{++} & HCO_3^- = 3 meq/L; HOCl = 2 mg/L; 10°C

Time	Final	Temp.	0.45 um Filtered Samples			30k Ultrafiltered Sample # 1			30k Ultrafiltered Sample # 2			Avg.	Bottle Conc. (mg/L)		HOCl
(min)	pH	(C)	Tube #	Fe (mg/L)	Mn (mg/L)	Tube #	Fe (mg/L)	Mn (mg/L)	Tube #	Fe (mg/L)	Mn (mg/L)	Ultra	Mn	Fe	(mg/L)
0	Acidified		1	99.99	0.609										ND
0	Acidified		2	103.36	0.602										ND
5	7	10.5	3	ND	0.378										ND
5	Adsorb		4	ND	0.389										ND
15	6.86	9.5	5	ND	0.355	6	ND	0.353	7	ND	0.347	0.35	0.58	95.24	ND
30	6.88	8.6	9	ND	0.308	10	ND	0.313	11	ND	0.319	0.32	0.62	106.15	ND
45	6.9	8.7	13	ND	0.263	14	ND	0.265	15	ND	0.26	0.26	0.62	105.09	ND
60	6.9	8.8	17	ND	0.217	18	ND	0.218	19	ND	0.212	0.22	0.60	97.24	ND
75	6.88	9	21	ND	0.155	22	ND	0.151	23	ND	0.145	0.15	0.61	100.89	ND
90	6.88	9	25	ND	0.114	26	ND	0.116	27	ND	0.111	0.11	0.64	103.84	ND

* Average Fe (8) = 101.5 +/- 3.84 & (2) 101.7 mg/L

Fe(II) Oxidized Prior to Mn(II) Addition

Table A-28: 9/11/94: pH = 7; Fe(II) Target = 100 mg/L; 0.5 mg/L as Mn(II); Ca^{++} & HCO_3^- = 3 meq/L; HOCl = 2 mg/L; 10°

Time	Final	Temp.	0.45 um Filtered Samples			0.45 um Filtered Samples			Avg.
(min)	pH	(C)	Tube #	Fe (mg/L)	Mn (mg/L)	Tube #	Fe (mg/L)	Mn (mg/L)	0.45 um
0	Acidified; Fe only		1	136.3	0.094	2	109	0.094	0.09
0	Acidified; Both		3	116.7	0.608	4	112.6	0.608	0.61
5	Adsorb		5	ND	0.491	6	ND	0.484	0.49
20			7	ND	0.373	8	ND	0.343	0.36
40	6.86	9.5	9	ND	0.245	10	ND	0.227	0.24
60	6.88	8.6	11	ND	0.158	12	ND	0.148	0.15
80	6.9	8.7	13	ND	0.056	14	ND	0.05	0.05
100	6.9	8.8	15	ND	0.016	16	ND	0.012	0.01
120	6.88	9	17	ND	0	18	ND	0	0.00

* Average Fe (3) = 112.77 +/- 3.85 & (5) 111.86+/- 5.66 mg/L

Also had a few samples from bottles used; Fe = 103.7 and 117.3 mg/L.

Table A-29: 12/28/94: pH = 8; Fe(II) Target = 100 mg/L; 0.5 mg/L as Mn(II); Ca^{++} & HCO_3^- = 3 meq/L; HOCl = 2 mg/L; 10°C

Time	Final	Temp.	0.45 um Filtered Samples			0.45 um Filtered Samples			HOCl	Avg.
(min)	pH	(C)	Tube #	Fe (mg/L)	Mn (mg/L)	Tube #	Fe (mg/L)	Mn (mg/L)	(mg/L)	0.45 um
0	Acidified; Fe only		1	93.75	0.019	2	95.5	0.016		0.02
0	Acidified; Both		3	94.2	0.5	4	92.7	0.507	1.41	0.50
5	Adsorb		5	ND	0.353	6	ND	0.363		0.36
10	8.02	9	7	ND	0.225	8	ND	0.218		0.22
20	7.98	9	9	ND	0.169	10	ND	0.164		0.17
30	8.01	9.3	11	ND	0.1054	12	ND	0.091		0.10
40	7.97	9.5	13	ND	0.063	14	ND	0.058		0.06
50	7.96	9.3	15	ND	0.031	16	ND	0.021		0.03
60	8.02	9.3	17	ND	0.005	18	ND	0.006	1.12	0.01

* Average Fe (4) = 94 +/- 1.16 mg/L; **PURE IRON GRADE**

Fe(II) Oxidized Prior to Mn(II) Addition

Table A-30: 12/29/94: pH = 8; Fe(II) Target = 15 mg/L; 0.5 mg/L as Mn(II); Ca^{++} & HCO_3^- = 3 meq/L; HOCl = 2 mg/L; 10°C

Time (min)	Final pH	Temp. (C)	0.45 um Filtered Samples			0.45 um Filtered Samples			HOCl (mg/L)	Avg. 0.45 um
			Tube #	Fe (mg/L)	Mn (mg/L)	Tube #	Fe (mg/L)	Mn (mg/L)		
0	Acidified; Fe only		21	15.36	0.023	22	15.78	0.021		0.02
0	Acidified; Both		23	18.65	0.492	24	17.94	0.501		0.50
5	Adsorb		25	ND	0.488	26	ND	0.472	1.73	0.48
30	7.92	9.5	27	ND	0.286	28	ND	0.273		0.28
60	7.85	10	29	ND	0.113	30	ND	0.103	1.47	0.11
90	7.74	10	31	ND	0.005	32	ND	0.002		0.00
120	7.78	9.8	33	ND	0.002	34	ND	0	1.23	0.00
150	7.74	11	35	ND	0.003	36	ND	0.001		0.00
180	7.74	11	37	ND	0	38	ND	0.001	1.27	0.00

* Average Fe (2) = 15.57 +/- 0.3 & (4) 16.93 mg/L; REGULAR IRON

Table A-31: 12/29/94: pH = 8; Fe(II) Target = 100 mg/L; 0.5 mg/L as Mn(II); Ca^{++} & HCO_3^- = 3 meq/L; HOCl = 2 mg/L; 10°C

Time (min)	Final pH	Temp. (C)	0.45 um Filtered Samples			HOCl (mg/L)
			Tube #	Fe (mg/L)	Mn (mg/L)	
0	Acidified; Fe only		Fe 0	94.8	0.1065	
0	Acidified; Both		Mn 0	95.9	0.564	
0	Acidified; Both		Mn 0	98.3	0.567	
5	Adsorb		AD	ND	0.354	1.95
10	7.97	10.5	10	ND	0.142	
20	7.92	10	20	ND	0.085	
30	8	9.8	30	ND	0.028	
40	8.02	9.2	40	ND	0	
50	8	9	50	ND	0	
60	7.98	9.2	60	ND	0	1.4

* Average Fe (3) = 96.33 +/- 1.79 mg/L REGULAR IRON

Predicted vs. Actual HOCl Requirements

Results Summarized from Data Previously Presented

Table A-32: Predicted vs. Actual HOCl Requirements pH 8

Reaction Time (min)	Fe = 4 mg/L						
	Mn (mg/L)	Δ Mn (mg/L)	HOCl (mg/L)	Est. Sorbed Mn (mg/L)	HOCl Required (mg/L)		
					Predicted	Predict Mn Oxed	Actual
0	0.54	0	2.1	0.02	0	0	0.00
30	0.46	0.07	1.98	0.02	0.09	0.07	0.12
60	0.39	0.15	1.91	0.02	0.19	0.17	0.19
120	0.26	0.28	1.87	0.02	0.37	0.34	0.23
180	0.12	0.41	1.76	0.01	0.54	0.52	0.34
240	0.03	0.51	1.66	0.00	0.66	0.66	0.44
300	0	0.54	1.61	0.00	0.70	0.70	0.49
Reaction Time (min)	Fe = 8 mg/L						
	Mn (mg/L)	Δ Mn (mg/L)	HOCl (mg/L)	Est. Sorbed Mn (mg/L)	HOCl Required (mg/L)		
					Predicted	Predict Mn Oxed	Actual
0	0.52	0	1.97	0.04	0	0	0.00
30	0.40	0.12	1.84	0.04	0.15	0.10	0.13
60	0.32	0.20	1.75	0.04	0.26	0.22	0.22
135	0.08	0.44	1.61	0.02	0.57	0.55	0.36
180	0	0.52	1.45	0.00	0.68	0.68	0.52
240	0	0.52	1.39	0.00	0.68	0.68	0.58
300	0	0.52	1.39	0.00	0.68	0.68	0.58
Reaction Time (min)	Fe = 15 mg/L						
	Mn (mg/L)	Δ Mn (mg/L)	HOCl (mg/L)	Est. Sorbed Mn (mg/L)	HOCl Required (mg/L)		
					Predicted	Predict Mn Oxed	Actual
0	0.49	0	1.73	0.08	0	0	ND
30	0.46	0.03	ND	0.07	0.04	n/a	ND
60	0.39	0.10	1.47	0.07	0.13	0.04	0.26
90	0.26	0.24	ND	0.06	0.31	0.23	ND
120	0.12	0.37	1.23	0.04	0.48	0.42	0.50
150	0.03	0.47	ND	0.01	0.60	0.59	ND
180	0	0.49	1.27	0.00	0.64	0.64	0.46
Reaction Time (min)	Fe = 20 mg/L						
	Mn (mg/L)	Δ Mn (mg/L)	HOCl (mg/L)	Est. Sorbed Mn (mg/L)	HOCl Required (mg/L)		
					Predicted	Predict Mn Oxed	Actual
0	0.52	0	2.03	0.10	0	0	ND
30	0.32	0.21	1.75	0.09	0.27	0.16	0.28
60	0.14	0.38	1.56	0.06	0.49	0.41	0.47
135	0.00	0.52	1.38	-0.06	0.68	0.68	0.65
180	0	0.52	1.42	0.00	0.68	0.68	0.61
240	0	0.52	1.35	0.00	0.68	0.68	0.68
300	0	0.52	1.35	0.00	0.68	0.68	0.68
Reaction Time (min)	Fe = 50 mg/L						
	Mn (mg/L)	Δ Mn (mg/L)	HOCl (mg/L)	Est. Sorbed Mn (mg/L)	HOCl Required (mg/L)		
					Predicted	Predict Mn Oxed	Actual
0	0.582	0	1.48	0.26	0	0	ND
20	0.13	0.46	ND	0.15	0.59	0.40	ND
40	0.01	0.57	ND	-0.03	0.74	0.74	ND
60	0.01	0.58	1.33	-0.08	0.75	0.75	0.15
80	0.00	0.58	ND	-0.21	0.76	0.76	ND
100	0.00	0.58	ND	-0.16	0.75	0.75	ND
120	0	0.58	1.27	0.00	0.76	0.76	0.21
Reaction Time (min)	Fe = 100 mg/L						
	Mn (mg/L)	Δ Mn (mg/L)	HOCl (mg/L)	Est. Sorbed Mn (mg/L)	HOCl Required (mg/L)		
					Predicted	Predict Mn Oxed	Actual
0	0.5	0	1.41	0.51	0	0	ND
10	0.22	0.28	ND	0.38	0.36	-0.13	ND
20	0.17	0.33	ND	0.34	0.43	-0.02	ND
30	0.10	0.40	ND	0.26	0.52	0.18	ND
40	0.06	0.44	ND	0.19	0.57	0.33	ND
50	0.03	0.47	ND	0.08	0.61	0.50	ND
60	0.01	0.49	1.12	-0.08	0.64	0.64	0.29

* For each case initial HOCl dose = 2 mg/L unless otherwise noted; 0.45 um results used; HOCl Req'd calculated from "0" value.

Predicted vs. Actual HOCl Requirements

Results Summarized from Data Previously Presented

Table A-33: Predicted vs. Actual HOCl Requirements pH 7

Reaction Time (min)	Fe = 2 mg/L						
	Mn (mg/L)	Δ Mn (mg/L)	HOCl (mg/L)	Est. Sorbed Mn (mg/L)	HOCl Required (mg/L)		
					Predicted	Predict Mn Oxed	Actual
0	0.52	0	2	0.00	0	0	ND
30	0.48	0.04	1.85	0.00	0.06	0.05	0.15
60	0.47	0.05	1.85	0.00	0.07	0.06	0.15
120	0.43	0.09	1.82	0.00	0.12	0.12	0.18
180	0.40	0.12	1.76	0.00	0.15	0.15	0.24
240	0.36	0.16	1.67	0.00	0.21	0.21	0.33
300	0.308	0.21	1.63	0.00	0.27	0.27	0.37
Reaction Time (min)	Fe = 8 mg/L						
	Mn (mg/L)	Δ Mn (mg/L)	HOCl (mg/L)	Est. Sorbed Mn (mg/L)	HOCl Required (mg/L)		
					Predicted	Predict Mn Oxed	Actual
0	0.52	0	1.66	0.01	0	0	ND
30	0.37	0.15	1.57	0.01	0.20	0.18	0.09
60	0.34	0.18	1.56	0.01	0.23	0.21	0.10
90	0.30	0.22	1.57	0.01	0.29	0.27	0.09
120	0.26	0.25	1.48	0.01	0.33	0.32	0.18
180	0.16	0.36	1.5	0.01	0.46	0.45	0.16
240	0.067	0.45	1.33	0.00	0.59	0.58	0.33
Reaction Time (min)	Fe = 10 mg/L						
	Mn (mg/L)	Δ Mn (mg/L)	HOCl (mg/L)	Est. Sorbed Mn (mg/L)	HOCl Required (mg/L)		
					Predicted	Predict Mn Oxed	Actual
0	0.53	0	1.84	0.02	0	0	ND
30	0.40	0.13	1.54	0.01	0.17	0.15	0.30
60	0.33	0.20	1.58	0.01	0.26	0.25	0.26
90	0.27	0.26	1.56	0.01	0.34	0.32	0.28
120	0.20	0.34	1.48	0.01	0.44	0.43	0.36
150	0.15	0.39	1.47	0.01	0.50	0.49	0.37
180	0.083	0.45	1.33	0.01	0.59	0.58	0.51
Reaction Time (min)	Fe = 20 mg/L						
	Mn (mg/L)	Δ Mn (mg/L)	HOCl (mg/L)	Est. Sorbed Mn (mg/L)	HOCl Required (mg/L)		
					Predicted	Predict Mn Oxed	Actual
0	0.56	0	1.81	0.03	0	0	ND
15	0.45	0.11	ND	0.03	0.14	0.10	ND
30	0.42	0.14	ND	0.03	0.18	0.14	ND
45	0.39	0.17	ND	0.03	0.22	0.19	ND
60	0.33	0.23	1.5	0.03	0.30	0.27	0.31
75	0.28	0.28	ND	0.03	0.36	0.33	ND
90	0.24	0.32	1.49	0.02	0.41	0.38	0.32

* For each case initial HOCl dose = 2 mg/L unless otherwise noted; 0.45 um results used; HOCl Req'd calculated from "0" value.

Mn(II) Oxidation onto MnO_X

Table A-34: 9/19/94: pH = 8; MnO_X Target = 0.525 mg/L; 0.5 mg/L as Mn(II); Ca^{++} & HCO_3^- = 3 meq/L; HOCl = 2 mg/L; 10°C

Time	Final	Temp.	0.45 um Samples		30k Sample # 1		30k Sample # 2		Avg.	HOCl
(min)	pH	(C)	Tube #	Mn (mg/L)	Tube #	Mn (mg/L)	Tube #	Mn (mg/L)	Ultra	(mg/L)
0	Extracted- MnOx		1	0.294	2	0.307				
0	Extracted- Both		3	0.793	4	0.852				
5-adsorb	8.02	10.8	5	0.47	6	0.454	7	0.456	0.46	ND
20	ND	ND	8	0.451	9	0.44	10	0.443	0.44	1.87
40	7.83	10	11	0.439	12	0.436	13	0.438	0.44	1.93
60	7.83	10.2	14	0.439	15	0.433	16	0.431	0.43	1.90
80	7.86	10.2	17	0.434	18	0.428	19	0.422	0.43	1.91
100	7.84	10.2	20	0.426	21	0.416	22	0.416	0.42	1.91
120	7.84	9	23	0.416	24	0.409	25	0.417	0.41	1.91

* Note: MnOx concentration ~ 0.47 mg/L.

Table A-35: 9/20/94: pH = 8; MnO_X Target = 1.77 mg/L; 0.5 mg/L as Mn(II); Ca^{++} & HCO_3^- = 3 meq/L; HOCl = 2 mg/L; 10°C

Time	Final	Temp.	0.45 um Samples		30k Sample # 1		30k Sample # 2		Avg.	HOCl
(min)	pH	(C)	Tube #	Mn (mg/L)	Tube #	Mn (mg/L)	Tube #	Mn (mg/L)	Ultra	(mg/L)
0	Extracted- MnOx		26	1.147	27	1.139				
0	Extracted- Both		28	1.543	29	1.667				
5-adsorb	8	10.8	30	0.448	31	0.428	32	0.42	0.42	ND
20	ND	ND	33	0.362	34	0.356	35	0.351	0.35	2.31
40	7.89	10.5	36	0.336	37	0.339	38	0.336	0.34	2.31
60	7.91	11	39	0.316	40	0.304	41	0.305	0.30	2.34
80	7.89	9.8	42	0.294	43	0.285	44	0.287	0.29	2.31
100	7.9	9.8	45	0.274	46	0.269	47	0.265	0.27	ND
120	7.89	10	48	0.252	49	0.249	50	0.247	0.25	2.34

* Note: MnOx concentration ~ 1.81 mg/L.

Table A-36: 9/21/94: pH = 8; MnO_X Target = 1.77 mg/L; 0.5 mg/L as Mn(II); Ca^{++} & HCO_3^- = 3 meq/L; HOCl = 2 mg/L; 10°C

Time	Final	Temp.	0.45 um Samples		30k Sample # 1		30k Sample # 2		Avg.	HOCl
(min)	pH	(C)	Tube #	Mn (mg/L)	Tube #	Mn (mg/L)	Tube #	Mn (mg/L)	Ultra	(mg/L)
0	Extracted- Both		51	1.305	52	1.257				
0	Filtered- Both		53	0.448	54	0.465				
5-adsorb	8.01	10.5	55	0.444	56	0.412	57	0.407	0.41	ND
30	ND	ND	58	0.377	59	0.36	60	0.35	0.36	2.22
60	7.78	9	61	0.329	62	0.326	63	0.333	0.33	2.15
120	7.97	9	64	0.292	65	0.285	66	0.284	0.28	2.16
180	7.89	9	67	0.244	68	0.238	69	0.24	0.24	2.10
240	ND	9.8	70	0.213	71	0.2	72	0.21	0.21	2.06
360	ND	8.5	73	0.135	74	0.125	75	0.128	0.13	2.01

* Note: MnOx concentration ~ 2.02 mg/L.

Table A-37: CSTR System: Before and After 4 mg/L HOCl Dose was Added

Influent = 0.5 mg/L as Mn(II), Fe(II) = 2 mg/L, Ca^{++} and HCO_3^- = 3 meq/L, pH = 6.85, 15°C, HOCl as indicated; θ_H = 1 hour

Time of Sampling	Total Elapsed Time (hr)	Mn Reactor 1; Fe(III) = 250 mg/L	Mn Reactor 2; Fe(III) = 500 mg/L	Mn Reactor 3; Fe(III) = 750 mg/L	Mn Mixer (mg/L)	Other/Comments
No HOCl Added; ~ 1 mg/L Residual in Tap Water						
10/10/94 10:40	0				0.875	
10/10/94 10:55	0:15	0.127	0.036	0.016		
10/10/94 11:10	0:30	0.156	0.065	0.026		
10/10/94 11:25	0:45	0.194	0.088	0.047		
10/10/94 11:40	1:00	0.219	0.113	0.064		
10/10/94 11:55	1:15	0.271	0.153	0.088		
10/10/94 12:10	1:30	0.297	0.204	0.121		
10/10/94 12:40	2:00	0.35	0.261	0.182		
10/10/94 13:10	2:30	0.393	0.318	0.233		
10/10/94 13:40	3:00	0.421	0.357	0.444		
10/10/94 14:10	3:30	0.401	0.337	0.334		
10/10/94 14:40	4:00	0.331	0.334	0.472		
10/10/94 15:10	4:30	0.466	0.172	0.187		
10/10/94 17:10	6:30	0.501	0.44	0.43		
10/10/94 17:40	7:00	0.511	0.497	0.472		
10/10/94 20:55	10:15	0.578	0.581	0.511		
10/11/94 12:55		0.539	0.594	0.555		
10/12/94 0:30	0	***Began HOCl Feed = 4 mg/L***				
10/12/94 0:45	0:15	0.404	0.329	0.417		
10/12/94 1:00	0:30	0.187	0.094	0.063		
10/12/94 1:15	0:45	0.173	0.062	0.057		
10/12/94 1:30	1:00	0.186	0.065	0.047		
10/12/94 1:45	1:15	0.171	0.055	0.031		
10/12/94 2:00	1:30	0.149	0.044	0.006		
10/12/94 2:15	1:45	0.135	0.028	0.005		
10/12/94 2:30	2:00	0.123	0.02	0		
10/12/94 2:45	2:15	0.098	0.01	0		
10/12/94 3:00	2:30	0.085	0.01	0.001		
10/12/94 3:15	2:45	0.071	0.008	0.004		
10/12/94 3:30	3:00	0.057	0.007	0.002	0.512	
10/12/94 12:40	12:10	0.007	0.001	0.001		
10/13/94 13:40	13:10	0.009	0.005	0.001	0.69	pH(1): 6.85; (2): 6.81; (3) 6.86
10/15/94 19:00	18:30					HOCl(1): 1.61; (2):1.44; (3): 1.67

Table A-38: 11/1/94 CSTR System:

HOCl = 4 mg/L, Fe = 2 mg/L Mn = 0.5 mg/L θ_H = 1 hour; pH = ~ 7.1, Temperature = 13°C

Time	Time	Reactor # 1	Reactor # 2	Reactor # 3	Mn Mixer	Mixer HOCl	Actual Concentrations		Acid Effluent; 1, 2, & 3 (mg/L)						HOCl or S.S. Conc. (mg/L); 1, 2, & 3					
(minutes)	(hours)	100 mg/L Fe	200 mg/L Fe	300 mg/L Fe	(mg/L)	(mg/L)	Mn (mg/L)	HOCl (mg/L)	Fe	Mn	Fe	Mn	Fe	Mn	Fe/S.S.	Mn/HOCl	Fe/S.S.	Mn/HOCl	Fe/S.S.	Mn/HOCl
15	0.25	0.051	0.161	0.143																
30	0.50	0.039	0.137	0.104																
45	0.75	0.041	0.097	0.052						0.382		0.33		0.274						
60	1.00	0.025	0.066	0.013	0.566		0.46													
75	1.25	0.031	0.06	0.007																
90	1.50	0.05	0.049	0.004																
105	1.75	0.035	0.03	0																
120	2.00	0.034	0.023	0																
150	2.50	0.015	0.002	0																
180	3.00	0.021	0.008	0.015																
210	3.50	0.01	0	0.016											85	2.2	134	12.4	468.8	8.2
240	4.00	0.012	0	0.022		3.80		3.11								0.28		0.22		0.22
315	5.25	0.004	0	0.017																
450	7.50	0.022	0.013	0.005	0.513		0.42													
900	15.00	0.004	0.005	0.002											18.1		22.8		129.9	
1470	24.50	0.015	0.003	0.001	0.648		0.53													
1530	25.50				0.578		0.47									1.24		1.6		1.36
SPILL OCCURRED AT 12:30 P.M.																				
1650	27.50														72		197		91	
2070	34.50	0.098	0.005	0.012	0.628	4.63	0.51	3.78												
2130	35.50	0.09	0.009	0.008		4.44		3.63							10		65		147	
2940	49.00	0.151	0.032	0.015	0.62		0.51		2.033	0.535	4.485	0.711	6.02	2.98						
3045	50.75	0.099	0.038	0.019																

Table A-39: 11/3/94 CSTR System:

Influent: HOCl = 2-3 mg/L, Fe = 2 mg/L, Mn = 0.5 mg/L, Ca^{++} and HCO_3^- = 3 meq/L, pH= 7.2, θ_H = 1 hour, 13°C

Time (min)	Time (hours)	Reactor # 1 100 mg/L	Reactor # 2 200 mg/L	Reactor # 3 300 mg/L	Mixer Mn (mg/L)	Mixer HOCl (mg/L)	Actual Concentrations Mn (mg/L)	Actual Concentrations HOCl (mg/L)	Acid Effluent; 1, 2, & 3 (mg/L) Fe	Mn	Fe	Mn	Fe	Mn	HOCl or S.S. Conc. (mg/L); 1, 2, & 3 Fe/S.S.	Mn/HOCl	Fe/S.S.	Mn/HOCl	Fe/S.S.	Mn/HOCl
HOCl = 2 mg/L																				
15	0.25	0.43	0.291	0.23	0.615		0.50													
30	0.50	0.336	0.308	0.236											18.1	1.46	22.8	0.99	129.9	3.27
45	0.75	0.347	0.33	0.26						0.382		0.33		0.274						
60	1.00	0.372	0.351	0.29																
75	1.25	0.379	0.367	0.301																
90	1.50	0.388	0.388	0.312																
105	1.75	0.389	0.402	0.322																
120	2.00	0.381	0.438	0.332																
135	2.25	0.375	0.445	0.334	0.637		0.52													
645	10.75	0.317	0.422	0.219	0.676		0.55													
975	16.25	0.353	0.405	0.245	0.66		0.54								85	2.2	134	12.4	468.8	8.2
1050	17.50					1.90		1.55								0.28		0.22		0.22
1425	23.75	0.342	0.374	0.331	0.652		0.53													
HOCl Dose Changed to 3 mg/L																				
1470	24.50	0.36	0.401	0.37											18.1		22.8		129.9	
1485	24.75	0.354	0.391	0.349																
1500	25.00	0.35	0.387	0.342																
1515	25.25	0.341	0.371	0.307																
1530	25.50	0.326	0.355	0.266																
1545	25.75	0.32	0.346	0.238																
1575	26.25	0.29	0.33	0.177																
1605	26.75	0.271	0.312	0.149																
2310	38.50	0.111	0.217	0.03	0.656	3.36	0.54	2.75								1.2		1.08		0.95
2430	40.50	0.191	0.318	0.03	0.61		0.50													
2475	41.25					3.46		2.83							34		27		85	
2745	45.75	0.2	0.317	0.037	0.657		0.54												136.8	23.4
3645	60.75	SHUTDN	SHUTDN	0.237	0.601		0.49						3.787	0.519						

Table A-40: 11/7/94 CSTR System Startup:

Influent: HOCl = 1-2 mg/L, Fe = 2 mg/L, Mn = 0.5 mg/L, Ca^{++} and HCO_3^- = 3 meq/L, pH= 6.8, θ_H = 2 hour, 15°C

Time	Time	Reactor # 1	Reactor # 2	Reactor # 3	Mixer Mn	Mixer HOCl	Actual Concentrations		Acid Effluent; 1, 2, & 3 (mg/L)						HOCl or S.S. Conc. (mg/L); 1, 2, & 3					
(min)	(hr)	100 mg/L	200 mg/L	300 mg/L	(mg/L)	(mg/L)	Mn (mg/L)	HOCl (mg/L)	Fe	Mn	Fe	Mn	Fe	Mn	Fe/S.S.	Mn/HOCl	Fe/S.S.	Mn/HOCl	Fe/S.S.	Mn/HOCl
STARTUP; HOCl = 2 mg/L																				
25	0.42	0.025	0.03	0.017	0.747		0.47													
45	0.75	0.051	0.073	0.051					4.82	0.082	10.04	0.094	5.98	0.061						
60	1.00	0.065	0.087	0.06																
90	1.50	0.086	0.12	0.082											87.8	1.91	189	2.12	306.9	2.34
120	2.00	0.098	0.145	0.103																
150	2.50	0.107	0.173	0.105																
180	3.00	0.108	0.196	0.12																
210	3.50	0.115	0.203	0.135	0.696	2.71	0.44	1.72												
750	12.50	0.058	0.059	0.035	0.695	2.63	0.44	1.67	2.368		3.424		3.957		87.8		189		306.9	
840	14.00	0.055	0.06	0.024											157.5		346.5		521.4	
945	15.75	0.047	0.06	0.033	0.665	2.75	0.42	1.75								0.34		0.28		0.3
1095	18.25	0.037	0.041	0.022	0.61	2.78	0.39	1.77												
1230	20.50	0.072	0.105	0.07	0.757		0.48													
1425	23.75	0.167	0.237	0.175	0.667		0.42			0.241		0.315		0.238						
2160	36.00	0.039	0.052	0.024	0.71		0.45													
2340	39.00	0.067	0.083	0.054	0.764		0.49								133.33		253.33		467	
2610	43.50	0.1	0.124	0.088	0.74	2.79	0.47	1.77	1.566	0.186	3.047	0.228	2.962	0.16						
2805	46.75	0.127	0.138	0.115	0.792	2.8	0.50	1.78	1.216		1.92		3.208							
Changed HOCl Dose from ~ 2 mg/L to 1 mg/L																				
2850	47.50	0.116	0.136	0.103	0.781		0.50								75.5	3.3	144.5	5.62	234.7	6.5
3030	50.50	0.361	0.392	0.353	0.772	1.48	0.49	0.94												
3510	58.50	0.622	0.638	0.673	0.831	1.57	0.53	1.00	1.317	0.665	1.561	0.664	3.744	0.732		0.16		0		0.25
3570	59.50														166.67		240			433.33
3645	60.75	0.622	0.691	0.68																
3720	62.00	0.609	0.683	0.676	0.818		0.52		0.871	0.657	2.663	0.754	4.612	0.761	115.3	4.271	140.4	4.16	216.2	4.85

Table A-41(a): 1/4/95 & 1/5/95 CSTR System:

Influent: HOCl = 2.5-3 mg/L, Fe = 2 mg/L, Mn = 0.5 mg/L, Ca^{++} and HCO_3^- = 3 meq/L, pH= 7; θ_H = 2 hour, 20°C

Date	Time of Day	Reactor # 1: 100 mg/.L					Reactor # 2: 200 mg/.L					Reactor # 3: 300 mg/.L				
		Filt. Effluent		Acid Effluent			Filt. Effluent		Acid Effluent			Filt. Effluent		Acid Effluent		
		Tube	Mn	Tube	Mn	Fe	Tube	Mn	Tube	Mn	Fe	Tube	Mn	Tube	Mn	Fe
1/4/95	8:30	***SYSTEM STARTUP; HOCl = 3 mg/L***														
	9:00	4	0.155	7	0.126	7.241	5	0.044	8	0.046	3.331	6	0.024	9	0.038	5.727
	9:30	10	0.117	13	0.138	2.296	11	0.07	14	0.054	3.214	12	0.045	15	0.027	4.918
	10:00	17	0.143				18	0.047				19	0.008			
	10:30	20	0.072	23	0.103	1.807	21	0.045	24	0.07	3.715	22	0.009	25	0.03	4.912
	11:00	26	0.054				27	0.053				28	0.006			
	11:30	29	0.042	32	0.081	1.889	30	0.054	33	0.08	3.356	31	0.006	34	0.032	4.882
	12:00	35	0.037				36	0.041				37	0.012			
	13:00	38	0.037	41	0.069	2.231	39	0.042	42	0.078	3.404	40	0.006	43	0.05	6.213
	14:00	45	0.018	48	0.062	2.2	46	0.029	49	0.061	3.473	47	0.003	50	0.032	4.956
	15:00	51	0.016	54	0.061	1.929	52	0.023	55	0.059	3.164	53	0.018	56	0.034	4.681
	16:30	58	0.014	61	0.054	2.089	59	0.016	62	0.055	4.45	60	0.007	63	0.041	5.078
	20:30	67	0.006	70	0.057	2.164	68	0.056	71	0.056	3.985	69	0.004	72	0.049	5.012
	23:00	80	0.007				81	0.004				82	0.001			
		CHANGE TO 2.5mg/L HOCl														
1/5/95	9:00	84	0.01	87	0.149	2.736	85	0.007	88	0.1	3.604	86	0.004	89	0.11	5.032
	10:30	91	0.006	94	0.157	2.757	92	0.005	95	0.156	5.576	93	0	96	0.149	6.685
	11:30	100	0.004				101	0.005				102	0.002			
	12:30	104	0.014	107	0.136	2.524	105	0.008	108	0.138	4.611	106	0.004	109	0.116	5.358
	13:30	110	0.008				111	0.004				112	0.004			
	14:30	121	0.01	124	0.17	2.772	122	0.01	125	0.144	3.852	123	0.006	126	0.123	5.081
	16:00	127	0.013				128	0.012				129	0.006			
	18:00	131	0.003	134	0.172	2.976	132	0.005	135	0.168	4.146	133	0.004	136	0.177	5.55
	20:00	139	0.019	143	0.195	2.651	140	0.019	144	0.188	4.504	141	0.004	145	0.174	ND
	21:30	146	0.017				147	0.015				148	0.01			
	22:30	149	0.03	152	0.187	2.553	150	0.027	153	0.19	4.141	151	0.011	154	0.172	5.41
	23:30	159	0.028				160	0.028				161	0.009			

* Note: Acidified effluent values do not account for dilutions

Acid Effluents: 4 mL and 5 drops nitric; as of 1/5/94 began using 5 mL sample; samples 7-9 4 mL sample 1 mL acid

In-Reactor Solids: 5 mL sample 2 mL acid; then 100:1

Generally temperatures held fairly constant at 20 degees C.

Table A-41(b): 1/4/95 & 1/5/95 CSTR System:

Influent: HOCl = 2.5-3 mg/L, Fe = 2 mg/L, Mn = 0.5 mg/L, Ca^{++} and HCO_3^- = 3 meq/L, pH= 7; θ_H = 2 hour, 20°C

Time of Day	Mn Mixer Tube #	Mn Mixer Conc. (mg/L)	HOCl Mixer (mL)	Actual Conc. Mn (mg/L)	Actual Conc. HOCl (mg/L)	Temp. (C)	pH 1	pH 2	pH 3	Effluent HOCl, In-Solids Conc., or Influent Lines (mg/L) Reactor # 1 Tube	Fe	Mn	HOCl	Reactor # 2 Tube	Fe	Mn	HOCl	Reactor # 3 Tube	Fe	Mn	HOCl	Comments
8:30				n/a	n/a					1	112	0.92		2	255	0.9		3	371	1.04		Mn Feed Line in Sink 8:30-9:00; added 0.4mL back!
9:00				n/a	n/a																	Avg. HNO_3 Drop = 0.03034 g
9:30				n/a	n/a																	HNO_3: 2.5 L = 7.8 lb; s = 1.42
10:00	16	0.59	2.25	0.53	3.01																	
10:30				n/a	n/a																	
11:00				n/a	n/a																	
11:30				n/a	n/a																	
12:00				n/a	n/a																	
13:00	44	0.545	1.94	0.49	2.59																	
14:00				n/a	n/a		6.76	6.92	6.96													Added 500mL Boost; pH effluent
15:00	57	0.56		0.51	n/a																	
16:30				n/a	n/a					64	101	2.46	0.71	65	226	2.69	0.52	66	318	2.84	0.52	
20:30	73	0.526	2.13	0.47	2.85		6.87	7.02	7.07													pH Effluent
23:00	83	0.572		0.52	n/a																	Added 500mL Boost
CHANGE TO 2.5mg/L HOCl																						
9:00	90	0.581	1.92	0.52	2.57																	
10:30			1.87	n/a	2.50		6.87	6.95	7.02				0.87				0.68				0.78	Tap [HOCl] = 1.28 mg/L as HOCl; pH Reactor
11:30	103	0.563	1.97	0.51	2.63					97	87.9	4.86		98	204	6.02		99	278	6.22		
12:30				n/a	n/a																	
13:30	113	0.435	1.98	0.39	2.65																	
14:30			1.86	n/a	2.49								0.71				0.56				0.74	
16:00	130	0.531	1.86	0.48	2.49																	Added 500mL Boost; HOCl and Mn after boost
18:00	138	0.538	1.85	0.49	2.47																	
20:00	142	0.605	1.84	0.55	2.46																	
21:30				n/a	n/a																	
22:30	155	0.568	1.51	0.51	2.02					156	85.4	6.3		157	194	7.95		158	247	7.1		500mL Boost; In-Reactor - 5 mL sample, 3 mL acid
23:30				n/a	n/a																	

Table A-41(c): 1/6/95 - 1/8/95 CSTR System (Continued Operation from 1/4 & 1/5):
Influent: HOCl = 2.5 mg/L, Fe = 2 mg/L, Mn = 0.5 mg/L, Ca^{++} and HCO_3^- = 3 meq/L, pH= 7; θ_H = 2 hour, 20°C

Date	Time of Day	Reactor # 1: 100 mg/.L					Reactor # 2: 200 mg/.L					Reactor # 3: 300 mg/.L				
		Filt. Effluent		Acid Effluent			Filt. Effluent		Acid Effluent			Filt. Effluent		Acid Effluent		
		Tube	Mn	Tube	Mn	Fe	Tube	Mn	Tube	Mn	Fe	Tube	Mn	Tube	Mn	Fe
1/6/95	10:00	*RESTART SYSTEM AFTER HAS CLEANING (Mixer Empty b/c Constant Head Tank Froze); HOCl = 2.5 mg/L*														
	11:00	162	0.201	165	0.412		163	0.159	166	0.4		164	0.007	167	0.282	
	12:30	169	0.085	175	0.432		170	0.076	176	0.429		171	0.024	177	0.336	
	14:30	178	0.035	181	0.273		179	0.059	182	0.306		180	0.001	183	0.35	
	16:30	185	0.069	188	0.38	3.687	186	0.066	189	0.395	6.395	187	0.008	190	0.334	6.869
	18:30	1	0.06	4	0.211	2.968	2	0.065	5	0.247	6.086	3	0.025	6	0.235	6.569
	20:30	7	0.061				8	0.053				9	0.011			
1/7/95	0:30	10	0.036	13	0.275	2.997	11	0.042	14	0.271	4.793	12	0.018	15	0.194	5.426
	10:30	20	0.021	23	0.304	3.431	21	0.014	24	0.261	6.047	22	0	25	0.366	8.04
	14:00	27	0.023	31	0.272	2.672	28	0.017	32	0.252	4.931	29	0.008	33	0.315	6.299
	16:30	37	0.01	40	0.31	2.89	38	0.011	41	0.36	4.377	39	0.008	42	0.346	5.934
	18:00	43	0.018	46	0.291	2.752	44	0.011	47	0.33	3.664	45	0.007	48	0.327	5.922
	19:30	49	0.009				50	0.007				51	0.002			
	20:30	52	0.004				53	0.003				54	0			
	23:00	59	0.003	62	0.202	2.678	60	0.004	1	0.292	3.82	61	0.003	2	0.192	5
1/8/95	10:00	6	0.01	10	0.367	3.216	7	0.007	11	0.498	6.5	8	0.005	12	0.453	6.51
	15:00	13	0.007	17	0.481	2.808	14	0.006	18	0.324	3.74	15	0.005	19	0.353	4.9
	22:00	23	0.012	27	0.225	2.107	24	0.013	28	0.228	2.87	25	0.006	29	0.357	5.03
1/9/95	11:00	33	0.004	37	0.141	2.709	34	0.004	38	0.325	3.73	35	0.006	39	0.313	4.97
	13:00	43	0.008				44	0.008				45	0.002			
	15:30	47	0.004	51	0.349		48	0.003	52	0.378		49	0	53	0.546	
	18:00	54	0.006	58	0.303		55	0.007	59	0.305		56	0.003	60	0.367	

* Note: Acidified effluent values do not account for dilutions

Acid Effluents: 5 mL sample and 5 drops nitric

In-Reactor Solids: see comments field for sampling info; then 100:1

Table A-41(d): 1/6/95 - 1/8/95 CSTR System (Continued Operation from 1/4 & 1/5):

Influent: HOCl = 2.5 mg/L, Fe = 2 mg/L, Mn = 0.5 mg/L, Ca^{++} and HCO_3^- = 3 meq/L, pH= 7; θ_H = 2 hour, 20°C

Time of Day	Mn Mixer Tube #	Mn Mixer Conc. (mg/L)	HOCl Mixer (mL)	Actual Conc. Mn (mg/L)	Actual Conc. HOCl (mg/L)	Temp. (C)	pH 1	pH 2	pH 3	Effluent HOCl, In-Solids Conc., or Influent Lines (mg/L) Reactor # 1 Tube	Reactor # 1 Fe	Reactor # 1 Mn	Reactor # 1 HOCl	Reactor # 2 Tube	Reactor # 2 Fe	Reactor # 2 Mn	Reactor # 2 HOCl	Reactor # 3 Tube	Reactor # 3 Fe	Reactor # 3 Mn	Reactor # 3 HOCl	Comments
11:00	168	0.587	1.54	0.53	2.06																	
12:30			1.43	n/a	1.91		7.07	7.16	7.54	172	84.8	7.12		173	180	8.78		174	256	10.6		500 mL Boost, 5mL w/3 mL acid (In)
14:30	184	0.568	1.51	0.51	2.02		6.78	6.48	6.86				0.31				0.28				0.43	
16:30	191	0.574		0.52	n/a																	500mL Boost after sampling
18:30				n/a	n/a																	
20:30				n/a	n/a																	
0:30	16	0.593		0.53	n/a					17	81.3	7.82		18	155	9.33		19	224	10.5		4 mL sample; 2 mL Acid (In Reactor)
10:30	26	0.57	1.60	0.51	2.14		6.84	6.86	6.84				0.5				0.41				0.47	1L Boost
14:00	30	0.56	1.53	0.51	2.04					34	72	12.3		35	147	10.5		36	196	12.2		2 mL each of sample and acid
16:30			1.48	n/a	1.98																	
18:00			1.47	n/a	1.96																	
19:30				n/a	n/a																	
20:30	55	0.478	1.40	0.43	1.87								0.43				0.36				0.43	
23:00			1.44	n/a	1.92					3	72.8	9.68		4	140	11.8		5	198	14.2		2 mL each of sample and acid
10:00	9	0.501	1.62	0.45	2.16		7.01	7.00	7.02													
15:00	16	0.476	1.55	0.43	2.07					20	67.4	10.1	0.62	21	127	12.8	0.52	22	162	13.8	0.62	2 mL each of sample and acid
22:00	26	0.458		0.41	n/a		7.09	7.10	7.10	30	67.2	10	0.62	31	121	12.6	0.52	32	157	13.6	0.62	2 mL each; New Fe Feed (10mL acid) & Mn 0 acid
11:00	36	0.462	1.64	0.42	2.19		7.7	7.71	7.73	40	62.2	11.4	0.64	41	113	13.3	0.59	42	137	14.4	0.65	Flows great; 2 mL each
13:00	46	0.484	1.65	0.44	2.20																	
15:30	50	0.508	1.61	0.46	2.15																	
18:00	57	0.564	0.78	0.51	1.04																	

Table A-42(a): 1/12/95 - 1/14/95 CSTR System:

Influent: HOCl = 1 mg/L, Fe = 2 mg/L, Mn = 0.5 mg/L, Ca^{++} and HCO_3^- = 3 meq/L, pH= 8; θH = 2.5 hour, 20°C

Date	Time of Day	Reactor # 1: 100 mg/.L					Reactor # 2: 200 mg/.L				
		Filt. Effluent		Acid Effluent			Filt. Effluent		Acid Effluent		
		Tube	Mn	Tube	Mn	Fe	Tube	Mn	Tube	Mn	Fe
1/12/95	11:30	***SYSTEM STARTUP***									
	12:30	3	0.231	6	0.259	4.434	4	0.01	7	0.029	7.031
	13:30	8	0.139	10	0.197	5.123	9	0.042	11	0.044	6.279
	15:15	12	0.2	15	0.297	8.714	13	0.086	16	0.069	9.458
	16:30	17	0.262	19	0.314	7.01	18	0.061	20	0.091	8.134
	17:30	21	0.288	24	0.353	7.596	22	0.074	25	0.107	7.324
1/13/95	0:00	28	0.389	31	0.454	9.746	29	0.18	32	0.226	7.734
	10:00	35	0.398	38	0.471	7.404	36	0.309	39	0.365	7.452
	11:30	42	0.406	44	0.493	7.837	43	0.328	45	0.376	6.812
	13:00	47	0.411				48	0.329			
	16:00	50	0.409	53	0.465	6.169	51	0.29	54	0.359	8.002
	17:00	57	0.412	59	0.459	5.585	58	0.294	60	0.36	8.707
	18:30	62		64		6.114	63		65		8.83
1/14/95	11:30	68		71		6.535	69		72		ND

* Reactor # 1 & 3 actually used with ~ 200 and 300 mg/L as Fe respectively.

* Reactor 2 was used without solids to see effects.

Table A-42(b): 1/12/95 - 1/14/95 CSTR System:

Influent: HOCl = 1 mg/L, Fe = 2 mg/L, Mn = 0.5 mg/L, Ca^{++} and HCO_3^- = 3 meq/L,
pH= 8; θH = 2.5 hour, 20°C

Time of Day	Mn Mixer Tube #	Mn Mixer Conc. (mg/L	HOCl Mixer (mL)	Actual Conc. Mn (mg/L)	Actual Conc. HOCl (mg/L)	Temp. (C)	pH 1	pH 2	Effluent HOCl, In-Solids Conc., or Influent Lines (mg/L) Reactor # 1 Tube	Fe	Mn	HOCl	Reactor # 2 Tube	Fe	Mn	HOCl	Comments or Observations
11:30	5	0.53		0.48	n/a		8.00	8.01	1	219.2			2	345.8			In-Solids Taken at 12:15
12:30			0.97	n/a	1.30												
13:30			0.78	n/a	1.04		8.39	8.39									
15:15	14	0.5	0.74	0.45	0.99		8.05	8.03									
16:30			0.71	n/a	0.95		8.00	8.00									
17:30	23	0.54	0.68	0.49	0.91		8.05	8.05	26	193.4		0.163	27	320.2		0.163	
0:00	30	0.43	0.76	0.39	1.02		7.96	7.96	33	183.8			34	309.2			Mixer Mn taken before adjust; tube sample indicates new conc.
10:00	37	0.46	0.65	0.42	0.87		7.95	8.04	40	156.4			41	282.8			
11:30				n/a	n/a												# 2 Filter Effluent = Tube # 46
13:00	49	0.52	0.68	0.47	0.91		8.05	7.85				0.118				0.163	System down from 13:30 to 15:30 for pump repair
16:00	52	0.49	0.64	0.44	0.86				55	145.6			56	281.8			Found problem: bad pump tube # 3; changed all 3
17:00	61	0.5		0.45	n/a												
18:30		0.37	0.70	0.33	0.94		8.14	8.08	66	141			67	271.2			
11:30	70		0.64	n/a	0.86		8.11	8.10	73	115.6			74	213			

Table A-43(a): 1/17/95 - 1/26/95 CSTR System:

Influent: HOCl = varies, Fe = 2 mg/L, Mn = 0.5 mg/L, Ca^{++} and HCO_3^- = 3 meq/L, pH= 7; θ_H = 2.5 hour, 20°C

Date	Time of Day	Reactor # 1: 100 mg/.L					Reactor # 2: 200 mg/.L					Reactor # 3: 300 mg/.L				
		Filt. Effluent		Acid Effluent			Filt. Effluent		Acid Effluent			Filt. Effluent		Acid Effluent		
		Tube	Mn	Tube	Mn	Fe	Tube	Mn	Tube	Mn	Fe	Tube	Mn	Tube	Mn	Fe
1/17/95	14:30	***System Startup***														
	15:30	4	0.023	8	0.04	2.182	5	0.052	9	0.061	2.44	6	0.03	10	0.031	2.143
	16:30	11	0.069	14	0.093	4.034	12	0.085	15	0.104	3.301	13	0.052	16	0.062	3.736
	17:30	17	0.154	21	0.15	3.885	18	0.105	22	0.138	3.894	19	0.076	23	0.096	3.939
	18:30	24	0.138	28	0.189	4.883	25	0.211	29	0.167	4.227	26	0.104	30	0.119	5.73
	19:30	31	0.159	35	0.21	4.426	32	0.159	36	0.192	4.276	33	0.111	37	0.143	6.164
	20:30	41	0.188				42	0.157				43	0.115			
	21:30	44	0.177	47	0.234	5.018	45	0.172	48	0.198	4.573	46	0.128	49	0.156	6.774
	22:30	51	0.217				52	0.205				53	0.18			
	23:30	54	0.239	57	0.295	5.431	55	0.226	58	0.242	4.381	56	0.201	59	0.227	8.479
1/18/95	8:30	64	0.325	67	0.438	7.61	65	0.315	68	0.373	6.252	66	0.289	69	0.348	ND
	10:00	74	0.344				75	0.319				76	0.292			
	11:00	78	0.391	81	0.477	5.889	79	0.35	82	0.388	4.296	80	0.33	83	0.395	8.75
	12:00	84	0.386				85	0.352				86	0.338			
	13:00	87	0.419	90	0.503	5.953	88	0.368	91	0.406	3.952	89	0.377	92	0.449	8.753
	14:00	96	0.397				97	0.377				98	0.369			
	15:00	100	0.333	103	0.46	5.943	101	0.334	104	0.385	5.03	102	0.318	105	0.392	9.104
	16:00	106	0.319				107	0.304				108	0.279			
	17:30	109	0.292	112	0.403	4.618	110	0.278	113	0.336	4.528	111	0.25	114	0.34	9.154
	19:00	116	0.261	119	0.342	3.025	117	0.24	120	0.284	2.965	118	0.199	121	0.278	6.785
	21:00	126	0.178				127	0.178				128	0.137			
	22:00	129	0.175	132	0.286	3.627	130	0.155	133	0.211	3.402	131	0.115	134	0.209	6.762
	23:00	136	0.159				137	0.136				138	0.105			
1/19/95	0:30	139	0.162	142	0.186	2.578	140	0.139	143	0.181	2.668	141	0.116	144	0.18	5.775

* Note: Acidified effluent values do not account for dilutions

Acid Effluents: 5 mL and 5 drops nitric

In-Reactor Solids: 2 mL sample 2 mL acid; then 10:1 & 100:1

Generally temperatures held fairly constant at 20 degees C. (15 deg. in mixer)

Table A-43(b): 1/17/95 - 1/26/95 CSTR System:

Influent: HOCl = varies, Fe = 2 mg/L, Mn = 0.5 mg/L, Ca^{++} and HCO_3^- = 3 meq/L, pH= 7; θ_H = 2.5 hour, 20°C

Time of Day	Mn Mixer Tube #	Mn Mixer Conc. (mg/L)	HOCl Mixer (mL)	Actual Conc. Mn (mg/L)	Actual Conc. HOCl (mg/L)	Temp. (C)	pH 1	pH 2	pH 3	Effluent HOCl, In-Solids Conc., or Influent Lines (mg/L) Reactor # 1 Tube	Reactor # 1 Fe	Reactor # 1 Mn	Reactor # 1 HOCl	Reactor # 2 Tube	Reactor # 2 Fe	Reactor # 2 Mn	Reactor # 2 HOCl	Reactor # 3 Tube	Reactor # 3 Fe	Reactor # 3 Mn	Reactor # 3 HOCl	Comments
14:30			1.08	n/a	1.44		7.99	8.01	7.99	1	136	0.43		2	281	0.93		3	396	0.64		2 mL samp/2 mL acid; 1 mg/L HOCL; pre-cleaned
15:30	7	0.589	0.82	0.53	1.10																	HAS; OD to make up for rxns. No Mn Feed for 30 min.
16:30		0.478	0.67	0.43	0.90		8.01	8.04	8.06													6 mL 1N acid added initially
17:30	20	0.527	0.72	0.48	0.96																	500 mL Boost
18:30	27	0.504	0.70	0.45	0.94		8.09	8.10	8.07													Adjusted pH's to 8; added 1 mL acid to feed
19:30	34	0.504	0.74	0.45	0.99					38	117	1.28	0.19	39	283	1.68	0	40	380	1.66	0.19	
20:30			0.72	n/a	0.96																	
21:30	50	0.473		0.43	n/a		8.20	8.21	8.22													Add 1 mL acid; adjust to 8
22:30			0.70	n/a	0.94																	Add 3 mL acid adjust to 8
23:30	60	0.431	0.73	0.39	0.98					61	110	1.44		62	254	1.84		63	375	1.72		
8:30	70	0.468	0.83	0.42	1.11		8.10	8.09	8.11	71	80.4	4.98		72	238	6.3		73	308	6.16		Added 1 mL acid
10:00	77	0.628	0.83	0.57	1.11								0.15				0.15				0.16	
11:00		0.505		0.46	n/a																	Reactor # 1 looking washed out
12:00		0.516	0.77	0.47	1.03		8.10	8.10	8.10													Add 1 mL acid (13 mL total)
13:00			1.42	n/a	1.90					93	71.2	1.88	0.18	94	214	3.68	0.15	95	281	3.32	0.18	Changed HOCl feed to 2 mg/L
14:00	99	0.555	1.66	0.50	2.22		8.03	8.04	8.02													
15:00		0.482		0.43	n/a																	
16:00				n/a	n/a																	
17:30	115	0.519	1.46	0.47	1.95		8.03	8.05	8.05													
19:00	122	0.504		0.45	n/a					123	71.6	2.38		124	221	3.94		125	276	3.92		
21:00				n/a	n/a																	
22:00	135	0.488	1.46	0.44	1.95		8.10	8.11	8.08				0.36				0.22				0.28	
23:00			1.39	n/a	1.86																	
0:30	145	0.604	1.35	0.54	1.80		8.08	8.08	8.06	146				147				148				New Mn Feed (0.40 mL/min); in-solids samp. lost

Table A-43(c): 1/17/95 - 1/26/95 CSTR System:

Influent: HOCl = varies, Fe = 2 mg/L, Mn = 0.5 mg/L, Ca^{++} and HCO_3^- = 3 meq/L, pH= 7; θ_H = 2.5 hour, 20°C

Date	Time of Day	Reactor # 1: 100 mg/.L					Reactor # 2: 200 mg/.L					Reactor # 3: 300 mg/.L				
		Filt. Effluent		Acid Effluent			Filt. Effluent		Acid Effluent			Filt. Effluent		Acid Effluent		
		Tube	Mn	Tube	Mn	Fe	Tube	Mn	Tube	Mn	Fe	Tube	Mn	Tube	Mn	Fe
1/19/95	10:00	149	0.069	152	0.242	3.028	150	0.032	153	0.135	4.051	151	0.011	154	0.144	5.936
	12:00	159	0.063	163	0.327	4.456	160	0.022	164	0.118	3.63	161	0.01	165	0.118	5.54
	13:00	166	0.038	169	0.226	3.034	167	0.018	170	0.112	3.302	168	0.013	1	0.147	7.299
	14:00	3	0.033				4	0.011				5	0.002			
	15:30	6	0.005	9	0.185	2.631	7	0.003	10	0.091	2.757	8	0.005	11	0.118	4.917
	17:30	13	0.011	16	0.361	4.848	14	0.007	17	0.113	3.212	15	0.005	18	0.149	5.913
1/20/95	0:00	23	0.007	26	0.141	2.384	24	0.007	27	0.095	3.163	25	0.003	28	0.136	5.591
	10:00	33	0.009	36	0.155	2.756	34	0.003	37	0.141	4.329	35	0.003	38	0.155	6.305
	12:00	43	0.009				44	0.007				45	0			
	14:00	46	0.004	49	0.216	2.141	47	0.003	50	0.121	2.666	48	0.007	51	0.152	4.699
	16:00	53	0.006				54	0.005				55	0.003			
	17:30	59	0.006				60	0.004				61	0.004			
	18:30	63	0.008				64	0.004				65	0.004			
	21:30	66	0.035				67	0.009				68	0.008			
	23:30	69	0.102	75	0.421	2.772	70	0.034	76	0.221	3.327	71	0.03	77	0.298	5.282
	12:00	78	0.356	81	1.096	7.121	79	0.331	82	0.581	4.469	80	0.332	83	0.764	8.93
	14:00	201	0.367				202	0.377				203	0.372			
	23:30	204	0.428				205	0.451				206	0.434			

* Note: Acidified effluent values do not account for dilutions

Acid Effluents: 5 mL and 5 drops nitric

In-Reactor Solids: 2 mL sample 2 mL acid; then 10:1 & 100:1

Generally temperatures held fairly constant at 20 degees C. (15 deg. in mixer)

Table A-43(d): 1/17/95 - 1/26/95 CSTR System:

Influent: HOCl = varies, Fe = 2 mg/L, Mn = 0.5 mg/L, Ca^{++} and HCO_3^- = 3 meq/L, pH= 7; θ_H = 2.5 hour, 20°C

Time of Day	Mn Mixer Tube #	Mn Mixer Conc. (mg/L)	HOCl Mixer (mL)	Actual Conc. Mn (mg/L)	Actual Conc. HOCl (mg/L)	Temp. (C)	pH 1	pH 2	pH 3	Effluent HOCl, In-Solids Conc., or Influent Lines (mg/L) Reactor # 1 Tube	Fe	Mn	HOCl	Reactor # 2 Tube	Fe	Mn	HOCl	Reactor # 3 Tube	Fe	Mn	HOCl	Comments
10:00	155	0.575	1.49	0.52	1.99		8.15	8.11	8.08	156			0.46	157			0.3	158			0.36	Changed alkalinity feed; lost samples 156-158
12:00	162	0.569	2.18	0.51	2.91																	Switch to 3 mg/L; HOCl reading after change
13:00	2	0.537		0.48	n/a																	pH problems; new Fe feed
14:00			2.22	n/a	2.97		7.96	7.90	7.85													
15:30	12	0.473	2.12	0.43	2.83																	still pH problems; new Fe feed 0.5 mL acid/10L
17:30	19	0.601	2.04	0.54	2.73		7.90	7.86	7.86	20	55.2	4.22	0.77	21	179	6.74	0.5	22	214	6.38	0.61	
0:00	29	0.52	2.26	0.47	3.02		7.69	7.67	7.71	30	51	4.7	ND	31	183	7.9	0.41	32	200	7.44	0.78	
10:00	39	0.525	2.37	0.47	3.17		7.72	7.71	7.73	40	49	5.62	1.1	41	179	9.34	0.92	42	187	8.5	0.99	
12:00		0.474		0.43	n/a																	New HOCl feed (still 3 mg/L)
14:00	52	0.563	2.16	0.51	2.89		7.69	7.68	7.70													
16:00			2.27	n/a	3.03		7.68	7.72	7.73	56	50	6.3		57	174	10.2		58	178	9.22		4:30 Cut HOCl feed; added 20 mL PAO to quench
17:30	62	0.558	1.19	0.50	1.59																	Additional 10 mL PAO added
18:30		0.435		0.39	n/a		8.00	8.02	8.01													
21:30			0.68	n/a	0.91		8.21	8.23	8.26	72	50	6.2		73	172	10.9		74	164	9.24		New Fe Feed 14 mL acid/20L; pH ad. to 8
23:30		0.435		0.39	n/a		8.29	8.28	8.32	85	38.8	4.62		86	130	8.58		87	142	8.46		Added 5 mL more acid
12:00	84	0.526		0.47	n/a																	
14:00			0.56	n/a	0.75		8.23	8.22	8.24													
23:30	210	0.577	2.16	0.52	2.89		8.17	8.15	8.15	207	26.4	3.02		208	147	9.28		209	115	6.7		HOCl Feed started 2 mg/L

Table A-43(e): 1/17/95 - 1/26/95 CSTR System:

Influent: HOCl = varies, Fe = 2 mg/L, Mn = 0.5 mg/L, Ca^{++} and HCO_3^- = 3 meq/L, pH= 7; θ_H = 2.5 hour, 20°C

Date	Time of Day	Reactor # 1: 100 mg/.L					Reactor # 2: 200 mg/.L					Reactor # 3: 300 mg/.L				
		Filt. Effluent		Acid Effluent			Filt. Effluent		Acid Effluent			Filt. Effluent		Acid Effluent		
		Tube	Mn	Tube	Mn	Fe	Tube	Mn	Tube	Mn	Fe	Tube	Mn	Tube	Mn	Fe
1/22/95	11:00	211	0.15				212	0.065				213	0.048			
	17:00	218	0.077				219	0.02				220	0.02			
	20:00	225	0.097	228	0.376	1.766	226	0.016	229	0.188	2.219	227	0.029	230	0.311	3.781
	21:45	231	0.125				232	0.027				233	0.027			
1/23/95	11:00	238	0.053				239	0.014				240	0.006			
	14:00	245	0.064				246	0.028				247	0.012			
	17:00	1	0.046	4	0.261	1.824	2	0.007	5	0.169	2.041	3	0.005	6	0.203	2.324
	23:00	11	0.039				12	0.009				13	0.007			
1/24/95	12:00	18	0.046	21	0.27	1.824	19	0.011	22	0.204	1.941	20	0.011	23	0.307	2.498
	20:00	28	0.025	31	0.386	2.838	29	0.005	32	0.258	2.349	30	0.003	33	0.243	2.415
1/25/95	11:00	38	0.032	41	0.23	1.92	39	0.008	42	0.206	1.733	40	0.004	43	0.377	2.507
	18:00	1	0.053	4	0.314	2.61	2	0.008	5	0.194	1.67	3	0.01	6	0.268	2.149
	21:00	11	0.259				12	0.074				13	0.14			
1/26/95	9:30	14	0.11	17	1.013	6.632	15	0.061	18	0.235	1.513	16	0.065	19	0.36	2.782
	12:00	24	0.097				25	0.042				26	0.053			
	14:30	27	0.118	30	0.389	2.151	28	0.052	31	0.237	1.709	29	0.056	32	0.398	3.172

* Note: Acidified effluent values do not account for dilutions

Acid Effluents: 5 mL and 5 drops nitric

In-Reactor Solids: 2 mL sample 2 mL acid; then 10:1 & 100:1

Generally temperatures held fairly constant at 20 degees C. (15 deg. in mixer)

Table A-43(f): 1/17/95 - 1/26/95 CSTR System:

Influent: HOCl = varies, Fe = 2 mg/L, Mn = 0.5 mg/L, Ca^{++} and HCO_3^- = 3 meq/L, pH= 7; θ_H = 2.5 hour, 20°C

Time of Day	Mn Mixer Tube #	Mn Mixer Conc. (mg/L)	HOCl Mixer (mL)	Actual Conc. Mn (mg/L)	Actual Conc. HOCl (mg/L)	Temp. (C)	pH 1	pH 2	pH 3	Effluent HOCl, In-Solids Conc., or Influent Lines (mg/L) Reactor # 1 Tube	Fe	Mn	HOCl	Reactor # 2 Tube	Fe	Mn	HOCl	Reactor # 3 Tube	Fe	Mn	HOCl	Comments
11:00	217	0.57	1.52	0.51	2.03		8.23	8.20	8.21	214	25.6	3.16		215	144	10		216	108	7.1		Add 2 mL acid to 10L Fe
17:00	221	0.552	1.54	0.50	2.06		8.08	8.04	8.03	222	28.4	3.38	0.81	223	146	10.8	0.46	224	105	7.46	0.59	New HOCl Feed; Still 2 mg/L
20:00			1.51	n/a	2.02		8.12	8.09	8.10													500 mL Boost; 1 mL acid to 8L Fe
21:45	234	0.658	1.61	0.59	2.15					235	28.4	3.8		236	148	11.7		237	101	7.94		
11:00	241	0.585	1.48	0.53	1.98		8.16	8.13	8.20	242	28.4	4.12		243	148	13		244	93.6	8.56		500 mL boost; New HOCl
14:00	248	0.543		0.49	n/a																	New Fe/Ca Feed; 20 mL acid
17:00	7	0.57	1.51	0.51	2.02		8.12	8.07	8.08	8	28	4.6	0.4	9	150	14.8	0.28	10	96	10.1	0.31	2 mL aid to > 20 L
23:00	14	0.512	1.59	0.46	2.12		8.16	8.08	8.10	15	34.2	4.82		16	148	15.3		17	95.6	10.4		2 mL acid 20L
12:00	24	0.597	1.47	0.54	1.96		8.22	8.16	8.20	25	31.6	5.5	0.52	26	145	16.4	0.36	27	91.4	11.3	0.36	5 mL acid 16L
20:00	34	0.514	1.62	0.46	2.16					35	33.8	5.7		36	146	16.9		37	96.8	12.4		
11:00	44	0.498	1.50	0.45	2.00					45	34.2	5.04	0.22	46	152	16.7	0.33	47	97.6	11.7	0.37	
18:00	7	0.549	1.46	0.50	1.95		8.15	8.05	8.06	8	32.4	6.18		9	148	19.9		10	89.2	13.4		Added 8 mL Conc. Nitric to 8L; pH down
21:00				n/a	n/a		5.95	6.10	5.90													
9:30	20	0.497	1.50	0.45	2.00		6.18	6.20	6.05	21	11	2.06	0.34	22	153	20.1	0.27	23	92.6	13.5	0.27	
12:00				n/a	n/a																	
14:30	33	0.536	1.27	0.48	1.70					34	6.8	0.78		35	161	21.2		36	88	13.2		

Mn(II) Adsorption onto MnO_X

Table A-44: Mn(II) Adsorption onto MnO_X pH 8

2/1/95; pH = 8, $[Mn(II)]_0$ ~ 0.5 mg/L, Ca^{++} and HCO_3^- = 3 meq/L, NO Fe(II) or HOCl, MnO_X varies, 10°C

Initial Mn(II)		Acid Total Mn		Calculated	pH	Temp.	5 min Adsorb Sample		Calculated Adsorption Ratio
Sample #	(mg/L)	Sample #	(mg/L)	MnOx (mg/L)		(°C)	Sample #	Mn (mg/L)	mg Mn(II)/mg MnOx
pH = 8									
1	0.535	3	1.26	0.725	8.03	8	5	0.36	0.23
2	0.536	4	1.34	0.804			6	0.35	0.25
							7	0.35	0.24
Average	0.54		1.3	0.76			Average	0.35	0.24
8	0.545	10	1.32	0.775	8.04	9.8	12	0.358	0.24
9	0.547	11	1.35	0.803			13	0.344	0.26
							14	0.344	0.26
Average	0.55		1.335	0.79			Average	0.35	0.25
15	0.558	17	2.86	2.302	8.02	10.5	19	0.086	0.20
16	0.554	18	2.96	2.406			20	0.084	0.20
							21	0.078	0.20
Average	0.56		2.91	2.35			Average	0.08	0.20
22	0.579	24	4.54	3.961	8.03	10	26	0.014	0.14
23	0.577	25	4.51	3.933			27	0.008	0.14
							28	0.009	0.14
Average	0.58		4.525	3.95			Average	0.01	0.14
29	0.497	31	8.33	7.833	8.01	10	33	0.018	0.06
30	0.507	32	8.13	7.623			34	0.011	0.06
							35	0.01	0.06
Average	0.50		8.23	7.73			Average	0.01	0.06
36	0.579	38	10.78	10.201	8.01	10.8	40	0.005	0.06
37	0.586	39	10.8	10.214			41	0.004	0.06
							42	0.007	0.06
Average	0.58		10.79	10.21			Average	0.01	0.06

Mn(II) Adsorption onto MnO_x

Table A-45: Mn(II) Adsorption onto MnO_x pH 8

2/3/95; pH = 8, $[Mn(II)]_o$ ~ 1 mg/L, Ca^{++} and HCO_3^- = 3 meq/L, NO Fe(II) or HOCl, MnO_x varies, 10°C

Initial Mn(II)		Acid Total Mn		Calculated	pH	Temp.	5 min Adsorb Sample		Calculated Adsorption Ratio
Sample #	(mg/L)	Sample #	(mg/L)	MnOx (mg/L)		(°C)	Sample #	Mn (mg/L)	mg Mn(II)/mg MnOx
pH = 8									
1	1.021	3	4.84	3.819	8.01	7	5	0.18	0.22
2	1.012	4	4.73	3.718			6	0.22	0.21
							7	0.23	0.21
Average	1.02		4.785	3.77			Average	0.21	0.21
8	1.011	10	8.97	7.959	8	9.8	12	0.04	0.12
9	1.015	11	8.97	7.955			13	0.034	0.12
							14	0.031	0.12
Average	1.01		8.97	7.96			Average	0.04	0.12
15	1.036	17	12.75	11.714	8.03	9.5	19	0.011	0.09
16	1.031	18	12.92	11.889			20	0.012	0.09
							21	0.014	0.09
Average	1.03		12.835	11.80			Average	0.01	0.09
22	1.026	24	17.04	16.014	8.02	10.2	26	0.011	0.06
23	1.036	25	16.82	15.784			27	0.006	0.06
							28	0.008	0.06
Average	1.03		16.93	15.90			Average	0.01	0.06
31	1.02	33	1.71	0.69	8.01	10	35	0.916	0.17
32	1.023	34	1.6	0.577			36	0.922	0.16
							37	0.912	0.17
Average	1.02		1.655	0.63			Average	0.92	0.17
38	1.058	40	2.43	1.372	8.02	9	42	0.7	0.25
39	1.036	41	2.47	1.434			43	0.707	0.24
							44	0.687	0.26
Average	1.05		2.45	1.40			Average	0.70	0.25
45	1.085	47	3.7	2.615	8	10.6	49	0.449	0.24
46	1.055	48	3.67	2.615			50	0.448	0.24
							51	0.452	0.24
Average	1.07		3.685	2.62			Average	0.45	0.24
52	1.082	53	1.48	0.398	8.02	10	55	0.941	0.29
53	1.03	54	1.43	0.4			56	0.959	0.24
							57	0.964	0.23
Average	1.06		1.455	0.40			Average	0.95	0.25

Mn(II) Adsorption onto MnO_X

Table A-46: Mn(II) Adsorption onto MnO_X pH 7

2/4/95; pH = 7, $[Mn(II)]_0$ ~ 1 mg/L, Ca^{++} and HCO_3^- = 3 meq/L, NO Fe(II) or HOCl, MnO_X varies, 10°C

Initial Mn(II)		Acid Total Mn		Calculated	pH	Temp.	5 min Adsorb Sample		Calculated Adsorption Ratio
Sample #	(mg/L)	Sample #	(mg/L)	MnOx (mg/L)		(°C)	Sample #	Mn (mg/L)	mg Mn(II)/mg MnOx
pH = 8									
59	1.023	61	1.84	0.817	6.99	10.7	63	0.84	0.22
60	1.021	62	1.85	0.829			64	0.84	0.22
							65	0.83	0.23
Average	1.02		1.845	0.82			Average	0.84	0.22
66	1.025	68	3.27	2.245	7.02	10	70	0.545	0.21
67	1.025	69	3.36	2.335			71	0.54	0.21
							72	0.538	0.21
Average	1.03		3.315	2.29			Average	0.54	0.21
73	1.014	75	4.75	3.736	7.01	9.8	77	0.396	0.17
74	1.02	76	4.78	3.76			78	0.388	0.17
							79	0.374	0.17
Average	1.02		4.765	3.75			Average	0.39	0.17
80	1.019	82	6.34	5.321	6.98	9.4	84	0.181	0.16
81	1.018	83	6.31	5.292			85	0.175	0.16
							86	0.175	0.16
Average	1.02		6.325	5.31			Average	0.18	0.16
87	1.031	89	8.83	7.799	7	10.8	91	0.059	0.12
88	1.028	90	8.78	7.752			92	0.051	0.13
							93	0.045	0.13
Average	1.03		8.805	7.78			Average	0.052	0.13
94	1.032	96	11.15	10.118	6.97	10.3	98	0.076	0.09
95	1.021	97	11.07	10.049			99	0.066	0.10
							100	0.056	0.10
Average	1.03		11.11	10.08			Average	0.066	0.095
1	1.007	3	13.68	12.673	6.97	10.1	5	0.013	0.08
2	1.006	4	13.77	12.764			6	0.015	0.08
							7	0.015	0.08
Average	1.01		13.725	12.72			Average	0.014	0.078

Mn(II) Adsorption onto MnO_X

Table A-47: Mn(II) Adsorption onto MnO_X pH 8

2/4/95; pH = 8, $[Mn(II)]_0$ ~ 1 mg/L, Ca^{++} and HCO_3^- = 3 meq/L, NO Fe(II) or HOCl, MnO_X varies, 10°C

Initial Mn(II)		Acid Total Mn		Calculated	pH	Temp.	5 min Adsorb Sample		Calculated Adsorption Ratio
Sample #	(mg/L)	Sample #	(mg/L)	MnOx (mg/L)		(°C)	Sample #	Mn (mg/L)	mg Mn(II)/mg MnOx
pH = 8									
1	1.021	2	1.88		8.01	10.5	4	0.98	0.05
		3	1.86				5	0.96	0.07
							6	0.95	0.08
		Average	1.87	0.85			Average	0.96	0.06
7	1.005	8	2.18		8.01	10.5	10	0.808	0.17
		9	2.2				11	0.797	0.18
							12	0.78	0.19
		Average	2.19	1.19			Average	0.80	0.17
13	1.012	14	4.56		8.01	10	16	0.397	0.13
		15	4.72				17	0.411	0.13
							18	0.402	0.13
		Average	4.64	4.64			Average	0.40	0.13
19	1.016	20	5.19		8.01	10	22	0.3	0.14
		21	5.21				23	0.259	0.15
							24	0.238	0.15
		Average	5.2	5.20			Average	0.27	0.14

APPENDIX B

OPERATION AND DETECTION LIMIT DETERMINATION FOR ATOMIC ADSORPTION-SPECTROPHOTOMETER

Detection Limit Determination

a. Procedure. The detection limit of the AA-S used for analysis of all Fe(II) and Mn(II) samples was determined only for manganese as this is the most critical parameter under study. The test procedure used to determine the limit of detection was taken directly from the operating manual for the AA-S (Instructions for Perkin Elmer Atomic-Adsorption Spectrophotometer Model 703. Norwalk, CT. May 1978[63]). In general, two low concentration standards are prepared, the first at 5 times the estimated detection limit and the second at 10 times the estimated detection limit. The standards are analyzed alternately (reading a blank in between the two standard readings) twenty or more times once optimum operating conditions have been obtained. The absorbance means are determined by this procedure and are used to calculate the detection limit of the instrument for the element in question. This determination was conducted on two different occasions; both results are given in the following sections.

b. Detection Limit Determination 8/8/94. The average detection limit was found to be approximately 0.005 mg/L by this procedure. This value suggests that any value between 0.005 and 10 x 0.005 mg/L should be reported as **detect only** as the *quantification limit* is defined as 10 times the detection limit. Thus only values greater than the SMCL of 0.05 mg/L can be reported as **true numerical values.** Because the blank readings varied greatly form the beginning to the end of the test, the results were somewhat questionable. This phenomenon should not affect the results because the standard values are corrected by accounting for the discrepancy between the zero value and the value "seen" by the AA-S. The test was rerun on 8/26/94 to confirm the findings

of this determination. Table B-1 summarizes the data collected for this test procedure as well as providing a sample calculation for the detection limit value.

c. Detection Limit Determination 8/26/94. During the data collection for this procedure, the AA-S appeared to malfunction after the 20th reading. Therefore, two results will be reported; one for the first 20 readings which meets the minimum number required for this determination and the second for all 25 readings. By ignoring the final 5 readings, the detection limit is approximately 0.006 mg/L which compares well to the previously determined value. Also, the blank reading in this determination is less variable than the previous test. However if all the readings are used in the determination, the detection limit swells to 0.008 mg/L, and the blank readings appear very irregular for the final 5 readings. Tables B-2 and B-3 provide a listing of both cases discussed with Table B-2 being shaded after the 20th reading to indicate that these values were not used in the detection limit determination.

Operation

Standard operating procedures as recommended by the manufacturer were used during AA-S analysis.

Table B-1: Detection Limit Determination for Mn on AA-S 8/8/94
(25 of 25 Readings used for Calculation)

Reading Number	Blank (Zero)	Standard 1 (0.075 mg/L)	Blank (Zero)	Standard 2 (0.150 mg/L)	Corrected Values S 1	Corrected Values S 2
1	-0.001	0.072	-0.003	0.148	0.074	0.15
2	-0.001	0.073	-0.001	0.146	0.074	0.148
3	-0.003	0.068	-0.008	0.142	0.0735	0.147
4	-0.002	0.071	0	0.145	0.072	0.147
5	-0.004	0.071	-0.004	0.145	0.075	0.148
6	-0.002	0.072	-0.001	0.152	0.0735	0.1525
7	0	0.078	0	0.151	0.078	0.15
8	0.002	0.074	-0.005	0.143	0.0755	0.15
9	-0.009	0.069	-0.006	0.143	0.0765	0.1485
10	-0.005	0.066	-0.006	0.145	0.0715	0.1495
11	-0.003	0.07	-0.007	0.143	0.075	0.1485
12	-0.004	0.07	-0.002	0.146	0.073	0.1495
13	-0.005	0.071	-0.002	0.145	0.0745	0.149
14	-0.006	0.069	-0.005	0.143	0.0745	0.1485
15	-0.006	0.069	-0.006	0.143	0.075	0.148
16	-0.004	0.071	-0.005	0.145	0.0755	0.15
17	-0.005	0.07	-0.005	0.146	0.075	0.1505
18	-0.004	0.073	-0.005	0.143	0.0775	0.148
19	-0.005	0.067	-0.008	0.144	0.0735	0.153
20	-0.01	0.065	-0.008	0.141	0.074	0.1495
21	-0.009	0.064	-0.009	0.141	0.073	0.1505
22	-0.01	0.064	-0.01	0.137	0.074	0.1465
23	-0.009	0.063	-0.01	0.139	0.0725	0.1485
24	-0.009	0.065	-0.008	0.141	0.0735	0.151
25	-0.012	0.062	-0.011	0.138	0.0735	0.152
26	-0.017					
				STANDARD CONCENTRATION =	0.075	0.15
				MEAN =	0.0743	0.14934
					Ratio =	**2.01**
				STANDARD DEVIATION =	0.001541	0.001669

$$Detection\ Limit = \frac{S\tan dard\ Concentration \times 3\ S\tan dard\ Deviations}{Mean}$$

Detection Lmit (0.075 Standard) = 0.0047 mg/L
Detection Lmit (0.15 Standard) = 0.0050 mg/L

Average Detection Limit = **0.0048** mg/L

Table B-2: Detection Limit Determination for Mn on AA-S 8/26/94
(20 of 25 Readings used for Calculation)

Reading Number	Blank (Zero)	Standard 1 (0.075 mg/L)	Blank (Zero)	Standard 2 (0.150 mg/L)	Corrected Values	
					S 1	S 2
1	0.002	0.078	0.006	0.152	0.074	0.15
2	-0.002	0.078	0.001	0.15	0.0785	0.148
3	0.003	0.077	0	0.149	0.0755	0.149
4	0	0.076	0	0.149	0.076	0.149
5	0	0.079	0.004	0.151	0.077	0.148
6	0.002	0.079	0.002	0.152	0.077	0.1495
7	0.003	0.078	0.002	0.154	0.0755	0.152
8	0.002	0.079	0.003	0.152	0.0765	0.15
9	0.001	0.077	0	0.154	0.0765	0.1535
10	0.001	0.079	0.001	0.155	0.078	0.153
11	0.003	0.082	0.001	0.157	0.08	0.154
12	0.005	0.081	0.004	0.156	0.0765	0.152
13	0.004	0.081	0.003	0.154	0.0775	0.15
14	0.005	0.081	0.004	0.152	0.0765	0.149
15	0.002	0.078	0.006	0.157	0.074	0.1525
16	0.003	0.081	-0.005	0.153	0.082	0.155
17	0.001	0.077	-0.001	0.15	0.077	0.1505
18	0	0.081	0.002	0.151	0.08	0.1515
19	-0.003	0.078	0.003	0.153	0.078	0.151
20	0.001	0.078	0.001	0.155	0.077	0.1535
21	0.002	0.084	0.003	0.158	0.0815	0.1535
22	0.006	0.083	0.006	0.159	0.077	0.1525
23	0.007	0.084	0.003	0.156	0.079	0.152
24	0.005	0.071	0.001	0.144	0.068	0.148
25	-0.009	0.069	-0.012	0.147	0.0795	0.161
26	-0.016					
				STANDARD CONCENTRATION =	0.075	0.15
				MEAN =	0.07715	0.15105
					Ratio =	**1.96**
				STANDARD DEVIATION =	0.001941	0.00207

$$Detection\ Limit = \frac{S\,tan\,dard\ Concentration \times 3\ S\,tan\,dard\ Deviations}{Mean}$$

Detection Lmit (0.075 Standard) = 0.0057 mg/L
Detection Lmit (0.15 Standard) = 0.0062 mg/L

Average Detection Limit = **0.0059** mg/L

Table B-3: Detection Limit Determination for Mn on AA-S 8/26/94
(25 of 25 Readings used for Calculation)

Reading Number	Blank (Zero)	Standard 1 (0.075 mg/L)	Blank (Zero)	Standard 2 (0.150 mg/L)	Corrected Values	
					S 1	S 2
1	0.002	0.078	0.006	0.152	0.074	0.15
2	-0.002	0.078	0.001	0.15	0.0785	0.148
3	0.003	0.077	0	0.149	0.0755	0.149
4	0	0.076	0	0.149	0.076	0.149
5	0	0.079	0.004	0.151	0.077	0.148
6	0.002	0.079	0.002	0.152	0.077	0.1495
7	0.003	0.078	0.002	0.154	0.0755	0.152
8	0.002	0.079	0.003	0.152	0.0765	0.15
9	0.001	0.077	0	0.154	0.0765	0.1535
10	0.001	0.079	0.001	0.155	0.078	0.153
11	0.003	0.082	0.001	0.157	0.08	0.154
12	0.005	0.081	0.004	0.156	0.0765	0.152
13	0.004	0.081	0.003	0.154	0.0775	0.15
14	0.005	0.081	0.004	0.152	0.0765	0.149
15	0.002	0.078	0.006	0.157	0.074	0.1525
16	0.003	0.081	-0.005	0.153	0.082	0.155
17	0.001	0.077	-0.001	0.15	0.077	0.1505
18	0	0.081	0.002	0.151	0.08	0.1515
19	-0.003	0.078	0.003	0.153	0.078	0.151
20	0.001	0.078	0.001	0.155	0.077	0.1535
21	0.002	0.084	0.003	0.158	0.0815	0.1535
22	0.006	0.083	0.006	0.159	0.077	0.1525
23	0.007	0.084	0.003	0.156	0.079	0.152
24	0.005	0.071	0.001	0.144	0.068	0.148
25	-0.009	0.069	-0.012	0.147	0.0795	0.161
26	-0.016					
				STANDARD CONCENTRATION =	0.075	0.15
				MEAN =	0.07712	0.15152
					Ratio =	**1.96**
				STANDARD DEVIATION =	0.002762	0.002838

$$Detection\ Limit = \frac{S\ \text{tan}\ dard\ Concentration \times 3\ S\ \text{tan}\ dard\ Deviations}{Mean}$$

Detection Lmit (0.075 Standard) = 0.0081 mg/L
Detection Lmit (0.15 Standard) = 0.0084 mg/L

Average Detection Limit = **0.0082** mg/L

Table B-5: Summary of Operating Parameters Used for AA-S Analysis

Element	Lamp Current	Wavelength (nm)	Relative Noise	Sensitivity	Linear Range
Fe	30 mA	248.3	1.0	0.10 mg/L	5 mg/L
Mn	20 mA	279.5	1.0	0.052 mg/L	2 mg/L

** Note: All analysis performed with Nominal Spectrum Band Width = 0.2 nm (UV Range); Acetylene Flame (oxidizing) with air as oxidant.*

Appendix C: Calculations

Stock Solution Calculations:

Mn Stock: 0.5 *mg* Mn^{++} *per mL stock solution*

$$\frac{0.5\ mg\ Mn^{++}}{mL\ solution} \times \frac{169.01\ mg\ MnSO_4 \cdot H_2O}{54.94\ mg\ Mn^{++}} = 1.54\ mg\ MnSO_4 \cdot H_2O\ per\ mL\ solution$$

Fe Stock: 1 *mg* Fe^{++} *per mL stock solution*

$$\frac{1\ mg\ Fe^{++}}{mL\ solution} \times \frac{278.02\ mg\ FeSO_4 \cdot 7H_2O}{55.847\ mg\ Fe^{++}} = 4.98\ mg\ FeSO_4 \cdot 7H_2O\ per\ mL\ solution$$

Ca Stock: 1 *meq* Ca^{++} *per mL stock solution*

$$\frac{1\ meq\ Ca^{++}}{mL\ solution} \times \frac{20.04\ mg\ Ca^{++}}{meq\ as\ Ca^{++}} \times \frac{110.99\ mg\ CaCl_2}{40.08\ mg\ Cae^{++}} = 55.5\ mg\ CaCl_2\ per\ mL\ solution$$

$NaHCO_3^-$ *Stock*: 1 *meq* HCO_3^- *per mL stock solution*

$$\frac{1\ meq\ HCO_3^-}{mL\ solution} \times \frac{61.02\ mg\ HCO_3^-}{meq\ as\ HCO_3^-} \times \frac{84.01\ mg\ NaHCO_3^-}{61.02\ mg\ HCO_3^-} = 84.01\ mg\ HCO_3^-\ per\ mL\ solution$$

HOCl Stock: 1 *mg HOCl per mL stock solution*

$$\frac{1\ mg\ HOCl}{mL\ solution} \times \frac{1\ mole\ HOCl}{52.46 \times 10^3\ mg\ HOCl} \times \frac{1\ mole\ OCl^-}{1\ mole\ HOCl} \times \frac{1\ mole\ NaOCl}{1\ mole\ OCl^-} \times \frac{74.44 \times 10^3\ mg\ NaOCl}{1\ mole\ NaOCl} = 1.42\ mg\ NaOCl\ per\ mL\ solution$$

NaOCl Stock: 5.25% *Solution* = 52,500*mg* / *L* = 52.5*mg* / *mL*

Therefore. $\frac{52.5mg/mL}{1.42mg/mL} = 37$; *Dilute NaOCl Stock Solution* 37:1

Chlorine Chemistry.

$Cl_2 + H_2O \longleftrightarrow HOCl + H^+ + Cl^-$

$HOCl \longleftrightarrow H^+ + OCl^-$ $(pK_a = 7.5)$

Re*lationship Between HOCl and* Cl_2

$$\frac{1\,mg\ HOCl}{mL\ solution} \times \frac{1\,mole\ HOCl}{52.46 \times 10^3\,mg\ HOCl} \times \frac{1\,mole\ Cl_2}{1\,mole\ HOCl} \times \frac{70.906 \times 10^3\,mg\ Cl_2}{1\,mole\ Cl_2} = 1.35\,mg\ Cl_2\ per\ mL\ solution$$

Amperometric Titration Calculation and Mn/Cl_2 Ratio Determination:

$$Cl_2\,(mg/L) = \frac{(mL\ titrant)(normality\ of\ PAO)(mg/meq\ of\ Cl_2)}{Sample\ Volume\ in\ mL} = \frac{(mL\ titrant)(0.00564)(35450)}{200\,mL}$$

Example: 1.23*mL of PAO added as titrant to* 2:1 *diluted sample*

$$HOCl(mg/L) = \frac{(2 \times 1.23mL)(0.00564)(35450)}{200\,mL} \times \frac{1\,mg\ HOCl}{1.35\,mg\ Cl_2} = 1.82\,mg\ as\,HOCl/L$$

$$Mn^{++} + HOCl + H_2O \longrightarrow MnO_2 + Cl^- + 3H^+ \quad (1.30mg\ HOCl\ req'd\ per\ mg\ Mn^{++})$$

$$Mn^{++}] = \frac{0.5\,mg\ Mn^{++}}{L} \times \frac{1\,mole\ Mn^{++}}{54.94 \times 10^3\ mg\ Mn^{++}} = 9.1 \times 10^{-6}\,M$$

$$HOCl] = [Cl_2] = \frac{2\,mg\ HOCl}{L} \times \frac{1\,mole\ HOCl}{52.453 \times 10^3\ mg\ HOCl} = 3.81 \times 10^{-5}\,M$$

$$\frac{[Cl_2]}{[Mn^{++}]} = \frac{3.81 \times 10^{-5}\,M}{9.1 \times 10^{-6}\,M} = 4.2$$

$MnCO_3$ Interference

$K_{so} = 10^{-9.3} = [Mn^{++}][CO_3^{=}]$ **< NOT TEMPERATURE CORRECTED >**

$Mn^{++}] = 9.1 \times 10^{-6}\ M \quad \therefore [CO_3^{=}] \geq \dfrac{10^{-9.3}}{9.1 \times 10^{-6}} \Rightarrow 5.51 \times 10^{-5}\ M$ *for ppt. to occur*

$C_{T,CO_3} = 3meq\ /\ L = 3 \times 10^{-3}\ M;$

Carbonate System pK_a values corrected for temperature (10° C):

$pK_{a.1} = 6.46 \quad pK_{a.2} = 10.49$

$pH = 9;\ \alpha_1 = 0.9694 \quad \alpha_2 = 0.0306$

$0.0306 = \dfrac{[CO_3^{=}]}{3 \times 10^{-3}\ M}; \Rightarrow \quad [CO_3^{=}] = 9.2 \times 10^{-5}\ M; \quad \therefore ppt.\ will\ occur$

$pH = 8;\ \alpha_1 = 0.9945 \quad \alpha_2 = 0.0055$

$0.0055 = \dfrac{[CO_3^{=}]}{3 \times 10^{-3}\ M}; \Rightarrow \quad [CO_3^{=}] = 1.64 \times 10^{-5}\ M; \quad \therefore ppt.\ will\ not\ occur$

Statistical Analysis

Sample Data Set: Table A-18: 7/20/94: pH = 8; Fe(II) Target = 4 mg/L; 0.5 mg/L as Mn(II); Ca^{++} & HCO_3^- = 3 meq/L; HOCl = 2 mg/L; 10°C

Time (min)	Final pH	Temp. (C)	0.45 um Filtered Samples			30k Ultrafiltered Sample # 1			30k Ultrafiltered Sample # 2			Avg. Ultra	HOCl (mg/L)
			Tube #	Fe (mg/L)	Mn (mg/L	Tube #	Fe (mg/L)	Mn (mg/L	Tube #	Fe (mg/L)	Mn (mg/L		
0	8.04	11.5											
0	Acidified		127	4.552	**0.537**	128	4.621	0.545	129	4.634	0.542	**0.5435**	ND
5	Adsorb		124	-0.026	**0.493**	125	-0.024	0.501	126	-0.022	0.505	**0.503**	ND
30	7.88	10.8	1	-0.01	**0.464**	2	-0.017	0.452	3	-0.013	0.447	**0.4495**	0.00
60	7.87	11	4	-0.007	**0.391**	5	-0.011	0.404	6	0.003	0.398	**0.401**	0.00
120	7.87	11	7	-0.008	**0.256**	8	-0.008	0.261	9	-0.011	0.252	**0.2565**	0.00
180	7.83	10.2	10	-0.001	**0.124**	11	-0.011	0.12	12	-0.01	0.118	**0.119**	0.00
240	7.79	11	13	-0.013	**0.027**	14	-0.013	0.027	15	-0.021	0.025	**0.026**	0.00
300	7.79	11.2	16	-0.014	-0.001	17	-0.016	0.001	18	-0.019	0	0.00	0.00

* It is believed that the initial HOCl dose exceeded 2 mg/L; probably ~ 2.1 mg/L

Comparing the data sets highlighted above:

t-Test: Paired Two Sample for Means

	Variable 1	*Variable 2*
Mean	0.327428571	0.328357143
Variance	0.038461619	0.039525476
Observations	7	7
Pearson Correlation	0.999082723	
Hypothesized Mean Difference	0	
df	6	
t Stat	-0.276783756	
P(T<=t) one-tail	0.395617055	
t Critical one-tail	1.943180905	
P(T<=t) two-tail	0.791234109	
t Critical two-tail	2.446913641	

** Used to calculate variances

z-Test: Two Sample for Means

	Variable 1	*Variable 2*
Mean	0.327428571	0.328357143
Known Variance	0.038461619	0.039525476
Observations	7	7
Hypothesized Mean Difference	0	
z	-0.008797372	
P(Z<=z) one-tail	0.496490381	
z Critical one-tail	1.644853	
P(Z<=z) two-tail	0.248245191	
z Critical two-tail	1.959961082	

Since the z statistic is less than the critical value, the two sets of data are not significantly different from one another.

pH 8: Determination of Langmuir Isotherm Constants Mn(II) onto Fe(III)

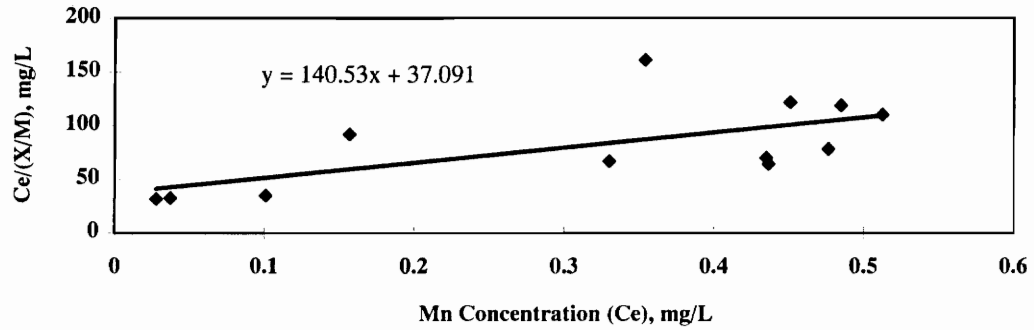

Slope = 1/a =	140.53
a =	0.007
y int. = 1/ab =	37.091
b=	3.79

pH 7: Determination of Langmuir Isotherm Constants Mn(II) onto Fe(III)

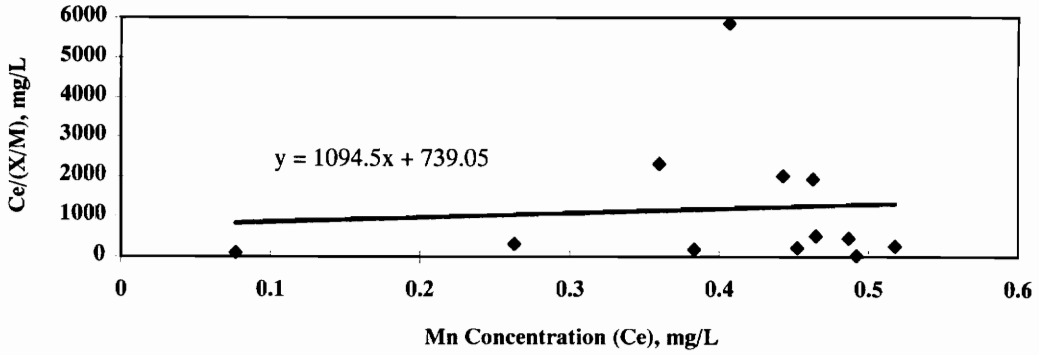

Slope = 1/a =	1094.5
a =	0.00091
y int. = 1/ab =	739.05
b=	1.48

pH 8: Determination of Freundlich Isotherm Constants
Mn(II) onto Fe(III)

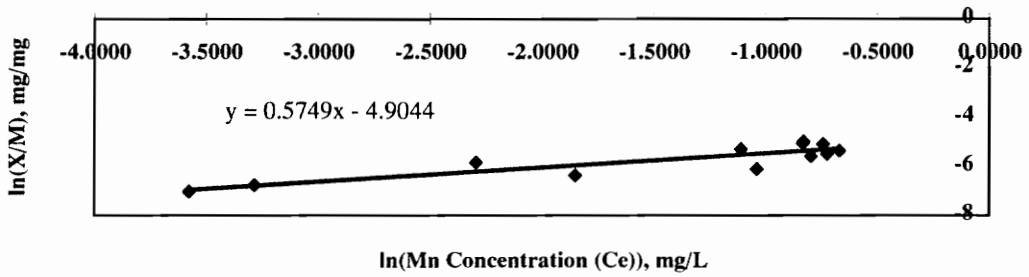

Slope = 1/n =	0.5749
n =	1.74
y int. = ln k =	-4.9044
k=	0.00741

pH 7: Determination of Freundlich Isotherm Constants
Mn(II) onto Fe(III)

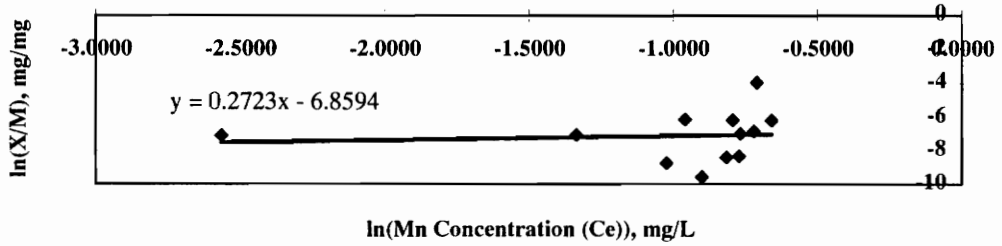

Slope = 1/n =	0.2723
n =	3.67
y int. = ln k =	-6.8594
k=	0.00105

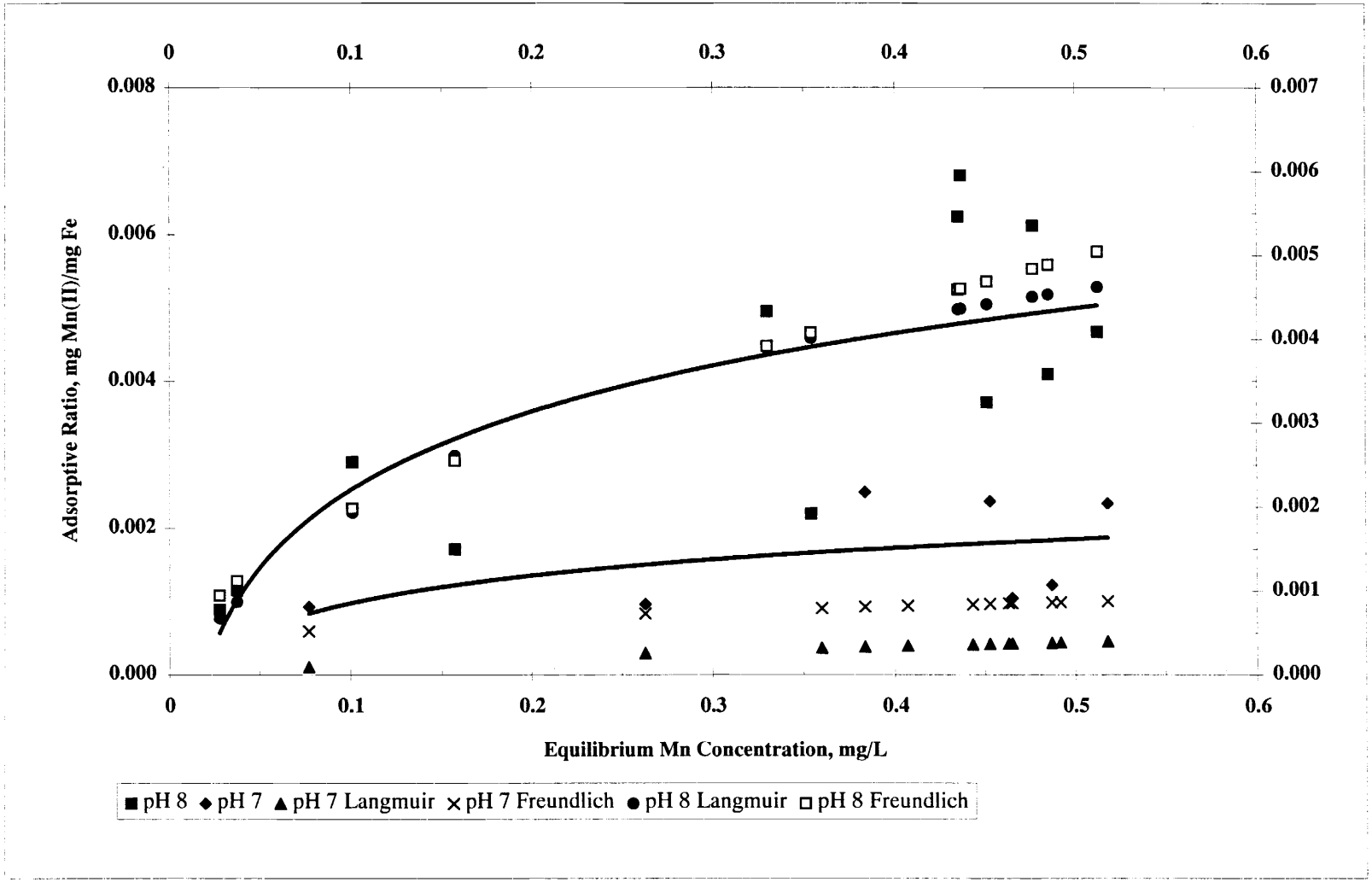

To Determine Best Fit of Langmuir or Freundlich Isotherms to Data Collected

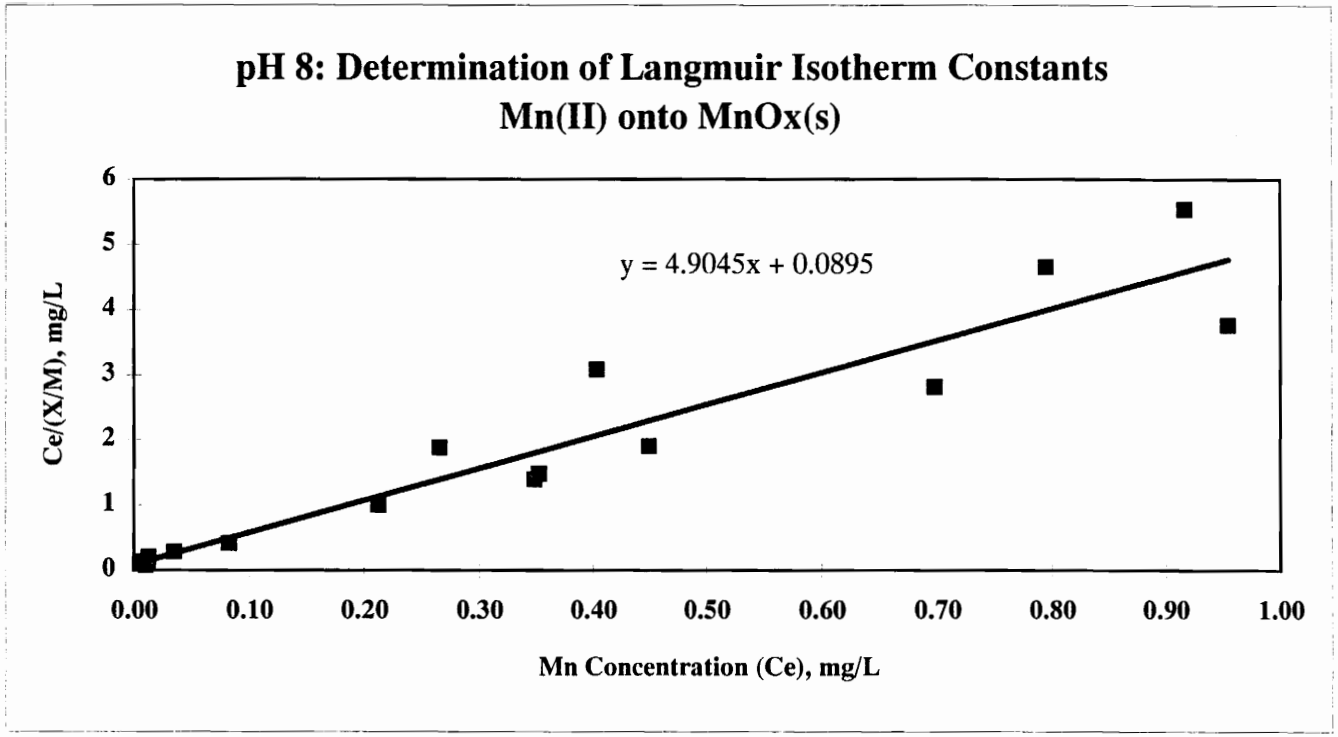

Slope = 1/a =	4.9045
a =	0.204
y int. = 1/ab =	0.0895
b=	54.80

Rate Constant k vs. Fe(III) Concentration pH 8

Fe(III) (mg/L)	Rate Constant (units)	Units = mg Mn/L-min
4.6	1.71E-03	
8.3	2.29E-03	
15.57	8.30E-03	
19.85	2.51E-03	
94	2.27E-02	(Pure)
96.3	5.39E-02	(Reg.)
50.48	Indeterm Data	
Avg.	1.52E-02	

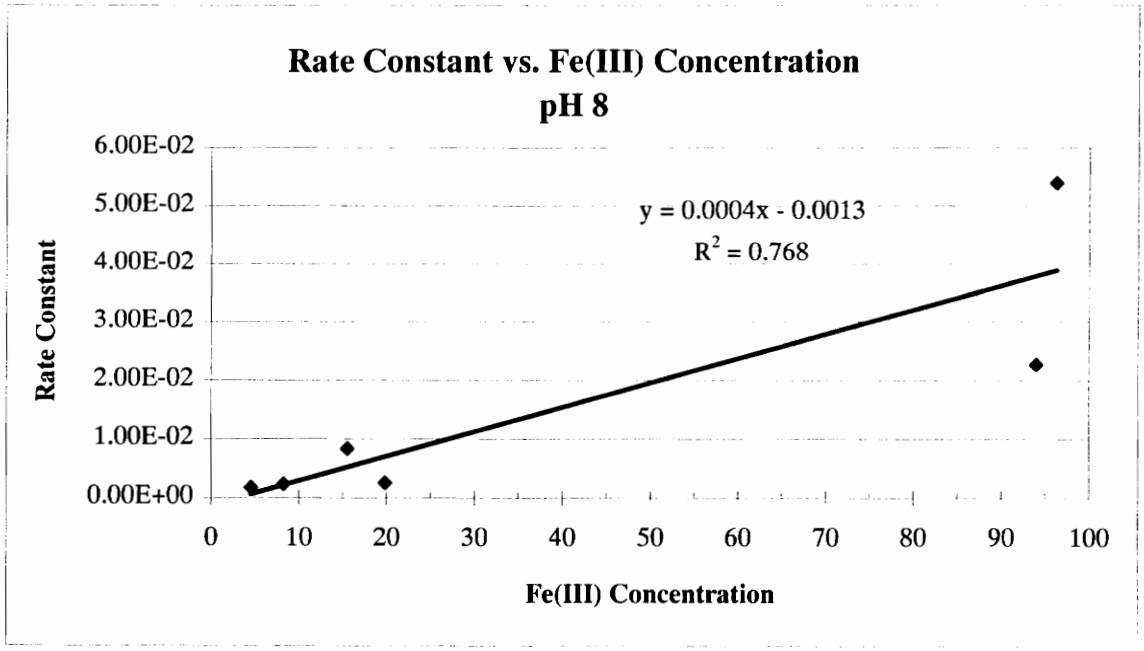

Reaction Rate Determination for Use in Model

INSTANTANEOUS RATES

pH 8; Fe(II) = 4 mg/L

Time (min)	0.45µm Mn (mg/L)	Rate (mg/L-min)	ln C	ln Rate
0	0.493	n/a	-0.707	
30	0.464	0.00097	-0.768	-6.942
60	0.391	0.00243	-0.939	-6.018
120	0.256	0.00225	-1.363	-6.097
180	0.124	0.00220	-2.087	-6.119
240	0.027	0.00162	-3.612	-6.427
300	0	0.00045		-7.706

Est. k — Actual Fe = 4.6 mg/L

9.46E-04
2.37E-03
2.17E-03
2.08E-03
1.46E-03
1.81E-03 Avg.

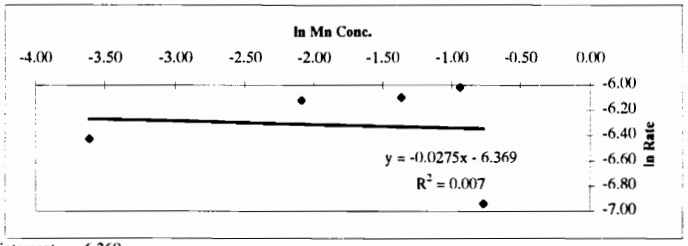

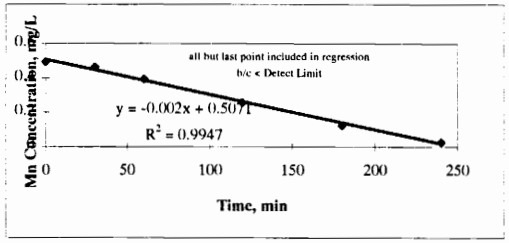

y intercept = -6.369
slope = -0.0275
k = 1.71E-03

pH 8; Fe(II) = 8 mg/L

Time (min)	0.45µm Mn (mg/L)	Rate (mg/L-min)	ln C	ln Rate
0	0.488	n/a	-0.717	
30	0.402	0.00287	-0.911	-5.855
60	0.317	0.00283	-1.149	-5.866
120	0.078	0.00398	-2.551	-5.526
180	0	0.00130		-6.645
240	0	0.00000		n/a
300	0	0.00000		n/a

Est. k — Actual Fe = 8.3 mg/L

2.36E-03
2.21E-03
2.30E-03

2.29E-03 Avg.

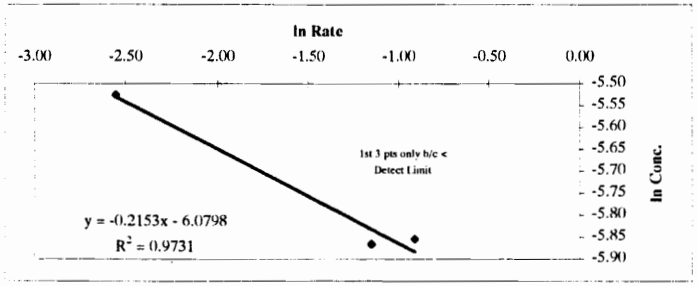

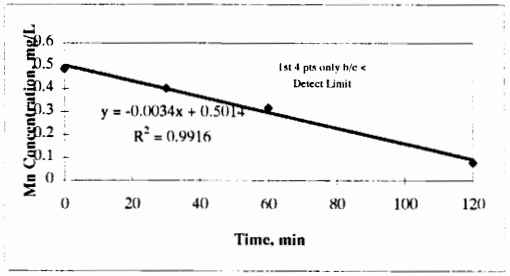

y intercept = -6.0798
slope = -0.2153
k = 2.29E-03

pH 8; Fe(II) = 20 mg/L

Time (min)	0.45µm Mn (mg/L)	Rate (mg/L-min)	ln C	ln Rate
0	0.438	n/a	-0.826	
30	0.315	0.00410	-1.155	-5.497
60	0.143	0.00573	-1.945	-5.161
135	0.002	0.00188	-6.215	-6.276
180	0	0.00004		-10.021
240	0	0.00000		n/a
300	0	0.00000		n/a

Est. k

2.51E-03
2.51E-03

2.51E-03

Actual Fe = 19.85 mg/L

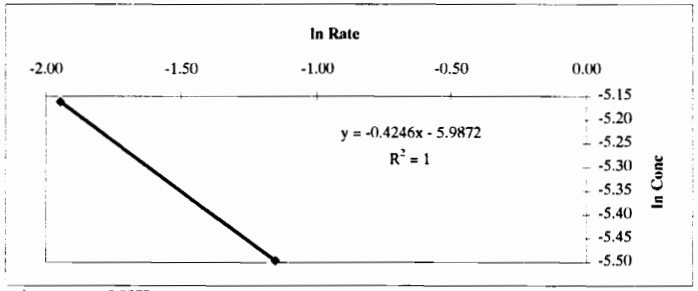

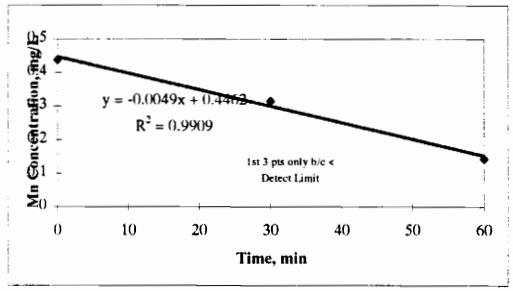

y intercept = -5.9872
slope = -0.4246
k = 2.51E-03

pH 8; Fe(II) = 50 mg/L

Time (min)	0.45µm Mn (mg/L)	Rate (mg/L-min)	ln C	ln Rate
0	0.344	n/a	-1.067	
20	0.127	0.01085	-2.064	-4.524
40	0.011	0.00580	-4.510	-5.150
60	0.006	0.00025	-5.116	-8.294
80	0	0.00030		-8.112
100	0	0.00000		n/a
120	0	0.00000		n/a

Est. k

1.35E-02
9.33E-03
4.29E-04

7.75E-03

Actual Fe = 50.48 mg/L

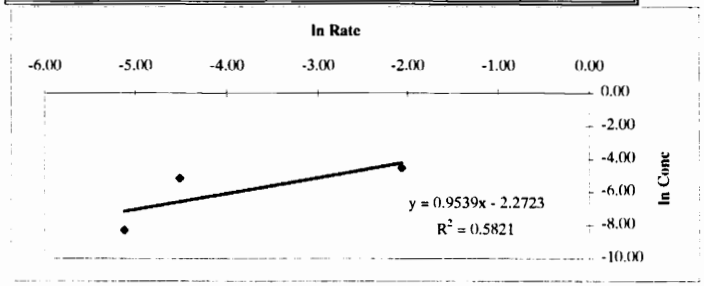

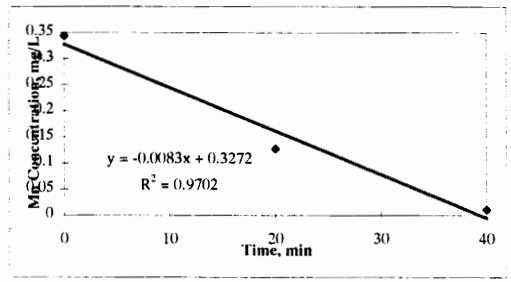

y intercept = -2.2723
slope = 0.9539
k = 1.03E-01

pH 8; Fe(II) = 100 mg/L Pure Iron

Time (min)	0.45µm Mn (mg/L)	Rate (mg/L-min)	ln C	ln Rate
0	0.353	n/a	-1.041	
10	0.225	0.01280	-1.492	-4.358
20	0.169	0.00560	-1.778	-5.185
30	0.1054	0.00636	-2.250	-5.058
40	0.063	0.00424	-2.765	-5.463
50	0.031	0.00320	-3.474	-5.745
60	0.005	0.00260	-5.298	-5.952

Est. k — Actual Fe = 94 mg/L

3.06E-02
1.58E-02
2.37E-02
2.13E-02
2.44E-02

2.32E-02

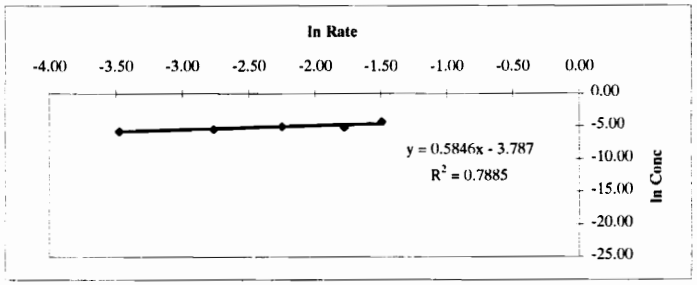

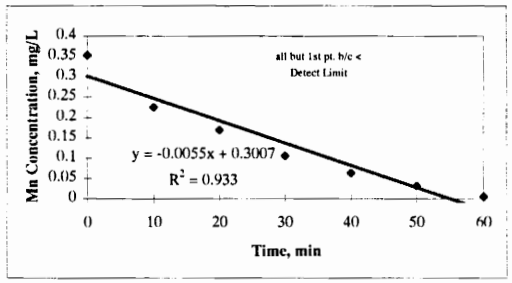

y intercept = -3.787
slope = 0.5846
k = 2.27E-02

pH 8; Fe(II) = 15 mg/L

Time (min)	0.45µm Mn (mg/L)	Rate (mg/L-min)	ln C	ln Rate
0	0.488	n/a	-0.717	
30	0.286	0.00673	-1.252	-5.001
60	0.113	0.00577	-2.180	-5.156
90	0.005	0.00360	-5.298	-5.627
120	0.002	0.00010	-6.215	-9.210
150	0.003	-0.00003	-5.809	#NUM!
180	0	0.00010		-9.210

Est. k — Actual Fe = 15.57 mg/L

8.30E-03
8.30E-03
8.72E-03
2.82E-04
-8.79E-05
8.30E-03 AVG.

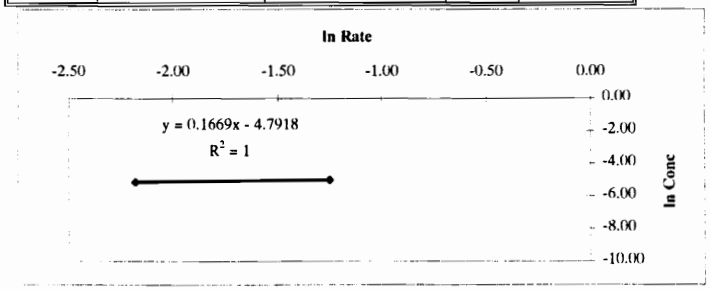

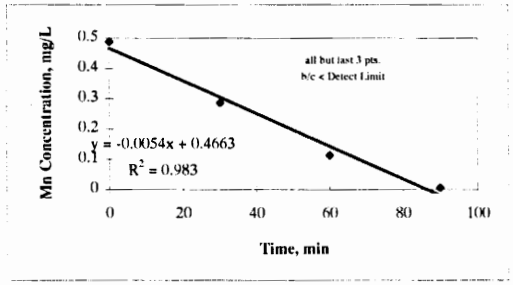

y intercept = -4.7918
slope = 0.1669
k = 8.30E-03

pH 8; Fe(II) = 100 mg/L

Time (min)	0.45µm Mn (mg/L)	Rate (mg/L-min)	ln C	ln Rate
0	0.354	n/a	-1.038	
10	0.142	0.02120	-1.952	-3.854
20	0.085	0.00570	-2.465	-5.167
30	0.028	0.00570	-3.576	-5.167
40	0.001	0.00270	-6.908	-5.915
50	0	0.00010		
60	0	0.00000		

Est. k

7.98E-02
3.04E-02
6.46E-02
2.94E-01

5.83E-02 AVG.

Actual Fe = 96.3 mg/L

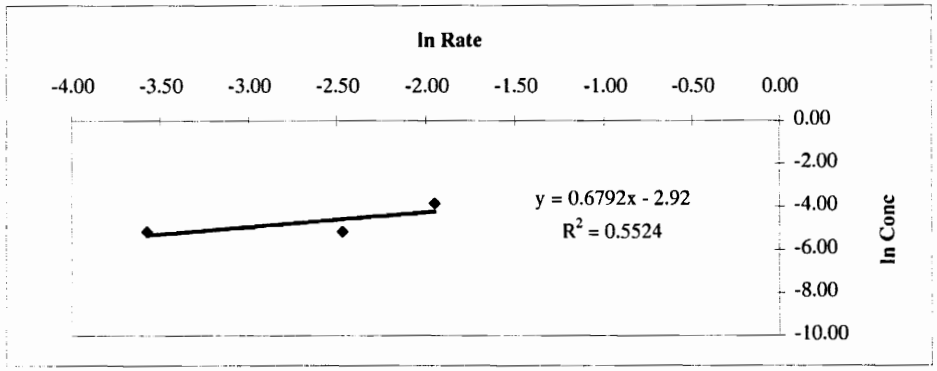

y intercept = -2.92
slope = 0.6792
k = 5.39E-02

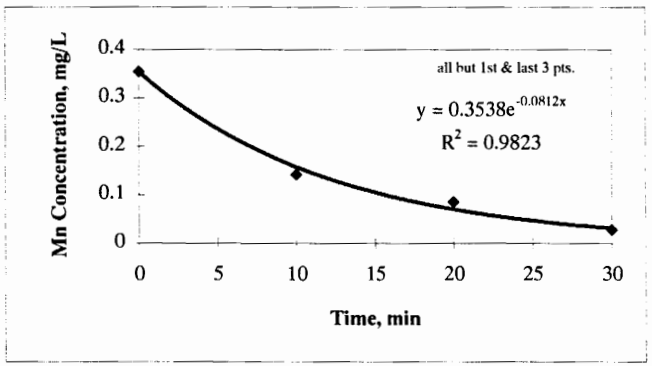

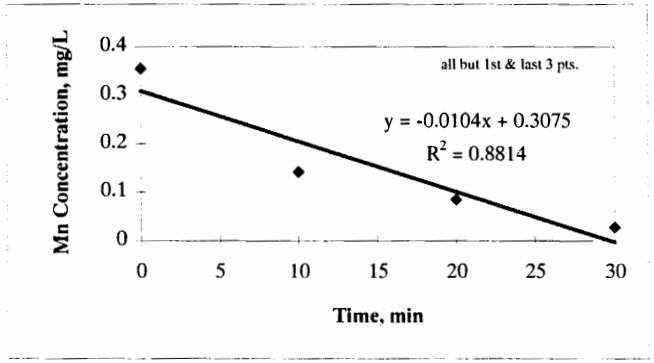

Rate Constant k vs. Fe(III) Concentration pH 7

Fe(III) (mg/L)	Rate Constant (units)
1.9	1.75E-04
8	2.13E-03
9.88	3.57E-03
21	2.92E-03
53.67	5.62E-03
101	2.01E-03
112.77	6.50E-03
Avg.	**3.28E-03**

Units = mg Mn/L-min

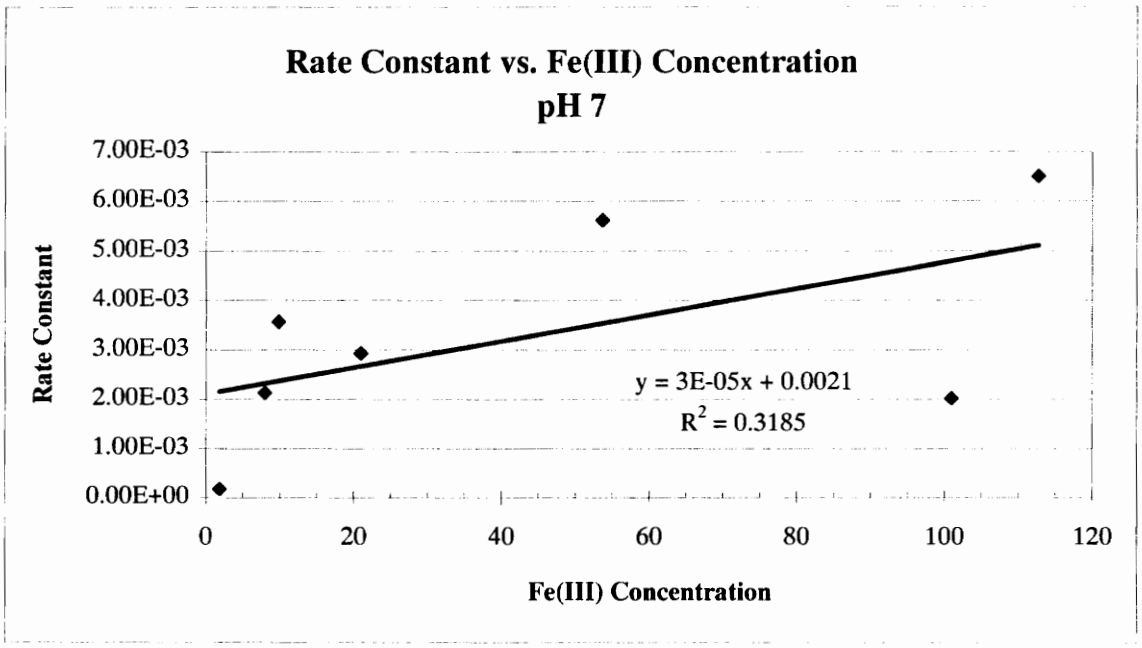

Reaction Rate Determination for Use in Model

INSTANTANEOUS RATES

pH 7; Fe(II) = 2 mg/L

Time (min)	0.45µm Mn (mg/L)	Rate (mg/L-min)	ln C	ln Rate	Est. k
0	0.495	n/a	-0.703		
30	0.475	0.00067	-0.744	-7.313	2.55E-04
60	0.466	0.00030	-0.764	-8.112	1.12E-04
120	0.426	0.00067	-0.853	-7.313	2.22E-04
180	0.399	0.00045	-0.919	-7.706	1.38E-04
240	0.357	0.00070	-1.030	-7.264	1.86E-04
300	0.308	0.00082	-1.178	-7.110	1.79E-04
					1.82E-04 Avg.

Actual Fe = 1.9

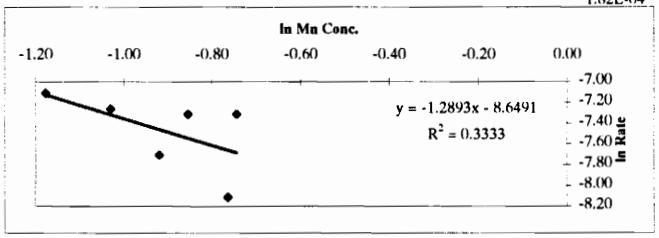

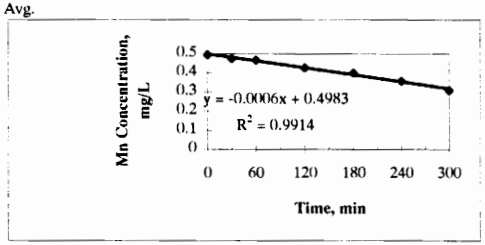

y intercept = -8.6491
slope = -1.2893
k = 1.75E-04

pH 7; Fe(II) = 8 mg/L

Time (min)	0.45µm Mn (mg/L)	Rate (mg/L-min)	ln C	ln Rate	Est. k
0	0.509	n/a	-0.675		
30	0.38	0.00430	-0.968	-5.449	4.87E-03
60	0.34	0.00133	-1.079	-6.620	1.53E-03
90	0.31	0.00100	-1.171	-6.908	1.16E-03
120	0.25	0.00200	-1.386	-6.215	2.39E-03
180	0.16	0.00150	-1.833	-6.502	1.90E-03
240	0.06	0.00167	-2.813	-6.397	2.40E-03
					2.38E-03 Avg.

Actual Fe = 8

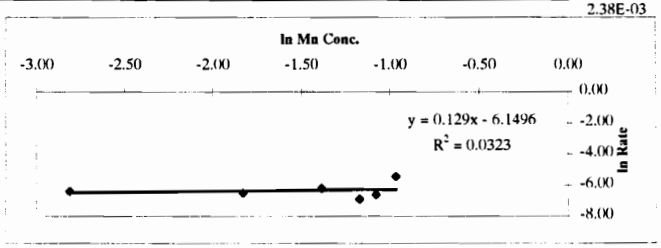

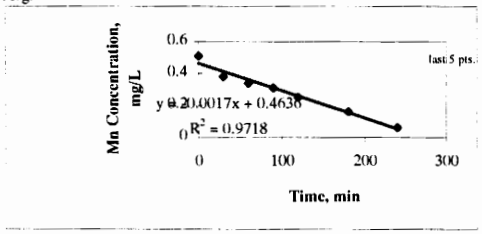

y intercept = -6.15
slope = 0.129
k = 2.13E-03

pH 7; Fe(II) = ~10 mg/L

Time (min)	0.45µm Mn (mg/L)	Rate (mg/L-min)	ln C	ln Rate	Est. k
0	0.517	n/a	-0.660		
30	0.403	0.00380	-0.909	-5.573	4.88E-03
60	0.332	0.00237	-1.103	-6.046	3.21E-03
90	0.274	0.00193	-1.295	-6.249	2.76E-03
120	0.196	0.00260	-1.630	-5.952	4.08E-03
150	0.148	0.00160	-1.911	-6.438	2.71E-03
180	0.083	0.00217	-2.489	-6.135	4.31E-03
					3.66E-03 Avg.

Actual Fe = 9.88

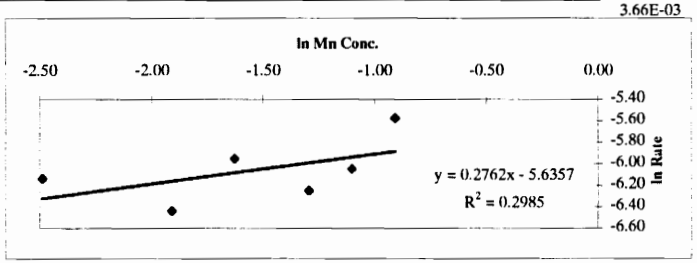

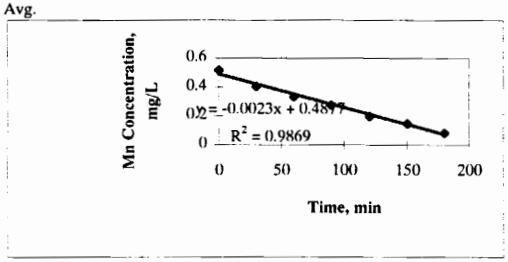

y intercept = -5.6357
slope = 0.2762
k = 3.57E-03

pH 7; Fe(II) = ~21 mg/L

Time (min)	0.45µm Mn (mg/L)	Rate (mg/L-min)	ln C	ln Rate	Est. k
0	0.518	n/a	-0.658		
15	0.451	0.00447	-0.796	-5.411	4.44E-03
30	0.424	0.00180	-0.858	-6.320	1.79E-03
45	0.387	0.00247	-0.949	-6.005	2.45E-03
60	0.328	0.00393	-1.115	-5.538	3.90E-03
75	0.281	0.00313	-1.269	-5.766	3.11E-03
90	0.241	0.00267	-1.423	-5.927	2.64E-03
					3.06E-03 Avg.

Actual Fe = 21

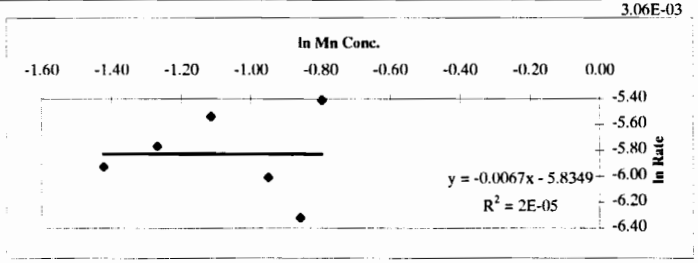

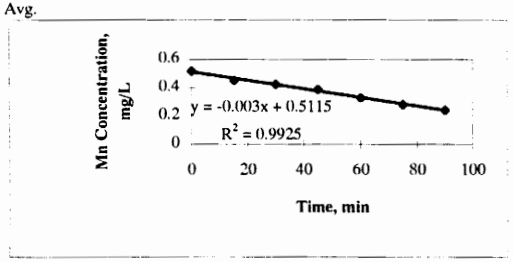

y intercept = -5.8349
slope = -0.0067
k = 2.92E-03

pH 7; Fe(II) = ~53 mg/L

Time (min)	0.45µm Mn (mg/L)	Rate (mg/L-min)	ln C	ln Rate	Est. k
0	0.458	n/a	-0.781		
30	0.29	0.00560	-1.238	-5.185	6.71E-03
50	0.22	0.00350	-1.514	-5.655	4.37E-03
75	0.11	0.00440	-2.207	-5.426	6.08E-03
95	0.04	0.00350	-3.219	-5.655	5.61E-03
105	0.01	0.00300	-4.605	-5.809	5.88E-03
135	0	0.00033		-8.006	
					5.69E-03 Avg.

Actual Fe = 53.67

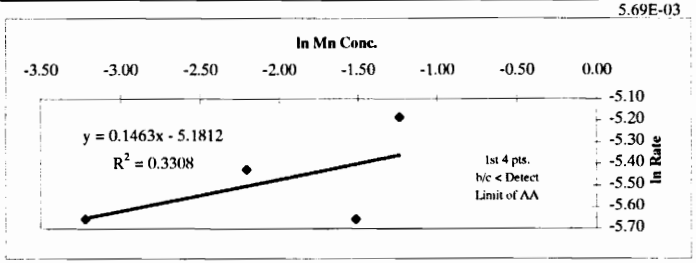

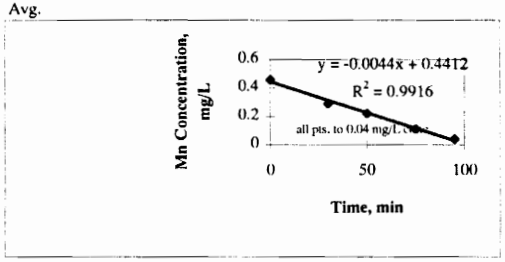

y intercept = -5.1812
slope = 0.1463
k = 5.62E-03

pH 7; Fe(II) = ~101 mg/L

Time (min)	0.45µm Mn (mg/L)	Rate (mg/L-min)	ln C	ln Rate	Est. k
0	0.389	n/a	-0.944		
15	0.35	0.00260	-1.050	-5.952	1.99E-03
30	0.32	0.00200	-1.139	-6.215	1.49E-03
45	0.26	0.00400	-1.347	-5.521	2.83E-03
60	0.22	0.00267	-1.514	-5.927	1.81E-03
75	0.15	0.00467	-1.897	-5.367	2.87E-03
90	0.11	0.00267	-2.207	-5.927	1.52E-03
					2.09E-03 Avg.

Actual Fe = 101

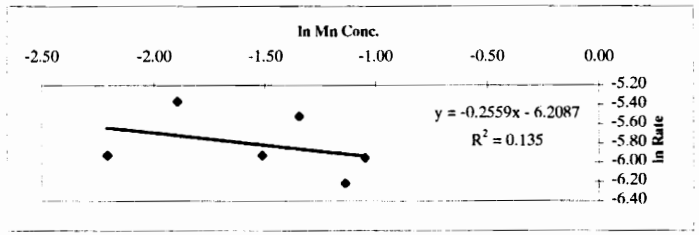

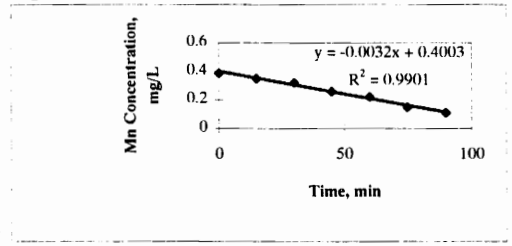

y intercept = -6.2087
slope = -0.2559
k = 2.01E-03

pH 7; Fe(II) = ~101 mg/L

Time (min)	0.45µm Mn (mg/L)	Rate (mg/L-min)	ln C	ln Rate
0	0.491	n/a	-0.711	
20	0.373	0.00590	-0.986	-5.133
40	0.245	0.00640	-1.406	-5.051
60	0.158	0.00435	-1.845	-5.438
80	0.056	0.00510	-2.882	-5.279
100	0.016	0.00200	-4.135	-6.215
120	0	0.00080		-7.131

Est. k

4.58E-03
4.47E-03
2.71E-03
2.44E-03
6.94E-04

3.55E-03 Avg.

Actual Fe = 112.7667

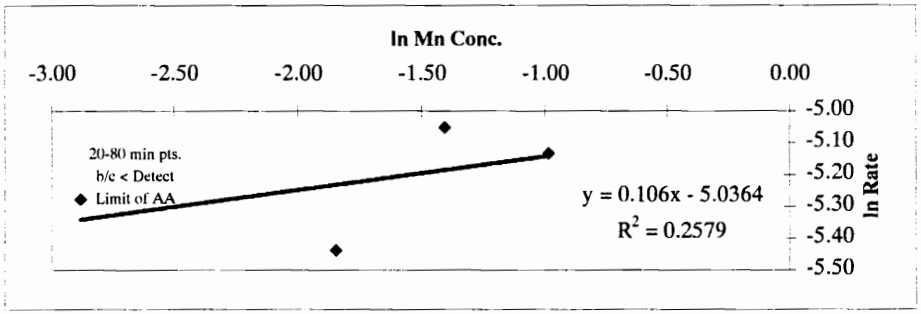

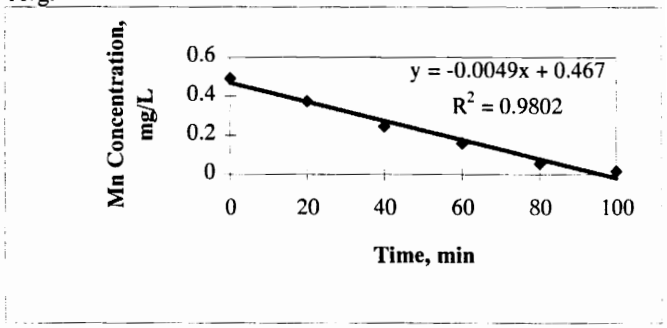

y intercept = -5.0364
slope = 0.106
k = 6.50E-03

APPENDIX D:

MODEL FORMULATION/

RELATED CALCULATIONS

BATCH SYSTEM MODEL

CALCULATIONS AND

FORMULATION

pH 8 Batch Model Results: Langmuir

pH 8; Fe = 4.6 mg/L; HOCl = 2 mg/L

Time, min	Observed	1.50E-02	2.00E-02	2.50E-02	3.43E-02
0	0.493	0.493	0.493	0.493	0.493
30	0.464	0.435	0.417	0.400	0.368
60	0.391	0.383	0.350	0.319	0.267
120	0.256	0.291	0.239	0.195	0.130
180	0.124	0.216	0.157	0.112	0.058
240	0.027	0.157	0.100	0.063	0.025
300	0	0.112	0.063	0.034	0.011
Sq. Residuals		**0.040**	**0.015**	**0.016**	**0.045**
			Best Fit		

pH 8; Fe = 8.3 mg/L; HOCl = 1.97 mg/L

Time, min	Observed	1.50E-02	2.00E-02	2.50E-02	3.43E-02
0	0.488	0.488	0.488	0.488	0.488
30	0.402	0.393	0.365	0.338	0.293
60	0.317	0.313	0.267	0.227	0.166
120	0.078	0.192	0.137	0.096	0.050
180	0	0.115	0.068	0.040	0.015
240	0	0.068	0.033	0.016	0.004
300	0	0.040	0.016	0.007	0.001
Sq. Residuals		**0.0325**	**0.0132**	**0.0143**	**0.0357**
			Best Fit		

pH 8; Fe = 19.85 mg/L; HOCl = 2.03 mg/L

Time, min	Observed	1.00E-02	1.50E-02	2.00E-02	3.43E-02
0	0.438	0.438	0.438	0.438	0.438
30	0.315	0.316	0.268	0.227	0.142
60	0.143	0.227	0.164	0.119	0.050
135	0.002	0.102	0.052	0.028	0.005
180	0	0.065	0.028	0.012	0.001
240	0	0.037	0.012	0.004	0.000
300	0	0.021	0.006	0.002	0.000
Sq. Residuals		**0.0230**	**0.0061**	**0.0092**	**0.0383**
			Best Fit		

pH 8; Fe = 50.48 mg/L; HOCl = 1.48 mg/L

Time, min	Observed	4.50E-02	5.00E-02	5.50E-02	6.00E-02	3.43E-02
0	0.344	0.344	0.344	0.344	0.344	0.344
20	0.127	0.115	0.105	0.096	0.088	0.143
40	0.011	0.056	0.049	0.043	0.038	0.077
60	0.006	0.032	0.027	0.023	0.019	0.047
80	0	0.019	0.016	0.013	0.011	0.031
100	0	0.012	0.010	0.008	0.006	0.021
120	0	0.008	0.006	0.005	0.004	0.015
Sq. Residuals		**0.0034**	**0.0027**	**0.0025**	**0.0026**	**0.0078**
				Best Fit		

pH 8; Fe = 94 mg/L; HOCl = 1.41 mg/L

Time, min	Observed	3.50E-02	4.00E-02	4.50E-02	3.43E-02
0	0.353	0.353	0.353	0.353	0.353
10	0.225	0.203	0.191	0.180	0.205
20	0.169	0.140	0.129	0.119	0.142
30	0.1054	0.108	0.098	0.090	0.109
40	0.063	0.087	0.079	0.072	0.089
50	0.031	0.074	0.067	0.061	0.075
60	0.005	0.064	0.058	0.053	0.065
Sq. Residuals		**0.0073**	**0.0072**	**0.0080**	**0.0074**
			Best Fit		

pH 8; Fe = 15.57 mg/L; HOCl = 1.73 mg/L

Time, min	Observed	2.50E-02	3.00E-02	3.50E-02	4.00E-02	3.43E-02
0	0.488	0.488	0.488	0.488	0.488	0.488
30	0.286	0.281	0.251	0.224	0.201	0.228
60	0.113	0.160	0.129	0.104	0.084	0.107
90	0.005	0.093	0.068	0.050	0.037	0.052
120	0.002	0.056	0.037	0.025	0.017	0.027
150	0.003	0.034	0.021	0.013	0.008	0.014
180	0	0.021	0.012	0.007	0.004	0.007
Sq. Residuals		**0.0143**	**0.0072**	**0.0066**	**0.0095**	**0.0064**
				Best Fit		

pH 8; Fe = 96.3 mg/L; HOCl = 1.95 mg/L

Time, min	Observed	4.50E-02	5.00E-02	5.50E-02	6.00E-02	3.43E-02
0	0.354	0.354	0.354	0.354	0.354	0.354
10	0.142	0.141	0.131	0.122	0.114	0.168
20	0.085	0.080	0.073	0.066	0.060	0.102
30	0.028	0.053	0.047	0.042	0.038	0.071
40	0.001	0.038	0.033	0.029	0.026	0.052
50	0	0.029	0.025	0.022	0.019	0.040
60	0	0.022	0.019	0.016	0.014	0.032
Sq. Residuals		**0.0033**	**0.0027**	**0.0025**	**0.0027**	**0.0081**
				Best Fit		

pH 8 Batch Model Results: Freundlich

pH 8; Fe = 4.6 mg/L; HOCl = 2 mg/L

Time, min	Observed	8.00E-02	9.00E-02	9.50E-02	1.53E-01
0	0.493	0.493	0.493	0.493	0.493
30	0.464	0.381	0.371	0.366	0.315
60	0.391	0.309	0.295	0.289	0.228
120	0.256	0.222	0.207	0.200	0.143
180	0.124	0.171	0.158	0.151	0.102
240	0.027	0.138	0.126	0.120	0.078
300	0	0.115	0.104	0.099	0.063
Sq. Residuals		**0.0426**	**0.0420**	**0.043**	**0.069**
			Best Fit		

pH 8; Fe = 8.3 mg/L; HOCl = 1.97 mg/L

Time, min	Observed	9.00E-02	9.50E-02	1.00E-01	1.53E-01
0	0.488	0.488	0.488	0.488	0.488
30	0.402	0.316	0.309	0.303	0.251
60	0.317	0.230	0.223	0.216	0.163
120	0.078	0.145	0.139	0.133	0.092
180	0	0.103	0.098	0.094	0.062
240	0	0.079	0.075	0.071	0.045
300	0	0.063	0.059	0.056	0.035
Sq. Residuals		**0.0402**	**0.03981**	**0.03983**	**0.05379**
			Best Fit		

pH 8; Fe = 19.85 mg/L; HOCl = 2.03 mg/L

Time, min	Observed	8.00E-02	8.50E-02	9.00E-02	9.50E-02	1.53E-01
0	0.438	0.438	0.438	0.438	0.438	0.438
30	0.315	0.223	0.216	0.209	0.203	0.148
60	0.143	0.143	0.136	0.130	0.124	0.081
135	0.002	0.088	0.083	0.079	0.075	0.034
180	0	0.051	0.047	0.044	0.042	0.024
240	0	0.037	0.034	0.032	0.030	0.017
300	0	0.028	0.026	0.024	0.023	0.012
Sq. Residuals		**0.02054**	**0.02052**	**0.0208**	**0.0214**	**0.0339**
			Best Fit			

pH 8; Fe = 50.48 mg/L; HOCl = 1.48 mg/L

Time, min	Observed	2.50E-01	3.00E-01	3.50E-01	4.00E-01	1.53E-01
0	0.344	0.344	0.344	0.344	0.344	0.344
20	0.127	0.096	0.081	0.070	0.062	0.139
40	0.011	0.049	0.040	0.033	0.028	0.080
60	0.006	0.030	0.024	0.020	0.017	0.053
80	0	0.021	0.017	0.014	0.012	0.039
100	0	0.016	0.013	0.010	0.009	0.030
120	0	0.013	0.010	0.008	0.007	0.024
Sq. Residuals		**0.00385**	**0.00377**	**0.0043**	**0.0049**	**0.0101**
			Best Fit			

pH 8; Fe = 94 mg/L; HOCl = 1.41 mg/L

Time, min	Observed	9.50E-02	1.00E-01	1.50E-01	2.00E-01	1.53E-01
0	0.353	0.353	0.353	0.353	0.353	0.353
10	0.225	0.233	0.229	0.193	0.166	0.191
20	0.169	0.171	0.166	0.128	0.102	0.126
30	0.1054	0.132	0.128	0.092	0.070	0.091
40	0.063	0.106	0.102	0.070	0.052	0.069
50	0.031	0.088	0.084	0.056	0.040	0.055
60	0.005	0.074	0.070	0.046	0.032	0.045
Sq. Residuals		**0.011**	**0.0091**	**0.0052**	**0.0101**	**0.0054**
				Best Fit		

pH 8; Fe = 15.57 mg/L; HOCl = 1.73 mg/L

Time, min	Observed	1.00E-01	1.50E-01	2.00E-01	2.50E-01	1.53E-01
0	0.488	0.488	0.488	0.488	0.488	0.488
30	0.286	0.259	0.207	0.171	0.145	0.205
60	0.113	0.171	0.125	0.097	0.079	0.123
90	0.005	0.125	0.087	0.065	0.052	0.085
120	0.002	0.097	0.065	0.048	0.037	0.064
150	0.003	0.079	0.052	0.037	0.029	0.050
180	0	0.065	0.042	0.030	0.023	0.041
Sq. Residuals		**0.038**	**0.0212**	**0.0213**	**0.0257**	**0.0210**
			Best Fit			

pH 8; Fe = 96.3 mg/L; HOCl = 1.95 mg/L

Time, min	Observed	1.50E-01	2.00E-01	2.50E-01	1.53E-01
0	0.354	0.354	0.354	0.354	0.354
10	0.142	0.155	0.126	0.105	0.153
20	0.085	0.089	0.066	0.052	0.087
30	0.028	0.058	0.041	0.031	0.057
40	0.001	0.041	0.028	0.021	0.040
50	0	0.031	0.021	0.015	0.030
60	0	0.024	0.016	0.012	0.024
Sq. Residuals		**0.0043**	**0.0022**	**0.0033**	**0.0040**
			Best Fit		

Runge-Kutta Estimation: Batch Studies Langmuir

Initial Parameters:

Δx =	0.05	
pH =	7	
k =	3.50E-02	
$OCl]_O$ =	2	mg/L as HOCl
C_O =	0.491	mg/L as Mn
a (iso) =	0.0011	
b (iso) =	2.34	
olume =	0.3	L
Fe =	112.8	mg/L as Fe
Λ =	0.002783181	

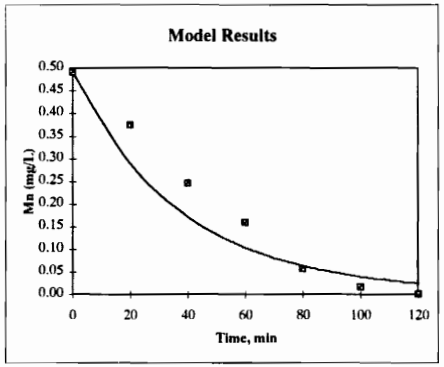

Time	Observed	3.50E-02	Res.
0	0.491	0.491	0
20	0.373	0.290	0.00688
40	0.245	0.172	0.005348
60	0.158	0.103	0.002993
80	0.056	0.063	4.96E-05
100	0.016	0.039	0.000528
120	0	0.024	0.000591
		0.0164	**0.016**

Mn(II) Concentration

x	Y_i	k_1	k_2	k_3	k_4	Y_{i+1}
0.00	0.491	-0.01280	-0.01279	-0.01279	-0.01279	0.490
0.05	0.490	-0.01278	-0.01278	-0.01278	-0.01277	0.490
0.10	0.490	-0.01277	-0.01276	-0.01276	-0.01276	0.489
0.15	0.489	-0.01275	-0.01275	-0.01275	-0.01274	0.488
0.20	0.488	-0.01274	-0.01273	-0.01273	-0.01272	0.488
0.25	0.488	-0.01272	-0.01271	-0.01271	-0.01271	0.487
0.30	0.487	-0.01270	-0.01270	-0.01270	-0.01269	0.487
0.35	0.487	-0.01269	-0.01268	-0.01268	-0.01268	0.486
0.40	0.486	-0.01267	-0.01267	-0.01267	-0.01266	0.485
0.45	0.485	-0.01266	-0.01265	-0.01265	-0.01265	0.485
0.50	0.485	-0.01264	-0.01264	-0.01264	-0.01263	0.484
0.55	0.484	-0.01263	-0.01262	-0.01262	-0.01262	0.483
0.60	0.483	-0.01261	-0.01261	-0.01261	-0.01260	0.483

HOCl Concentration

x	Y_i	k_1	k_2	k_3	k_4	Y_{i+1}
0.00	2.000	-0.01479	-0.01479	-0.01479	-0.01479	1.999
0.05	1.999	-0.01478	-0.01477	-0.01477	-0.01477	1.999
0.10	1.999	-0.01476	-0.01476	-0.01476	-0.01476	1.998
0.15	1.998	-0.01475	-0.01475	-0.01475	-0.01474	1.997
0.20	1.997	-0.01473	-0.01473	-0.01473	-0.01473	1.996
0.25	1.996	-0.01472	-0.01472	-0.01472	-0.01471	1.996
0.30	1.996	-0.01471	-0.01470	-0.01470	-0.01470	1.995
0.35	1.995	-0.01469	-0.01469	-0.01469	-0.01469	1.994
0.40	1.994	-0.01468	-0.01467	-0.01467	-0.01467	1.993
0.45	1.993	-0.01466	-0.01466	-0.01466	-0.01466	1.993
0.50	1.993	-0.01465	-0.01465	-0.01465	-0.01464	1.992
0.55	1.992	-0.01463	-0.01463	-0.01463	-0.01463	1.991
0.60	1.991	-0.01462	-0.01462	-0.01462	-0.01461	1.990

	C	D	E
1			
2			
3	**Initial Parameters:**		
4	Δx =	0.05	
5	pH =	7	
6	k =	0.035	
7	$[HOCl]_o$ =	2	mg/L as HOCl
8	C_o =	=L22	mg/L as Mn
9	a (iso) =	0.0011	
10	b (iso) =	2.34	
11	Volume =	0.3	L
12	Fe =	112.8	mg/L as Fe
13	A =	=$D$11*54.94/($D$12*52.5)	
14			Mn(II) Concentration
15	x	Y_i	k_1
16			
17	0	=$D$8	=(-$D$6*$T17*($D$9*$D$10*$D17/(1+$D$10*$D17))*$D$12)/($D$11+(((($D$9*$D$10)/((1+$D$10*$D17)^2))*$D$12))
18	=C17+$D$4	=I17	=(-$D$6*$T18*($D$9*$D$10*$D18/(1+$D$10*$D18))*$D$12)/($D$11+(((($D$9*$D$10)/((1+$D$10*$D18)^2))*$D$12))
19	=C18+$D$4	=I18	=(-$D$6*$T19*($D$9*$D$10*$D19/(1+$D$10*$D19))*$D$12)/($D$11+(((($D$9*$D$10)/((1+$D$10*$D19)^2))*$D$12))
20	=C19+$D$4	=I19	=(-$D$6*$T20*($D$9*$D$10*$D20/(1+$D$10*$D20))*$D$12)/($D$11+(((($D$9*$D$10)/((1+$D$10*$D20)^2))*$D$12))
21	=C20+$D$4	=I20	=(-$D$6*$T21*($D$9*$D$10*$D21/(1+$D$10*$D21))*$D$12)/($D$11+(((($D$9*$D$10)/((1+$D$10*$D21)^2))*$D$12))

	G
1	
2	
3	
4	
5	
6	
7	
8	
9	
10	
11	
12	
13	
14	Mn(II) Concentration
15	k_3
16	
17	=(-$D$6*$T17*($D$9*$D$10*($D17+(0.5*$D$4*$F17))/(1+$D$10*($D17+(0.5*$D$4*$F17))))*$D$12)/($D$11+(($D$9*$D$10)/((1+$D$10*($D17+(0.5*$D$4*$F17)))^2))*$D$12))
18	=(-$D$6*$T18*($D$9*$D$10*($D18+(0.5*$D$4*$F18))/(1+$D$10*($D18+(0.5*$D$4*$F18))))*$D$12)/($D$11+(($D$9*$D$10)/((1+$D$10*($D18+(0.5*$D$4*$F18)))^2))*$D$12))
19	=(-$D$6*$T19*($D$9*$D$10*($D19+(0.5*$D$4*$F19))/(1+$D$10*($D19+(0.5*$D$4*$F19))))*$D$12)/($D$11+(($D$9*$D$10)/((1+$D$10*($D19+(0.5*$D$4*$F19)))^2))*$D$12))
20	=(-$D$6*$T20*($D$9*$D$10*($D20+(0.5*$D$4*$F20))/(1+$D$10*($D20+(0.5*$D$4*$F20))))*$D$12)/($D$11+(($D$9*$D$10)/((1+$D$10*($D20+(0.5*$D$4*$F20)))^2))*$D$12))
21	=(-$D$6*$T21*($D$9*$D$10*($D21+(0.5*$D$4*$F21))/(1+$D$10*($D21+(0.5*$D$4*$F21))))*$D$12)/($D$11+(($D$9*$D$10)/((1+$D$10*($D21+(0.5*$D$4*$F21)))^2))*$D$12))

	H	I
1		
2		
3		
4		
5		
6		
7		
8		
9		
10		
11		
12		
13		
14	Mn(II) Concentration	
15	k_4	Y_{i+1}
16		
17	=(-$D$6*$T17*($D$9*$D$10*($D17+($D$4*$G17))/(1+$D$10*($D17+($D$4*$G17))))*$D$12)/($D$11+(((($D$9*$D$10)/((1+$D$10*($D17+($D$4*$G17)))^2))*$D$12))	=D17+(($D$4/6)*(E17+2*F17+2*G17+H17))
18	=(-$D$6*$T18*($D$9*$D$10*($D18+($D$4*$G18))/(1+$D$10*($D18+($D$4*$G18))))*$D$12)/($D$11+(((($D$9*$D$10)/((1+$D$10*($D18+($D$4*$G18)))^2))*$D$12))	=D18+(($D$4/6)*(E18+2*F18+2*G18+H18))
19	=(-$D$6*$T19*($D$9*$D$10*($D19+($D$4*$G19))/(1+$D$10*($D19+($D$4*$G19))))*$D$12)/($D$11+(((($D$9*$D$10)/((1+$D$10*($D19+($D$4*$G19)))^2))*$D$12))	=D19+(($D$4/6)*(E19+2*F19+2*G19+H19))
20	=(-$D$6*$T20*($D$9*$D$10*($D20+($D$4*$G20))/(1+$D$10*($D20+($D$4*$G20))))*$D$12)/($D$11+(((($D$9*$D$10)/((1+$D$10*($D20+($D$4*$G20)))^2))*$D$12))	=D20+(($D$4/6)*(E20+2*F20+2*G20+H20))
21	=(-$D$6*$T21*($D$9*$D$10*($D21+($D$4*$G21))/(1+$D$10*($D21+($D$4*$G21))))*$D$12)/($D$11+(((($D$9*$D$10)/((1+$D$10*($D21+($D$4*$G21)))^2))*$D$12))	=D21+(($D$4/6)*(E21+2*F21+2*G21+H21))

	S	T	U	V
1				
2				
3				
4				
5				
6				
7				
8				
9				
10				
11				
12				
13				
14			HOCl Concentration	
15	x	Y_i	k_1	k_2
16				
17	0	=$D$7	=-$D$6*$T17*$D$9*$D$10*$D17/($D$13*(1+$D$10*$D17))	=-$D$6*(0.5*$D$4*$U17+$T17)*$D$9*$D$10*$D17/($D$13*(1+$D$10*$D17))
18	=S17+$D$4	=Y17	=-$D$6*$T18*$D$9*$D$10*$D18/($D$13*(1+$D$10*$D18))	=-$D$6*(0.5*$D$4*$U18+$T18)*$D$9*$D$10*$D18/($D$13*(1+$D$10*$D18))
19	=S18+$D$4	=Y18	=-$D$6*$T19*$D$9*$D$10*$D19/($D$13*(1+$D$10*$D19))	=-$D$6*(0.5*$D$4*$U19+$T19)*$D$9*$D$10*$D19/($D$13*(1+$D$10*$D19))
20	=S19+$D$4	=Y19	=-$D$6*$T20*$D$9*$D$10*$D20/($D$13*(1+$D$10*$D20))	=-$D$6*(0.5*$D$4*$U20+$T20)*$D$9*$D$10*$D20/($D$13*(1+$D$10*$D20))
21	=S20+$D$4	=Y20	=-$D$6*$T21*$D$9*$D$10*$D21/($D$13*(1+$D$10*$D21))	=-$D$6*(0.5*$D$4*$U21+$T21)*$D$9*$D$10*$D21/($D$13*(1+$D$10*$D21))

	W	X	Y
1			
2			
3			
4			
5			
6			
7			
8			
9			
10			
11			
12			
13			
14		HOCl Concentration	
15	k_3	k_4	Y_{i+1}
16			
17	=-$D$6*(0.5*$D$4*$V17+$T17)*$D$9*$D$10*$D17/($D$13*(1+$D$10*$D17))	=-$D$6*($D$4*$W17+$T17)*$D$9*$D$10*$D17/($D$13*(1+$D$10*$D17))	=T17+(($D$4/6)*(U17+2*V17+2*W17+X17))
18	=-$D$6*(0.5*$D$4*$V18+$T18)*$D$9*$D$10*$D18/($D$13*(1+$D$10*$D18))	=-$D$6*($D$4*$W18+$T18)*$D$9*$D$10*$D18/($D$13*(1+$D$10*$D18))	=T18+(($D$4/6)*(U18+2*V18+2*W18+X18))
19	=-$D$6*(0.5*$D$4*$V19+$T19)*$D$9*$D$10*$D19/($D$13*(1+$D$10*$D19))	=-$D$6*($D$4*$W19+$T19)*$D$9*$D$10*$D19/($D$13*(1+$D$10*$D19))	=T19+(($D$4/6)*(U19+2*V19+2*W19+X19))
20	=-$D$6*(0.5*$D$4*$V20+$T20)*$D$9*$D$10*$D20/($D$13*(1+$D$10*$D20))	=-$D$6*($D$4*$W20+$T20)*$D$9*$D$10*$D20/($D$13*(1+$D$10*$D20))	=T20+(($D$4/6)*(U20+2*V20+2*W20+X20))
21	=-$D$6*(0.5*$D$4*$V21+$T21)*$D$9*$D$10*$D21/($D$13*(1+$D$10*$D21))	=-$D$6*($D$4*$W21+$T21)*$D$9*$D$10*$D21/($D$13*(1+$D$10*$D21))	=T21+(($D$4/6)*(U21+2*V21+2*W21+X21))

CSTR MODEL:

FORMULATION AND

SIMULATIONS

CSTR Model: Model Simulations

Initial Parameters:

Δx =	1	min
pH =	8	
Q =	0.01917	L/min
Volume =	2.3	L
C_{in} =	0.5	mg/L
k =	3.43E-02	
a (Fe iso) =	0.0070	
b (Fe iso) =	3.79	
M_{Fe} =	280	mg/L as FeO
$HOCl_o$ =	2	mg/L
a (Mn iso) =	0.204	
b (Mn iso) =	54.8	
M_{Mn} =	0	mg/L MnO_x
Fe_{in} =	2	mg/L
A =	0.008596054	
B =	0	
k2 (Fe) =	3.990202751	
k3 (Mn) =	0	

Note: Assume MnOx = 0 and no growth

θH = 120 min

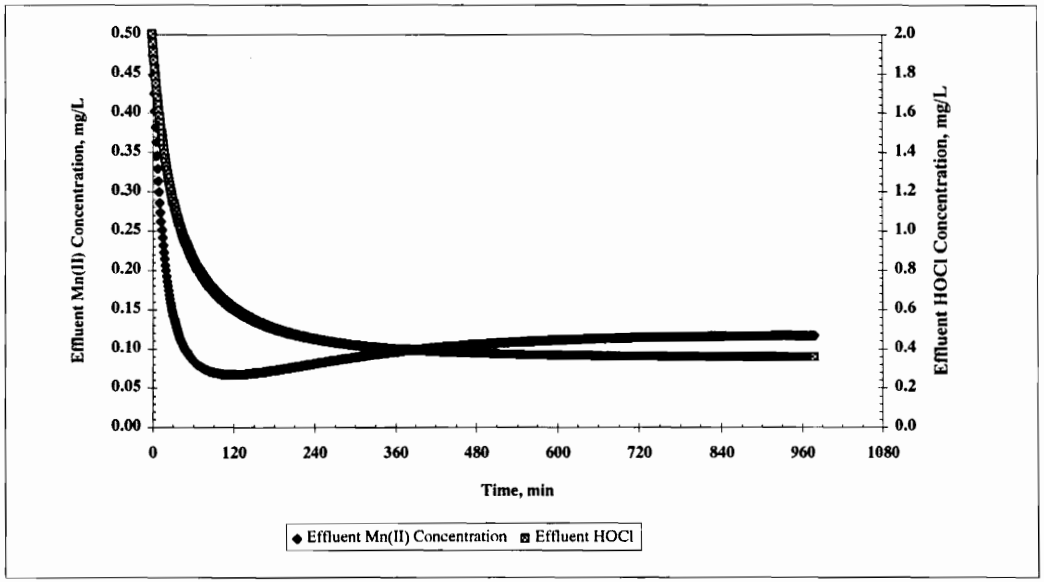

Mn(II) Concentration

x	Y_i	k_1	k_2	k_3	k_4	Y_{i+1}
0.00	0.500	-0.02762	-0.02699	-0.02701	-0.02638	0.473
1.00	0.473	-0.02576	-0.02516	-0.02518	-0.02458	0.448
2.00	0.448	-0.02401	-0.02345	-0.02346	-0.02290	0.424
3.00	0.424	-0.02238	-0.02184	-0.02186	-0.02133	0.403
4.00	0.403	-0.02085	-0.02035	-0.02036	-0.01987	0.382
5.00	0.382	-0.01942	-0.01895	-0.01897	-0.01850	0.363

HOCl Concentration

x	Y_i	k_1	k_2	k_3	k_4	Y_{i+1}
0.00	2.000	-0.04724	-0.04661	-0.04661	-0.04599	1.953
1.00	1.953	-0.04530	-0.04471	-0.04472	-0.04413	1.909
2.00	1.909	-0.04345	-0.04289	-0.04290	-0.04234	1.866
3.00	1.866	-0.04168	-0.04115	-0.04116	-0.04063	1.825
4.00	1.825	-0.03999	-0.03949	-0.03949	-0.03900	1.785
5.00	1.785	-0.03837	-0.03790	-0.03790	-0.03743	1.747

	A	B	C
28	CSTR Model		
29			
30	x	Y_i	k_1
31			
32	0	=$B$8	=($B$6*$H$8-$B$6*$B32-$B$9*$J32*(($B$10*$B$11*$B32)/(1+$B$11*$B32))*$B$12-$B$9*$J32*(($B$14*$B$15*$B32)/(1+$B$15*$B32))*$B$16)/($B$7+((($H$10*$B$11)/((1+$B$11*$B32)^2))*$B$12+(($B$14*$B$15)/((1+$B$14*$B$16)^2))*$B$16)
33	=A32+$B$4	=G32	=($B$6*$H$8-$B$6*$B33-$B$9*$J33*(($B$10*$B$11*$B33)/(1+$B$11*$B33))*$B$12-$B$9*$J33*(($B$14*$B$15*$B33)/(1+$B$15*$B33))*$B$16)/($B$7+((($H$10*$B$11)/((1+$B$11*$B33)^2))*$B$12+(($B$14*$B$15)/((1+$B$14*$B$16)^2))*$B$16)
34	=A33+$B$4	=G33	=($B$6*$H$8-$B$6*$B34-$B$9*$J34*(($B$10*$B$11*$B34)/(1+$B$11*$B34))*$B$12-$B$9*$J34*(($B$14*$B$15*$B34)/(1+$B$15*$B34))*$B$16)/($B$7+((($H$10*$B$11)/((1+$B$11*$B34)^2))*$B$12+(($B$14*$B$15)/((1+$B$14*$B$16)^2))*$B$16)
35	=A34+$B$4	=G34	=($B$6*$H$8-$B$6*$B35-$B$9*$J35*(($B$10*$B$11*$B35)/(1+$B$11*$B35))*$B$12-$B$9*$J35*(($B$14*$B$15*$B35)/(1+$B$15*$B35))*$B$16)/($B$7+((($H$10*$B$11)/((1+$B$11*$B35)^2))*$B$12+(($B$14*$B$15)/((1+$B$14*$B$16)^2))*$B$16)
36	=A35+$B$4	=G35	=($B$6*$H$8-$B$6*$B36-$B$9*$J36*(($B$10*$B$11*$B36)/(1+$B$11*$B36))*$B$12-$B$9*$J36*(($B$14*$B$15*$B36)/(1+$B$15*$B36))*$B$16)/($B$7+((($H$10*$B$11)/((1+$B$11*$B36)^2))*$B$12+(($B$14*$B$15)/((1+$B$14*$B$16)^2))*$B$16)
37	=A36+$B$4	=G36	=($B$6*$H$8-$B$6*$B37-$B$9*$J37*(($B$10*$B$11*$B37)/(1+$B$11*$B37))*$B$12-$B$9*$J37*(($B$14*$B$15*$B37)/(1+$B$15*$B37))*$B$16)/($B$7+((($H$10*$B$11)/((1+$B$11*$B37)^2))*$B$12+(($B$14*$B$15)/((1+$B$14*$B$16)^2))*$B$16)
38	=A37+$B$4	=G37	=($B$6*$H$8-$B$6*$B38-$B$9*$J38*(($B$10*$B$11*$B38)/(1+$B$11*$B38))*$B$12-$B$9*$J38*(($B$14*$B$15*$B38)/(1+$B$15*$B38))*$B$16)/($B$7+((($H$10*$H$11)/((1+$B$11*$B38)^2))*$B$12+(($B$14*$B$15)/((1+$B$14*$B$16)^2))*$B$16)
39	=A38+$B$4	=G38	=($B$6*$H$8-$B$6*$B39-$B$9*$J39*(($B$10*$B$11*$B39)/(1+$B$11*$B39))*$B$12-$B$9*$J39*(($B$14*$B$15*$B39)/(1+$B$15*$B39))*$B$16)/($B$7+((($H$10*$B$11)/((1+$B$11*$B39)^2))*$B$12+(($B$14*$B$15)/((1+$B$14*$B$16)^2))*$B$16)
40	=A39+$B$4	=G39	=($B$6*$H$8-$B$6*$B40-$B$9*$J40*(($B$10*$B$11*$B40)/(1+$B$11*$B40))*$B$12-$B$9*$J40*(($B$14*$B$15*$B40)/(1+$B$15*$B40))*$B$16)/($B$7+((($H$10*$B$11)/((1+$B$11*$B40)^2))*$B$12+(($B$14*$B$15)/((1+$B$14*$B$16)^2))*$B$16)
41	=A40+$B$4	=G40	=($B$6*$H$8-$B$6*$B41-$B$9*$J41*(($B$10*$B$11*$B41)/(1+$B$11*$B41))*$B$12-$B$9*$J41*(($B$14*$B$15*$B41)/(1+$B$15*$B41))*$B$16)/($B$7+((($H$10*$B$11)/((1+$B$11*$B41)^2))*$B$12+(($B$14*$B$15)/((1+$B$14*$B$16)^2))*$B$16)
42	=A41+$B$4	=G41	=($B$6*$H$8-$B$6*$B42-$B$9*$J42*(($B$10*$B$11*$B42)/(1+$B$11*$B42))*$B$12-$B$9*$J42*(($B$14*$B$15*$B42)/(1+$B$15*$B42))*$B$16)/($B$7+((($H$10*$B$11)/((1+$B$11*$B42)^2))*$B$12+(($B$14*$B$15)/((1+$B$14*$B$16)^2))*$B$16)
43	=A42+$B$4	=G42	=($B$6*$H$8-$B$6*$B43-$B$9*$J43*(($B$10*$B$11*$B43)/(1+$B$11*$B43))*$B$12-$B$9*$J43*(($B$14*$B$15*$B43)/(1+$B$15*$B43))*$B$16)/($B$7+((($H$10*$B$11)/((1+$B$11*$B43)^2))*$B$12+(($B$14*$B$15)/((1+$B$14*$B$16)^2))*$B$16)
44	=A43+$B$4	=G43	=($B$6*$H$8-$B$6*$B44-$B$9*$J44*(($B$10*$B$11*$B44)/(1+$B$11*$B44))*$B$12-$B$9*$J44*(($B$14*$B$15*$B44)/(1+$B$15*$B44))*$B$16)/($B$7+((($H$10*$B$11)/((1+$B$11*$B44)^2))*$B$12+(($B$14*$B$15)/((1+$B$14*$B$16)^2))*$B$16)
45	=A44+$B$4	=G44	=($B$6*$H$8-$B$6*$B45-$B$9*$J45*(($B$10*$B$11*$B45)/(1+$B$11*$B45))*$B$12-$B$9*$J45*(($B$14*$B$15*$B45)/(1+$B$15*$B45))*$B$16)/($B$7+((($H$10*$B$11)/((1+$B$11*$B45)^2))*$B$12+(($B$14*$B$15)/((1+$B$14*$B$16)^2))*$B$16)

	D
28	CSTR Model
29	Mn(II) Concentration
30	k2
31	
32	=$I$56*$I$8* $I$56^($I$32+0.5*$I$4*$C32) $I$9*$J32*((($I$10*$I$11*$I$32+0.5*$I$4*$C32)/(1+$I$11*($I$32+0.5*$I$4*$C32)))*$I$12 $I$9*$J32*((($I$14*$I$15*($I$32+0.5*$I$4*$C32)/(1+$I$15*($I$32+0.5*$I$4*$C32)))*$I$16)/($I$7+(($I$10*$I$11)/(1+$I$11*($I$32+0.5*$I$4*$C32)^2))*$I$12+(($I$14*$I$15)/(1+$I$14*$I$16)^2)+$I$16)
33	=$I$56*$I$8 $I$56^($I$33+0.5*$I$4*$C33) $I$9*$J33*((($I$10*$I$11*$I$33+0.5*$I$4*$C33)/(1+$I$11*($I$33+0.5*$I$4*$C33)))*$I$12 $I$9*$J33*((($I$14*$I$15*($I$33+0.5*$I$4*$C33)/(1+$I$15*($I$33+0.5*$I$4*$C33)))*$I$16)/($I$7+(($I$10*$I$11)/(1+$I$11*($I$33+0.5*$I$4*$C33)^2))*$I$12+(($I$14*$I$15)/(1+$I$14*$I$16)^2)+$I$16)
34	=$I$56*$I$8 $I$56^($I$34+0.5*$I$4*$C34) $I$9*$J34*((($I$10*$I$11*$I$34+0.5*$I$4*$C34)/(1+$I$11*($I$34+0.5*$I$4*$C34)))*$I$12 $I$9*$J34*((($I$14*$I$15*($I$34+0.5*$I$4*$C34)/(1+$I$15*($I$34+0.5*$I$4*$C34)))*$I$16)/($I$7+(($I$10*$I$11)/(1+$I$11*($I$34+0.5*$I$4*$C34)^2))*$I$12+(($I$14*$I$15)/(1+$I$14*$I$16)^2)+$I$16)
35	=$I$56*$I$8 $I$56^($I$35+0.5*$I$4*$C35) $I$9*$J35*((($I$10*$I$11*$I$35+0.5*$I$4*$C35)/(1+$I$11*($I$35+0.5*$I$4*$C35)))*$I$12 $I$9*$J35*((($I$14*$I$15*($I$35+0.5*$I$4*$C35)/(1+$I$15*($I$35+0.5*$I$4*$C35)))*$I$16)/($I$7+(($I$10*$I$11)/(1+$I$11*($I$35+0.5*$I$4*$C35)^2))*$I$12+(($I$14*$I$15)/(1+$I$14*$I$16)^2)+$I$16)
36	=$I$56*$I$8 $I$56^($I$36+0.5*$I$4*$C36) $I$9*$J36*((($I$10*$I$11*$I$36+0.5*$I$4*$C36)/(1+$I$11*($I$36+0.5*$I$4*$C36)))*$I$12 $I$9*$J36*((($I$14*$I$15*($I$36+0.5*$I$4*$C36)/(1+$I$15*($I$36+0.5*$I$4*$C36)))*$I$16)/($I$7+(($I$10*$I$11)/(1+$I$11*($I$36+0.5*$I$4*$C36)^2))*$I$12+(($I$14*$I$15)/(1+$I$14*$I$16)^2)+$I$16)
37	=$I$56*$I$8 $I$56^($I$37+0.5*$I$4*$C37) $I$9*$J37*((($I$10*$I$11*$I$37+0.5*$I$4*$C37)/(1+$I$11*($I$37+0.5*$I$4*$C37)))*$I$12 $I$9*$J37*((($I$14*$I$15*($I$37+0.5*$I$4*$C37)/(1+$I$15*($I$37+0.5*$I$4*$C37)))*$I$16)/($I$7+(($I$10*$I$11)/(1+$I$11*($I$37+0.5*$I$4*$C37)^2))*$I$12+(($I$14*$I$15)/(1+$I$14*$I$16)^2)+$I$16)
38	=$I$56*$I$8 $I$56^($I$38+0.5*$I$4*$C38) $I$9*$J38*((($I$10*$I$11*$I$38+0.5*$I$4*$C38)/(1+$I$11*($I$38+0.5*$I$4*$C38)))*$I$12 $I$9*$J38*((($I$14*$I$15*($I$38+0.5*$I$4*$C38)/(1+$I$15*($I$38+0.5*$I$4*$C38)))*$I$16)/($I$7+(($I$10*$I$11)/(1+$I$11*($I$38+0.5*$I$4*$C38)^2))*$I$12+(($I$14*$I$15)/(1+$I$14*$I$16)^2)+$I$16)
39	=$I$56*$I$8 $I$56^($I$39+0.5*$I$4*$C39) $I$9*$J39*((($I$10*$I$11*$I$39+0.5*$I$4*$C39)/(1+$I$11*($I$39+0.5*$I$4*$C39)))*$I$12 $I$9*$J39*((($I$14*$I$15*($I$39+0.5*$I$4*$C39)/(1+$I$15*($I$39+0.5*$I$4*$C39)))*$I$16)/($I$7+(($I$10*$I$11)/(1+$I$11*($I$39+0.5*$I$4*$C39)^2))*$I$12+(($I$14*$I$15)/(1+$I$14*$I$16)^2)+$I$16)
40	=$I$56*$I$8 $I$56^($I$40+0.5*$I$4*$C40) $I$9*$J40*((($I$10*$I$11*$I$40+0.5*$I$4*$C40)/(1+$I$11*($I$40+0.5*$I$4*$C40)))*$I$12 $I$9*$J40*((($I$14*$I$15*($I$40+0.5*$I$4*$C40)/(1+$I$15*($I$40+0.5*$I$4*$C40)))*$I$16)/($I$7+(($I$10*$I$11)/(1+$I$11*($I$40+0.5*$I$4*$C40)^2))*$I$12+(($I$14*$I$15)/(1+$I$14*$I$16)^2)+$I$16)
41	=$I$56*$I$8 $I$56^($I$41+0.5*$I$4*$C41) $I$9*$J41*((($I$10*$I$11*$I$41+0.5*$I$4*$C41)/(1+$I$11*($I$41+0.5*$I$4*$C41)))*$I$12 $I$9*$J41*((($I$14*$I$15*($I$41+0.5*$I$4*$C41)/(1+$I$15*($I$41+0.5*$I$4*$C41)))*$I$16)/($I$7+(($I$10*$I$11)/(1+$I$11*($I$41+0.5*$I$4*$C41)^2))*$I$12+(($I$14*$I$15)/(1+$I$14*$I$16)^2)+$I$16)
42	=$I$56*$I$8 $I$56^($I$42+0.5*$I$4*$C42) $I$9*$J42*((($I$10*$I$11*$I$42+0.5*$I$4*$C42)/(1+$I$11*($I$42+0.5*$I$4*$C42)))*$I$12 $I$9*$J42*((($I$14*$I$15*($I$42+0.5*$I$4*$C42)/(1+$I$15*($I$42+0.5*$I$4*$C42)))*$I$16)/($I$7+(($I$10*$I$11)/(1+$I$11*($I$42+0.5*$I$4*$C42)^2))*$I$12+(($I$14*$I$15)/(1+$I$14*$I$16)^2)+$I$16)
43	=$I$56*$I$8 $I$56^($I$43+0.5*$I$4*$C43) $I$9*$J43*((($I$10*$I$11*$I$43+0.5*$I$4*$C43)/(1+$I$11*($I$43+0.5*$I$4*$C43)))*$I$12 $I$9*$J43*((($I$14*$I$15*($I$43+0.5*$I$4*$C43)/(1+$I$15*($I$43+0.5*$I$4*$C43)))*$I$16)/($I$7+(($I$10*$I$11)/(1+$I$11*($I$43+0.5*$I$4*$C43)^2))*$I$12+(($I$14*$I$15)/(1+$I$14*$I$16)^2)+$I$16)
44	=$I$56*$I$8 $I$56^($I$44+0.5*$I$4*$C44) $I$9*$J44*((($I$10*$I$11*$I$44+0.5*$I$4*$C44)/(1+$I$11*($I$44+0.5*$I$4*$C44)))*$I$12 $I$9*$J44*((($I$14*$I$15*($I$44+0.5*$I$4*$C44)/(1+$I$15*($I$44+0.5*$I$4*$C44)))*$I$16)/($I$7+(($I$10*$I$11)/(1+$I$11*($I$44+0.5*$I$4*$C44)^2))*$I$12+(($I$14*$I$15)/(1+$I$14*$I$16)^2)+$I$16)
45	=$I$56*$I$8 $I$56^($I$45+0.5*$I$4*$C45) $I$9*$J45*((($I$10*$I$11*$I$45+0.5*$I$4*$C45)/(1+$I$11*($I$45+0.5*$I$4*$C45)))*$I$12 $I$9*$J45*((($I$14*$I$15*($I$45+0.5*$I$4*$C45)/(1+$I$15*($I$45+0.5*$I$4*$C45)))*$I$16)/($I$7+(($I$10*$I$11)/(1+$I$11*($I$45+0.5*$I$4*$C45)^2))*$I$12+(($I$14*$I$15)/(1+$I$14*$I$16)^2)+$I$16)

	E
28	Vm(II) Concentration
29	k3
30	k4
31	
32	=$IB$6*$IB$8-$IB$6*($B32+0.5*$IB$4*$D32)-$IB$9*$J32*(($IB$10*$IB$11*($B32+0.5*$IB$4*$D32)/(1+$IB$11*($B32+0.5*$IB$4*$D32))+$IB$12-$IB$9*$J32*(($IB$14*$IB$15*($B32+0.5*$IB$4*$D32)/(1+$IB$15*($B32+0.5*$IB$4*$D32)))*$IB$16/($IB$7+(($IB$10*$IB$11)/(1+$IB$11*($B32+0.5*$IB$4*$D32)))^2)*$IB$12+(($IB$14*$IB$15)/(1+$IB$14*$IB$16)^2)*$IB$16)
33	=$IB$6*$IB$8-$IB$6*($B33+0.5*$IB$4*$D33)-$IB$9*$J33*(($IB$10*$IB$11*($B33+0.5*$IB$4*$D33)/(1+$IB$11*($B33+0.5*$IB$4*$D33)))+$IB$12-$IB$9*$J33*(($IB$14*$IB$15*($B33+0.5*$IB$4*$D33)/(1+$IB$15*($B33+0.5*$IB$4*$D33)))*$IB$16/($IB$7+(($IB$10*$IB$11)/(1+$IB$11*($B33+0.5*$IB$4*$D33)))^2)*$IB$12+(($IB$14*$IB$15)/(1+$IB$14*$IB$16)^2)*$IB$16)
34	=$IB$6*$IB$8-$IB$6*($B34+0.5*$IB$4*$D34)-$IB$9*$J34*(($IB$10*$IB$11*($B34+0.5*$IB$4*$D34)/(1+$IB$11*($B34+0.5*$IB$4*$D34)))+$IB$12-$IB$9*$J34*(($IB$14*$IB$15*($B34+0.5*$IB$4*$D34)/(1+$IB$15*($B34+0.5*$IB$4*$D34)))*$IB$16/($IB$7+(($IB$10*$IB$11)/(1+$IB$11*($B34+0.5*$IB$4*$D34)))^2)*$IB$12+(($IB$14*$IB$15)/(1+$IB$14*$IB$16)^2)*$IB$16)
35	=$IB$6*$IB$8-$IB$6*($B35+0.5*$IB$4*$D35)-$IB$9*$J35*(($IB$10*$IB$11*($B35+0.5*$IB$4*$D35)/(1+$IB$11*($B35+0.5*$IB$4*$D35)))+$IB$12-$IB$9*$J35*(($IB$14*$IB$15*($B35+0.5*$IB$4*$D35)/(1+$IB$15*($B35+0.5*$IB$4*$D35)))*$IB$16/($IB$7+(($IB$10*$IB$11)/(1+$IB$11*($B35+0.5*$IB$4*$D35)))^2)*$IB$12+(($IB$14*$IB$15)/(1+$IB$14*$IB$16)^2)*$IB$16)
36	=$IB$6*$IB$8-$IB$6*($IB36+0.5*$IB$4*$D36)-$IB$9*$J36*(($IB$10*$IB$11*($IB36+0.5*$IB$4*$D36)/(1+$IB$11*($IB36+0.5*$IB$4*$D36)))+$IB$12-$IB$9*$J36*(($IB$14*$IB$15*($IB36+0.5*$IB$4*$D36)/(1+$IB$15*($IB36+0.5*$IB$4*$D36)))*$IB$16/($IB$7+(($IB$10*$IB$11)/(1+$IB$11*($IB36+0.5*$IB$4*$D36)))^2)*$IB$12+(($IB$14*$IB$15)/(1+$IB$14*$IB$16)^2)*$IB$16)
37	=$IB$6*$IB$8-$IB$6*($B37+0.5*$IB$4*$D37)-$IB$9*$J37*(($IB$10*$IB$11*($B37+0.5*$IB$4*$D37)/(1+$IB$11*($B37+0.5*$IB$4*$D37)))+$IB$12-$IB$9*$J37*(($IB$14*$IB$15*($B37+0.5*$IB$4*$D37)/(1+$IB$15*($B37+0.5*$IB$4*$D37)))*$IB$16/($IB$7+(($IB$10*$IB$11)/(1+$IB$11*($B37+0.5*$IB$4*$D37)))^2)*$IB$12+(($IB$14*$IB$15)/(1+$IB$14*$IB$16)^2)*$IB$16)
38	=$IB$6*$IB$8-$IB$6*($B38+0.5*$IB$4*$D38)-$IB$9*$J38*(($IB$10*$IB$11*($B38+0.5*$IB$4*$D38)/(1+$IB$11*($B38+0.5*$IB$4*$D38)))+$IB$12-$IB$9*$J38*(($IB$14*$IB$15*($B38+0.5*$IB$4*$D38)/(1+$IB$15*($B38+0.5*$IB$4*$D38)))*$IB$16/($IB$7+(($IB$10*$IB$11)/(1+$IB$11*($B38+0.5*$IB$4*$D38)))^2)*$IB$12+(($IB$14*$IB$15)/(1+$IB$14*$IB$16)^2)*$IB$16)
39	=$IB$6*$IB$8-$IB$6*($B39+0.5*$IB$4*$D39)-$IB$9*$J39*(($IB$10*$IB$11*($B39+0.5*$IB$4*$D39)/(1+$IB$11*($B39+0.5*$IB$4*$D39)))+$IB$12-$IB$9*$J39*(($IB$14*$IB$15*($B39+0.5*$IB$4*$D39)/(1+$IB$15*($B39+0.5*$IB$4*$D39)))*$IB$16/($IB$7+(($IB$10*$IB$11)/(1+$IB$11*($B39+0.5*$IB$4*$D39)))^2)*$IB$12+(($IB$14*$IB$15)/(1+$IB$14*$IB$16)^2)*$IB$16)
40	=$IB$6*$IB$8-$IB$6*($B40+0.5*$IB$4*$D40)-$IB$9*$J40*(($IB$10*$IB$11*($B40+0.5*$IB$4*$D40)/(1+$IB$11*($B40+0.5*$IB$4*$D40)))+$IB$12-$IB$9*$J40*(($IB$14*$IB$15*($B40+0.5*$IB$4*$D40)/(1+$IB$15*($B40+0.5*$IB$4*$D40)))*$IB$16/($IB$7+(($IB$10*$IB$11)/(1+$IB$11*($B40+0.5*$IB$4*$D40)))^2)*$IB$12+(($IB$14*$IB$15)/(1+$IB$14*$IB$16)^2)*$IB$16)
41	=$IB$6*$IB$8-$IB$6*($B41+0.5*$IB$4*$D41)-$IB$9*$J41*(($IB$10*$IB$11*($B41+0.5*$IB$4*$D41)/(1+$IB$11*($B41+0.5*$IB$4*$D41)))+$IB$12-$IB$9*$J41*(($IB$14*$IB$15*($B41+0.5*$IB$4*$D41)/(1+$IB$15*($B41+0.5*$IB$4*$D41)))*$IB$16/($IB$7+(($IB$10*$IB$11)/(1+$IB$11*($B41+0.5*$IB$4*$D41)))^2)*$IB$12+(($IB$14*$IB$15)/(1+$IB$14*$IB$16)^2)*$IB$16)
42	=$IB$6*$IB$8-$IB$6*($B42+0.5*$IB$4*$D42)-$IB$9*$J42*(($IB$10*$IB$11*($B42+0.5*$IB$4*$D42)/(1+$IB$11*($B42+0.5*$IB$4*$D42)))+$IB$12-$IB$9*$J42*(($IB$14*$IB$15*($B42+0.5*$IB$4*$D42)/(1+$IB$15*($B42+0.5*$IB$4*$D42)))*$IB$16/($IB$7+(($IB$10*$IB$11)/(1+$IB$11*($B42+0.5*$IB$4*$D42)))^2)*$IB$12+(($IB$14*$IB$15)/(1+$IB$14*$IB$16)^2)*$IB$16)
43	=$IB$6*$IB$8-$IB$6*($B43+0.5*$IB$4*$D43)-$IB$9*$J43*(($IB$10*$IB$11*($B43+0.5*$IB$4*$D43)/(1+$IB$11*($B43+0.5*$IB$4*$D43)))+$IB$12-$IB$9*$J43*(($IB$14*$IB$15*($B43+0.5*$IB$4*$D43)/(1+$IB$15*($B43+0.5*$IB$4*$D43)))*$IB$16/($IB$7+(($IB$10*$IB$11)/(1+$IB$11*($B43+0.5*$IB$4*$D43)))^2)*$IB$12+(($IB$14*$IB$15)/(1+$IB$14*$IB$16)^2)*$IB$16)
44	=$IB$6*$IB$8-$IB$6*($B44+0.5*$IB$4*$D44)-$IB$9*$J44*(($IB$10*$IB$11*($B44+0.5*$IB$4*$D44)/(1+$IB$11*($B44+0.5*$IB$4*$D44)))+$IB$12-$IB$9*$J44*(($IB$14*$IB$15*($B44+0.5*$IB$4*$D44)/(1+$IB$15*($B44+0.5*$IB$4*$D44)))*$IB$16/($IB$7+(($IB$10*$IB$11)/(1+$IB$11*($B44+0.5*$IB$4*$D44)))^2)*$IB$12+(($IB$14*$IB$15)/(1+$IB$14*$IB$16)^2)*$IB$16)
45	=$IB$6*$IB$8-$IB$6*($B45+0.5*$IB$4*$D45)-$IB$9*$J45*(($IB$10*$IB$11*($B45+0.5*$IB$4*$D45)/(1+$IB$11*($B45+0.5*$IB$4*$D45)))+$IB$12-$IB$9*$J45*(($IB$14*$IB$15*($B45+0.5*$IB$4*$D45)/(1+$IB$15*($B45+0.5*$IB$4*$D45)))*$IB$16/($IB$7+(($IB$10*$IB$11)/(1+$IB$11*($B45+0.5*$IB$4*$D45)))^2)*$IB$12+(($IB$14*$IB$15)/(1+$IB$14*$IB$16)^2)*$IB$16)

	E
28	CSTR Model
29	Min(B) Concentration
30	k1
31	
32	=$B56*$I$8 $I$6*(($B32+0.5*$I$4*$D32)-$B59*$J32*(($I$10*$R$11*($B32+0.5*$I$4*$D32)/(1+$R$11*($B32+0.5*$I$4*$D32))+$I$12 $I$59*$J32*($I$14*$I$15*($B32+0.5*$I$4*$D32)/(1+$I$15*($B32+0.5*$I$4*$D32)))*$I$16)/$I$7+(($I$10*$I$11)/((1+$I$11*($B32+0.5*$I$4*$D32))^2))*$I$12+(($I$14*$I$15)/((1+$I$14*$I$16)^2))*$I$16)
33	=$B56*$I$8 $I$6*(($B33+0.5*$I$4*$D33)-$B59*$J33*(($I$10*$R$11*($B33+0.5*$I$4*$D33)/(1+$R$11*($B33+0.5*$I$4*$D33))+$I$12 $I$59*$J33*($I$14*$I$15*($B33+0.5*$I$4*$D33)/(1+$I$15*($B33+0.5*$I$4*$D33)))*$I$16)/$I$7+(($I$10*$I$11)/((1+$I$11*($B33+0.5*$I$4*$D33))^2))*$I$12+(($I$14*$I$15)/((1+$I$14*$I$16)^2))*$I$16)
34	=$B56*$I$8 $I$6*(($B34+0.5*$I$4*$D34)-$B59*$J34*(($I$10*$R$11*($B34+0.5*$I$4*$D34)/(1+$R$11*($B34+0.5*$I$4*$D34))+$I$12 $I$59*$J34*($I$14*$I$15*($B34+0.5*$I$4*$D34)/(1+$I$15*($B34+0.5*$I$4*$D34)))*$I$16)/$I$7+(($I$10*$I$11)/((1+$I$11*($B34+0.5*$I$4*$D34))^2))*$I$12+(($I$14*$I$15)/((1+$I$14*$I$16)^2))*$I$16)
35	=$B56*$I$8 $I$6*(($B35+0.5*$I$4*$D35)-$B59*$J35*(($I$10*$R$11*($B35+0.5*$I$4*$D35)/(1+$R$11*($B35+0.5*$I$4*$D35))+$I$12 $I$59*$J35*($I$14*$I$15*($B35+0.5*$I$4*$D35)/(1+$I$15*($B35+0.5*$I$4*$D35)))*$I$16)/$I$7+(($I$10*$I$11)/((1+$I$11*($B35+0.5*$I$4*$D35))^2))*$I$12+(($I$14*$I$15)/((1+$I$14*$I$16)^2))*$I$16)
36	=$B56*$I$8 $I$6*(($B36+0.5*$I$4*$D36)-$B59*$J36*(($I$10*$R$11*($B36+0.5*$I$4*$D36)/(1+$R$11*($B36+0.5*$I$4*$D36))+$I$12 $I$59*$J36*($I$14*$I$15*($B36+0.5*$I$4*$D36)/(1+$I$15*($B36+0.5*$I$4*$D36)))*$I$16)/$I$7+(($I$10*$I$11)/((1+$I$11*($B36+0.5*$I$4*$D36))^2))*$I$12+(($I$14*$I$15)/((1+$I$14*$I$16)^2))*$I$16)
37	=$B56*$I$8 $I$6*(($B37+0.5*$I$4*$D37)-$B59*$J37*(($I$10*$R$11*($B37+0.5*$I$4*$D37)/(1+$R$11*($B37+0.5*$I$4*$D37))+$I$12 $I$59*$J37*($I$14*$I$15*($B37+0.5*$I$4*$D37)/(1+$I$15*($B37+0.5*$I$4*$D37)))*$I$16)/$I$7+(($I$10*$I$11)/((1+$I$11*($B37+0.5*$I$4*$D37))^2))*$I$12+(($I$14*$I$15)/((1+$I$14*$I$16)^2))*$I$16)
38	=$B56*$I$8 $I$6*(($B38+0.5*$I$4*$D38)-$B59*$J38*(($I$10*$R$11*($B38+0.5*$I$4*$D38)/(1+$R$11*($B38+0.5*$I$4*$D38))+$I$12 $I$59*$J38*($I$14*$I$15*($B38+0.5*$I$4*$D38)/(1+$I$15*($B38+0.5*$I$4*$D38)))*$I$16)/$I$7+(($I$10*$I$11)/((1+$I$11*($B38+0.5*$I$4*$D38))^2))*$I$12+(($I$14*$I$15)/((1+$I$14*$I$16)^2))*$I$16)
39	=$B56*$I$8 $I$6*(($B39+0.5*$I$4*$D39)-$B59*$J39*(($I$10*$R$11*($B39+0.5*$I$4*$D39)/(1+$R$11*($B39+0.5*$I$4*$D39))+$I$12 $I$59*$J39*($I$14*$I$15*($B39+0.5*$I$4*$D39)/(1+$I$15*($B39+0.5*$I$4*$D39)))*$I$16)/$I$7+(($I$10*$I$11)/((1+$I$11*($B39+0.5*$I$4*$D39))^2))*$I$12+(($I$14*$I$15)/((1+$I$14*$I$16)^2))*$I$16)
40	=$B56*$I$8 $I$6*(($B40+0.5*$I$4*$D40)-$B59*$J40*(($I$10*$R$11*($B40+0.5*$I$4*$D40)/(1+$R$11*($B40+0.5*$I$4*$D40))+$I$12 $I$59*$J40*($I$14*$I$15*($B40+0.5*$I$4*$D40)/(1+$I$15*($B40+0.5*$I$4*$D40)))*$I$16)/$I$7+(($I$10*$I$11)/((1+$I$11*($B40+0.5*$I$4*$D40))^2))*$I$12+(($I$14*$I$15)/((1+$I$14*$I$16)^2))*$I$16)
41	=$B56*$I$8 $I$6*(($B41+0.5*$I$4*$D41)-$B59*$J41*(($I$10*$R$11*($B41+0.5*$I$4*$D41)/(1+$R$11*($B41+0.5*$I$4*$D41))+$I$12 $I$59*$J41*($I$14*$I$15*($B41+0.5*$I$4*$D41)/(1+$I$15*($B41+0.5*$I$4*$D41)))*$I$16)/$I$7+(($I$10*$I$11)/((1+$I$11*($B41+0.5*$I$4*$D41))^2))*$I$12+(($I$14*$I$15)/((1+$I$14*$I$16)^2))*$I$16)
42	=$B56*$I$8 $I$6*(($B42+0.5*$I$4*$D42)-$B59*$J42*(($I$10*$R$11*($B42+0.5*$I$4*$D42)/(1+$R$11*($B42+0.5*$I$4*$D42))+$I$12 $I$59*$J42*($I$14*$I$15*($B42+0.5*$I$4*$D42)/(1+$I$15*($B42+0.5*$I$4*$D42)))*$I$16)/$I$7+(($I$10*$I$11)/((1+$I$11*($B42+0.5*$I$4*$D42))^2))*$I$12+(($I$14*$I$15)/((1+$I$14*$I$16)^2))*$I$16)
43	=$B56*$I$8 $I$6*(($B43+0.5*$I$4*$D43)-$B59*$J43*(($I$10*$R$11*($B43+0.5*$I$4*$D43)/(1+$R$11*($B43+0.5*$I$4*$D43))+$I$12 $I$59*$J43*($I$14*$I$15*($B43+0.5*$I$4*$D43)/(1+$I$15*($B43+0.5*$I$4*$D43)))*$I$16)/$I$7+(($I$10*$I$11)/((1+$I$11*($B43+0.5*$I$4*$D43))^2))*$I$12+(($I$14*$I$15)/((1+$I$14*$I$16)^2))*$I$16)
44	=$B56*$I$8 $I$6*(($B44+0.5*$I$4*$D44)-$B59*$J44*(($I$10*$R$11*($B44+0.5*$I$4*$D44)/(1+$R$11*($B44+0.5*$I$4*$D44))+$I$12 $I$59*$J44*($I$14*$I$15*($B44+0.5*$I$4*$D44)/(1+$I$15*($B44+0.5*$I$4*$D44)))*$I$16)/$I$7+(($I$10*$I$11)/((1+$I$11*($B44+0.5*$I$4*$D44))^2))*$I$12+(($I$14*$I$15)/((1+$I$14*$I$16)^2))*$I$16)
45	=$B56*$I$8 $I$6*(($B45+0.5*$I$4*$D45)-$B59*$J45*(($I$10*$R$11*($B45+0.5*$I$4*$D45)/(1+$R$11*($B45+0.5*$I$4*$D45))+$I$12 $I$59*$J45*($I$14*$I$15*($B45+0.5*$I$4*$D45)/(1+$I$15*($B45+0.5*$I$4*$D45)))*$I$16)/$I$7+(($I$10*$I$11)/((1+$I$11*($B45+0.5*$I$4*$D45))^2))*$I$12+(($I$14*$I$15)/((1+$I$14*$I$16)^2))*$I$16)

	F
28	CSTR Model
29	Mn(II) Concentration
30	Kd
31	
32	=($I$56*$I$58-$I$56*($I$32+$I$54*$E32)-$I$59*$J32*((($I$10*$I$11*($I$32+$I$54*$E32))/(1+$I$11*($I$32+$I$54*$E32)))*$I$12-$I$59*$J32*((($I$14*$I$15*($I$32+$I$54*$E32))/(1+$I$15*($I$32+$I$54*$E32)))*$I$16))/($I$7+((($I$10*$I$11)/(1+$I$11*($I$32+$I$54*$E32)))^2))*$I$12+((($I$14*$I$15)/(1+$I$14*$I$16)^2))*$I$16)
33	=($I$56*$I$58-$I$56*($I$33+$I$54*$E33)-$I$59*$J33*((($I$10*$I$11*($I$33+$I$54*$E33)))/(1+$I$11*($I$33+$I$54*$E33)))*$I$12-$I$59*$J33*((($I$14*$I$15*($I$33+$I$54*$E33)))/(1+$I$15*($I$33+$I$54*$E33)))*$I$16))/($I$7+((($I$10*$I$11)/(1+$I$11*($I$33+$I$54*$E33)))^2))*$I$12+((($I$14*$I$15)/(1+$I$14*$I$16)^2))*$I$16)
34	=($I$56*$I$58-$I$56*($I$34+$I$54*$E34)-$I$59*$J34*((($I$10*$I$11*($I$34+$I$54*$E34)))/(1+$I$11*($I$34+$I$54*$E34)))*$I$12-$I$59*$J34*((($I$14*$I$15*($I$34+$I$54*$E34)))/(1+$I$15*($I$34+$I$54*$E34)))*$I$16))/($I$7+((($I$10*$I$11)/(1+$I$11*($I$34+$I$54*$E34)))^2))*$I$12+((($I$14*$I$15)/(1+$I$14*$I$16)^2))*$I$16)
35	=($I$56*$I$58-$I$56*($I$35+$I$54*$E35)-$I$59*$J35*((($I$10*$I$11*($I$35+$I$54*$E35)))/(1+$I$11*($I$35+$I$54*$E35)))*$I$12-$I$59*$J35*((($I$14*$I$15*($I$35+$I$54*$E35)))/(1+$I$15*($I$35+$I$54*$E35)))*$I$16))/($I$7+((($I$10*$I$11)/(1+$I$11*($I$35+$I$54*$E35)))^2))*$I$12+((($I$14*$I$15)/(1+$I$14*$I$16)^2))*$I$16)
36	=($I$56*$I$58-$I$56*($I$36+$I$54*$E36)-$I$59*$J36*((($I$10*$I$11*($I$36+$I$54*$E36)))/(1+$I$11*($I$36+$I$54*$E36)))*$I$12-$I$59*$J36*((($I$14*$I$15*($I$36+$I$54*$E36)))/(1+$I$15*($I$36+$I$54*$E36)))*$I$16))/($I$7+((($I$10*$I$11)/(1+$I$11*($I$36+$I$54*$E36)))^2))*$I$12+((($I$14*$I$15)/(1+$I$14*$I$16)^2))*$I$16)
37	=($I$56*$I$58-$I$56*($I$37+$I$54*$E37)-$I$59*$J37*((($I$10*$I$11*($I$37+$I$54*$E37)))/(1+$I$11*($I$37+$I$54*$E37)))*$I$12-$I$59*$J37*((($I$14*$I$15*($I$37+$I$54*$E37)))/(1+$I$15*($I$37+$I$54*$E37)))*$I$16))/($I$7+((($I$10*$I$11)/(1+$I$11*($I$37+$I$54*$E37)))^2))*$I$12+((($I$14*$I$15)/(1+$I$14*$I$16)^2))*$I$16)
38	=($I$56*$I$58-$I$56*($I$38+$I$54*$E38)-$I$59*$J38*((($I$10*$I$11*($I$38+$I$54*$E38)))/(1+$I$11*($I$38+$I$54*$E38)))*$I$12-$I$59*$J38*((($I$14*$I$15*($I$38+$I$54*$E38)))/(1+$I$15*($I$38+$I$54*$E38)))*$I$16))/($I$7+((($I$10*$I$11)/(1+$I$11*($I$38+$I$54*$E38)))^2))*$I$12+((($I$14*$I$15)/(1+$I$14*$I$16)^2))*$I$16)
39	=($I$56*$I$58-$I$56*($I$39+$I$54*$E39)-$I$59*$J39*((($I$10*$I$11*($I$39+$I$54*$E39)))/(1+$I$11*($I$39+$I$54*$E39)))*$I$12-$I$59*$J39*((($I$14*$I$15*($I$39+$I$54*$E39)))/(1+$I$15*($I$39+$I$54*$E39)))*$I$16))/($I$7+((($I$10*$I$11)/(1+$I$11*($I$39+$I$54*$E39)))^2))*$I$12+((($I$14*$I$15)/(1+$I$14*$I$16)^2))*$I$16)
40	=($I$56*$I$58-$I$56*($I$40+$I$54*$E40)-$I$59*$J40*((($I$10*$I$11*($I$40+$I$54*$E40)))/(1+$I$11*($I$40+$I$54*$E40)))*$I$12-$I$59*$J40*((($I$14*$I$15*($I$40+$I$54*$E40)))/(1+$I$15*($I$40+$I$54*$E40)))*$I$16))/($I$7+((($I$10*$I$11)/(1+$I$11*($I$40+$I$54*$E40)))^2))*$I$12+((($I$14*$I$15)/(1+$I$14*$I$16)^2))*$I$16)
41	=($I$56*$I$58-$I$56*($I$41+$I$54*$E41)-$I$59*$J41*((($I$10*$I$11*($I$41+$I$54*$E41)))/(1+$I$11*($I$41+$I$54*$E41)))*$I$12-$I$59*$J41*((($I$14*$I$15*($I$41+$I$54*$E41)))/(1+$I$15*($I$41+$I$54*$E41)))*$I$16))/($I$7+((($I$10*$I$11)/(1+$I$11*($I$41+$I$54*$E41)))^2))*$I$12+((($I$14*$I$15)/(1+$I$14*$I$16)^2))*$I$16)
42	=($I$56*$I$58-$I$56*($I$42+$I$54*$E42)-$I$59*$J42*((($I$10*$I$11*($I$42+$I$54*$E42)))/(1+$I$11*($I$42+$I$54*$E42)))*$I$12-$I$59*$J42*((($I$14*$I$15*($I$42+$I$54*$E42)))/(1+$I$15*($I$42+$I$54*$E42)))*$I$16))/($I$7+((($I$10*$I$11)/(1+$I$11*($I$42+$I$54*$E42)))^2))*$I$12+((($I$14*$I$15)/(1+$I$14*$I$16)^2))*$I$16)
43	=($I$56*$I$58-$I$56*($I$43+$I$54*$E43)-$I$59*$J43*((($I$10*$I$11*($I$43+$I$54*$E43)))/(1+$I$11*($I$43+$I$54*$E43)))*$I$12-$I$59*$J43*((($I$14*$I$15*($I$43+$I$54*$E43)))/(1+$I$15*($I$43+$I$54*$E43)))*$I$16))/($I$7+((($I$10*$I$11)/(1+$I$11*($I$43+$I$54*$E43)))^2))*$I$12+((($I$14*$I$15)/(1+$I$14*$I$16)^2))*$I$16)
44	=($I$56*$I$58-$I$56*($I$44+$I$54*$E44)-$I$59*$J44*((($I$10*$I$11*($I$44+$I$54*$E44)))/(1+$I$11*($I$44+$I$54*$E44)))*$I$12-$I$59*$J44*((($I$14*$I$15*($I$44+$I$54*$E44)))/(1+$I$15*($I$44+$I$54*$E44)))*$I$16))/($I$7+((($I$10*$I$11)/(1+$I$11*($I$44+$I$54*$E44)))^2))*$I$12+((($I$14*$I$15)/(1+$I$14*$I$16)^2))*$I$16)
45	=($I$56*$I$58-$I$56*($I$45+$I$54*$E45)-$I$59*$J45*((($I$10*$I$11*($I$45+$I$54*$E45)))/(1+$I$11*($I$45+$I$54*$E45)))*$I$12-$I$59*$J45*((($I$14*$I$15*($I$45+$I$54*$E45)))/(1+$I$15*($I$45+$I$54*$E45)))*$I$16))/($I$7+((($I$10*$I$11)/(1+$I$11*($I$45+$I$54*$E45)))^2))*$I$12+((($I$14*$I$15)/(1+$I$14*$I$16)^2))*$I$16)

	G
28	
29	
30	Y_{i+1}
31	
32	=B32+(($B$4/6)*(C32+2*D32+2*E32+F32))
33	=B33+(($B$4/6)*(C33+2*D33+2*E33+F33))
34	=B34+(($B$4/6)*(C34+2*D34+2*E34+F34))
35	=B35+(($B$4/6)*(C35+2*D35+2*E35+F35))
36	=B36+(($B$4/6)*(C36+2*D36+2*E36+F36))
37	=B37+(($B$4/6)*(C37+2*D37+2*E37+F37))
38	=B38+(($B$4/6)*(C38+2*D38+2*E38+F38))
39	=B39+(($B$4/6)*(C39+2*D39+2*E39+F39))
40	=B40+(($B$4/6)*(C40+2*D40+2*E40+F40))
41	=B41+(($B$4/6)*(C41+2*D41+2*E41+F41))
42	=B42+(($B$4/6)*(C42+2*D42+2*E42+F42))
43	=B43+(($B$4/6)*(C43+2*D43+2*E43+F43))
44	=B44+(($B$4/6)*(C44+2*D44+2*E44+F44))
45	=B45+(($B$4/6)*(C45+2*D45+2*E45+F45))

	I	J	K
28	CSTR Model		
29			HOCl Concentration
30	x	Y_i	k_1
31			
32	0	=$B$13	=($B$6*$B$13-$B$6*$J32-$B$20*$J32*(($B$10*$B$11*$B32)/(1+$B$11*$B32))*$B$7-$B$21*$J32*(($B$14*$B$15*$B32)/(1+$B$15*$B32))*$B$7-0.64*$B$17*$B$6)/$B$7
33	=I32+$B$4	=O32	=($B$6*$B$13-$B$6*$J33-$B$20*$J33*(($B$10*$B$11*$B33)/(1+$B$11*$B33))*$B$7-$B$21*$J33*(($B$14*$B$15*$B33)/(1+$B$15*$B33))*$B$7-0.64*$B$17*$B$6)/$B$7
34	=I33+$B$4	=O33	=($B$6*$B$13-$B$6*$J34-$B$20*$J34*(($B$10*$B$11*$B34)/(1+$B$11*$B34))*$B$7-$B$21*$J34*(($B$14*$B$15*$B34)/(1+$B$15*$B34))*$B$7-0.64*$B$17*$B$6)/$B$7
35	=I34+$B$4	=O34	=($B$6*$B$13-$B$6*$J35-$B$20*$J35*(($B$10*$B$11*$B35)/(1+$B$11*$B35))*$B$7-$B$21*$J35*(($B$14*$B$15*$B35)/(1+$B$15*$B35))*$B$7-0.64*$B$17*$B$6)/$B$7
36	=I35+$B$4	=O35	=($B$6*$B$13-$B$6*$J36-$B$20*$J36*(($B$10*$B$11*$B36)/(1+$B$11*$B36))*$B$7-$B$21*$J36*(($B$14*$B$15*$B36)/(1+$B$15*$B36))*$B$7-0.64*$B$17*$B$6)/$B$7
37	=I36+$B$4	=O36	=($B$6*$B$13-$B$6*$J37-$B$20*$J37*(($B$10*$B$11*$B37)/(1+$B$11*$B37))*$B$7-$B$21*$J37*(($B$14*$B$15*$B37)/(1+$B$15*$B37))*$B$7-0.64*$B$17*$B$6)/$B$7
38	=I37+$B$4	=O37	=($B$6*$B$13-$B$6*$J38-$B$20*$J38*(($B$10*$B$11*$B38)/(1+$B$11*$B38))*$B$7-$B$21*$J38*(($B$14*$B$15*$B38)/(1+$B$15*$B38))*$B$7-0.64*$B$17*$B$6)/$B$7
39	=I38+$B$4	=O38	=($B$6*$B$13-$B$6*$J39-$B$20*$J39*(($B$10*$B$11*$B39)/(1+$B$11*$B39))*$B$7-$B$21*$J39*(($B$14*$B$15*$B39)/(1+$B$15*$B39))*$B$7-0.64*$B$17*$B$6)/$B$7
40	=I39+$B$4	=O39	=($B$6*$B$13-$B$6*$J40-$B$20*$J40*(($B$10*$B$11*$B40)/(1+$B$11*$B40))*$B$7-$B$21*$J40*(($B$14*$B$15*$B40)/(1+$B$15*$B40))*$B$7-0.64*$B$17*$B$6)/$B$7
41	=I40+$B$4	=O40	=($B$6*$B$13-$B$6*$J41-$B$20*$J41*(($B$10*$B$11*$B41)/(1+$B$11*$B41))*$B$7-$B$21*$J41*(($B$14*$B$15*$B41)/(1+$B$15*$B41))*$B$7-0.64*$B$17*$B$6)/$B$7
42	=I41+$B$4	=O41	=($B$6*$B$13-$B$6*$J42-$B$20*$J42*(($B$10*$B$11*$B42)/(1+$B$11*$B42))*$B$7-$B$21*$J42*(($B$14*$B$15*$B42)/(1+$B$15*$B42))*$B$7-0.64*$B$17*$B$6)/$B$7
43	=I42+$B$4	=O42	=($B$6*$B$13-$B$6*$J43-$B$20*$J43*(($B$10*$B$11*$B43)/(1+$B$11*$B43))*$B$7-$B$21*$J43*(($B$14*$B$15*$B43)/(1+$B$15*$B43))*$B$7-0.64*$B$17*$B$6)/$B$7
44	=I43+$B$4	=O43	=($B$6*$B$13-$B$6*$J44-$B$20*$J44*(($B$10*$B$11*$B44)/(1+$B$11*$B44))*$B$7-$B$21*$J44*(($B$14*$B$15*$B44)/(1+$B$15*$B44))*$B$7-0.64*$B$17*$B$6)/$B$7
45	=I44+$B$4	=O44	=($B$6*$B$13-$B$6*$J45-$B$20*$J45*(($B$10*$B$11*$B45)/(1+$B$11*$B45))*$B$7-$B$21*$J45*(($B$14*$B$15*$B45)/(1+$B$15*$B45))*$B$7-0.64*$B$17*$B$6)/$B$7

	L
28	CSTR Model
29	HOCl Concentration
30	k_2
31	
32	=($B$6*$B$13-$B$6*($J32+0.5*$B$4*$K32)-$B$20*($J32+0.5*$B$4*$K32)*(($B$10*$B$11*$B32)/(1+$B$11*$B32))*$B$7-$B$21*($J32+0.5*$B$4*$K32)*(($B$14*$B$15*$B32)/(1+$B$15*$B32))*$B$7-0.64*$B$17*$B$6)/$B$7
33	=($B$6*$B$13-$B$6*($J33+0.5*$B$4*$K33)-$B$20*($J33+0.5*$B$4*$K33)*(($B$10*$B$11*$B33)/(1+$B$11*$B33))*$B$7-$B$21*($J33+0.5*$B$4*$K33)*(($B$14*$B$15*$B33)/(1+$B$15*$B33))*$B$7-0.64*$B$17*$B$6)/$B$7
34	=($B$6*$B$13-$B$6*($J34+0.5*$B$4*$K34)-$B$20*($J34+0.5*$B$4*$K34)*(($B$10*$B$11*$B34)/(1+$B$11*$B34))*$B$7-$B$21*($J34+0.5*$B$4*$K34)*(($B$14*$B$15*$B34)/(1+$B$15*$B34))*$B$7-0.64*$B$17*$B$6)/$B$7
35	=($B$6*$B$13-$B$6*($J35+0.5*$B$4*$K35)-$B$20*($J35+0.5*$B$4*$K35)*(($B$10*$B$11*$B35)/(1+$B$11*$B35))*$B$7-$B$21*($J35+0.5*$B$4*$K35)*(($B$14*$B$15*$B35)/(1+$B$15*$B35))*$B$7-0.64*$B$17*$B$6)/$B$7
36	=($B$6*$B$13-$B$6*($J36+0.5*$B$4*$K36)-$B$20*($J36+0.5*$B$4*$K36)*(($B$10*$B$11*$B36)/(1+$B$11*$B36))*$B$7-$B$21*($J36+0.5*$B$4*$K36)*(($B$14*$B$15*$B36)/(1+$B$15*$B36))*$B$7-0.64*$B$17*$B$6)/$B$7
37	=($B$6*$B$13-$B$6*($J37+0.5*$B$4*$K37)-$B$20*($J37+0.5*$B$4*$K37)*(($B$10*$B$11*$B37)/(1+$B$11*$B37))*$B$7-$B$21*($J37+0.5*$B$4*$K37)*(($B$14*$B$15*$B37)/(1+$B$15*$B37))*$B$7-0.64*$B$17*$B$6)/$B$7
38	=($B$6*$B$13-$B$6*($J38+0.5*$B$4*$K38)-$B$20*($J38+0.5*$B$4*$K38)*(($B$10*$B$11*$B38)/(1+$B$11*$B38))*$B$7-$B$21*($J38+0.5*$B$4*$K38)*(($B$14*$B$15*$B38)/(1+$B$15*$B38))*$B$7-0.64*$B$17*$B$6)/$B$7
39	=($B$6*$B$13-$B$6*($J39+0.5*$B$4*$K39)-$B$20*($J39+0.5*$B$4*$K39)*(($B$10*$B$11*$B39)/(1+$B$11*$B39))*$B$7-$B$21*($J39+0.5*$B$4*$K39)*(($B$14*$B$15*$B39)/(1+$B$15*$B39))*$B$7-0.64*$B$17*$B$6)/$B$7
40	=($B$6*$B$13-$B$6*($J40+0.5*$B$4*$K40)-$B$20*($J40+0.5*$B$4*$K40)*(($B$10*$B$11*$B40)/(1+$B$11*$B40))*$B$7-$B$21*($J40+0.5*$B$4*$K40)*(($B$14*$B$15*$B40)/(1+$B$15*$B40))*$B$7-0.64*$B$17*$B$6)/$B$7
41	=($B$6*$B$13-$B$6*($J41+0.5*$B$4*$K41)-$B$20*($J41+0.5*$B$4*$K41)*(($B$10*$B$11*$B41)/(1+$B$11*$B41))*$B$7-$B$21*($J41+0.5*$B$4*$K41)*(($B$14*$B$15*$B41)/(1+$B$15*$B41))*$B$7-0.64*$B$17*$B$6)/$B$7
42	=($B$6*$B$13-$B$6*($J42+0.5*$B$4*$K42)-$B$20*($J42+0.5*$B$4*$K42)*(($B$10*$B$11*$B42)/(1+$B$11*$B42))*$B$7-$B$21*($J42+0.5*$B$4*$K42)*(($B$14*$B$15*$B42)/(1+$B$15*$B42))*$B$7-0.64*$B$17*$B$6)/$B$7
43	=($B$6*$B$13-$B$6*($J43+0.5*$B$4*$K43)-$B$20*($J43+0.5*$B$4*$K43)*(($B$10*$B$11*$B43)/(1+$B$11*$B43))*$B$7-$B$21*($J43+0.5*$B$4*$K43)*(($B$14*$B$15*$B43)/(1+$B$15*$B43))*$B$7-0.64*$B$17*$B$6)/$B$7
44	=($B$6*$B$13-$B$6*($J44+0.5*$B$4*$K44)-$B$20*($J44+0.5*$B$4*$K44)*(($B$10*$B$11*$B44)/(1+$B$11*$B44))*$B$7-$B$21*($J44+0.5*$B$4*$K44)*(($B$14*$B$15*$B44)/(1+$B$15*$B44))*$B$7-0.64*$B$17*$B$6)/$B$7
45	=($B$6*$B$13-$B$6*($J45+0.5*$B$4*$K45)-$B$20*($J45+0.5*$B$4*$K45)*(($B$10*$B$11*$B45)/(1+$B$11*$B45))*$B$7-$B$21*($J45+0.5*$B$4*$K45)*(($B$14*$B$15*$B45)/(1+$B$15*$B45))*$B$7-0.64*$B$17*$B$6)/$B$7

	M
28	CSTR Model
29	HOCl Concentration
30	k_3
31	
32	=($B$6*$B$13-$B$6*($J32+0.5*$B$4*$L32)-$B$20*($J32+0.5*$B$4*$L32)*(($B$10*$B$11*$B32)/(1+$B$11*$B32))*$B$7-$B$21*($J32+0.5*$B$4*$L32)*(($B$14*$B$15*$B32)/(1+$B$15*$B32))*$B$7-0.64*$B$17*$B$6)/$B$7
33	=($B$6*$B$13-$B$6*($J33+0.5*$B$4*$L33)-$B$20*($J33+0.5*$B$4*$L33)*(($B$10*$B$11*$B33)/(1+$B$11*$B33))*$B$7-$B$21*($J33+0.5*$B$4*$L33)*(($B$14*$B$15*$B33)/(1+$B$15*$B33))*$B$7-0.64*$B$17*$B$6)/$B$7
34	=($B$6*$B$13-$B$6*($J34+0.5*$B$4*$L34)-$B$20*($J34+0.5*$B$4*$L34)*(($B$10*$B$11*$B34)/(1+$B$11*$B34))*$B$7-$B$21*($J34+0.5*$B$4*$L34)*(($B$14*$B$15*$B34)/(1+$B$15*$B34))*$B$7-0.64*$B$17*$B$6)/$B$7
35	=($B$6*$B$13-$B$6*($J35+0.5*$B$4*$L35)-$B$20*($J35+0.5*$B$4*$L35)*(($B$10*$B$11*$B35)/(1+$B$11*$B35))*$B$7-$B$21*($J35+0.5*$B$4*$L35)*(($B$14*$B$15*$B35)/(1+$B$15*$B35))*$B$7-0.64*$B$17*$B$6)/$B$7
36	=($B$6*$B$13-$B$6*($J36+0.5*$B$4*$L36)-$B$20*($J36+0.5*$B$4*$L36)*(($B$10*$B$11*$B36)/(1+$B$11*$B36))*$B$7-$B$21*($J36+0.5*$B$4*$L36)*(($B$14*$B$15*$B36)/(1+$B$15*$B36))*$B$7-0.64*$B$17*$B$6)/$B$7
37	=($B$6*$B$13-$B$6*($J37+0.5*$B$4*$L37)-$B$20*($J37+0.5*$B$4*$L37)*(($B$10*$B$11*$B37)/(1+$B$11*$B37))*$B$7-$B$21*($J37+0.5*$B$4*$L37)*(($B$14*$B$15*$B37)/(1+$B$15*$B37))*$B$7-0.64*$B$17*$B$6)/$B$7
38	=($B$6*$B$13-$B$6*($J38+0.5*$B$4*$L38)-$B$20*($J38+0.5*$B$4*$L38)*(($B$10*$B$11*$B38)/(1+$B$11*$B38))*$B$7-$B$21*($J38+0.5*$B$4*$L38)*(($B$14*$B$15*$B38)/(1+$B$15*$B38))*$B$7-0.64*$B$17*$B$6)/$B$7
39	=($B$6*$B$13-$B$6*($J39+0.5*$B$4*$L39)-$B$20*($J39+0.5*$B$4*$L39)*(($B$10*$B$11*$B39)/(1+$B$11*$B39))*$B$7-$B$21*($J39+0.5*$B$4*$L39)*(($B$14*$B$15*$B39)/(1+$B$15*$B39))*$B$7-0.64*$B$17*$B$6)/$B$7
40	=($B$6*$B$13-$B$6*($J40+0.5*$B$4*$L40)-$B$20*($J40+0.5*$B$4*$L40)*(($B$10*$B$11*$B40)/(1+$B$11*$B40))*$B$7-$B$21*($J40+0.5*$B$4*$L40)*(($B$14*$B$15*$B40)/(1+$B$15*$B40))*$B$7-0.64*$B$17*$B$6)/$B$7
41	=($B$6*$B$13-$B$6*($J41+0.5*$B$4*$L41)-$B$20*($J41+0.5*$B$4*$L41)*(($B$10*$B$11*$B41)/(1+$B$11*$B41))*$B$7-$B$21*($J41+0.5*$B$4*$L41)*(($B$14*$B$15*$B41)/(1+$B$15*$B41))*$B$7-0.64*$B$17*$B$6)/$B$7
42	=($B$6*$B$13-$B$6*($J42+0.5*$B$4*$L42)-$B$20*($J42+0.5*$B$4*$L42)*(($B$10*$B$11*$B42)/(1+$B$11*$B42))*$B$7-$B$21*($J42+0.5*$B$4*$L42)*(($B$14*$B$15*$B42)/(1+$B$15*$B42))*$B$7-0.64*$B$17*$B$6)/$B$7
43	=($B$6*$B$13-$B$6*($J43+0.5*$B$4*$L43)-$B$20*($J43+0.5*$B$4*$L43)*(($B$10*$B$11*$B43)/(1+$B$11*$B43))*$B$7-$B$21*($J43+0.5*$B$4*$L43)*(($B$14*$B$15*$B43)/(1+$B$15*$B43))*$B$7-0.64*$B$17*$B$6)/$B$7
44	=($B$6*$B$13-$B$6*($J44+0.5*$B$4*$L44)-$B$20*($J44+0.5*$B$4*$L44)*(($B$10*$B$11*$B44)/(1+$B$11*$B44))*$B$7-$B$21*($J44+0.5*$B$4*$L44)*(($B$14*$B$15*$B44)/(1+$B$15*$B44))*$B$7-0.64*$B$17*$B$6)/$B$7
45	=($B$6*$B$13-$B$6*($J45+0.5*$B$4*$L45)-$B$20*($J45+0.5*$B$4*$L45)*(($B$10*$B$11*$B45)/(1+$B$11*$B45))*$B$7-$B$21*($J45+0.5*$B$4*$L45)*(($B$14*$B$15*$B45)/(1+$B$15*$B45))*$B$7-0.64*$B$17*$B$6)/$B$7

	N
28	CSTR Model
29	HOCl Concentration
30	k_4
31	
32	=($B$6*$B$13-$B$6*($J32+$B$4*$M32)-$B$20*($J32+$B$4*$M32)*(($B$10*$B$11*$B32)/(1+$B$11*$B32))*$B$7-$B$21*($J32+$B$4*$M32)*(($B$14*$B$15*$B32)/(1+$B$15*$B32))*$B$7-0.64*$B$17*$B$6)/$B$7
33	=($B$6*$B$13-$B$6*($J33+$B$4*$M33)-$B$20*($J33+$B$4*$M33)*(($B$10*$B$11*$B33)/(1+$B$11*$B33))*$B$7-$B$21*($J33+$B$4*$M33)*(($B$14*$B$15*$B33)/(1+$B$15*$B33))*$B$7-0.64*$B$17*$B$6)/$B$7
34	=($B$6*$B$13-$B$6*($J34+$B$4*$M34)-$B$20*($J34+$B$4*$M34)*(($B$10*$B$11*$B34)/(1+$B$11*$B34))*$B$7-$B$21*($J34+$B$4*$M34)*(($B$14*$B$15*$B34)/(1+$B$15*$B34))*$B$7-0.64*$B$17*$B$6)/$B$7
35	=($B$6*$B$13-$B$6*($J35+$B$4*$M35)-$B$20*($J35+$B$4*$M35)*(($B$10*$B$11*$B35)/(1+$B$11*$B35))*$B$7-$B$21*($J35+$B$4*$M35)*(($B$14*$B$15*$B35)/(1+$B$15*$B35))*$B$7-0.64*$B$17*$B$6)/$B$7
36	=($B$6*$B$13-$B$6*($J36+$B$4*$M36)-$B$20*($J36+$B$4*$M36)*(($B$10*$B$11*$B36)/(1+$B$11*$B36))*$B$7-$B$21*($J36+$B$4*$M36)*(($B$14*$B$15*$B36)/(1+$B$15*$B36))*$B$7-0.64*$B$17*$B$6)/$B$7
37	=($B$6*$B$13-$B$6*($J37+$B$4*$M37)-$B$20*($J37+$B$4*$M37)*(($B$10*$B$11*$B37)/(1+$B$11*$B37))*$B$7-$B$21*($J37+$B$4*$M37)*(($B$14*$B$15*$B37)/(1+$B$15*$B37))*$B$7-0.64*$B$17*$B$6)/$B$7
38	=($B$6*$B$13-$B$6*($J38+$B$4*$M38)-$B$20*($J38+$B$4*$M38)*(($B$10*$B$11*$B38)/(1+$B$11*$B38))*$B$7-$B$21*($J38+$B$4*$M38)*(($B$14*$B$15*$B38)/(1+$B$15*$B38))*$B$7-0.64*$B$17*$B$6)/$B$7
39	=($B$6*$B$13-$B$6*($J39+$B$4*$M39)-$B$20*($J39+$B$4*$M39)*(($B$10*$B$11*$B39)/(1+$B$11*$B39))*$B$7-$B$21*($J39+$B$4*$M39)*(($B$14*$B$15*$B39)/(1+$B$15*$B39))*$B$7-0.64*$B$17*$B$6)/$B$7
40	=($B$6*$B$13-$B$6*($J40+$B$4*$M40)-$B$20*($J40+$B$4*$M40)*(($B$10*$B$11*$B40)/(1+$B$11*$B40))*$B$7-$B$21*($J40+$B$4*$M40)*(($B$14*$B$15*$B40)/(1+$B$15*$B40))*$B$7-0.64*$B$17*$B$6)/$B$7
41	=($B$6*$B$13-$B$6*($J41+$B$4*$M41)-$B$20*($J41+$B$4*$M41)*(($B$10*$B$11*$B41)/(1+$B$11*$B41))*$B$7-$B$21*($J41+$B$4*$M41)*(($B$14*$B$15*$B41)/(1+$B$15*$B41))*$B$7-0.64*$B$17*$B$6)/$B$7
42	=($B$6*$B$13-$B$6*($J42+$B$4*$M42)-$B$20*($J42+$B$4*$M42)*(($B$10*$B$11*$B42)/(1+$B$11*$B42))*$B$7-$B$21*($J42+$B$4*$M42)*(($B$14*$B$15*$B42)/(1+$B$15*$B42))*$B$7-0.64*$B$17*$B$6)/$B$7
43	=($B$6*$B$13-$B$6*($J43+$B$4*$M43)-$B$20*($J43+$B$4*$M43)*(($B$10*$B$11*$B43)/(1+$B$11*$B43))*$B$7-$B$21*($J43+$B$4*$M43)*(($B$14*$B$15*$B43)/(1+$B$15*$B43))*$B$7-0.64*$B$17*$B$6)/$B$7
44	=($B$6*$B$13-$B$6*($J44+$B$4*$M44)-$B$20*($J44+$B$4*$M44)*(($B$10*$B$11*$B44)/(1+$B$11*$B44))*$B$7-$B$21*($J44+$B$4*$M44)*(($B$14*$B$15*$B44)/(1+$B$15*$B44))*$B$7-0.64*$B$17*$B$6)/$B$7
45	=($B$6*$B$13-$B$6*($J45+$B$4*$M45)-$B$20*($J45+$B$4*$M45)*(($B$10*$B$11*$B45)/(1+$B$11*$B45))*$B$7-$B$21*($J45+$B$4*$M45)*(($B$14*$B$15*$B45)/(1+$B$15*$B45))*$B$7-0.64*$B$17*$B$6)/$B$7

	O
28	CSTR Model
29	HOCl Concentration
30	Y_{i+1}
31	
32	=J32+(($B$4/6)*(K32+2*L32+2*M32+N32))
33	=J33+(($B$4/6)*(K33+2*L33+2*M33+N33))
34	=J34+(($B$4/6)*(K34+2*L34+2*M34+N34))
35	=J35+(($B$4/6)*(K35+2*L35+2*M35+N35))
36	=J36+(($B$4/6)*(K36+2*L36+2*M36+N36))
37	=J37+(($B$4/6)*(K37+2*L37+2*M37+N37))
38	=J38+(($B$4/6)*(K38+2*L38+2*M38+N38))
39	=J39+(($B$4/6)*(K39+2*L39+2*M39+N39))
40	=J40+(($B$4/6)*(K40+2*L40+2*M40+N40))
41	=J41+(($B$4/6)*(K41+2*L41+2*M41+N41))
42	=J42+(($B$4/6)*(K42+2*L42+2*M42+N42))
43	=J43+(($B$4/6)*(K43+2*L43+2*M43+N43))
44	=J44+(($B$4/6)*(K44+2*L44+2*M44+N44))
45	=J45+(($B$4/6)*(K45+2*L45+2*M45+N45))

CSTR Model: Model Simulations

Initial Parameters:

Δx =	1	min
pH =	8	
Q =	0.01917	L/min
Volume =	2.3	L
C_{in} =	0.5	mg/L
k =	3.43E-02	
a (Fe iso) =	0.0070	
b (Fe iso) =	3.79	
M_{Fe} =	280	mg/L as FeO
$HOCl_0$ =	**3**	**mg/L**
a (Mn iso) =	0.204	
b (Mn iso) =	54.8	
M_{Mn} =	0	mg/L MnO_x
Fe_{in} =	2	mg/L
A =	0.008596054	
B =	0	
k2 (Fe) =	3.990202751	
k2 (Mn) =	0	

Note: Assume MnOx = 0 and no growth

θH = 120 min

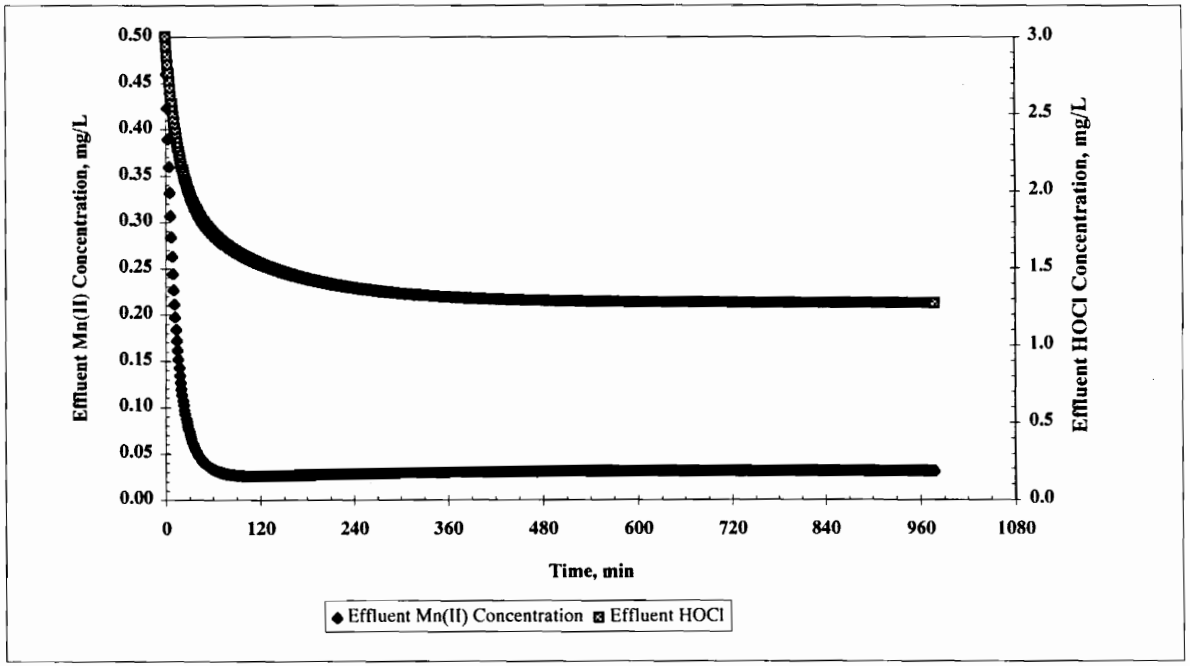

CSTR Model: Model Simulations

Initial Parameters:

Δx =	1	min
pH =	8	
Q =	0.01917	L/min
Volume =	2.3	L
C_{in} =	0.5	mg/L
k =	3.43E-02	
a (Fe iso) =	0.0070	
b (Fe iso) =	3.79	
M_{Fe} =	**150**	**mg/L as FeO**
$HOCl_0$ =	**2**	**mg/L**
a (Mn iso) =	0.204	
b (Mn iso) =	54.8	
M_{Mn} =	0	mg/L MnO_x
Fe_{in} =	2	mg/L
A =	0.016045968	
B =	0	
k2 (Fe) =	2.137608617	
k2 (Mn) =	0	

Note: Assume MnOx = 0 and no growth

θH = 120 min

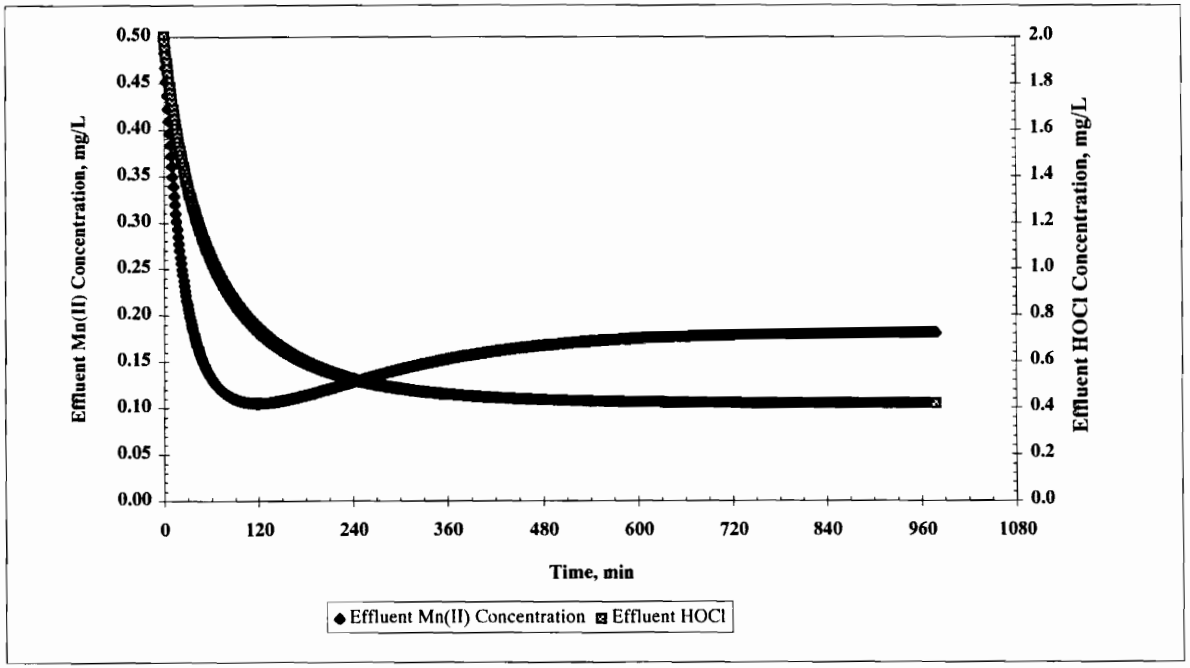

CSTR Model: Model Simulations

Initial Parameters:

Δx =	1	min
pH =	8	
Q =	**0.01917**	**L/min**
Volume =	2.3	L
C_{in} =	0.5	mg/L
k =	3.43E-02	
a (Fe iso) =	0.0070	
b (Fe iso) =	3.79	
M_{Fe} =	280	mg/L as FeO
$HOCl_0$ =	**4**	**mg/L**
a (Mn iso) =	0.204	
b (Mn iso) =	54.8	
M_{Mn} =	0	mg/L MnO_X
Fe_{in} =	2	mg/L
A =	0.008596054	
B =	0	
k2 (Fe) =	3.990202751	
k2 (Mn) =	0	

Note: Assume MnOx = 0 and no growth

θH = 120 min

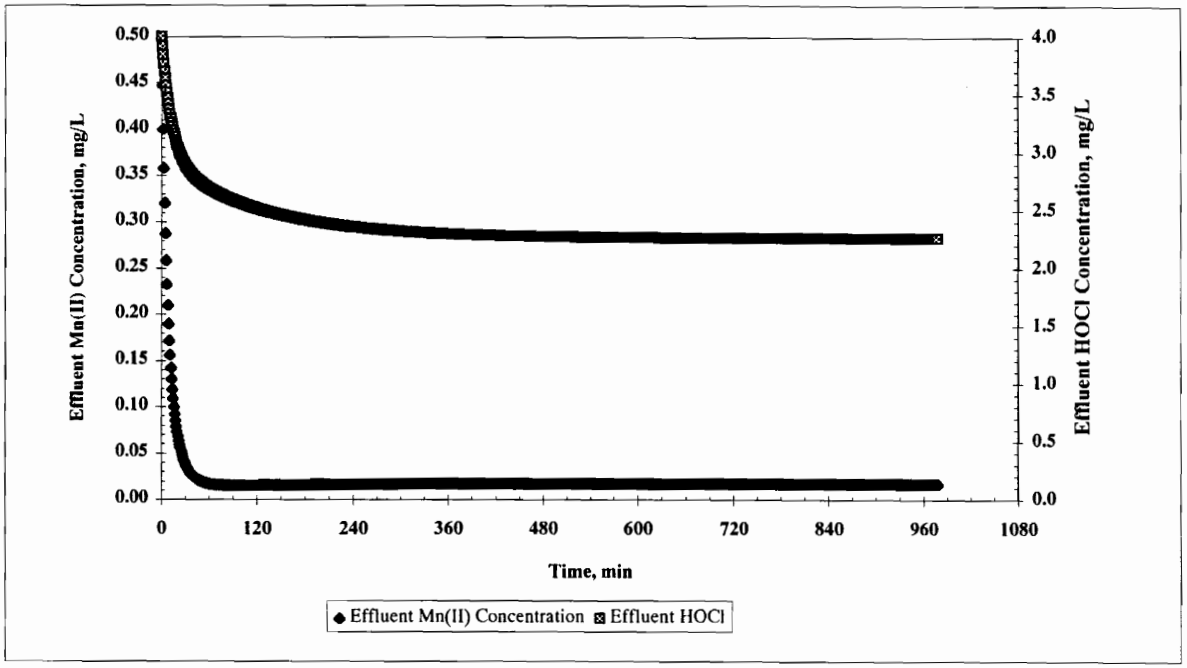

CSTR Model: Model Simulations

Initial Parameters:

Δx =	1	min
pH =	8	
Q =	0.01917	L/min
Volume =	2.3	L
C_{in} =	0.5	mg/L
k =	3.43E-02	
a (Fe iso) =	0.0070	
b (Fe iso) =	3.79	
M_{Fe} =	280	mg/L as FeO
$HOCl_0$ =	**3**	**mg/L**
a (Mn iso) =	0.204	
b (Mn iso) =	54.8	
M_{Mn} =	**3**	**mg/L MnO_x**
Fe_{in} =	2	mg/L
A =	0.008596054	
B =	0.802298413	
k2 (Fe) =	3.990202751	
k2 (Mn) =	0.042752172	

Note: Assume MnOx = 0 and no growth

θH = 120 min

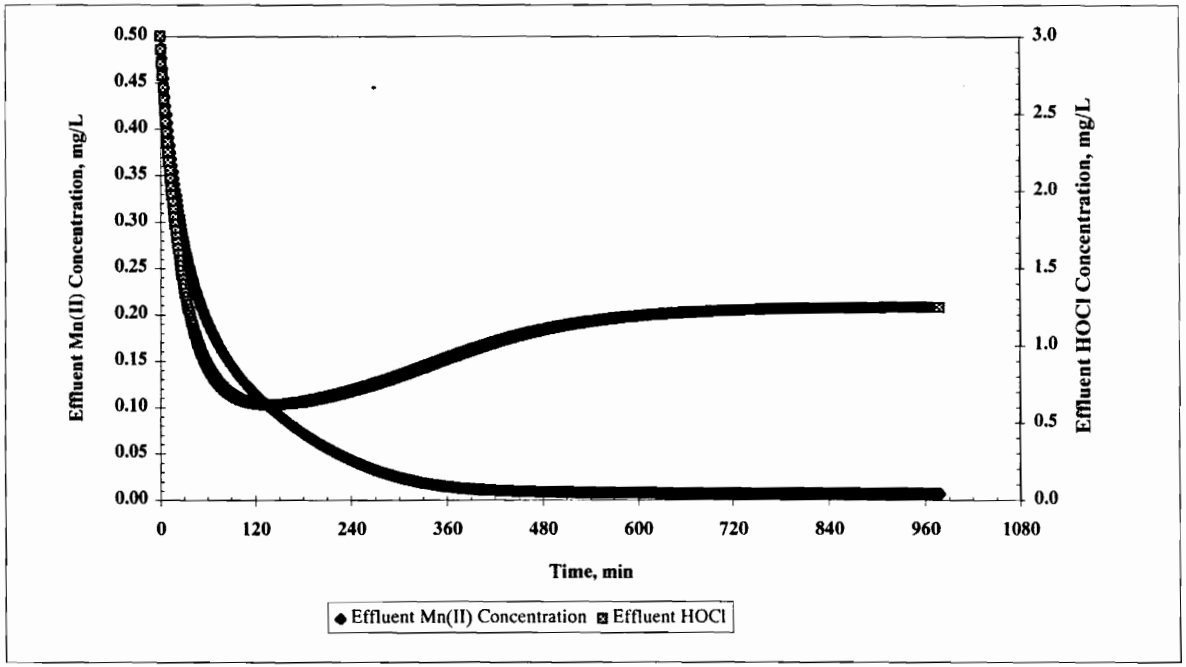

VITA

William Scott Dewhirst II was born in 1971 in Richmond, Virginia and attended high school in Henrico County at Hermitage High School. Upon completion of his high school career, he enrolled at Virginia Polytechnic Institute and State University (Virginia Tech) to pursue an undergraduate degree in civil engineering. Immediately following his undergraduate work and receipt of a Bachelors of Science in Civil Engineering, he continued on to receive a Masters of Science in Environmental Engineering at Virginia Tech. At the time of this writing, he resides in Greenville, South Carolina where he is employed with Black & Veatch Consulting Engineers.